University of Naples Federico II

Polytechnic School and of Basic Sciences
Department of Earth, Environment and Resources Sciences

Doctoral School in Earth Sciences
Ph.D. Program in Internal Dynamics of Volcanic Systems and Hydrogeological-Environmental Risks (XXVII Cycle)

Ph.D. Program Coordinator Prof. Benedetto De Vivo

Ph.D. Thesis in Applied Hydrogeology

Groundwater recharge in karst aquifers of southern Apennines: estimation at different spatial and temporal scale and effect of climate variability

Supervisor

Prof. Vincenzo Allocca

Ph.D. Student

Ferdinando Manna

Co-supervisor

Prof. Pantaleone De Vita

March 2015

Abstract

Karst aquifers represent, in large areas of the world, a strategic socio-economic and environmental resource providing drinkable water, a great biodiversity and amazing landscape. Ford and Williams (2007) estimated that about 25% of the world's population depends on water coming from karst aquifers. For this reason, from the 70's, several studies on European karst aquifers have been carried out, in order to create conceptual models and reproduce the hydrogeological behavior. The main issue of these models was the hydraulic role of the epikarst and the "duality" (Kiraly, 1994) of infiltration process (diffuse and rapid) , groundwater flow field (low velocity in the matrix and high in conduits) and discharge condition (low and constant and high and variable), which is a direct consequence of the heterogeneous structure of these aquifers. In Italy, only from the late 70's hydrologists and hydrogeologists focused their studies on karst aquifers, for enhancing the protection, usability and exploitation of water resources. Different models were proposed for the Alpine (Civita et alii, 1991; Vigna, 2007) and the southern Apennines (Celico, 1978; Celico, 1983a; Celico, 1986; Celico et alii, 2001; Allocca et alii, 2007) karst aquifers.

The latter are currently important sources also for several bottling plants and feed different aqueduct systems. In order to avoid pollution and over-exploitation and for a fair management of the resource, the correct estimation at various space-time scales of groundwater recharge processes, corresponding to mean annual replenishment of aquifers by infiltration processes through the vadose zone, is a fundamental and challenging issue, also considering the climate variability affecting the area.

On a regional scale, the impact of long-term climate variability on groundwater recharge was analysed by using regional indexes of precipitations, temperature, effective precipitations and spring discharges. In order to calculate these climate indexes, times series of precipitations and air temperature were gathered, from 1921 to 2012, from 18 rain gauge stations and 9 thermometric stations, chosen in function of the continuity of functioning and spatial distribution over the territory. Moreover, for the same period, discharge data were collected from three karst springs. A strong correlation was found between the climate indexes and the pattern of the North Atlantic Oscillation Index, analysed using different statistical techniques (using smoothing numerical techniques, cross-correlation and Fourier analysis).

On a basin scale, an original Annual Groundwater Recharge Coefficient (AGRC) was created, by means of an integrated approach based on hydrogeological, hydrological, geomorphological, land use and soil cover analyses. The coefficient represent the ratio between net groundwater outflow and the precipitation minus actual evapotranspiration (P-ETR) for a karst aquifer. To estimate P-ETR mean value for each considered aquifer, was constructed a model for the whole southern Apennines, based on the relation with the altitude, the orographic barrier and the rain shadow effect. The AGRC values found for the sample aquifers ranges from 50% to 79% and are consistent with those estimated for karst aquifers in Europe from other authors. Moreover, considering the peculiar geomorphological feature of the karst aquifers, characterized by huge summit plateau and endorheic areas, namely by a total infiltration and no runoff, an additional coefficient was assessed in order to estimate the recharge for the slope areas only ($AGRC_S$).

In addition, was studied the effect of the parameters affecting recharge on the estimated AGRC. A multiple linear regression between the AGRC, lithology and the summit plateau and endorheic areas was found. The latter is a valid tool for estimate recharge and, consequently, the mean annual runoff also for those aquifers characterized by a lack of spring discharge time series.
On a local scale, the groundwater recharge of a test perched karstic aquifer, belonging to the Mount Terminio hydrogeological structure was estimated. For such a purpose, an improvement of the Water Table Fluctuation (WTF) method, known as Episodic Master Recession (EMR) method (Nimmo et alii, 2015), was applied to estimate the Recharge to Precipitation Ratio (RPR) coefficient, which represents the amount of precipitation recharging groundwater. RPR values varies between 35% and 97%, with an annual annual RPR value (73%) resulted well matching with the AGRC estimated for that portion of Terminio karst aquifer (70%) and with the evapotranspiration value (30%) assessed through the use of Thornthwaite-Mather's method. By a multiple regression analysis, RPR values are recognized as chiefly influenced, mainly, by the rainfall intensity and, secondly, by the antecedent soil water content.
The different methods used at different spatial and temporal scale represent an advancement of the understanding of the hydrological behavior of karst aquifers and in particular of the recharge process. For the first time, has been establish a link between a large-scale atmospheric cycle and the groundwater recharge of carbonate karst aquifers. Furthermore, has been carried out an original coefficient (AGRC) through a multidisciplinary approach that can substitute those heuristically calculated (Celico, 1986; Allocca et alii, 2007) in the water balance calculations. Moreover, the EMR method has been applied in a heterogeneous perched karstic aquifer of the southern Italy, whereas, until now, was used in few porous aquifers, with homogeneous hydraulic properties (Nimmo et alii, 2015).

Acknowledgements

This thesis was prepared at the Department of Earth, Environment and Resources Sciences and supervised by Prof. Vincenzo Allocca. I want to thank him for his support in my post-graduate path, for the passion for the hydrogeology that transmitted me day after day and for all the professional and non-professional suggestions that has given me over these years.
I am also grateful to Prof. Pantaleone De Vita, essential presence for my scientific growth and for the incentive to improve my scientific background every day.
Without you two, this dissertation would not have been possible.
Thanks to Dr. John Nimmo of the United States Geological Survey headquarters of Menlo Park, CA for being by my side during my time of visiting, for his patience and helpfulness. Thank you for broadening my hydrogeological knowledge and sharing some specific aspects of his research.
Thanks also to Kim Perkins. Although there was no possibility to collaborate on the same study, I always appreciated the availability and the suggestions you gave me.
I want to thank Prof. De Vivo, coordinator of my Ph.D. course, the whole Ph.D. committee and Prof. Fulvio Celico, referee of the thesis.
Thanks to the Univesity of Naples that partially funds my visiting period at the USGS with "*Programma di scambi internazionali con Università ed Istituti di ricerca stranieri per la mobilità di breve durata di docenti, ricercatori e studiosi* – Decreto Rettorale: 432 del 13/02/2014".

List of publications

1. De Vita P., Allocca V., Manna F. and Fabbrocino S., 2012. *Coupled decadal variability of the North Atlantic Oscillation, regional rainfall and karst spring discharges in the Campania region (southern Italy)*. Hydrol. Earth Syst. Sci., 16, 1389-1399.
2. Allocca V., De Vita P., Manna F., 2012. *Impact of the NAO on the hydrological cycle of karst aquifers in southern Apennines.* Proceedings of Flowpath 2012. Bologna (Italy), 20-22 June 2012.
3. Manna F., Allocca V., De Vita P., Fusco F. and Napolitano E., 2013a. *Groundwater recharge assessment in karst aquifers of southern Apennines (Italy).* Rend. Online Soc. Geol. It, 24, 202 - 204.
4. Fusco F., De Vita P., Napolitano E., Allocca V. and Manna F., 2013. *Monitoring the soil suction regime of landslide prone ash-fall pyroclastics deposits covering slopes in the Sarno area (Campania – southern Italy)*. Rend. Online Soc. Geol. It, 24, 146 - 148.
5. Manna F., Allocca V., Fusco F., Napolitano E. & De Vita P., 2013b. *Effect of the North Atlantic Oscillation on groundwater recharge in karst aquifers of the Cilento Geopark (Italy).* Rend. Online Soc. Geol. It, 24, 106 - 109.
6. Allocca V., Manna F., De Vita P., 2014. *Estimating annual groundwater recharge coefficient for karst aquifers of the southern Apennines (Italy).* Hydrol. Earth Syst. Sci., 18, 803-817, doi:10.5194/hess-18-803-2014, 2014.
7. Manna F., Nimmo J., Allocca V. and De Vita P., 2014. *Assessment of groundwater recharge in an ash-fall mantled karst aquifer of southern Italy.* AGU Fall Meeting Abstract.
8. De Vita P., Allocca V., Di Clemente E., Fusco F., Manna F., Mastrogiovanni G. and Napolitano E., 2015. *The instability of Colluvial Mantle in Turbidite Flysch series of the Cilento region (Campania – southern Italy): the November 26, 2010 Ostigliano Translational Slide*. Engineering Geology for Society and Territory, Volume 2, 1045-1048.
9. Napolitano E., De Vita P., Fusco F., Allocca V. and Manna F., 2015. *Long-term hydrological modelling of pyroclastic soil mantled slopes for assessing rainfall threshold Triggering Debris Flows: The Case of the Sarno Mountains (Campania—Southern Italy).* Engineering Geology for Society and Territory, Volume 2, 1567-1570.
10. Manna F., Nimmo J., Allocca V. and De Vita P., 2015. *Recharge in karst aquifers: from regional to local and annual to episodic scale.* Accepted on Rend. Online Soc. Geol. It.
11. Allocca V., De Vita P., Manna F. and Nimmo J.,2015. *Groundwater recharge assessment at local and episodic scale in a perched karstic aquifer mantled by pyroclastic soils (Southern Italy).* Submitted.
12. Manna F., Nimmo J., Allocca V. and De Vita P., 2015. *Different spatial and temporal approaches in the estimation of recharge in karst aquifer of southern Apennines.* In preparation.

List of figures

List of tables

List of acronyms and abbreviations

ADS	Annex to drains systems (Mangin, 1975)
AGRC	Annual Groundwater Recharge Coefficient
$AGRC_S$	Annual Groundwater Recharge Coefficient for slope areas
ARC	Annual Runoff Coefficient
AWC	Available Water holding Capacity
Csa	Warm temperate climate with dry and hot summer (Geiger, 1954)
Csb	Warm temperate climate with dry and warm summer (Geiger, 1954)
EMR	Episodic Master Recession
ETP	Potential evapotranspiration
ETR	Actual evapotranspiration
FC	Field Capacity
GIS	Geographical Information System
LPV	Low Permeability Volume (Drogue, 1971; Kiraly, 1975)
LS	Loamy Sand
MADI	Mean Annual Discharge Index
MAEPI	Mean Annual Effective Precipitation Index
MAPI	Mean Annual Precipitation Index
MATI	Mean Annual Temperature Index
MRC	Master Recession Curve
NAO	North Atlantic Oscillation
NAOI	North Atlantic Oscillation Index
P	Precipitation
PWP	Permanent Wilting Point
R	Recharge
RO	Surface runoff
RPR	Recharge to Precipitation Ratio
SCS	Soil Conservation Service
SI	Storm Intensity
SL	Sandy Loam
SWAT	Soil and Water Assessment Tool
SWC	Soil Water Content
Sy	Specific yield
T	Air temperature
UTM	Universal Transverse Mercator
WTF	Water Table Fluctuation

ZOODRM Zoom Object-Oriented Distributed Recharge Model

List of symbols

A_E	Cumulative extension of summit plateau areas and/or endorheic watersheds
AEP_{ji}	Annual Effective Precipitation for the j rain gauge station and the i year
AP_{ji}	Annual Precipitation for the j rain gauge station and the i year
A_T	Total area of the karst aquifer
AT_{ki}	Annual air Temperature for the k air temperature gauge station and the i year
C_P	Cl- concentration from rainfall and dry precipitation
C_R	Cl- concentration from the recharge water
C_{RO}	Cl- concentration from surface runoff water
E	Summit plateau areas and/or endorheic watersheds area
K	Coefficient that depends on mean monthly hours of solar radiation in function of the month and latitude
I	Annual heat index
L	Limestone area
MAD	Mean Annual Discharge of the whole time series
MADi	Mean Annual Discharge for the i year
$MADI_i$	Mean Annual Discharge Index for the i year
$MAEPI_i$	Mean Annual Effective Precipitation Index for the i year
$MAEP_j$	Mean Annual Effective Precipitation of the whole time series for the j rain gauge station
$MAPI_i$	Mean Annual Precipitation Index for the i year
MAP_j	Mean Annual Precipitation of the whole time series for the j rain gauge station
$MATI_i$	Mean Annual air Temperature Index for the i year
MAT_k	Mean Annual air Temperature of the whole time series for the k air temperature gauge station
Qs	Mean annual spring discharge
Qt	Mean annual tapped discharge
t_i	Mean monthly air temperature for the i month
U_i	Mean annual groundwater inflow from adjoining aquifers and other allogenic recharge
U_o	Mean annual groundwater outflow through adjoining aquifers
V_{inflow}	Volume inflowing aquifers
$V_{outflow}$	Volume outflowing aquifers
Δh	Peak water-table rise
ΔWr	Interannual variation of groundwater reserves
ΔSW	Variation of the soil water content

Index

1. Introduction

Karst is a type of landscape formed from the dissolution of soluble rocks such as limestone (mainly), dolostone, marl and gypsum. Karst topography shows typical landforms: poljes, dolines and sinkholes, karren, swallow holes that affect greatly the groundwater circulation. Large areas of the ice-free continental area of the Earth are underlain by karst developed on carbonate rocks (Fig. 1/1) and roughly 20–25% of the world's population depends on karst water (Ford and Williams, 2007). In the United States 20% of the land surface is made of karst (Davies et alii, 1984) and 40% of the groundwater used for drinking comes from karst aquifers (Quinlan and Ewers, 1989). In India about 3 % of total land surface is occupied by carbonate rocks that are mostly karstified and constitute a significant source of groundwater. The groundwater drawn from these aquifers matches the water demand of ~35 million people (Dar et alii, 2014). In Europe, carbonate terrains occupy about 35% of the land surface and many important cities are supplied totally or partly with karst waters, including Bristol, London, Paris, Rome and Vienna (Ford and Williams, 2007).

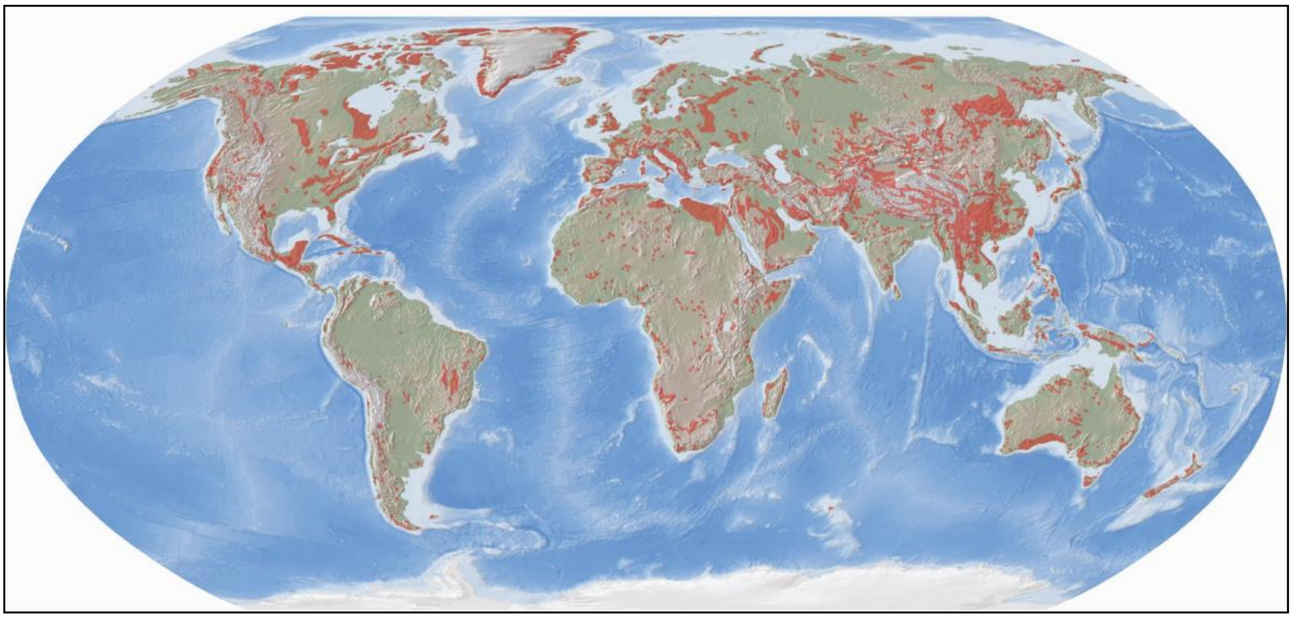

Fig. 1/1 – Major outcrops of carbonate rocks of the world (Ford and Williams, 2007).

In Italy and, especially in southern Italy, they constitute the main source of drinkable water with a mean groundwater yield of 4100×10^{6} m^{3} $year^{-1}$ and a mean specific groundwater yield varying between 0.025 and 0.400 m^{3} s^{-1} km^{-2} (Celico, 1983a; Celico, 1983 b; Celico et alii, 2000; Allocca et alii, 2007).

In the light of these considerations, it is fundamental a correct management and the preservation of these aquifers in order to prevent pollution and over-exploitation, also considering the long-trend climate variability (De Vita et alii, 2012, Manna et alii, 2013b) and the tropicalization of the weather (Mazzarella, 1999) in the Mediterranean area. To this purpose, in the past years, have been developed several methodologies (Aller et alii, 1987; Civita, 1988; 1994; 1997; Celico, 1996; 1998) for a better assessment of the intrinsic vulnerability and the definition of the protection areas. Conversely, there is a lack of studies

aimed at more in-depth evaluation of the potential groundwater resources of karst aquifer. In fact, so far, for karst aquifers of the southern Apennines, only heuristical estimations of the potential infiltration coefficient were carried out (Celico, 1988; Allocca et alii, 2007). Therefore, a correct assessment of the infiltration coefficients with an organic approach that consider the parameters affecting recharge, at different spatial and temporal scale, is needed.
Given that, the main objectives of this Ph.D. thesis are:

- the evaluation, on a regional scale, of the effects of long-trend climate variability in southern Apennines on groundwater recharge and spring discharges in karst aquifers;
- the assessment of groundwater recharge in karst aquifers, at basin and mean annual scale, by estimating of an original Annual Groundwater Recharge Coefficient (AGRC) and its regionalization to southern Apennines;
- the estimation of groundwater recharge, at local and episodic scale, by estimating an innovative Recharge Precipitation Ratio (RPR) coefficient in a perched karst aquifer of the southern Apennines.

The thesis is organized as follows: a review of hydrogeological conceptual models and the hydrogeological features of karst aquifers (European and southern Apennines karst aquifers) and a review of methods for the estimation of groundwater recharge in karst aquifer are described in Section 2. A description of the study area fields is reported in Section 3. A summary of dataset and used methods, results and conclusions are reported in Sections 4, 5 and 6 respectively. Finally, a sequence of the papers published during the three years of Ph.D. program, which constitute the results of the research activity, is provided.

2. Karst aquifers: literature review

2.1 Hydrogeological features of European karst aquifers

Starting from 70's, several studies on karst aquifers have been carried out focusing mainly on the creation of different conceptual models able to summarize the complex pattern of groundwater flow and to reproduce, as far as possible, the hydrogeological behavior.
One early attempt of conceptualizing karst aquifer focused attention on geological and hydrogeological setting. White (1969) recognized three types of karst aquifers:

- *Diffuse flow* (Fig. 2.1/1) occurs in less soluble rocks. In diffuse flow carbonate aquifers, integrated conduits are rare; caves are small and irregular and often represent only joints modified by the dissolution of rocks. For these aquifers, groundwater outflows in numerous small springs and the Darcy's law is applicable;

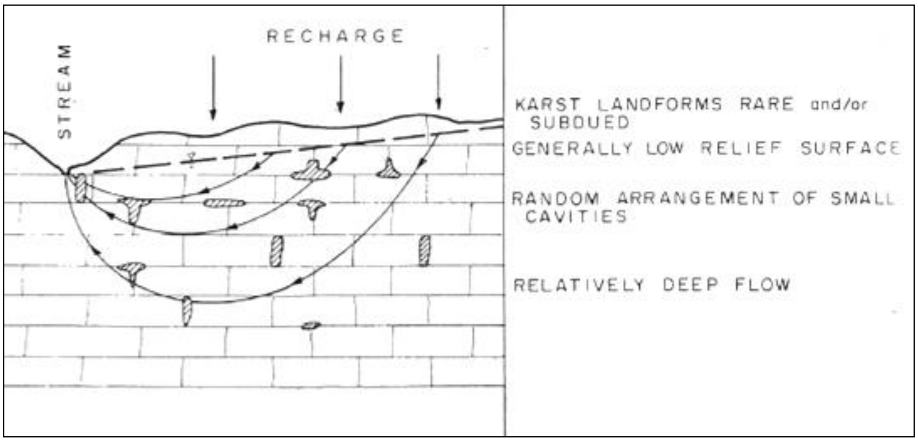

Fig. 2.1/1– Schematic diagram of a diffuse flow carbonate aquifer (White, 1969).

- *Free flowing* carbonate aquifers have well-developed subsurface drainage systems similar in pattern to surface drainage systems. In this type aquifer, groundwater flow paths have been enlarged by solutioning into a well-integrated conduit system (Fig. 2.1/2). Flow velocities in free flowing carbonate aquifers can reach tenths of meters/second and are often in the turbulent regime while the surrounding rocks have low porosity and permeability. Groundwater outflows in huge basal springs, with high discharge. Inputs to the subsurface may be from sinking surface streams, as well as flow from sinkholes and general infiltration. Among free flowing aquifers, it is possibile to distinguish "perched aquifers" (Fig. 2.1/2), with impermeable rocks over the base level and "deep aquifers" with karst system extended below the base level (Fig. 2.1/3);

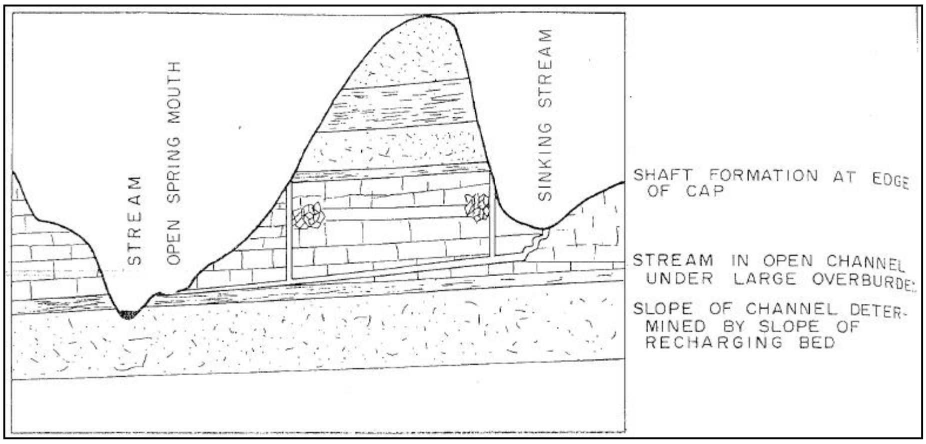

Fig. 2.1/2 – Schematic diagram of a free flow aquifer with both capping and perching beds (White, 1969).

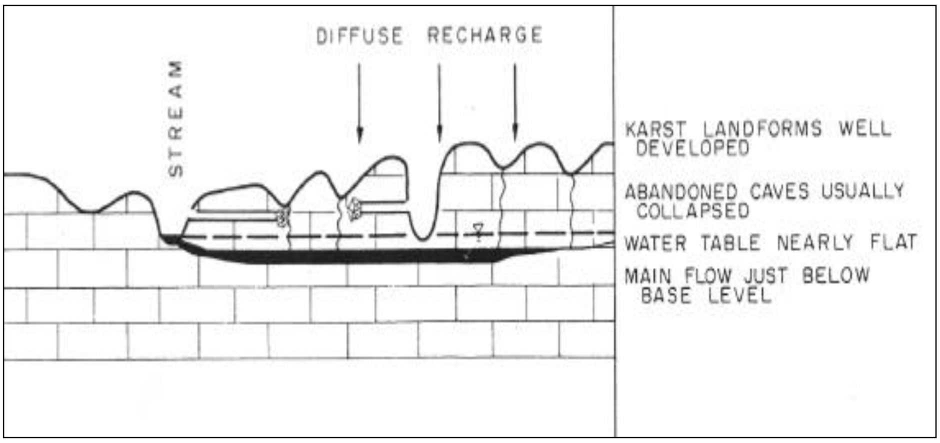

Fig. 2.1/3 – Schematic diagram of a maturely karst free flow aquifer (White, 1969).

- *Confined flow* aquifers are characterized by slow flow under artesian environments (Fig. 2.1/4) or in thin beds sandwiched between impervious rocks (Fig. 2.1/5). Confined flow carbonate aquifers possess network cave patterns because of a lack of concentrated recharge, which is inhibited by overlying rocks of low permeability. Hence, solutioning takes place along any available joint and generates a dense cave network.

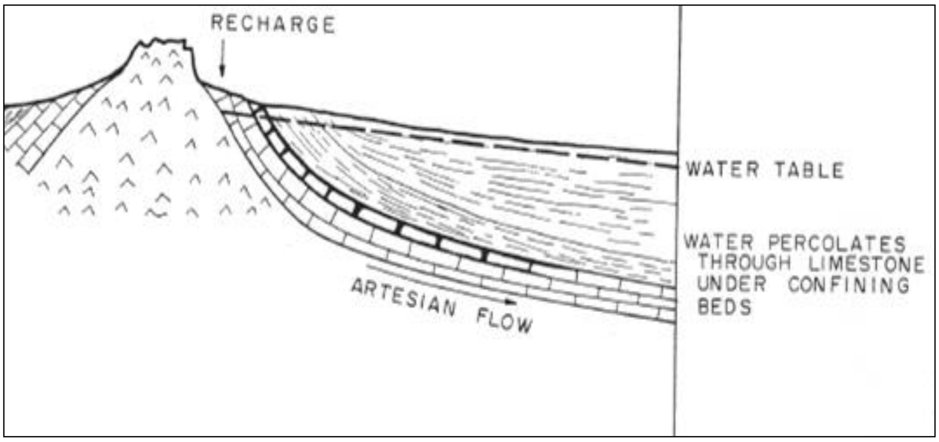

Fig. 2.1/4 – Schematic diagram of an artesian carbonate aquifer system (White, 1969).

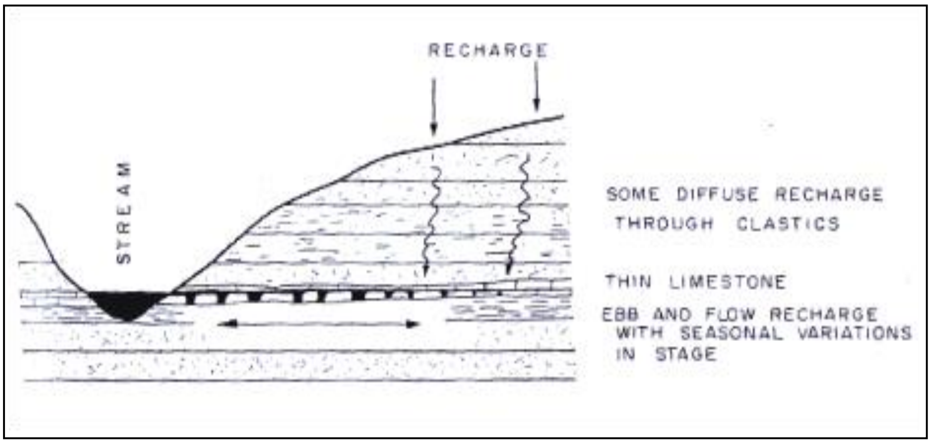

Fig. 2.1/5 – Schematic diagram of a sandwich type carbonate aquifer system (White, 1969).

In 1975 was published by Mangin (1975) one of the most important study in karst modeling (Fig. 2.1/6). He inferred structural information of the system such as storage, memory effect, degree of karstification, type of infiltration from the analysis of springs hydrographs. The particularity of Mangin's model is that the storage occurs in the "annex-to-drain system", i.e. a conduit system which transmit infiltration water towards karst springs.

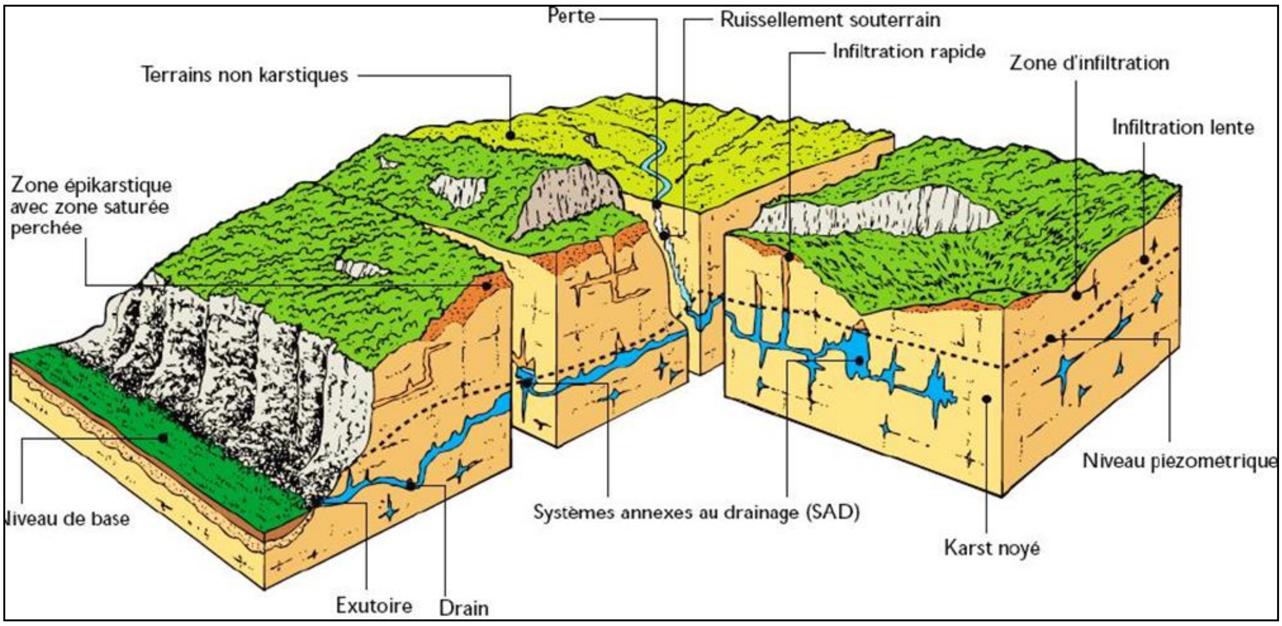

Fig. 2.1/6 – Schematic model of a karst system (Mangin, 1975).

Mangin (1974) was the first one to introduce the concept of "epikarst": a shallow, high permeability karstified zone just below the soil, able to storage part of the infiltration water and create a perched aquifer (Fig. 2.1/7). After Mangin (1974), the epikarst has been considered a fundamental part of the karst aquifer and ecosystem.

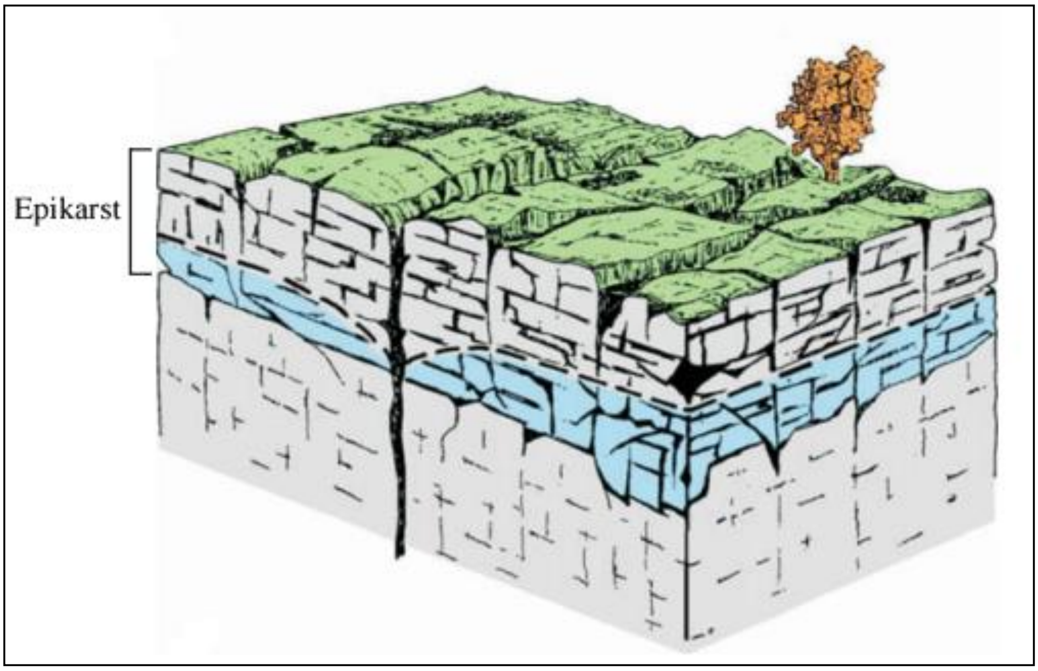

Fig. 2.1/7 – Schematic model of the epikarst system (Mangin, 1974).

Williams (1983; 1985) provided more experimental evidence for the existence of the epikarst, also referred to as the subcutaneous zone. The epikarst may be visualized as a horizon of a few meters thickness with high porosity and high permeability as a result of enhanced dissolutional activity near the land surface due to large supply of CO_2. During the evolution of the epikarst, a major volume of water inflows through fractures in the vadose zone. The enlargement of the fracture leads to the development of sinkholes, which concentrate the recharge (Fig. 2.1/8). The base of the epikarstic zone may be formed by reduced fracture frequency, a capillary barrier in the narrowing fissures or by clay residues from the dissolution process blocking the fissures. A perched temporary water table defines the upper surface, which slopes toward areas of rapid vertical percolation. The storage capacity depends on the balance between volume of water inflow and outflow; the latter is a function of the hydraulic conductivity of the underlying transmission zone.

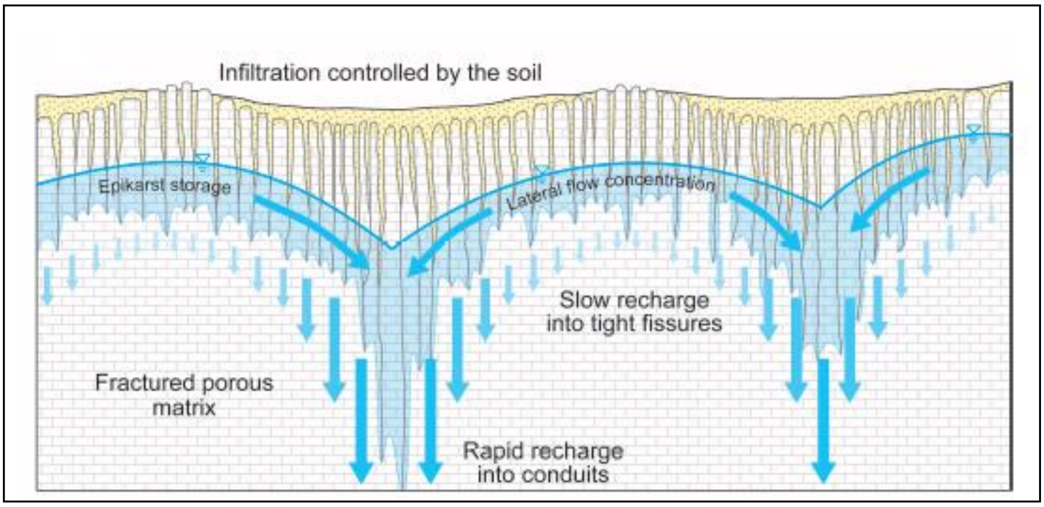

Fig. 2.1/8 - Water stored in the subcutaneous zone constitutes an epikarstic aquifer that is perched above a leaky capillary barrier. Dolines gain topographic expression because of the focusing of flow and dissolution down major leakage paths (Williams 1983; modified in Hartmann et alii, 2012).

It is evident, therefore, that the epikarst is under-drained. Solution dolines are a topographic manifestation of the focusing of flow and dissolution associated with this process (Williams 1985), and they penetrate most of the thickness of the epikarst (Fig. 2.1/9).

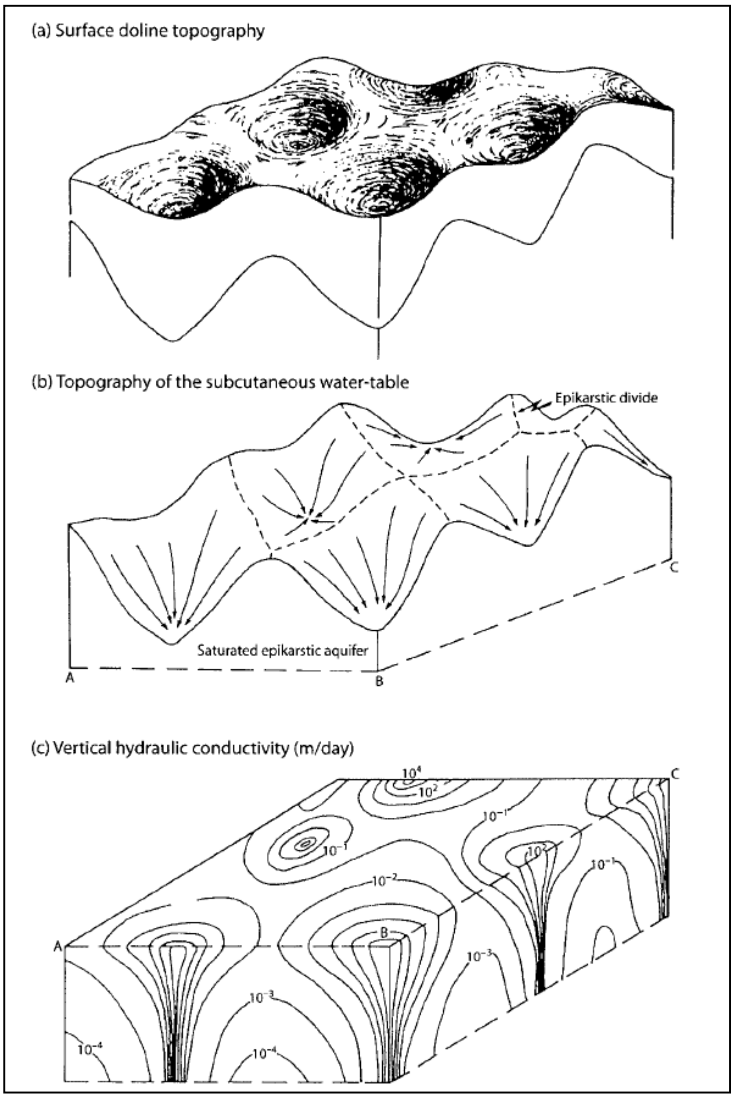

Fig. 2.1/9- (a) Solution dolines are a topographic expression of sites of centripetal drainage through the epikarst. (b) Beneath the surface the subcutaneous water table marks the upper surface of the epikarst aquifer and is drawn down over the main leakage paths developed down major joints. (c) Drainage of the epikarst is focused by zones of high hydraulic conductivity. These sites are the headwaters of autogenic cave streams (Williams, 1985).

The epikarst strongly influences the distribution and the temporal delay of groundwater recharge. Gunn (1981) distinguished six components in flow from dolines, some of them exhibiting large time lags and thus pointing to significant near-surface storage (Gunn, 1983). Williams in 1993 stated that the rising volume of water within the epikarst aquifer during storm (or snowmelt) events increases hydraulic head and so produces a pressure pulse that stimulates a transfer of water. This *pulse-trough* effect is different from the *flow-through* of Bakalowicz (1995) consisting in the slow transit of water from the epikarst to the vadose zone. The same author in 1974, from the interpretation of isotopic and geochemical analysis, asserted that the recharge is partially delayed by a first storage near the surface.

The first author to give a complete and accepted definition of epikarst was Klimchouk (1997). He defined epikarst as the uppermost zone of exposed karstified rocks, in which permeability due to fissuring and diffuse karstification is substantially greater, as compared to the underlying main vadose zone. He also summarized the considerations made from other authors (Mangin, 1975; Gunn, 1981; Williams, 1985; Klimchouk 2000, among others) on epikarst:

- Vertical hydraulic conductivity is high and almost homogeneous at the land surface;
- Hydraulic conductivity decreases with the depth because of the diminishing joints and fractures density;
- Infiltration in the top of the epikarst zone is much easier than drainage out of it; this causes that retention of percolation and storage of groundwater occurs in the epikarst zone;
- Infiltration water is stored in the epikarst (because of the different hydraulic conductivity with depth) and percolates slowly to the vadose zone;
- Water in the epikarst flows laterally towards the vertical fractures or joints.

Thanks to its storage capacity, the epikarst helps to maintain a base flow in the swallow holes and in the basal aquifer during dry periods. Moreover, an important function of the epikarst is to direct the flow from the surface to the depth like a funnel; for this reason, the effect is called "*funneling effect*".

Kiraly (1998), analyzing the spring hydrographs, hypothesized the existence of the epikarst to justify the peaks of the hydrographs. In fact, without concentration of the diffuse infiltration, the hydrograph should be too flat with respect to the reality.
An important consequence of the existence of an epikarst layer, as modelled by Kiraly (1998), is the "Faraday cage" effect (Fig. 2.1/10). In concentrating infiltration, epikarst limits greatly the recharge of the low permeability volumes by diffuse infiltration through the unsaturated zone. In a deep phreatic zone karst configuration, the low permeability volumes can still be recharged by inversion of gradients during flood events, but in the case of shallow karst configuration, the recharge of low permeability volume can be non-existent.

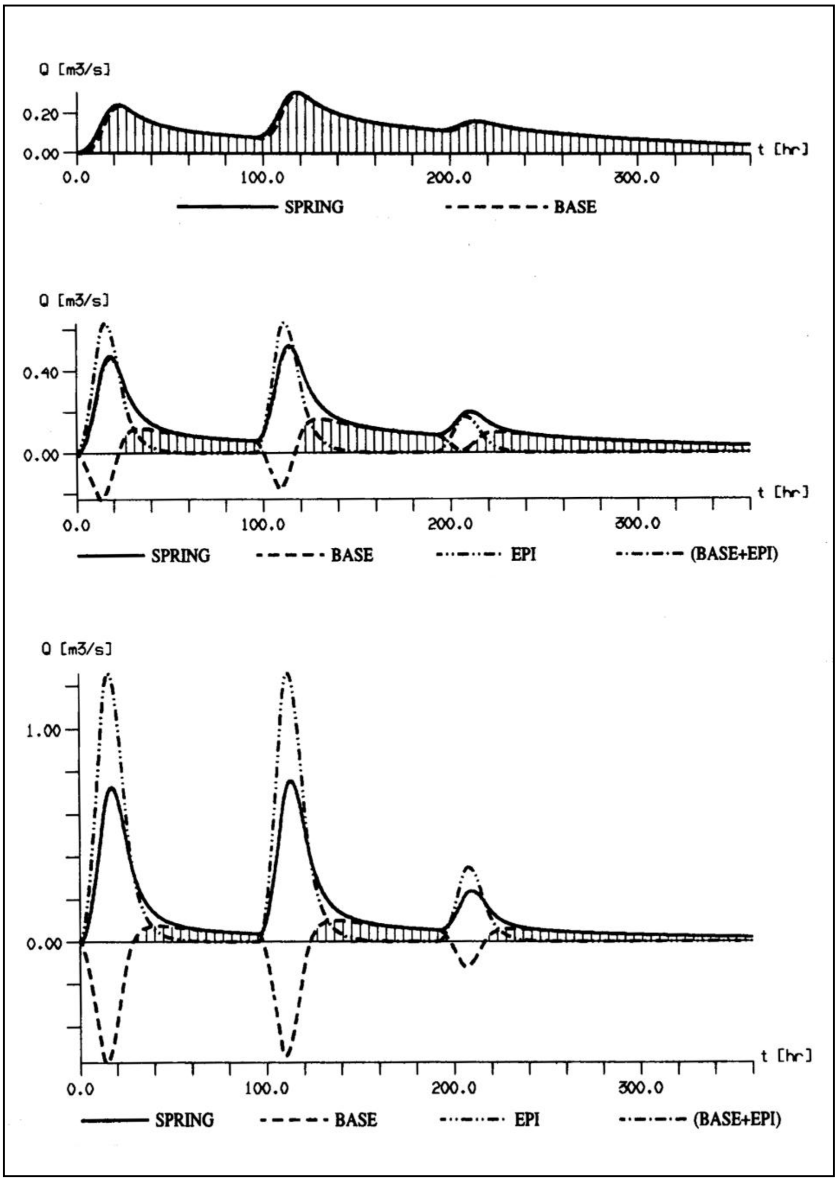

Fig. 2.1/10 - Simulations of karst spring hydrographs. There is no epikarst in the upper graph; epikarst concentrates 50 % of infiltration in the middle graph and 100 % in the lower graph (Kiraly, 1998). Hydrographs are separated in springflow, baseflow, and epiflow (rapid concentrated infiltration).

Klimchouk (2000) considered that part of the spring base flow origins from the water stored in the epikarst and canalized in conduits, because of the “funneling effect” (Fig. 2.1/11). The epikarst has an average depth between 3 and 15 m with a high variability depending on lithology and geomorphology and a hydraulic conductivity three order of magnitude more than that of the vadose zone. According to Kiraly (2002), more than 50% of the infiltration comes from concentrated flow from the epikarst. He also considered, in opposition to Bakalowicz (2004), the dolines part of the epikarst because they are the results of the hydrologic processes occurring in a certain phase of the epikarst evolution (Fig. 2.1/12).

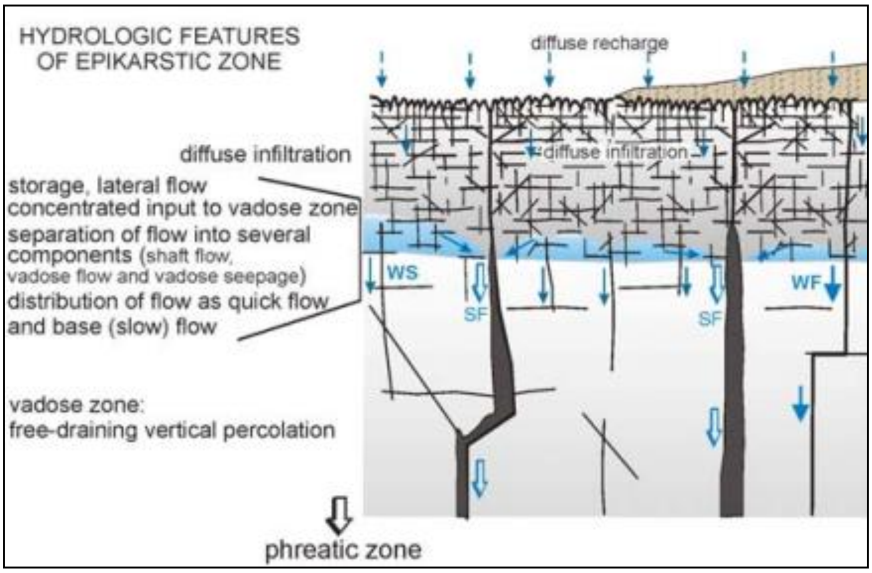

Fig. 2.1/11 – Hydrologic features of epikarst zone (Klimchouk, 2000)

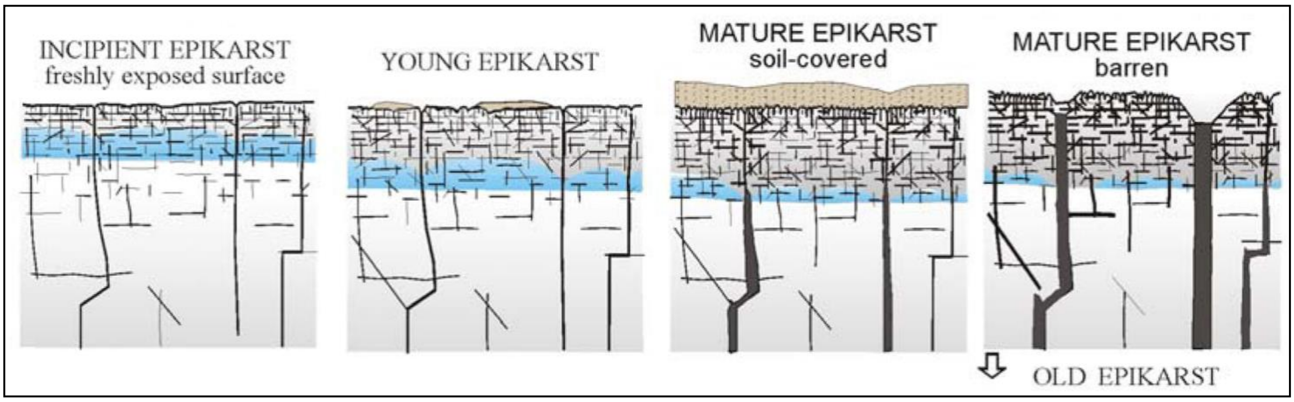

Fig. 2.1/12 – Evolution of the epikarst (Klimchouk, 2000).

Coming back the karst model, Drogue (1971) proposed a structural approach in which the author assumes that the phreatic zone is hydraulically continuous, with a relatively low permeability. Consequently, the karst aquifer may be considered as a two-continuum medium, a saturated matrix porosity drained by conduits. The same model was used by Kiraly (1988) to simulate karst spring hydrographs. The main limitation of the model is that is necessary a deep knowledge of the geometry of the aquifer.

Kiraly (1975), accordingly with Rhodes and Sinacori (1941), Swinnerton (1949), LeGrand and Stringfield (1966), Mandel (1966) and Bedinger (1966), represents graphically the development of karst (Fig. 2.1/13). Dissolution begins in a fractured (no karstified) rock and increases with the flow. The competition for drainage between high conductivity zones leads to the capture of the branches, developed slower, and contributes to the unification of the system of karstic channels. The karst springs, thus, decrease in number, but become more important with regard to the volumes.

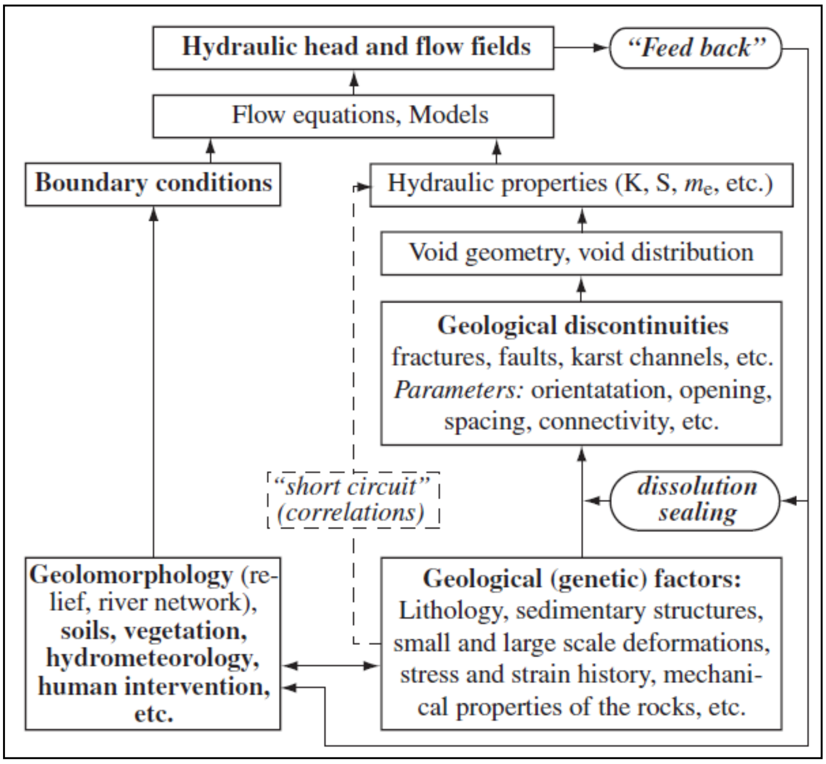

Fig. 2.1/13 – Schematic representation of the relation between groundwater flow, hydraulic properties and geological factors (Kiraly, 1975).

Atkinson (1977) and Gunn (1985) classified the flow in two categories: a diffuse flow, laminar flow in small size karst fractures and turbulent flow, a fast flow in conduits or fractures (> 10 mm diameter).

Gunn (1985) distinguished four recharge types (Fig. 2.1/14):

- diffuse autogenic recharge from precipitations;
- concentrated autogenic recharge
- diffuse allogenic recharge from stream-sink;
- concentrate allogenic recharge feeding important conduits.

Moreover he recognized four storage zones:

- soil and surficial deposits;
- epikarst;
- phreatic karst conduits and fractures (>10 mm);
- saturated matrix rock.

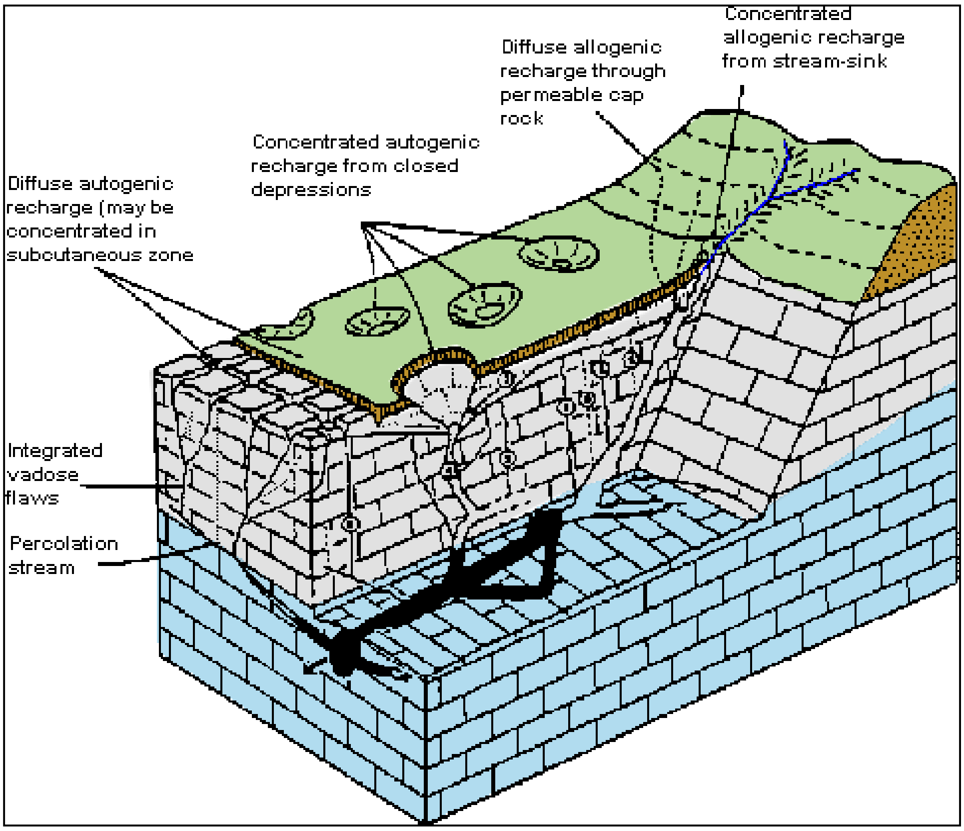

Fig. 2.1/14– Schematic representation of the recharge types in a karst system (Gunn, 1985)

In a "mature" aquifer, the heterogeneity may be schematized by a high permeability channel network "immersed" in a low permeability fractured limestone volume well connected to a local discharge area (Kiraly, 1998). A direct consequence of this structure is the *duality* of karst:

- Infiltration process: diffuse, slow infiltration in matrix and concentrated and rapid in conduits (Fig. 2.1/15);
- Groundwater flow field: low velocity in the matrix and high velocity in the karst conduits (Fig. 2.1/16);
- Discharge condition: low and constant discharge during dry periods when matrix flow is dominating and high and variable flow during the wet seasons when flow in conduits is dominant (Fig. 2.1/16).

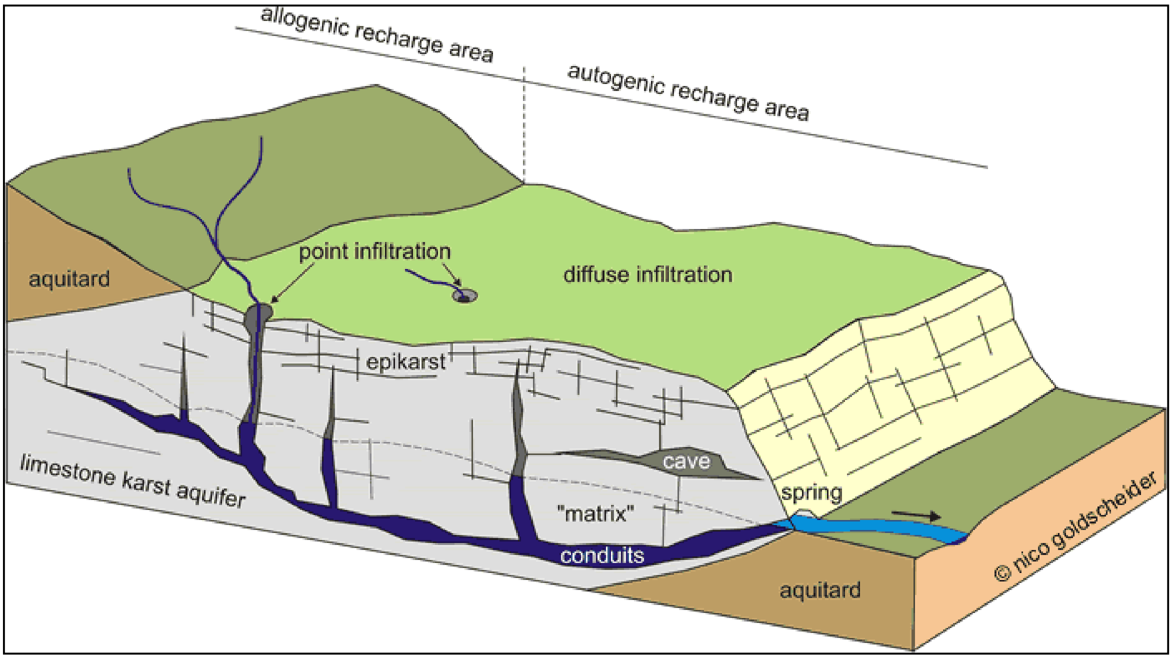

Fig. 2.1/15 – Block diagram illustrating the hydrogeological functioning of a karst aquifer (from Goldscheider & Drew 2007).

Bonacci (1993) connected the type of flow with the spring hydrograph. In particular, for a fast flow the hydrograph shows a peak and a fast decline with a small value of base flow; for a diffuse flow, the peak is shorter and there is a delay from rainfall to discharge; in a combined system (diffuse and fast) there is an intermediate situation (Fig. 2.1/16).

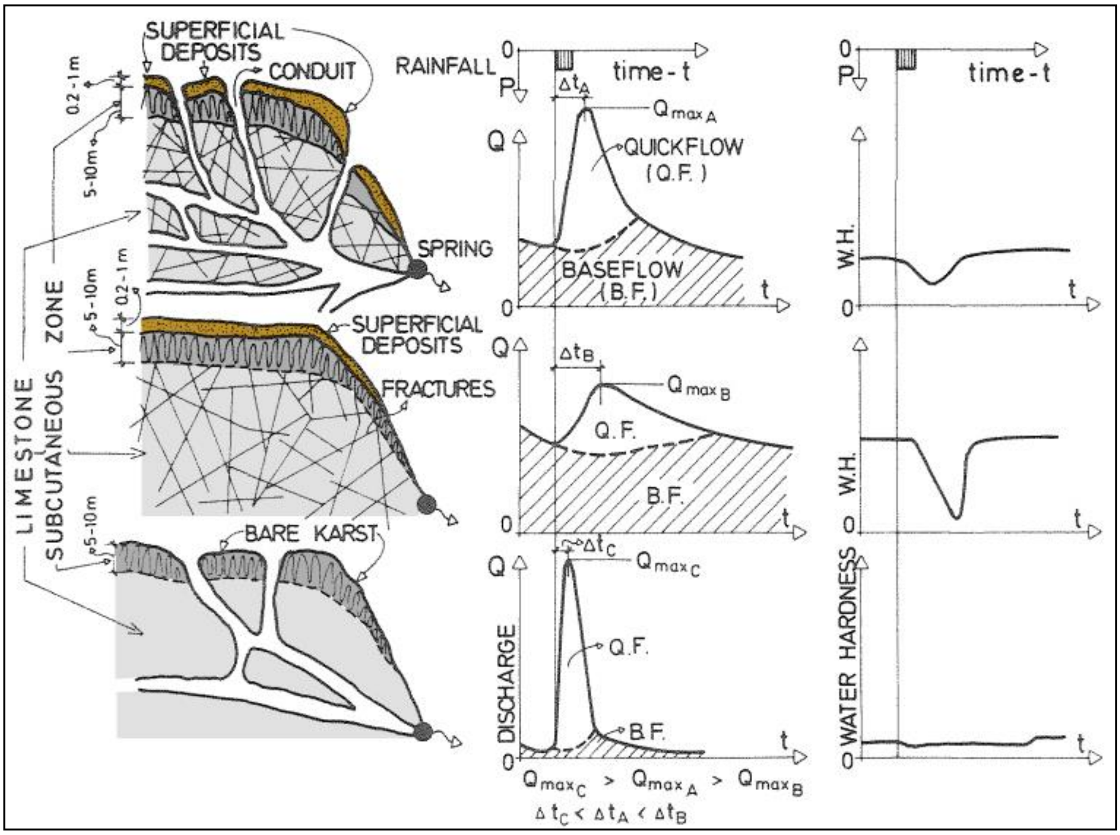

Fig. 2.1/16– Different spring hydrographs and water hardness graphs related to different karst system flow. The upper case is a combined flow system; the middle is diffuse flow system; the lower in conduit flow system (Bonacci, 1993).

Bakalowicz (2003) summarized the proposed models for the phreatic zone:

- According to Drogue (1974), Mudry (1990) and Kiraly (1997) water is stored in the matrix. i.e. primary and secondary rock porosity.
- According to Mangin (1994), groundwater is stored in karstic voids developing around the conduits and connected to them by high water head loss zones; the phreatic zone should be hydraulically discontinuous.
- Groundwater storage in the phreatic zone does not exist. The karst network drains groundwater from the vadose zone. The particularly high heterogeneity in the infiltration zone may act as a buffer delaying most of the recharge (Lastennet et alii, 1995).

Bakalowicz (2003) also described the various types of recharge and functions in the vadose and phreatic zones of a karst system (Fig. 2.1/17).

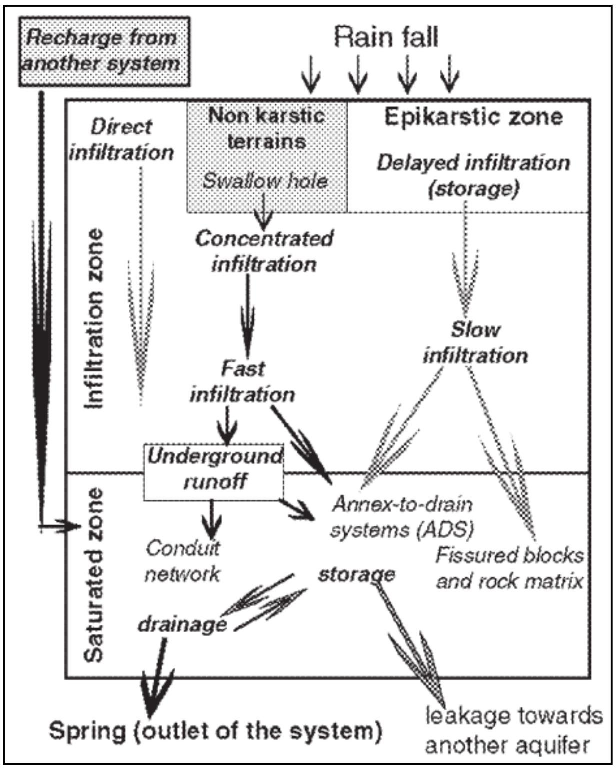

Fig. 2.1/17- General conceptual model describing the various types of recharge and functions in the vadose and phreatic zones of a karst system (Bakalowicz 2003).

Perrin (2003) proposed a model with a “waterfall system”: soil, epikarst, unsaturated zone and phreatic zone. He identified three types of karst systems with comparable soil and epikarst zones and different phreatic zones: deep phreatic karst system, shallow karst system and allogenic karst system (Fig. 2.1/18).

During flood events, fresh water should recharge the Low Permeability Volumes (LPV) because of the hydraulic gradient inversion between conduits and LPV. This inversion will stop the contribution of phreatic storage to spring discharge (Kiraly, 1998). This can be true for models 1 and 2. Hence groundwater participating to flood events is mainly issued from the reservoirs of the unsaturated zone. Under steady-state conditions, models of type 1 (deep phreatic systems) assume an important role to the storage in the phreatic zone. This storage is in the

LPV (Drogue, 1971; Kiraly, 1975), or in annex-to drains systems (ADS, Mangin, 1975). These models are based on observations at the spring and in piezometers. However the actual contribution of phreatic storage to spring flow was never clearly demonstrated.
In addition, the study of tracers leads to a conceptual model of flow storage with five phases. In the phase 0, in steady-state condition, the system is fed by water stored in the epikarst. Discharge and chemistry are stable. In phase 1, after a rainfall, the soil water is pushed down and feeds the system. There is a response in discharge but not in chemistry. During phase 2, if the rain continues, soil water bypasses the epikarst reaching directly karst conduits; soil water has some differences in chemistry, being unsaturated with respect to calcite. If rain continues, (phase 3), freshwater reaches directly conduits system. In this situation, stable isotope values will change, because isotopic concentration in rainfall is different from values in soil and epikarst. Phase 4 is the recession period after the event.

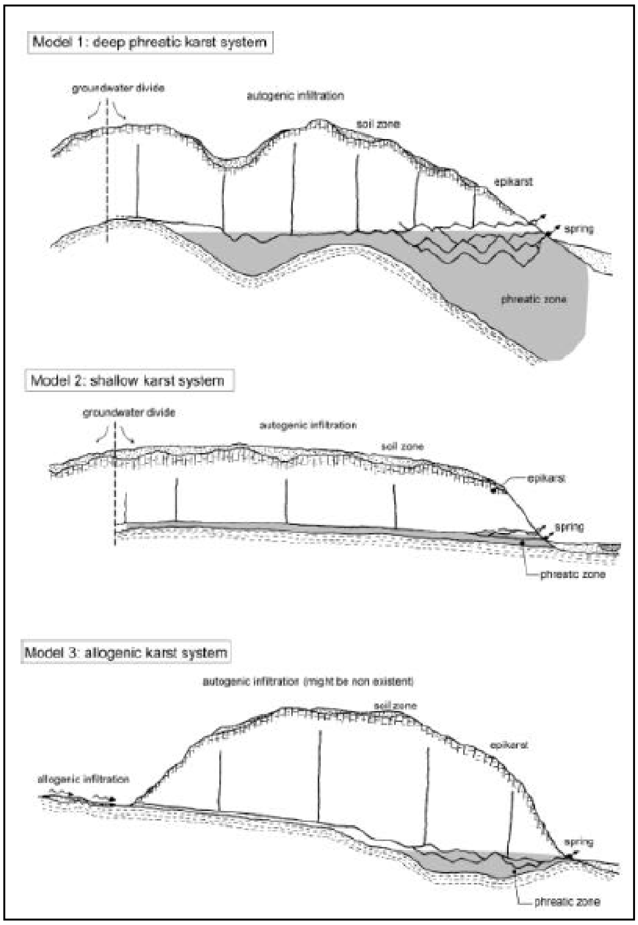

Fig. 2.1/18- Three main geometrical models of karst systems discharging at springs (Perrin, 2003)

Trček (2006) proposed a model based on three hydrogeologic zones (Fig. 2.1/19):

1) Upper vadose (unsaturated) zone:
- Soil moisture storage;
- Epikarst storage.
2) Lower vadose (unsaturated) zone:
- Diffuse vadose storage;
- Vadose conduit storage.

3) Phreatic (saturated) zone
- Phreatic conduit storage
- Diffuse phreatic storage

The recharge depends on the hydraulic behavior of the epikarst. In response to a pluviometric event, the water is stored at the bottom of the epikarst: if it is a small volume, water percolates slowly in the small fractures; conversely, if it is a big volume, there is formation of the epiflow (flow in conduit or large fractures) and, after, a diffuse recharge process.

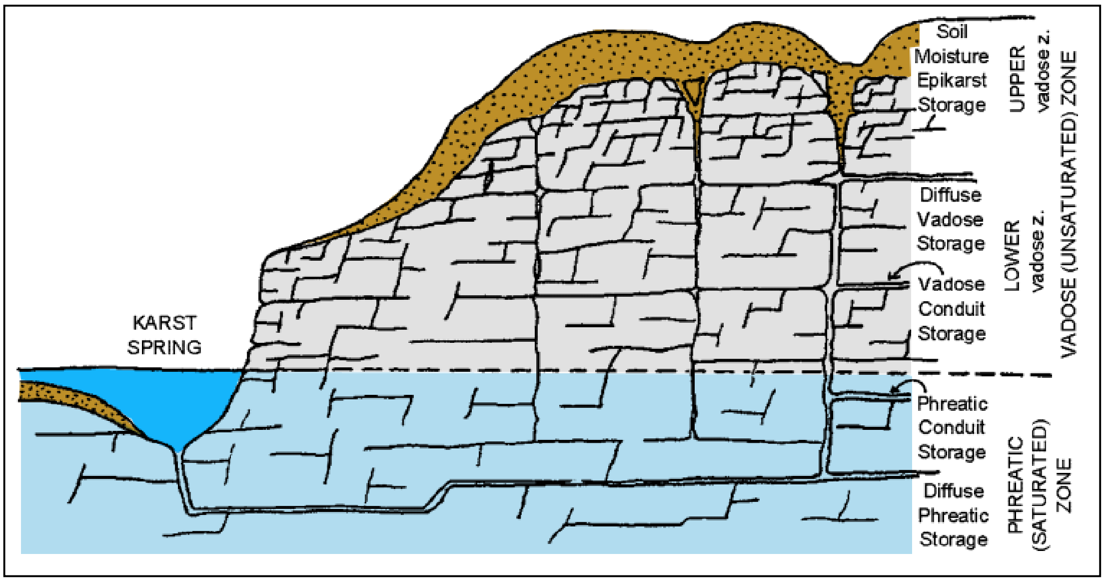

Fig. 2.1/19 – Conceptual model of karst aquifer (Trček e Krothe, 2002).

Ebrahimi (2007) stated that in a karst aquifer, the main volume of water is stored in the matrix but the main volume flows in the conduits. He studied the recession curves applying the approaches of Mangin (1975), Coutagne (1968) and Maillet (1905). According to Bonacci (1993), in a "mature" karst aquifer, with well-interconnected conduits, the response of the springs is immediate; conversely, the response is slow when diffuse recharge prevails.

2.2 Hydrogeological features of Italian karst aquifers

In Italy, only in recent decades, hydrogeologists, hydrologists and speleologists have focused their studies and works on karst aquifers for enhancing the protection, usability and exploitation of water resources. This time discrepancy between the national and European literature manifests itself in a lack of depth studies on karst aquifers Italian and, therefore, in a limited development of theories designed to describe their possible function and the identification of possible groundwater flow models.

2.2.1 Alpine karst aquifers

Civita et alii (1991), with regard to alpine karst landscape of the northern Italy, classified the karst aquifers, depending on the response to rainfall events, in three types:

- Dominant conduit system;
- Interconnected conduits system;
- Dispersed circulation system.

The same classification was adopted also by Vigna (2007). The dominant conduit system carbonate aquifers (Fig. 2.2/1) have a high degree of karstification and a lack of the saturated zone; infiltration water mixes very slightly with resident water and arrives rapidly to the discharge with a hourly response time. The hydrographs shows narrow peaks.

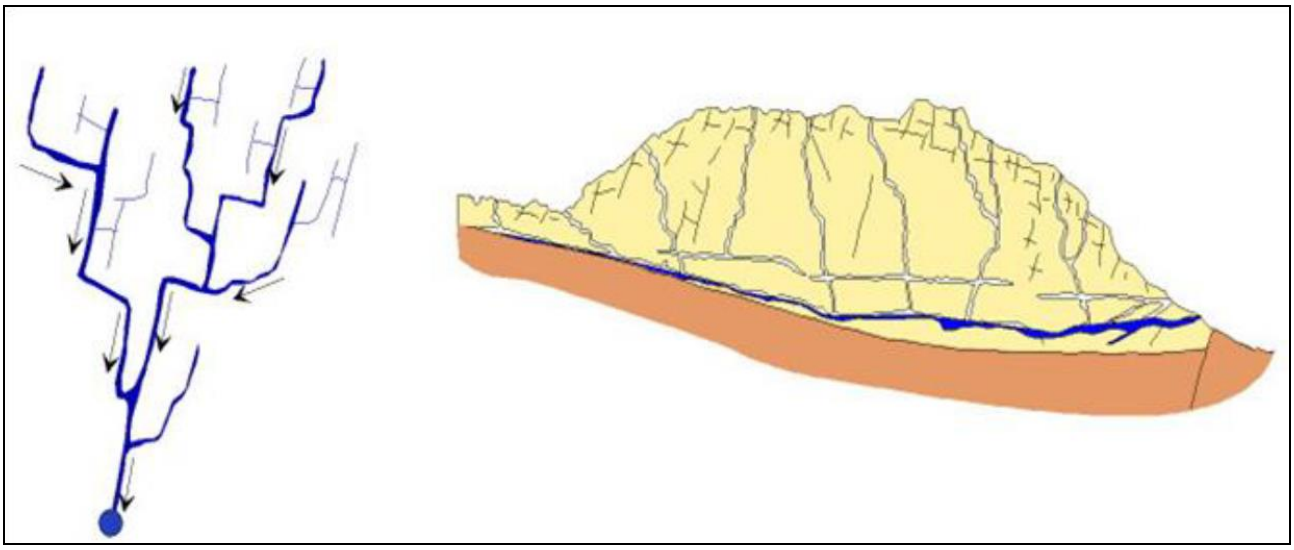

Fig. 2.2/1– Plan and section of a dominant conduit system (Vigna, 2007)

The carbonate aquifers with interconnected conduit systems (Fig. 2.2/2) generally have a medium degree of karstification and are characterized by the presence of phreatic conduits. A saturated zone is present at a depth close to the springs level. During rainfall events, the conduits cannot transfer the whole volume of incoming water, causing a water level rise and high hydraulic pressure in fractures and phreatic conduits. The response, called "piston flow (Vigna, 2002; Galleani et alii, 2011), generates a rise of the water level, electric conductivity and temperature at the springs because of the interactions with resident water.

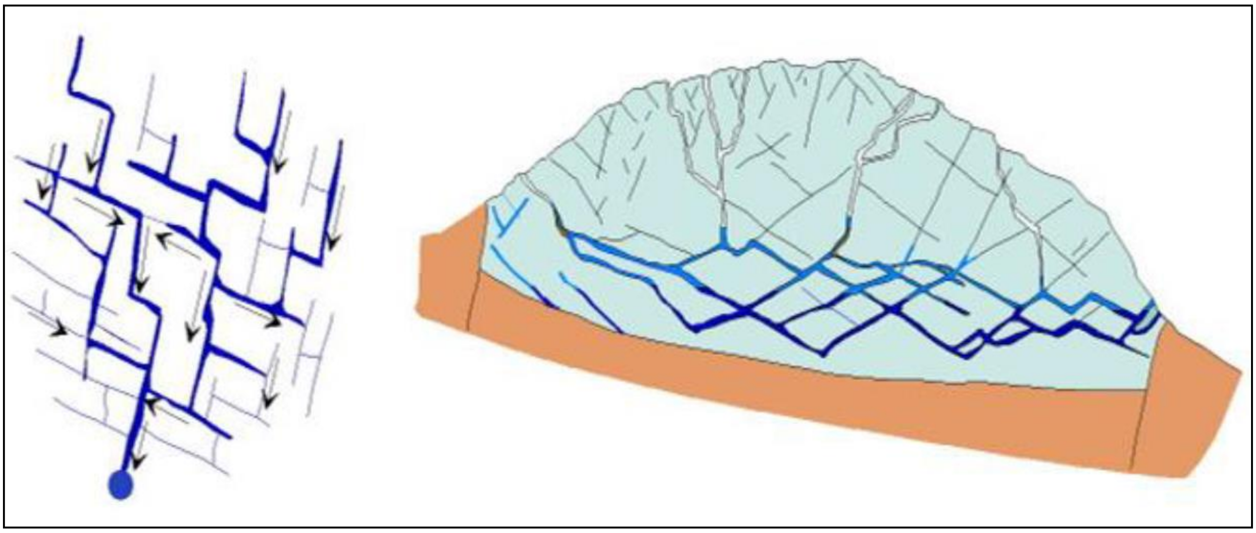

Fig. 2.2/2 - Plan and section of an interconnected conduit system (Vigna, 2007)

In highly fractured carbonate aquifers, with a dense network of joints and fractures, is typical the dispersed circulation systems (Fig. 2.2/3). It is characterized by a lack of preferential pathways and a homogeneous flow system. The permeability is lower because of the small size of the fractures and, consequently, flow velocities are low. The infiltration water, in contact with rocks, does not change its physical and chemical composition because of the high quantity of dissolved salt. This response is called “homogenization” (Vigna, 2002; Galleani et alii, 2011).

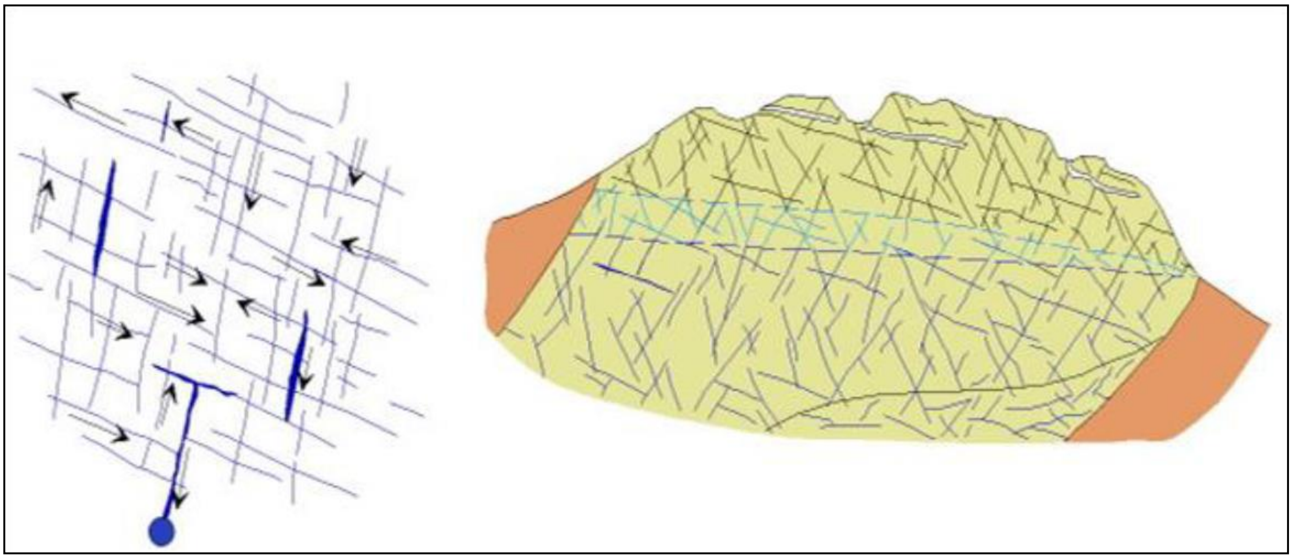

Fig. 2.2/3- Plan and section of a dispersed circulation system (Vigna, 2007)

2.2.2 Southern Apennines karst aquifers

About 8560 km^2 of the territory of the southern Italy (Fig. 2.2/4) consists of carbonate aquifers, fractured and karstified. These carbonate karst aquifers are mainly characterized by Triassic-Liassic dolomites and calcareous-dolomitic rocks, and Jurassic limestones of the Mesozoic carbonate platform Campania-Lucania (Apennine carbonate platform) of southern Apennines.

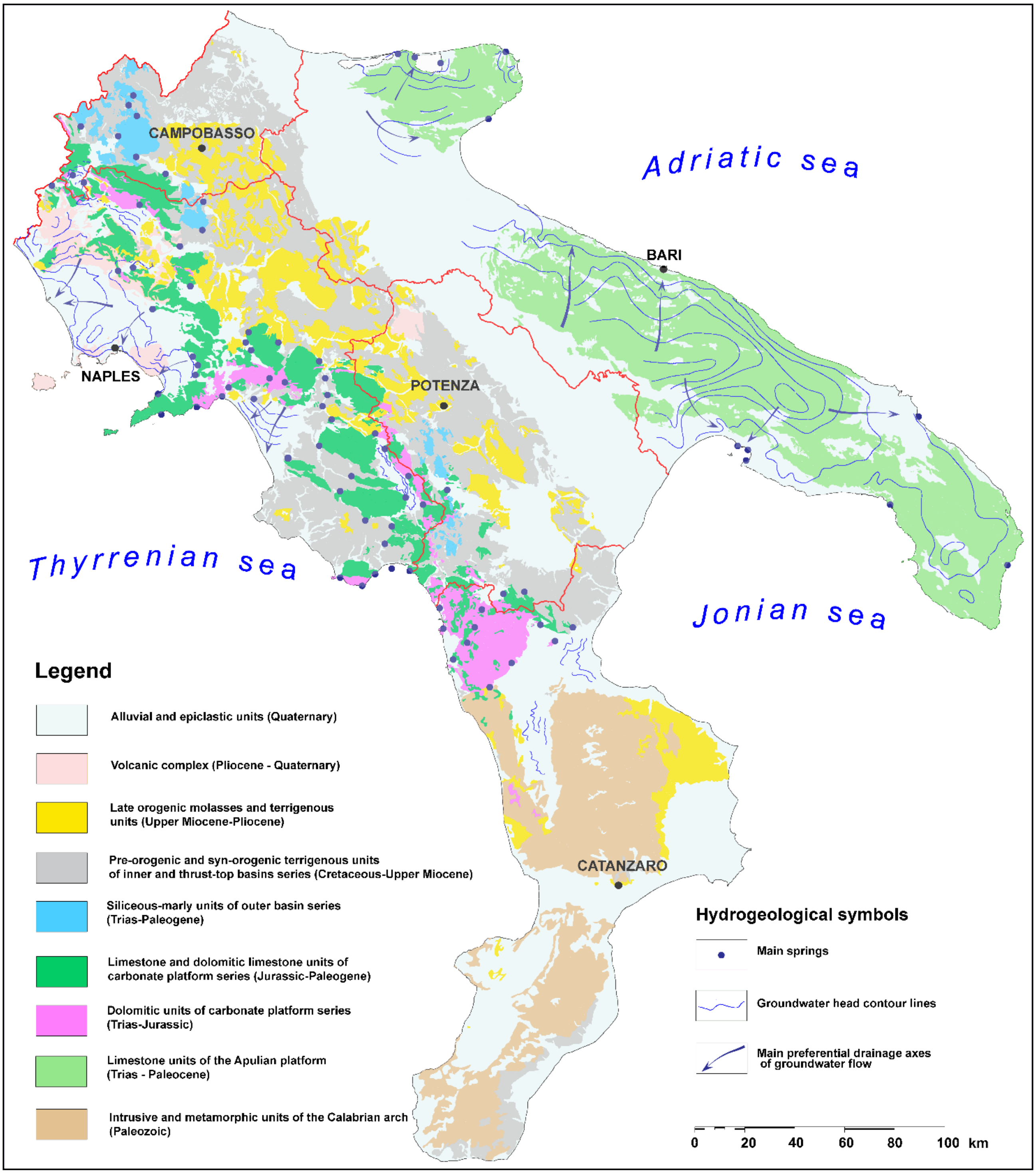

Fig. 2.2/4– Hydrogeological map of southern Italy (Allocca et alii, 2007).

Unlike other European karst aquifers, the karst aquifers of the southern Apennines are characterized by Mediterranean-type climate and covered by pyroclastic soils.

The groundwater of these carbonate karst aquifers represent the main source of water for the populations of the southern Italy and a strategic resource for the socio-economic and environmental development.

Celico (1978; 1983a; 1986) proposed one of the first conceptual models to describe the main hydrogeological features of karst aquifers of southern Apennines.

This conceptual model, also summarized in Celico et alii (2001) and Allocca et alii (2007), has been validated experimentally by means of: i) aquifers water balance and estimation of the groundwater's outflows, through systematic monitoring of the basal springs and streams discharges; ii) hydrochemical and isotopic surveys of groundwater and springs; iii) analysis of karst discharge springs hydrographs; iv) thermal infrared surveys in submarine springs and coastal karst aquifers; v) geophysical surveys and geotechnical investigations; vi) pumping tests, tracer tests and Lugeon tests in field sites and in experimental sites.

The key hydrogeological aspects of the conceptual model proposed (Celico, 1978; 1983a; 1986; Celico et alii, 2001; Allocca et alii, 2007), that make it different from other conceptual models found in the literature (White, 1969; Mangin, 1975; Kiraly, 1975; Drouge, 1992; Bonacci, 1993; Klimchouk, 2000; Civita et alii, 1992), can be listed as follows. Each karst aquifer is a groundwater body (hydrogeological units) well confined by terrigenous deposits with low permeability. The karst aquifers are characterized by a basal groundwater, outflowing in huge basal springs (Q_{mean} up to 5.5 m^3/s), located in the lowest point of the "impermeable boundary" composed by flysch deposits or alluvial sediments (Fig. 2.2/5a and 2.2/5b).

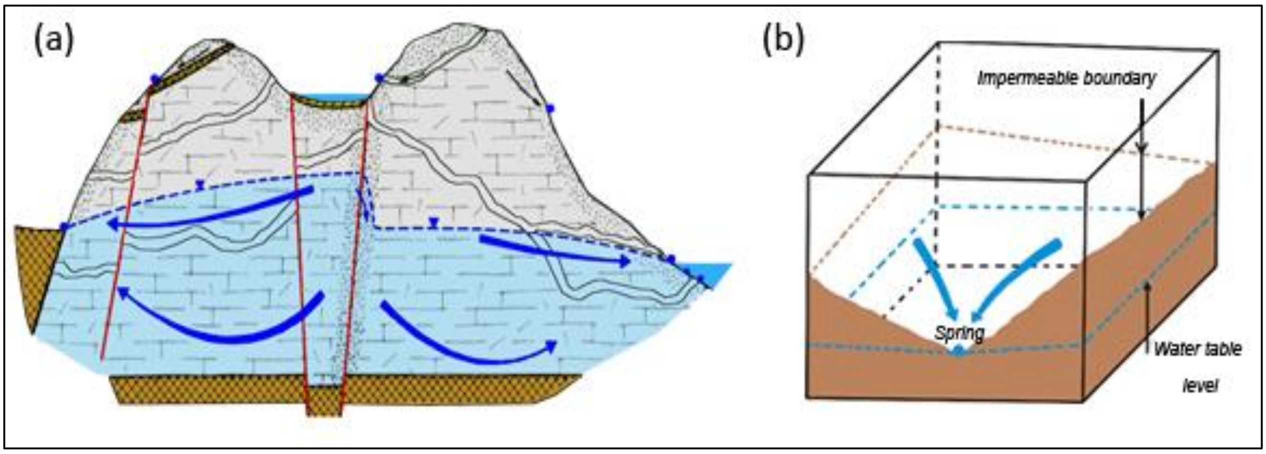

Fig. 2.2/5 – (a) Hydrogeological model of a karst aquifer of southern Apennine; (b) Example of spring location depending on the geometry of the impermeable boundary (Celico, 1986).

The saturated zone of the basal aquifer is separated in a zone with active circulation (over the basal piezometric level) and a zone with slow circulation (deep aquifer). Considering the depth of groundwater flow, it is very difficult to investigate the basal aquifer directly and the only information about can be inferred by the analysis of the spring hydrographs and of the chemical and physical parameters of the water springs.

Perched groundwater flow also occurs in the surficial part of carbonate karst aquifers, where the different thickness and hydraulic characteristics of the karst, as well as stratigraphic-structural factors and/or the presence of karst conduit, can generate high-altitude seasonal/temporary springs, characterized by low flow (Q_{mean} < 0.01 m^3/s).

Petrella et alii (2009) studied the genesis of high-altitude springs in a test area belonging to the Mount Matese karst aquifer using geophysical, hydrogeological, hydrochemical and isotopic investigations. The research demonstrated that the activation of these springs is due to the unusually high level of the groundwater head, that allows the spring to flow (Fig. 2.2/6).

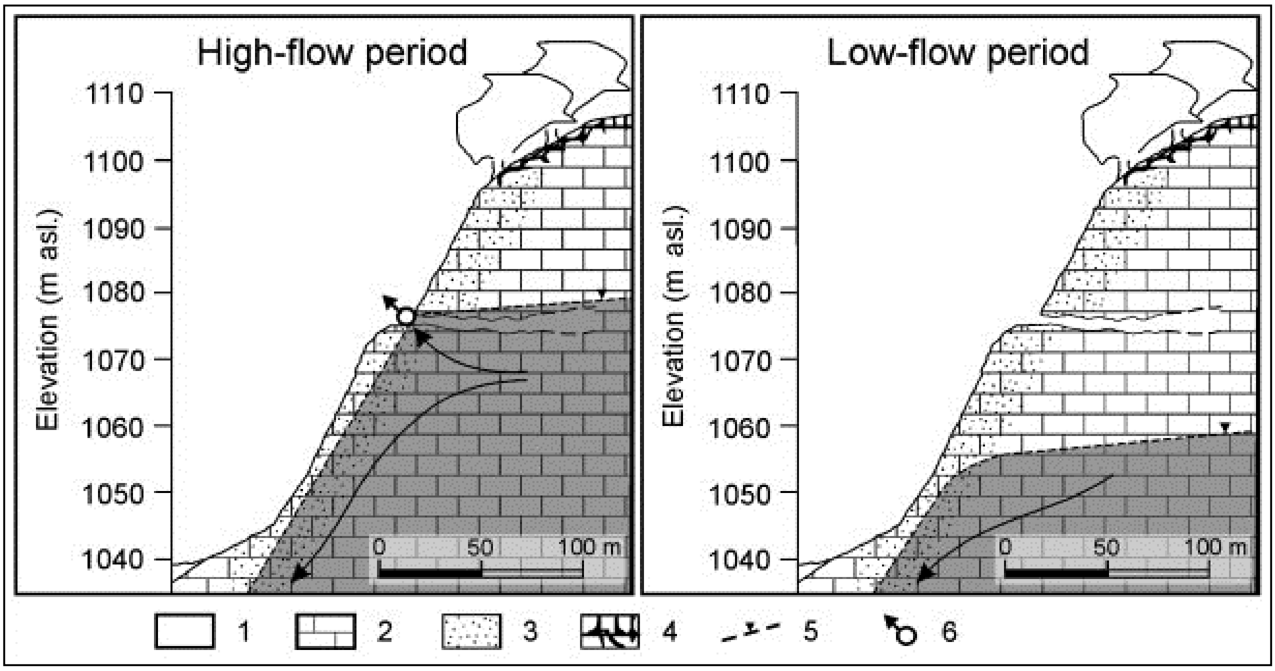

Fig. 2.2/6 – Schematic activation model of the high-altitude temporary spring (1: pyroclastic soil; 2: limestone; 3: cataclastic zone; 4: epikarst; 5: hydraulic head; 6: temporary spring) (Petrella et alii, 2009).

The activation of such a spring also depends on relationships between a low-permeability fault core and a karst system. When the hydraulic head does not reach the karst system, the great and concentrated head loss within the fault core does not allow the spring to flow, because the groundwater entirely flows through the fault zone towards the downgradient (Fig. 2.2/6) (Petrella et alii, 2009).

An important role in groundwater circulation is played by the tectonic structures. Celico et alii (2006) using site-scale investigations demonstrated the existence of fault zones, with a permeability low as that of siliciclastic rocks representing the regional aquitard of the carbonate aquifers, that act as a barriers or low-flow boundaries. These fault zones cause a change in the hydraulic gradient and allow a discrete groundwater flow through and an interdependence between the zones up- and down-gradient the faults. Because of this effect, the aquifer looks like a basins-in-series system. In some cases, along these faults, the groundwater table reaches the ground surface, causing the activation of seasonal springs (Fig. 2.2/7).

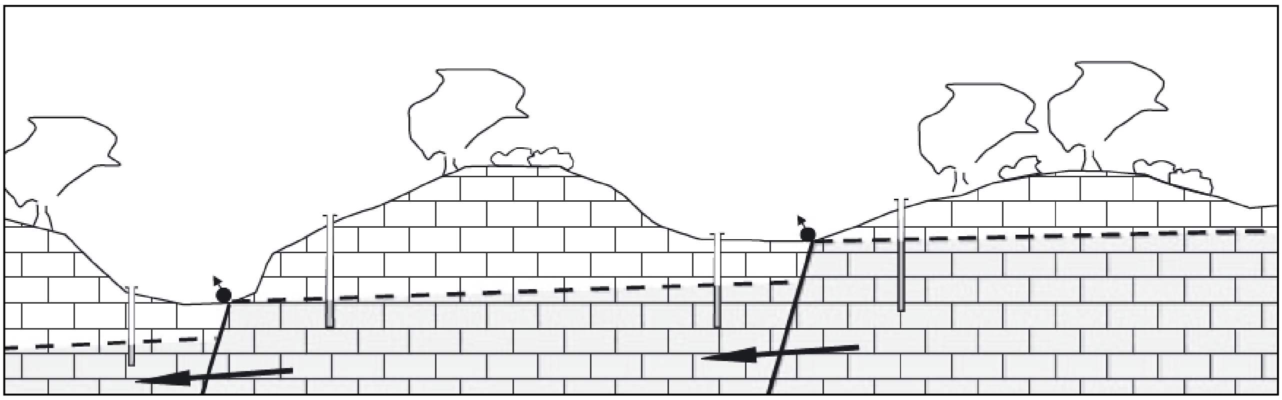

Fig. 2.2/7 – Schematic representation of a basins-in-series aquifer system (the arrows represent the groundwater flow through in fault zones) (Celico et alii, 2006).

Later, Petrella et alii (2014) refine the conceptualization of subsurface flow in faulted carbonate aquifers using a statistical approach to analyze the interaction between two wells located up- and down-gradient of a tectonic structure and the relationship between rainfalls and piezometric levels. The results of this study suggest that low-permeability fault zones influence the configuration of hydraulic head (step-like head profiles with concentrated head losses within the fault cores) and the relationships between sub-basins within the compartmentalized aquifer system. Moreover, the low permeability of different fault core zones can cause delay in groundwater head changes within compartmentalized system and an abrupt change in the hydraulic gradient (Fig. 2.2/8).

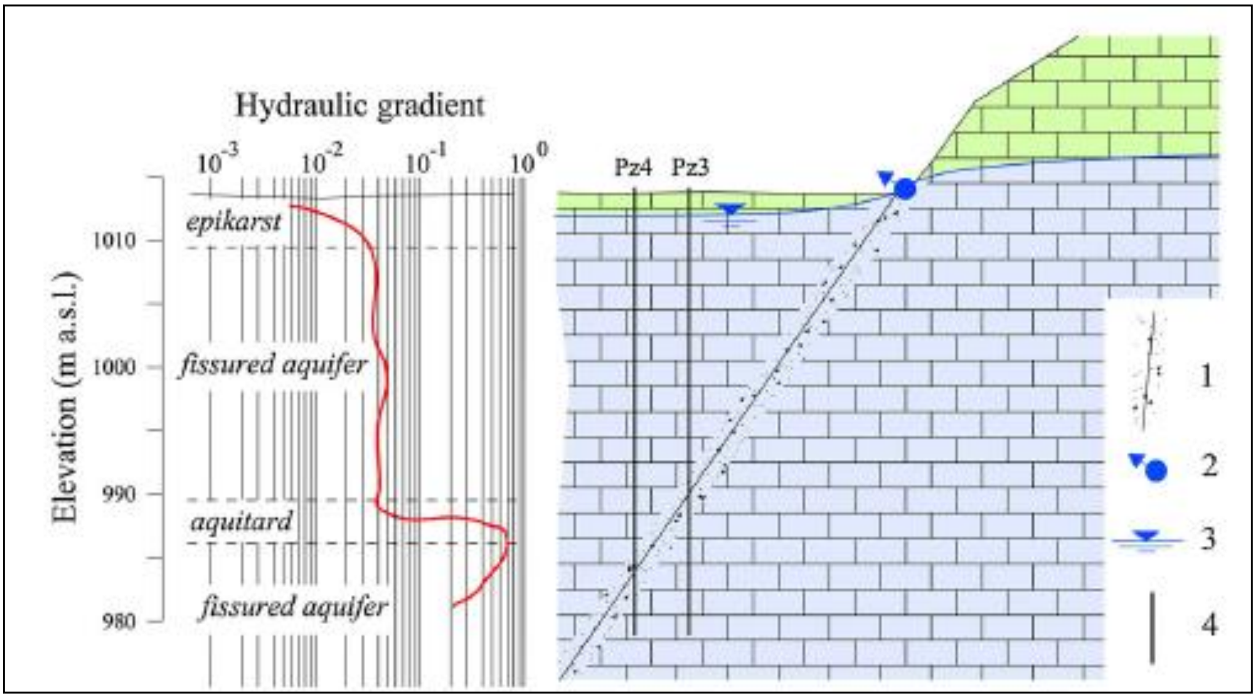

Fig. 2.2/8 – Evolution of the hydraulic gradient between two wells crossing a dipping fault zone (legend: 1-low-permeability fault core; 2-spring; 3-groundwater level; 4-observation well) (Petrella et alii, 2014).

At basin scale, the basal flow is in laminar regime in the fractured medium; therefore, the aquifer system can be considered as an "equivalent porous medium", hence the continuum approach and the Darcy's law can be applied. Turbulent flow is restricted into the karst conduits zones, that, when interconnected with the basal springs, cause strong discharge rise in response with intense rainfall events. The statement is confirmed by the analysis of the hydrographs of the basal springs, which are characterized by short peaks and a delay between rainfall event and spring discharge. The observation of the hydrographs induced to affirm that in these aquifer systems, unlike the majority of the European one, diffuse flow is predominant. Hydrographs with high peaks and fast response were found in high altitude springs due to the short travel time of rainwater and to the different hydraulic characteristics of the epikarst horizons (Petrella et alii, 2007).

The diffuse and basal flow is influenced by the distribution and architecture of fractures and karst channels; this implies that the aquifer systems are particularly heterogeneous and anisotropic, with important consequences for the local productivity of the aquifers, where the karst rocks present low values of transmissivity or specific discharge.

The mean groundwater yield ranges between a maximum of about 0,045 m^3 s^{-1} km^2 and a minimum of 0,015 m^3 s^{-1} km^2. The high productivity of karst aquifers is due to the high permeability of the karst rocks, the presence of large endorheic zones (Manna et alii, 2013a; Allocca et alii, 2014) (Figs. 2.2/9a and 2.2/9b) and the existence of a "pyroclastic soils-vegetation" surface system, acting as a temporary water storage tank and a distribution system for infiltrating rainwater into carbonate substrate (Figs. 2.2/9c; 2.2/9d; 2.2/9e and 2.2/9f). The annual groundwater recharge occurs by diffuse infiltration, through the pyroclastic soils and epikarst, and secondary or concentrated infiltration in endorheic zones, located on the top of the massifs and connected to karst conduits by swallow holes at the bottom (Fig. 2.2/9g).

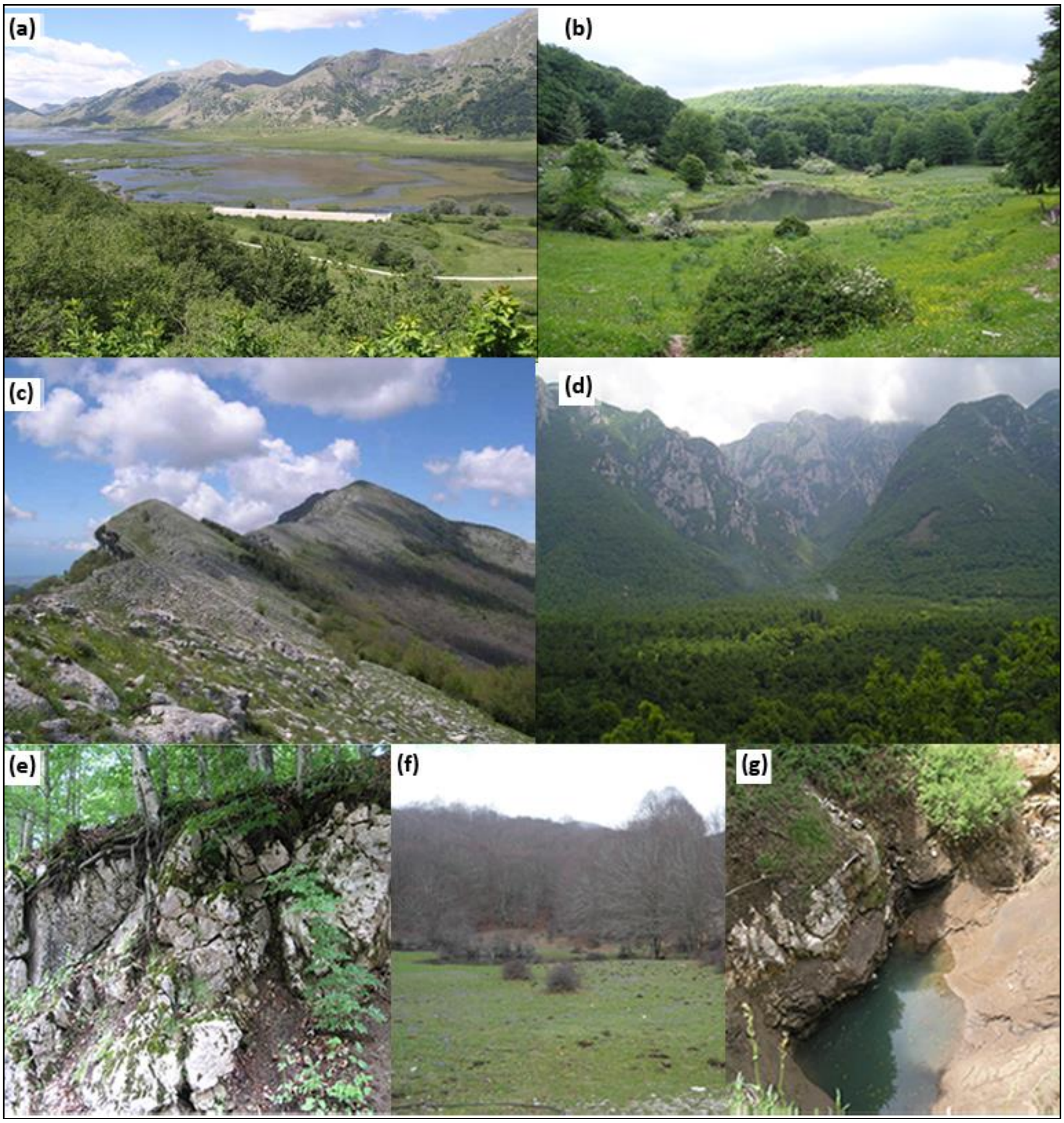

Fig. 2.2/9 – Pictures of typical features of southern Apennines karst aquifers. (a) Endorheic area of Matese Mount; (b) Endorheic area of "Acqua della Madonna" (Terminio Mount); (c and d) Slope areas; (e) "pyroclastic soils-vegetation" surface system on a slope area; (f) "pyroclastic soils-vegetation" surface system on a plain area; (g) Swallow hole.

An impotant fraction of the recharge occurs in this portion of the carbonate massifs mainly because of the topographic conditions.
Celico and Petrella (2008), in order to improve the hydrogeological knowledge of carbonate karst aquifer of the southern Italy, characterized from a hydrogeological and hydraulic point of view the epikarst in the test area "Acqua dei Faggi" and compared its features with those found by European authors (Mangin, 1975; Gunn, 1981; Williams, 1983; Williams, 1985; Klimchouk, 2000; Perrin et al., 2003; Perrin, 2003). Using geophysical and hydrogeological methods, they identified three horizons with different properties in the epikarst (Fig. 2.2/10) (Petrella et alii, 2007; Petrella et alii, 2008). A first layer of 5 meters depth highly karstified with high hydraulic conductivity and effective porosity (ep1). A second horizon highly fractured but less karstified with respect to the first layer, a well interconnected network of fractures and medium high values of hydraulic conductivity and effective porosity (ep2). The third horizon is fractured but not significantly karstified (f). On the whole, this horizon is characterized by a lower hydraulic conductivity and a lower effective porosity.

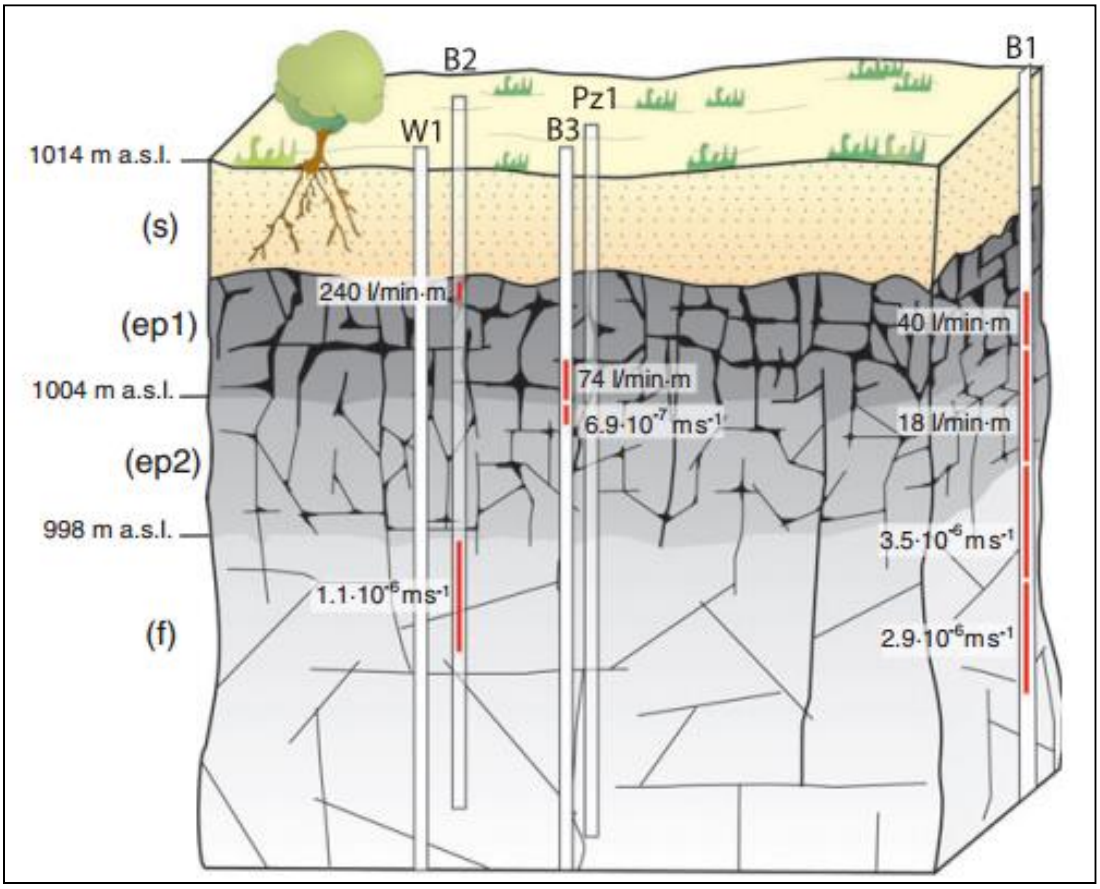

Fig. 2.2/10 – Schematic model of the epikarst in "Acqua dei Faggi" test area (Petrella et alii, 2007).

Using tracer tests, Petrella et alii (2008) characterized hydraulically the different horizons. Wider conduits and narrower fractures coexist within the lower epikarst (ep2). The adjusted aperture of the opening network (105 lm) suggests that conduits are subordinately developed. This horizon is hydraulically similar to granular porous media and Darcy's law can be applied to describe groundwater flow. A small value of longitudinal dispersivity (0.13 m) shows that

variations in the velocity field in the direction of flow are less significant than those typical of (13.6 m day^{-1}).
The different physical characteristics of the three horizons affect also the amplitude and magnitude of the piezometric fluctuation: in response to the same amount of rainfall, different rates of rise and decline of the groundwater level occur. When the water table is in the upper epikarst (ep1) there are restrained fluctuations, while huge variations occur when the water table is in the lower epikarst (ep2)(Fig. 2.2/11).

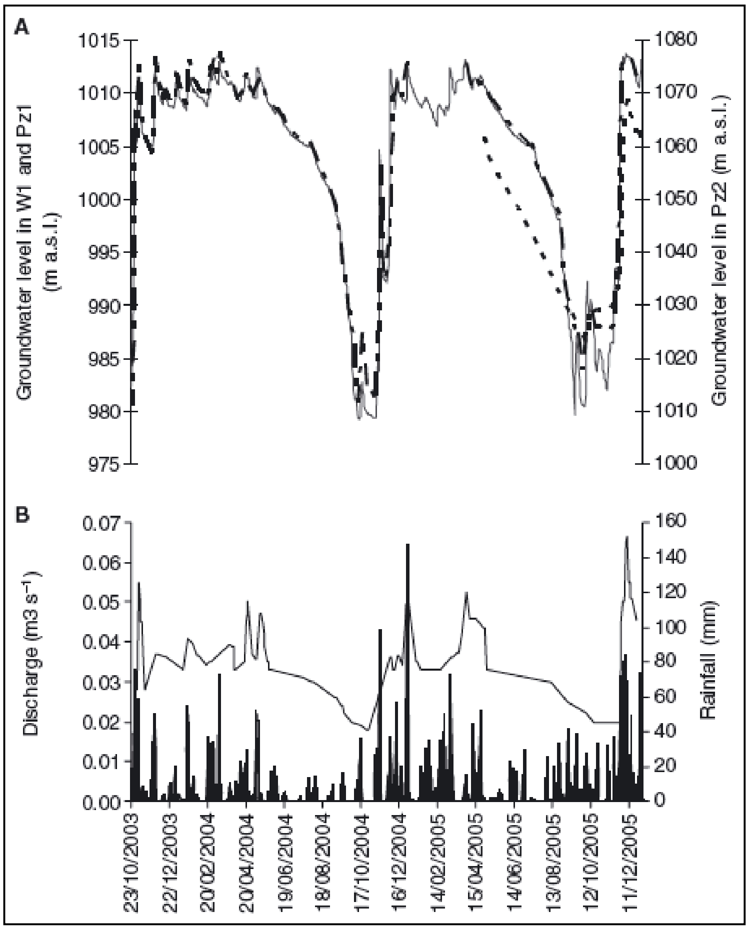

Fig. 2.2/11 – (A) Groundwater level fluctuations in W1 (line), in Pz1 (dashed line) and in Pz2 (dotted line); (B) spring hydrograph and daily rainfall (Petrella et alii, 2007).

The resulting conceptual models can be summarized as follow:

- Epikarst has 10 meters of depth underneath the soil and is formed of three horizons with decreasing degree of karstification;
- The mean tracer velocities calculated in ep1 (3.7 m day^{-1}) and ep2 (13.6 m day^{-1}) are both relatively low compared to velocities usually observed in highly karstified media;
- Diffuse infiltration and diffuse flow are dominating;
- Difference of permeability at the bottom does not allow a storage in a perched temporary aquifer; it can happen only in correspondence of high rainfall events;
- Due to high density and good interconnections of fractures at the base of the epikarst, percolation is observed below the epikarstic zone;

- Groundwater flow is expected to be laminar in the fractured bedrock below the epikarstic zone because of the significant decrease in diffuse karstification and hydraulic conductivities similar to conductivity of the fractured component of the lower epikarstic horizon;
- The “funnelling” effect within larger shafts does not play a predominant role on the hydrogeologic behavior of the carbonate medium.

This karst field site shows an unusual behavior with respect to the European literature probably because of rock mass fracturing caused by different tectonic phases and of the presence of pyroclastic soils on the top of the epikarst (Petrella et alii, 2007).

The hypothesis that the pyroclastic soil plays a significant role in governing epikarst evolution and thickening is supported by the relationship between soil thickness and epikarst thickness (Celico et alii, 2010). The loamy sand soil allows a homogenous and diffuse recharge within the aquifer system and causes a change in the pH of the infiltration water because of the presence of CO_2 and organic carbon coming from microbial metabolism. In addition, an increase of CO_2 is due to the spreading of a huge volume of manure, for agricultural purposes especially in karst depression where the thickness is greater, which induces oxidation processes (Celico et alii, 2010) (Fig. 2.2/12).

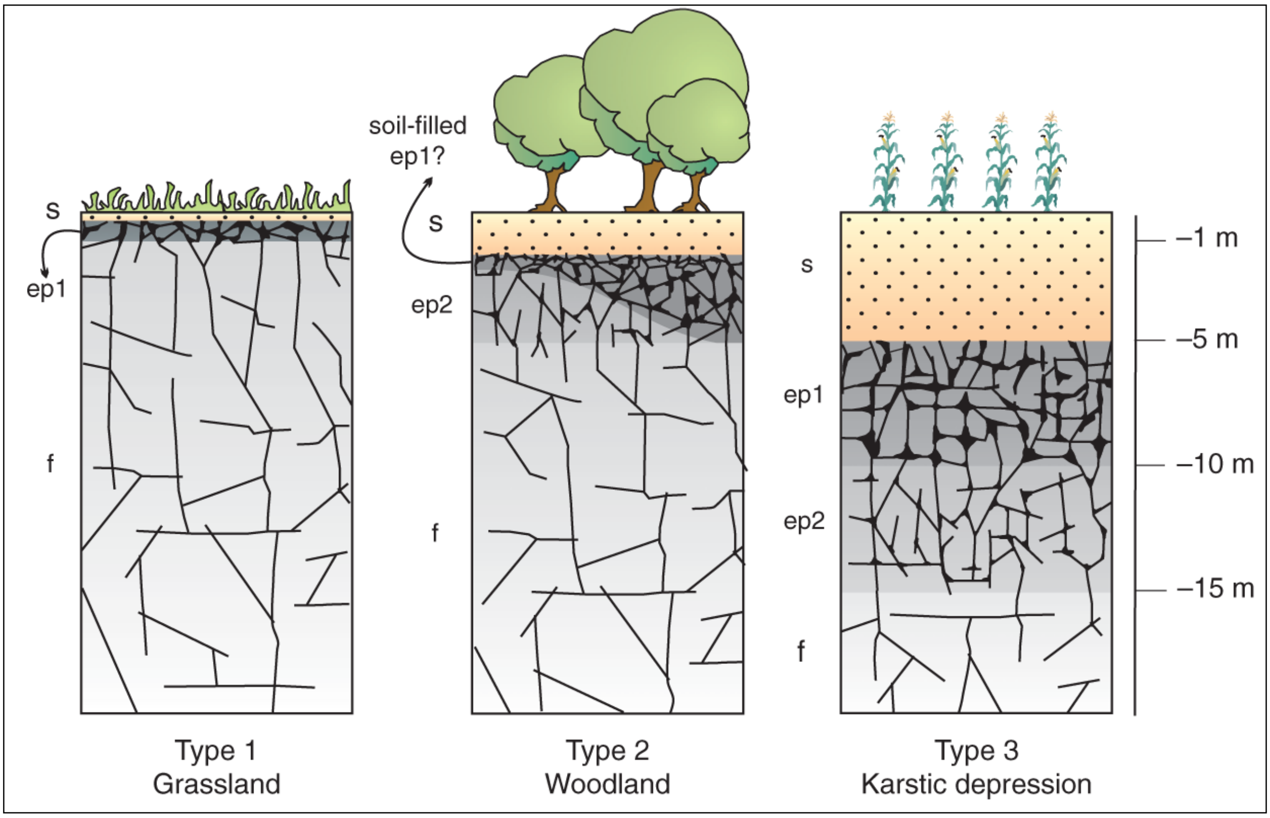

Fig. 2.2/12 – Main pedogeological settings (s is pyroclastic soil, ep1 is epikarst with pervasive karstification, ep2 is epikarst with non-pervasive karstification, f is fractured limestone) (Celico et alii, 2010).

2.3 Groundwater recharge methods in karst aquifers

Global-scale, regional and basin methods

Most of the methods for the recharge assessment used for karst aquifers have been developed for detrital aquifers and then adapted to karst without take into consideration the peculiarity characteristics of these aquifers. In fact, as seen in the introduction the heterogeneity of karst aquifers leads to a complex hydrological and hydrogeological behavior.
Methods to assess recharge in karst aquifers can be grouped in water budget methods, modeling methods and tracer methods.
The water budget method is the most widely used in the scientific literature. It is based on the assumption that water entry should be equal to the amount discharged plus or minus the variation in the volume of water that is stored (Andreo et alii, 2008). Fluid-mass-balance is calculated for the entire aquifer or separately for the vadose zone (soil moisture- balance) and the phreatic zone (groundwater balance) (Jukic and Jukic, 2008). The general equation of the water budget for a basin is:

$$\mathrm{P} - \mathrm{ETR} = \mathrm{RO} + \left(\mathrm{Q_s} + \mathrm{Q_t}\right) + \left(\mathrm{U_o} - \mathrm{U_i}\right) \pm \Delta \mathrm{W_r} \quad (2.3/1)$$

where, P is the mean annual precipitation, ETR is the mean annual actual evapotranspiration, RO is the mean annual runoff, Q_s is the mean annual spring discharge, Q_t is the mean annual tapped discharge, U_o is the mean annual groundwater outflow through adjoining aquifers, U_i is the mean annual groundwater inflow from adjoining aquifers and other allogenic recharge, and $\pm W_r$ is the interannual variation of groundwater reserves.
The uncertainity of the methods comes from the fact that the only parameter easily measurable is the precipitation. The evapotranspiration can be assessed through the application of several approaches: Thornthwaite and Mather (1955) and Turc (1954) are the most used.
Thornthwaite and Mather (1955) found an exponential relation between the potential evapotranspiration and monthly air temperature:

$$ETP = \sum_{i=1}^{12} K \times \left[1.6 \times \left(\frac{t_i}{I}\right)^a\right] \quad (2.3/2)$$

where:
ETP = annual potential evapotraspiration (mm);
K = coefficient that depends on mean monthly hours of solar radiation in function of the month and latitude;
t_i = mean monthly air temperature for the i month (°C);
$a = 675 \times 10^{-9} \times I^3 - 771 \times 10^{-7} \times I^2 + 1792 \times 10^{-5} \times I + 0.49239$;
I = annual heat index.

Turc's formula (1954) is based on annual runoff, air temperature and precipitation of 254 drainage basins distributed in different climates and continents.

$$ETR = \frac{P}{\sqrt{0.9 + \left(\frac{P}{300 + 25 \cdot T + 0.05 \cdot T^3} \right)^2}} \qquad (2.3/3)$$

where:
ETR = the mean annual actual evapotranspiration (mm);
P = the mean annual precipitation (mm);
T = the mean annual air temperature (°C).

The main result of the application of the water budget method is the estimation of coefficients, representing the percentage of afflux becoming recharge.
The most used is the Effective Infiltration Coefficient (EIC) defined as the ratio between the groundwater replenishment, corresponding to the net groundwater outflow, and the rainfall in a specified time scale (usually monthly or yearly) and at the aquifer scale (Drogue, 1971; Bonacci, 2001).
Therefore this ratio incorporates complex processes existing in the vadose zone such as water storage, evapotranspiration, runoff and percolation to the saturated zone; it was conceived as a practical tool to assess monthly or annual groundwater recharge of an aquifer by the rainfall measurements. Several application of this approach exist in the scientific literature in different areas of the world as summarized in Manna et alii, 2013 and Allocca et alii, 2014. In Europe, Kessler (1965) in Hungary found a value of 51.6%; Burdon (1965) and Soulios (1984) found values between 45% and 49% for a Greek karst aquifer; Drogue in Saugras basin, in France, about 50%; for different calcareous basins AEIC was variable from 23% to 77% with a mean value of 54% (Vilimonovic, 1965), (Bonacci, 2001 and Horvat and Rubinic, 2006). Sodeman and Tysinger (1965) assessed smaller value for a dolomitic basin in Tennessee.
In Italy, for the southern Apennines, Allocca et alii (2014) created an original coefficient, Annual Groundwater Recharge Coefficient, similar to the EIC but taking into account the effect of the evapotranspiration.
Starting from the general water budget equation (1), the mean AGRC is the ratio between the mean annual net groundwater outflow [$Q_{OUT} = (Q_s + Q_t) + (U_o - U_i)$] and the mean annual precipitation minus actual evapotranspiration (P-ETR), where both are related to the whole recharge area:

$$AGRC = \frac{(Q_s + Q_t) + (U_o - U_i)}{P - ETR} \qquad (2.3/4)$$

Other applications of the water budget method at different spatial and temporal scale exist in literature (Jocson et alii, 2002; Carter and Driscoll, 2006; Le-Moine et alii, 2008; Sheffer et alii, 2011; Hartmann et alii, 2012; Hartmann et alii, 2014; Guardiola-Albert et alii, 2014).
Numerical modeling approaches have been widely used to estimate recharge (Andreu et alii, 2011) and are a valid tool to forecast recharge (Scanlon et alii, 2002; Hartmann et alii, 2012).
The most important part of the numerical modelling methods is constituted by the spatially distributed methods. Since the final goal of the recharge estimation is the management of water resources, the studies conducted on basin and regional scale play a key role.

Sophocleous (1992), Fayer et alii (1996) and Civita and De Maio (2001) connected the soil water budget method with Geographical Information System in order to have a spatial distribution of recharge.

Specific models, based on water budget methods, have been developed, especially in Spain (Tohuami et alii, 2013): Visual Balan and Gis-Balan (Samper et alii, 2007), Hydrobal (Bellot et alii, 1999, 2001; Chirino, 2003) among others.

Samper et alii (1999) developed a software (Balan and Visual Balan) to estimate aquifer recharge. The code requires input parameters (precipitation and irrigation) and balances equation in soil, unsaturated zone and the aquifer. It permits the discretization of the different components of the water balance (runoff, evapotranspiration, interception, hypodermic flux, and groundwater flow). The infiltration is calculated by using the Horton equation (Horton 1933) or the SCS Curve Number method (SCS 1993). The code has been used by Spanish and Latin American hydrologists in many different fields (Samper 1997; Blasco et alii 2004).

Hydrobal is a model based on previous works by Nizinski and Saugier (1989) and Samper and García Vera (1997). It computes soil water balance using the input data: daily precipitation, temperature, soil parameters (field capacity, wilting point and initial soil moisture) and vegetation cover. The potential evapotranspiration is assessed through the Hargreaves–Samani's method (Hargreaves and Samani, 1982). The output of the model are the different percentage of the components of the water budget (interception, runoff, infiltration) for each each day for vegetation cover type.

Other spatially distributed models present in literature are illustrated here:

SWAT (acronyms for Soil and Water Assessment Tool) (Arnold et alii, 1998; Arnold and Fohrer, 2005) is a basin-scale that works on a daily time step and is able to predict the impact of management on water, sediment, and agricultural chemical yields in ungauged watersheds. The watershed is divided in sub-units, named hydrologic response units (HRUs) with homogeneous or dominant land use and soil characteristics. Within the watershed, it calculates surface runoff, return flow, percolation, evapotranspiration, transmission losses, pond and reservoir storage, crop growth and irrigation, groundwater flow. The model, developed by USDA, is used worldwide and several implementations for karst environments are present (Baffaut and Benson, 2009; Amatya et alii, 2011).

ZOODRM is a distributed modeling code for calculating spatial and temporal variations in groundwater recharge (Mansour and Hughes, 2004). It considers the different types of recharge: direct from the soil, indirect from water surface, urban recharge and irrigation recharge. Recharge is simulated from the base of the soil zone using a Penman-Grindley soil moisture balance approach (Penman, 1948; Grindley, 1967). Hughes et alii, 2008 applyied the code in order to assess the recharge in a structurally complex upland karst limestone aquifer situated in a semi-arid environment

Andreo et alii (2008) proposed a method, named APLIS, based on the variables altitude, slope, lithology, infiltration landform and soil type. In particular, for eight aquifers of the southern Spain they found that the recharge is higher where precipitation is abundant and where there are extensive limestone outcrops, because in such terrain there are abundant exokarstic preferential infiltration landforms, especially if the slope is slight (<8%). From this result, they scored the parameters and carried out an equation to calculate the recharge rate.

Hartmann et alii (2012) developed a recharge model that is based on a conceptual model of the epikarst transforming the spatial variability into statistical variables and applying an iterative calibration strategy in which more and more data was added to the calibration. Hartmann et alii (2014) presented the first simulations of groundwater recharge in all karst regions in Europe with a parsimonious karst hydrology model.

Allocca et alii (2014) created an equation to assess recharge on a regional scale. In particular, comparing the results of the water budget methods of fours sample aquifers with the variables affecting the recharge, they found a connection between the AGRC, lithology and extension of endorheic areas. On the base of their multivariate analysis, they concluded that recharge is mainly influenced by the presence of endorheic areas and, in second place, by the extension of limestone outcrop in the aquifer.

For the same area, Fiorillo et alii (2014) calculated the recharge on annual and daily scale using a GIS tool. The values of the coefficients of recharge found, although based on total rainfall, are similar to those estimated by Allocca et alii (2014) for the same aquifers.

Lumped models have been created also by Rimmer and Salingar (2006); Fleury et alii (2007), Geyer et alii (2008), Jukic and Denic-Jukic (2009) and Tritz et alii (2011).

Several geochemical tracers have been used in the estimation of groundwater recharge at both point and areal scale: tritium, oxygen and deuterium, chloride, bromide (Br^-), nitrate ($NO^{3\,-}$), fluorescein ($C^{2}0H^{12}O^{5}$), dissolved gases chlorofluorocarbons (CFCs) and noble gases such as helium (He) and argon (Ar).

For example, Plummer et alii (1998) studied the relation between a karst aquifer and a river by investigating data on transient tracers and other dissolved substances, including Cl^-, 3 H, tritiogenic helium-3 (3 He), chlorofluorocarbons (CFC-11, CFC-12, CFC-113), organic C (DOC), O2 (DO), H^2S, CH^4, $\delta^{18}O$, δD and ^{14}C. Aquilina et alii (2005) combined stable isotopic ratios ($\delta^{18}O$ and δD) with Cl^- concentration to estimate he evapotranspiration coefficients.

Information about past recharge conditions can be obtained using environmental tracers like chlorofluorocarbons (CFSs), 3H/3He relationships (Cook and Solomon, 1997; Dunkle et alii, 1993) or chloride (Johnston, 1987; Wood and Sanford, 1995)

The most important geochemical method to establish the recharge rate in karst aquifer is the chloride mass balance (Eriksson and Khunakasem, 1969) especially when there is no other source of chloride than rainfall. It is based on the conservative behavior of the chloride ion. In a steady state condition, the recharge is:

$$R \times C_R = (P \times C_P) - (RO \times C_{RO}) \quad (2.3/5)$$

where R is the recharge, C_R is the Cl^- concentration from the recharge water, P is the precipitation, C_P is the Cl^- concentration from rainfall and dry precipitation, E_S is the runoff water, C_E is the Cl^- concentration from surface runoff water.

If CMB is applied for a long time period, in a karst basin, runoff can be negligible as stated by Frot and van Wesemael (2009) and Cantón et alii (2010). A crucial point is the correct estimation of C_P from wet and dry precipitation, because the errors depend mainly on this parameter. Alcala and Custodio (2008), Alcala et alii (2011) and Guardiola Albert et alii (2014) applied the methods for different karst aquifer of the Spain.

Somaratne (2014) used the method in four karst aquifers of southern Australia, and stated that it is questionable due to theoretical limitations and key assumptions not being met. In fact, under point recharge situations, there is not a steady chloride mass flux crossing the watertable and variation of the method is needed in order to consider both point and diffuse recharge components.

Local scale methods

Rare are the cases of recharge estimation at local scale in karst aquifers especially because of their heterogeneity. It is difficult to represent the local areas of preferential recharge with presented models. Moreover, as said in the previous chapter, the main goal of most of the studies of karst aquifers is the management of water resources, that is based on basin scale observations.

Sheffer (2011) in a limestone cave in Central Israel, calculate rates and volumes of infiltration collecting water dripping in the cave. The observed drip rates on a semi-log graph show that three distinct flow regimes can be distinguished (quick flow, intermediate flow, slow flow). Sheffer (2011) also found a threshold rainfall value of 100 mm; only after reaching the threshold the cave drips react to precipitation events in an intermittent behavior. The percolation ranges from 10 to 66% of precipitation with a mean of about 35%.

Ries et alii (2015) modeled the infiltration process in a karst aquifer of the Mediterranean area by using a software (Hydrus – 1d) and soil moisture data at different depth. The coefficient found varies from 0 to 66% with average values of 20%-28% and depend mainly on the climatic conditions of the studied site.

Somaratne (2014) suggested application of: water table fluctuation, numerical groundwater modelling, Darcy flow calculation or water budget methods for recharge estimation in a point recharge dominant aquifer. Geochemical tracers methods and lysimeter methods can also be applied in karst aquifers on a local scale. Some examples of application of the Water Table Fluctuation method in fractured rock aquifers are present in literature. The main issue, is the correct quantification of the specific yield (Healy and Cook, 2002).

3. Study areas

Hydrogeological and climate characteristics

Regional scale

On a regional scale, it is possible identify 40 karst aquifers (total area 8,560 km^2) with an autonomous groundwater circulation (Fig. 3/1a). These aquifers are formed by carbonate massifs, which represent the highest mountains of southern Apennines.
Carbonate Mesozoic rocks are the main components of these aquifers, highly fractured due to their brittle mechanical behavior and tectonic stresses. Furthermore, due to their chemical composition, these rocks are subject to karst phenomena, through which percolating water enlarges the original fracture network. This network of discontinuities gives these mountains a very high infiltration capacity.
According to the hydrogeological characteristics observable on a large scale, the carbonate aquifers can be subdivided into three groups:

- Limestone aquifer (average yield: 3700×10^6 m^3 $year^{-1}$; mean groundwater yield: 0.016 and 0.035 m^3 s^{-1} km^{-2});
- Carbonate aquifers consisting of alternating limestone, limestone with chert, marly limestone and subordinately marls (average yield: 100×10^6 m^3 $year^{-1}$; mean groundwater yield: 0.009 and 0.015 m^3 s^{-1} km^{-2});
- Mainly dolomitic aquifers (average yield: 300×10^6 m^3 $year^{-1}$; mean groundwater yield: 0.013 and 0.021 m^3 s^{-1} km^{-2}).

The hydrogeological behaviour of these aquifers is in accordance with principal conceptual models proposed for karst aquifers of southern Apennines described in 2.2.2 chapter.
Particularly, the patterns of groundwater flow are greatly conditioned both by the altimetry of the boundary with the juxtaposing lower-permeability flysch deposits, as well as by the position and permeability of cataclastic bands associated with main faults and thrusts. The latter, behaving as aquitards, determine the fractioning of the groundwater flow into several groundwater basins (Petrella et alii, 2009; Celico et alii, 2010; Petrella et alii, 2014).
The basal springs, which constitute the main outflow volume, are located along the hydrogeological boundaries between carbonate and Miocene terrigenous formations and Plio-Quaternary deposits, which constitute the relative impermeable. The mean discharge varies from 0.1 to 5.5 m^3/s. Conversely, where the Plio-Quaternary deposits are formed by high permeability rocks, a groundwater exchange can exist.
Usually the water table of the basal flow present a very low slope, in the order of 0.3%, unless there exist tectonic zones which can produce cataclastic rocks with a strong difference in term of hydraulic conductivity, that can cause a jump in the water table (Petrella et alii, 2014).
Perched groundwater flow also occurs in the surficial part of carbonate karst aquifers, where the different thickness and hydraulic characteristics of the karst, as well as stratigraphic-structural factors and/or the presence of karst conduit, can generate high-altitude seasonal/temporary springs, characterized by low flow (Q_{mean} < 0.01 m^3/s).
The recharge occurs mainly in concentrated areas (dolines, swallow holes, endorheic zones and summit plateau) and subordinately in a diffuse way on the whole massif. In particular, the

presence of summit plateau, areas with a slope less than 5%, is a peculiar characteristic of the aquifer of southern Apennines.

In the recharge process, for these aquifers, an important role is played by the presence of ash-fall deposit that mantles the karst bedrock. Pyroclastic products, coming from the eruptions of the near volcanic centres, cover the slopes with a variable thickness and fill the concavity of the topography controlling the infiltration process.

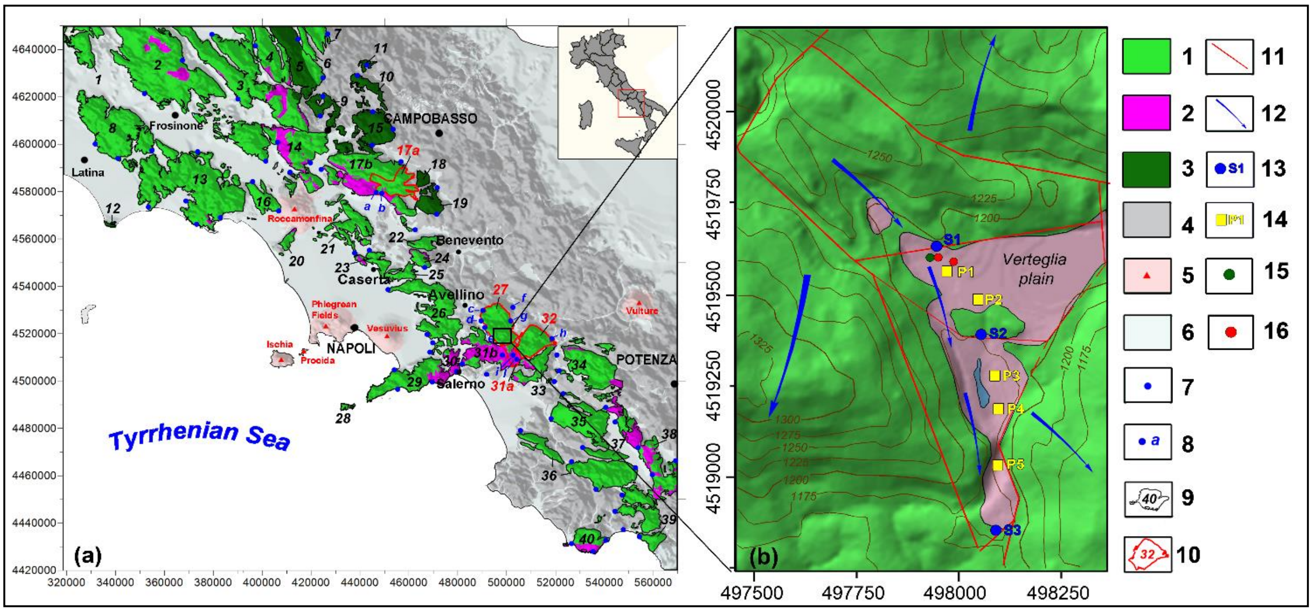

Fig. 3/1 – (a) Hydrogeological map of the karst aquifers of the southern Apennines. (b) Hydrogeological map of *Acqua della Madonna* perched karst aquifer. Key to symbols: 1) limestone and dolomitic limestone units of the carbonate platform series (Jurassic-Paleogene); 2) dolomitic units of the carbonate platform series (Trias-Liassic); 3) calcareous-marly units of the outer basin series (Trias-Paleogene); 4) pre-, syn- and late- orogenic molasses and terrigenous units (Cretaceous-Pliocene); 5) volcanic centres (Pliocene-Quaternary); 6) alluvial and epiclastic units (Quaternary); 7) main basal springs of karst aquifers; 8) basal karst springs considered in the hydrological budget (a and b: Maretto and Torano; c: Salza Irpina; d and e: Serino; f: Baiardo; g: Cassano Irpino; h: Sanità; i: Avella; l: Ausino-Ausinetto); 9) hydrogeological boundary and identification number of the karst aquifers; 10) hydrogeological boundary and identification number of the karst aquifers considered for the hydrological budget; 11) main faults; 12) groundwater flow direction; 13) perched springs; 14) piezometers; 15) soil water content sensor; 16) soil temperature sensor.

The climate in the study area varies from warm temperate climate with dry and hot summer (Csa) in the coastal sector to warm temperate climate with dry and warm summer (CSb) in the inland areas (Geiger, 1954). For the Geiger's classification of climate, the only difference is in the regime of temperature with Csa zone having $T_{max} \geq 22°C$ and Csb $T_{max} \leq 22°C$ and at least four moths with $T_{min} \geq 10°C$.

Following the geomorphological setting, the lowest mean annual air temperature (10 - 12°C) are along the Apennine ridge while values of 12-13°C and 13-15°C are, respectively, in the plains surrounded by mountains and in the coastal area. Rainfall regimes vary from the coastal or Mediterranean type to the Apennine sublittoral (Bandini, 1931), which is characterised by a principal maximum in autumn-winter and a minimum in the summer as reported on the diagram of the distribution of the mean monthly precipitation (Fig. 3/2).

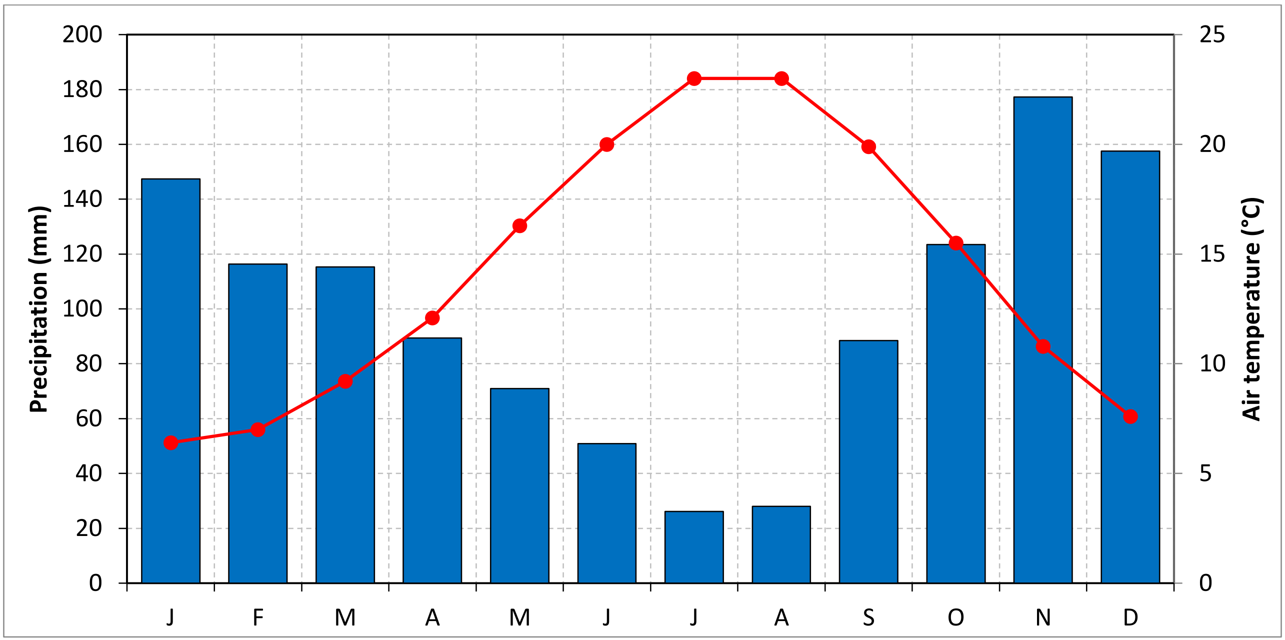

Fig. 3 /2 – Distribution of the mean monthly precipitation (blue bars) and air temperature (red line).

Like the air temperature, also the spatial distribution of the precipitation is influenced by the topography. In fact the Apennine chain works as a barrier against the humid masses coming from the Thyrrenian Sea, causing highest precipitation (about 2000 mm y^{-1}) on the top of the morphological divide (Roe, 2005; Houze, 2012) and lowest eastward of the divide (700-900 mm y^{-1}).

In the Mediterranean area, and therefore for the study area, has been demonstrate the effect of the North Atlantic Oscillation (NAO) on the long-term trend of precipitation and air temperature. The oscillation of the NAO affects the areas of origin of the humid masses that controls the regime of precipitation causing periods with precipitation value higher than the average and dry periods with deficient rainfalls (De Vita et alii, 2007; De Vita et alii, 2012).

Basin scale

On a basin scale, were studied Matese (a), Accellica (a), Terminio and Cervialto karst aquifers, which, for their characteristics, are representative of the other karst aquifers of southern Apennines (Fig. 3/1a). The choice was based on the availability of long time series of springs discharge.

Reflecting the regional geological setting, the sample aquifer are formed mainly by cretaceous limestone highly fractured and karstified and secondly by Triassic dolomitic units. The carbonate sedimentary series were piled up in the thrust-belt Apennine structure together with basinal and flysch series, during the Miocene orogenesis.

Mount Terminio is almost totally made of Cretaceous limestone and dolomitic limestone belonging to the "*Monti Picentini-Taburno*" stratigraphic unit (Allocca et alii, 2007) tectonically bounded by less permeable terrigenous deposits outcropping in the northern-eastern sector of the aquifer. The groundwater circulation within the aquifer is influenced by the orientation of the main faults and thrusts and outflows in four huge basal springs: Cassano Irpino (Q_{mean} = 3 m^3 s^{-1}), Serino (Q_{mean} = 2.3 m^3 s^{-1}), Baiardo (Q_{mean} = 0.25 m^3 s^{-1}) and Sorbo Serpico (Q_{mean} = 0.2 m^3 s^{-1}). The location of the springs, the geological setting and the structural features allowed to identify several groundwater basins (Celico, 1983a) that cannot be considered as autonomous basins. Mount Terminio represents the most productive aquifer of southern Apennines with a mean groundwater yield of about 0.045 $m^3\ s^{-1}\ km^{-2}$ and its water feeds important aqueducts system of the Campania, Basilicata and Apulia regions.

Like the Terminio Mount, also Cervialto karst aquifer is made of limestone of the "*Monti Picentini-Taburno*" stratigraphic unit. The aquifer is well isolated, in the northern part, by the presence of important regional faults causing the contact with flysch deposits and, in the southern part, by the presence of less permeable dolomitic units of the Accellica Mount. Because of this geological setting, Cervialto Mount has a sole groundwater outflow (Sanità karst springs, Q_{mean} = 3.95 $m^3\ s^{-1}$) located in the lowest point of the impermeable boundary. The mean groundwater yield of the carbonate unit is about 0.034 $m^3\ s^{-1}\ km^{-2}$ (Celico, 1983a; Mattia and Celico, 2002).

Matese (a) is a sub-catchment of the whole Mount Matese aquifer. It is made up, almost totally, of limestone bounded by less permeable dolomitic unit and flysch deposits. The main outflowing points are the springs Maretto and Torano (Q_{mean} = 3 $m^3\ s^{-1}$). Matese karst aquifer has been widely studied in the past years. The main studies have been summarized in the chapter 2.2.2.

Accellica (a) is a sub-catchment of the whole Accellica karst aquifer. Unlike the previous sample aquifers, it is formed mainly of dolomitic unit, which is relatively less fractured and karstified influencing the hydraulic behaviour of the aquifer. The basal flow is in this formation, feeding the main springs (Avella and Ausino-Ausinetto). The mean groundwater yield is about 0.029 $m^3\ s^{-1}\ km^{-2}$ (Celico, 1983a).

Local scale

The test area "Acqua della Madonna" is located in the central-southern sector of the Terminio Mount karst aquifer at 1179 m a.s.l. and is made of karst bedrock mantled by ash fall deposits (Fig. 3 /1b) (Fig. 1, Allocca et alii, 2015). It hosts a perched aquifer bounded laterally by direct faults that locally produce significant cataclastic zones that are characterized by a low hydraulic conductivity (lower than $1.0 \times 10^{-6}\ m\ s^{-1}$) (Allocca et alii, 2008).

The unconfined aquifer goes up to 60 meters depth as confirmed by boreholes in the area; the latter have not identified any stratigraphic or structural factor, which could perch the aquifer. According to the geological settings of the area, it is supposed that these factors (Celico, 1988) could be found below the depths reached by the drillings. In fact, Celico (1988), during the execution of different boreholes in the Terminio karst aquifer, found a sudden drop of the water table of 45 meters after drilled a less permeable layer of only 8 meters, which constitute a hydrological barrier (Fig. 3/3).

In the test area, the faults locally can produce a fractioning of the perched aquifer in a basin-in-series system with presence of perennial and seasonal springs along the tectonic zones. The annual fluctuation of groundwater levels crosses the boundary between pyroclastic cover and fractured carbonate bedrock.

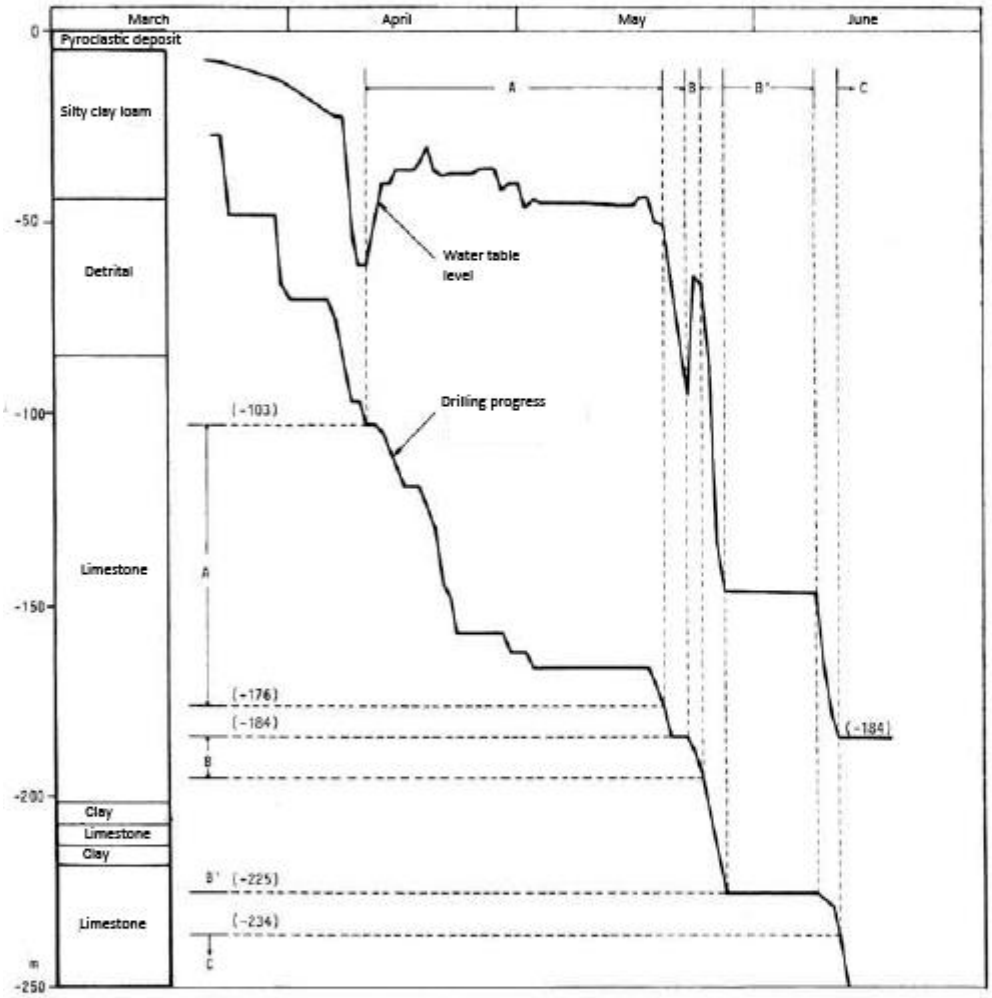

Fig. 3/3 – Water table level evolution in response to the execution of borehole in the higher part of Terminio karst aquifer (Celico, 1988).

The climate characteristics of "Acqua della Madonna" site area are consistent with those observed on regional scale for the carbonate reliefs. The mean annual precipitation is about 2000 mm y^{-1} with main events occur during the winter and a very dry periods corresponding with summer seasons. Events with high intensity precipitation (> 100 mm day^{-1}) are typical of the area. The temperature ranges from about 20°C of the summer to 2° of the winter period. The snow blanket generally persists less than a few days after precipitation and often with a discontinuous distribution within the pasture area.

4. Data and methodologies

Regional and mean-annual scale

North Atlantic Oscillation data

The North Atlantic Oscillation (NAO) is an oscillation with complex periodicity of the atmospheric masses over the tropical zone of the Azores Islands (barometric high) and Iceland (barometric low). It is described by an index, which is the barometric anomaly, with respect to the standard difference, between Iceland's barometric low and the Azores's barometric high. Different NAOIs exist depending on the barometric stations and on the period of the year considered (Hurrell et alii, 2003). For the case study, the analyses were performed with a subset (1921-2010) of the winter NAOI (December through March mean - DJFM) time series, calculated from the records of the Lisbon (Portugal) and Stikkishlomur (Iceland) barometric stations since 1864 (http://www.cgd.ucar.edu/cas/jhurrell/indices.html).

Hydrological data

To study the recharge of karst aquifers of southern Apennines and its variability have been collected pluviometric and air temperature data from 1921 to 2000 from the annals of the National Hydrographic and Tidal Service and and from the Regional Civil Protection Agency databases (www.protezionecivile.gov.it) for the remaining interval from 2000 to 2012. In this first phase of the study, have been reported, for each rain gauge and air temperature station, information regarding the year of functioning, the correct location (UTM coordinates and altitude) and the type of instrumentation. Moreover, was carried out a preliminary screening to eliminate those years for which the data were incomplete, i.e. those years for which were missed some monthly data. In total, were gathered data from 387 rain gauge stations and 228 air temperature-monitoring stations. About 50% of the station function for more than 30 years with lowest number (52) during the Second World War (1943) and a maximum of 229 in 1978. The average number of rain gauge station functioning per year is 172. The monitoring network cover an area of about 19.339 km^2 divided in 5 regions and 12 provinces and a very heterogeneous territory, from the coastal areas to the Apennines ridge.

Regional climate indexes

In order to study the influence of the North Atlantic Oscillation Index on the climatic regime of the southern Apennines, regional indexes of precipitation (MAPI), air temperature (MATI), effective precipitation (precipitation minus evapotranspiration) (MAEPI), evapotranspiration (MAEI) and recharge (MARI) were created.

From the collected hydrological data, 18 rain gauge stations (Cusano Mutri, Pescosannita, Sessa Aurunca, Caiazzo, Caserta, Altavilla Irpina, Torella dei Lombardi, Montevergine, Napoli Istituto di Fisica Terrestre, Palma Campania, Muro Lucano, Sorrento, Nocera Inferiore, Eboli, Sant'Angelo a Fasanella, Castellabate, Gioi Cilento and Morigerati) and 9 thermometric stations

(Gaeta, Atina, Ariano Irpino, Avellino, Montevergine, Napoli, Scafati, Capaccio and Morigerati) were chosen on the basis of the years of functioning and of the spatial distribution.
The Mean Annual Precipitation Index was calculated as follow:

$$MAPI_i = \frac{\sum_{j=1}^{18} \frac{AP_{ji} - MAP_j}{MAP_j}}{\sum_{j=1}^{18} j} \quad (4/1)$$

where
$MAPI_i$ = Mean Annual Precipitation Index for the *i* year (%);
AP_{ji} = Annual Precipitation for the *j* rain gauge station and the *i* year (mm);
MAP_j = Mean Annual Precipitation of the whole time series for the *j* rain gauge station (mm).

Similarly and with reference to the identical observation period (1921-2010), the Mean Annual air Temperature Index (hereafter MATI) was calculated as follows:

$$MATI_i = \frac{\sum_{k=1}^{9} \frac{AT_{ki} - MAT_k}{MAT_k}}{\sum_{k=1}^{9} k} \quad (4/2)$$

where
$MATI_i$ = Mean Annual air Temperature Index for the *i* year (%);
AT_{ki} = Annual air Temperature for the *k* air temperature gauge station and the *i* year (°C);
MAT_k = Mean Annual air Temperature of the whole time series for the *k* air temperature gauge station (°C).
In order to calculate the Mean Annual Evapotranspiration Index (MAEII) and the Mean Annual Effective Precipitation Index (MAEPI), for each rain gauge station, have been assessed the real evapotranspiration and, subsequently, the precipitation minus evapotranspiration.
To assess the real evapotranspiration was used the Turc's formula (1956). The reliability of this formula was confirmed by several studies in the Mediterranean (Santoro, 1970) and European areas (Parajka and Szolgay, 1998; Horvat and Rubinic, 2006).

$$ETR_j = \frac{P_j}{\sqrt{0.9 + \left(\frac{P_j}{300 + 25 \cdot T_j + 0.05 \cdot T_j^3}\right)^2}} \quad (4/3)$$

where ETR_j is the mean annual actual evapotranspiration (mm) for the j rain gauge station; P_j is the mean annual precipitation (mm) for the j rain gauge station; and T_j is the mean annual air temperature (°C) for the j air temperature-rain gauge station.

For those stations without the temperature monitoring equipment the value of mean annual temperature was extracted by a regional linear equation found between mean annual air temperature and its monitoring station.

$$T_j = -0.0064 \times h_j + 16.528 \quad (4/4)$$

T_j is the mean annual air temperature (°C) for the j air temperature-rain gauge station and h_j is the elevation of the rain gauge station.
MAEPI were calculated as:

$$MAEPI_i = \frac{\sum_{j=1}^{18} \frac{AEP_{ji} - MAEP_j}{MAEP_j}}{\sum_{j=1}^{18} j} \quad (4/5)$$

where
$MAEPI_i$ = Mean Annual Effective Precipitation Index for the *i* year (%);
AEP_{ji} = Annual Effective Precipitation for the *j* rain gauge station and the *i* year (mm);
$MAEP_j$ = Mean Annual Effective Precipitation of the whole time series for the *j* rain gauge station (mm).

MAEI has the same structure but using the Annual evapotranspiration value instead of the Annual Precipitation or Annual Effective Precipitation.

$$MAEI_i = \frac{\sum_{j=1}^{18} \frac{AE_{ji} - MAE_j}{MAE_j}}{\sum_{j=1}^{18} j} \quad (4/6)$$

where
$MAEI_i$ = Mean Annual Evapotranspiration Index for the *i* year (%);
AE_{ji} = Annual Evapotranspiration for the *j* rain gauge station and the *i* year (mm);
MAE_j = Mean Annual Evapotranspiration of the whole time series for the *j* rain gauge station (mm).

For MARI has been used the net infiltration derived from the overlay of the precipitation maps for the *i* year with the potential infiltration coefficient (c.i.p.) (Celico et alii, 1986; Allocca et alii, 2007).

$$MARI_i = \frac{\sum_{k=1}^{40} \frac{AR_{ki} - MAR_k}{MAR_k}}{\sum_{k=1}^{40} j} \quad (4/7)$$

where
$MARI_i$ = Mean Annual Recharge Index for the *i* year (%);

AR_{ki} = Annual Recharge for the *k* aquifer and the *i* year (mm);
MAR_j = Mean Annual Recharge of the whole time series for the *k* rain gauge station (mm).

Spring discharge indexes

To verify the influence of the NAOI on the recharge, were created also spring discharges indexes (MADI) of three karst springs. Mean Annual Discharge Index was calculated for Sanità (belonging to Cervialto karst aquifer), Cassano Irpino (belonging to Terminio karst aquifer) and Maretto (belonging to Matese (a) karst aquifer) springs as follow:

$$MADI_i = \frac{MAD_i - MAD}{MAD} \qquad (4/8)$$

where
$MADI_i$ = Mean Annual Discharge Index for the *i* year (%);
MAD_i = Mean Annual Discharge for the *i* year (m^3/year);
MAD = Mean Annual Discharge of the whole time series (m^3/year).

Basin and mean-annual scale

Spring discharge data

For four sample karst aquifers, long time series of daily spring discharge were collected. Specifically: *Sanità di Caposele*, which represent the only groundwater outflow of Cervialto karst aquifer, from 1921 to 2012; *Cassano Irpino* (1965-2010), *Serino* (1887-2010), *Baiardo* and *Salza Irpina* (1970-2000) for Terminio aquifer; *Avella* and *Ausino-Ausinetto* springs (recording period 1967-1989) for the Accellica (a) aquifer and *Maretto* and *Torano* (respectively 1967-2000 and 1957-2000) for Matese (a) aquifer.

Lithology, soil type, land use and geomorphological data

To assess the recharge on regional scale, were studied the parameters affecting the recharge processes. Information about outcrop's lithology were assessed by the analysis of the hydrogeological map of southern Apennines, 1:250000 scale (Allocca et alii, 2007). Soil type data were excerpt from the Ecopedological Map of Italy, 1:250000 and from the Land System Map of the Campania Region, 1:250,000 scale (www.risorsa.info). Land use data for the study area were collected from Corine Land Cover 2006 (www.eea.europa.eu).
Moreover, topographic and geomorphological feature were studied by using a national 20-m grid Digital elevation Model from the National Environmental Information System (http://www.sinanet.isprambiente.it).

Water budget method and AGRC estimation

The most used method to assess groundwater recharge is water budget method. The attractiveness of the method lies in its simplicity but exist uncertainties related to the errors in the estimation of the "known" parameters. In our study, for each sample aquifer, the Annual

Groundwater Recharge Coefficient (AGRC) has been calculated by applying the general equation of the water budget:

$$P - ETR = RO + (Q_s + Q_t) + (U_o - U_i) \pm \Delta W_r \quad (4/9)$$

where, P is the mean annual precipitation, ETR is the mean annual actual evapotranspiration, R is the mean annual runoff, Q_s is the mean annual spring discharge, Q_t is the mean annual tapped discharge, U_o is the mean annual groundwater outflow through adjoining aquifers, U_i is the mean annual groundwater inflow from adjoining aquifers and other allogenic recharge, and $\pm\Delta W_r$ is the interannual variation of groundwater reserves.
On a long term, the interannual variation can be consider negligible and the equation can be consider without last term.
The AGRC was estimated, by comparing terms of the hydrological budget, as the ratio between the mean annual net groundwater outflow (spring and other groundwater discharges) and the mean annual precipitation minus evapotranspiration:

$$AGRC = \frac{(Q_s + Q_t) + (U_o - U_i)}{P - ETR} \quad (4.10)$$

where Q_s is the mean annual spring discharge; Q_t is the mean annual tapped discharge; U_o is the mean annual groundwater outflow through adjoining aquifers; U_i is the mean annual groundwater inflow from adjoining aquifers and other allogenic recharge; P is the mean annual precipitation; ETR is the mean annual actual evapotranspiration; R is the mean annual runoff.

Like for the creation of the regional climatic indexes, for the calculation of the real evapotranspiration was used Turc's formula (1956) (4/3).
Considering the peculiar geomorphological feature of the karst aquifers, characterized by huge summit plateau and endorheic areas, namely by a total infiltration and no runoff, an additional coefficient was assessed in order to estimate the recharge for the slope areas only:

$$AGRC_S = \left[\frac{(AGRC \times A_T) - (1 \times A_E)}{A_T - A_E} \right] \times 100 \quad (4.11)$$

where: $AGRC_S$ is the Annual Groundwater Recharge Coefficient for slope areas; A_T is the total area of the karst aquifer (km^2); A_E is the cumulative extension of summit plateau areas and/or endorheic watersheds (km^2). A complementary value of the $AGRC_S$ was calculated and named Annual Runoff Coefficient (ARC):

$$ARC = 100 - AGRC_S \quad (4.12)$$

Local and episodic scale

Hydrological data

For “Acqua della Madonna” karst aquifer, the instrumentation consists of an air temperature and rain gauge station, five deep piezometers (up to 80 m), sensors for monitoring the temperature of the soil at 10 cm and 50 cm depth and sensors for soil water content at 10 cm depth.

Pluviometric and air temperature data have been collected. In particular, were used daily data from January to December 2008 from *S. Salvatore* thermo-pluviometric station (40° 49’ 36’’; 15° 01’ 46’’; elevation 980 m a.s.l.), which is part of *Alto Calore Spa* network (http://www.altocalore.eu/).

For the same period have been collected piezometric level daily data from the P1 piezometer, 60 m deep, whose stratigraphic setting is characterized, form the top, by 8.5 m of ash fall pyroclastic deposits and 51.5 m of karstified limestone and dolomitic-limestone.

In the same area have been collected data of volumetric soil water content at 10 cm. This depth is representative because evapotranspiration process occurs in the surficial part of the soil because of the limited depth of root apparatuses of grassy vegetation.

Groundwater recharge assessment

The assessment of recharge on a local scale was accomplished by the application of Water Table Fluctuation method (WTF). It is based on relating changes in measured water-table elevation with changes in the amount of water stored in the aquifer (Meinzer, 1923; Healy and Cook, 2002):

$$R = Sy \times \Delta h \quad (4.13)$$

where R (mm) is the recharge, Sy is specific yield (dimensionless), and Δh is the peak water-table rise attributed to the recharge period (mm).

Particularly, among the different approaches of the WTF method, was applied the approach of Nimmo et alii (2014), fitted for a complex hydrogeological setting. The method consists of two phases: the first is the individuation of the Master Recession Curve (MRC) and the second, Episodic Master Recession (EMR), is the recognition and quantification of recharge episodes with the assessment of Recharge to Precipitation Ratio (RPR).

To construct the Master Recession Curve and understand the relation between the decline rate of the piezometric level and the elevation, was used the MRC code (Nimmo et alii, 2015). The assumptions inherent to this approach are: 1) there exist a characteristic functional relation between water-table elevation and water-table decline rate in the absence of recharge (the basis for the MRC); 2) the measured well hydrograph data depict only natural water-table fluctuations caused by ground-water recharge and discharge (Heppner and Nimmo 2005; Heppner et alii 2007; Delin et alii 2007).

The input data required from the code are the precipitation and the water-table data in function of time; moreover, the codes requires two user-supplied parameters: the degree of the polynomial master recession curve and the storm recovery time value, which represent a characteristics of the system being the time between last precipitation event and the start of recession period.

This algorithm uses a subset of the original data, which represent the pure water-table recession data, formed by data not affected by input from recent precipitation. The intervals for MRC evaluation are considered to begin at a specified time interval after the end of the most recent precipitation in which there is a water table decreasing.

The MRC is the curve that best fits the dH/dt vs H extracted points and represents the average behavior for a declining water-table at that site. Typically it indicates faster decline at greater H, as observed by others (Heppner and Nimmo 2005, Nimmo et alii., 2014).

The Episodic Master Recharge code identifies discrete episodes of recharge at a hydrological site, based on the water-table dynamics and precipitation record at the site during a given time period. It requires data (water table level and cumulative precipitation) and user-supplied parameters (MRC type, specific yield, time lag and fluctuation tolerance). The latter two parameters characterize the methods: the fluctuation tolerance is a threshold of the noise that must be exceeded for the fluctuation H(t) to be considered significant; the time lag is the time between a precipitation event and the associated recharge response. To estimate the time lag, has been carried out a cross-correlation analysis between the water table rate of change and the precipitation. The MRC parameters are the intercept and the coefficients of the curve and derive from MRC code results while the specific yield is a characteristic of the medium.

The first step of the EMR code is to identify the recharge episodes. An episode is defined as a period during which the observed water-table rate of change, dH/dT, exceeds the Master Recession Curve (MRC)-predicted water-table rate of change, dH/dT_{MRC}, by an amount greater than the fluctuation tolerance.

The initiation of a single recharge episode starts one lag time before dH/dt crosses the tolerance interval of the dH/dt_{MRC} curve. Similarly, the end a single recharge episode finishes one lag time before dH/dt re-entries within the tolerance interval of the dH/dt_{MRC} curve (Fig. 5). The precipitation event associated with an episode begins one lag time before the start of the episode, and ends one lag time before the end of the episode.

The recharge in an episode is the product of the specific yield and the difference of two extrapolations that indicate the H that would have happened without recharge and the H that would have preceded the post-episode recession if there had been pure recession unaffected by overshoot. The overshoot is the component of the water table rise that does not depend from recharge but only from other causes like air trapping, change in atmospheric pressure or in temperature.

For each episode the algorithm calculated start and end time, duration, recharge, precipitation and Recharge to Precipitation Ratio (RPR), i.e. the amount of precipitation that becomes recharge.

Soil water balance

To understand deeply the processes affecting the unsaturated zone, the potential evapotranspiration was assessed using the formula of Thornthwaite and Mather (1955) that found an exponential relation between the potential evapotranspiration and monthly air temperature:

$$ETP = \sum_{i=1}^{12} K \times \left[1.6 \times \left(\frac{t_i}{I} \right)^a \right] \quad (4.14)$$

where:
ETP = annual potential evapotraspiration (mm);
K = coefficient that depends on mean monthly hours of solar radiation in function of the month and latitude;
t_i = mean monthly air temperature for the i month (°C);
$a = 675 \times 10^{-9} \times I^3 - 771 \times 10^{-7} \times I^2 + 1792 \times 10^{-5} \times I + 0.49239$;
I = annual heat index.
The monthly actual evapotranspiration (ETR_i) was calculated by the soil water balance method (Thornthwaite-Mather, 1955; 1957).
Besides Ep_i, this method considers the monthly precipitation (P_i) and the total available water content ($\Delta\theta_{TAW}$) stored in the evapotranspiration zone, which corresponds to the difference between field capacity value (θ_{FWC}) and Permanent Wilting Point (θ_{PWP}).
During humid season, when the soil water content exceeds the θ_{FWC} due to rainfall, monthly runoff (R_i) and net infiltration (I_{ei}) arise, namely groundwater recharge occurs. Differently, during months with rainfall amounts lower than Ep_i, ETR_i can equal Ep_i due to the loss of water content stored in the evapotranspiration zone in the antecedent month ($\theta_{i-1} - \theta_{PWP}$).
To calculate the actual evapotranspiration it is needed to know the field capacity, permanent wilting point, the available water holding capacity (difference between the first two) and the depth of the roots.
In study case, the field capacity (θ_{FWC}) is 36.9%, the permanent wilting point (θ_{PWP}) is 11.0%, the available water holding capacity ($\Delta\theta_{TAW}$) is 25.9% and the depth of the roots is 600 mm. Subsequently, the available water capacity, which is the product of water holding capacity and depth of roots, is 155.4 mm.

5. Results

Regional and mean-annual scale

Correlation of NAOI, regional climate indexes and MADI

The regional climate indexes were analyzed, in first analysis, by observing the linear trend (Fig. 5/1). For MAPI and MAEPI, was observed a decreasing rate with respect to the mean value. In particular for MAPI, -0.13% with respect to the mean annual value of 1160.2 mm and for MAEPI -0.26% respect to the annual mean (652.2 mm). MATI shows, conversely, an increasing rate of 0.6% respect to the mean 14.3°C.

Subsequently, observing the 11-year moving average trend of the single indexes a complex cyclical oscillation was found (Fig. 5/1). In two periods (1930 – 1944 and 1958-1978) the MAPI was below the normal value, while for three periods (before 1930, 1944-1958 and 1980-2005) it was above it. This trend is inversely correspondent with NAOI trend. The maximum values of the time series were as follows: +31% (1933), +35% (1969) and +41% (2010). The same complex cyclical oscillation is displayed by MATI, with a minimum of -15% in the 1944 and a maximum of 14% in 1994. Long-term trend of MAEPI is similar to MAPI but with a major fluctuation range around the mean value. In fact the extreme were -61% (2001) and +72% (1933). The amplification effect is due to the non-linear behaviour of the actual evapotranspiration (De Vita et alii, 2012).

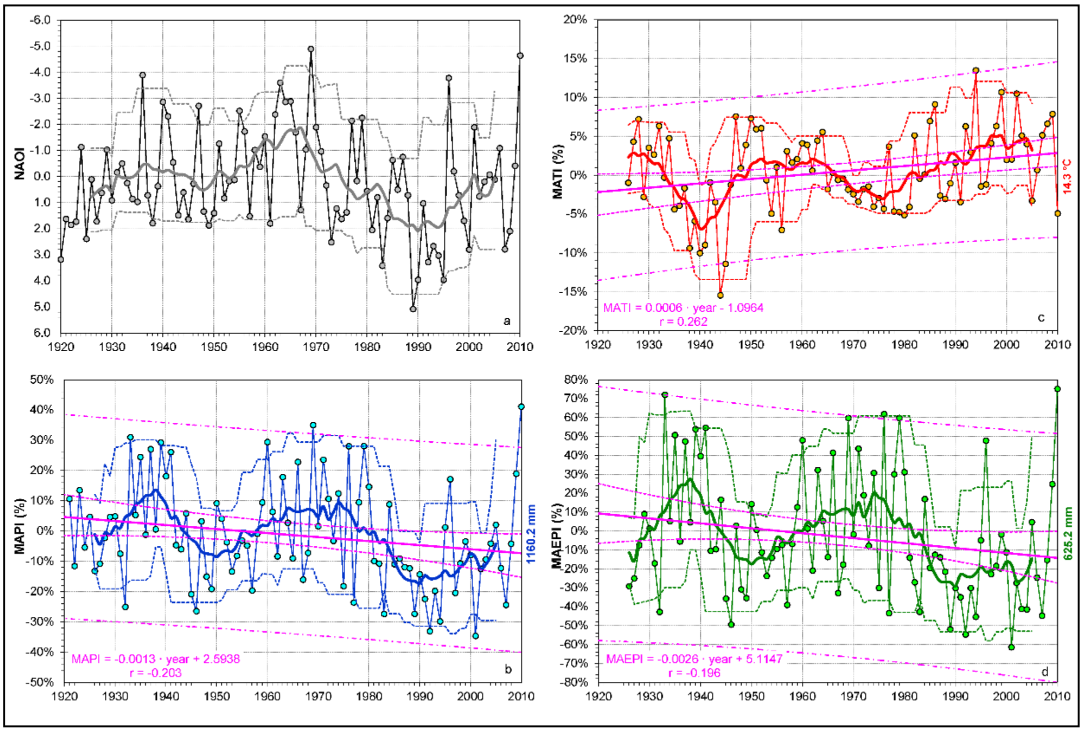

Fig. 5/1- Time series of a) winter NAOI time series monitored between Lisbon (Portugal) and Stykkisholmur/Reykjavik (Iceland). b) MAPI; c) MATI; d) MAEPI. Key to symbols: continuous magenta lines = linear trend of the whole time series (equation and coefficient of correlation in the lower left corner); dashed magenta lines = 95% confidence interval of the expected mean value; dash-dotted magenta lines = 95% prediction interval of the expected value; continuous thick line = 11-year moving average centred on the sixth year; dashed lines = 11-year moving 5th and 95th percentiles centred on the sixth year; number on right side of the graphs = absolute mean value of the whole time series (De Vita et alii, 2012).

Analyzing the 11 year moving average of MAPI, MAEPI, MATI, MAEI and MARI was found a strong overlapping of the peaks with NAOI (Fig. 5/2). To verify the correlation between the indexes, a cross correlation analysis was carried out using raw data and filtered data. For MAPI, the highest value of correlation was found at time lag of zero both with raw data($r = -0.422$; Prob. t-Student < 0.1%) and filtered data ($r = -0.767$; Prob. t-Student < 0.1%) (Figs 4 and 5, De Vita et alii, 2012). Similar results were found also for MAEPI, MATI, MAEI and MARI (Allocca et alii, 2012).
MADI of Sanità di Caposele spring displays a decrease of -14% was found respect to the mean value (3.95 m^3/s) ranging from +38% (1941) and -25% (2002) (Fig. 6, De Vita et alii, 2012). Considering the 11-year moving average the same trend observed for NAOI, MAPI, MATI and MAEPI was recognised with two positive phase (1930 – 1944 and 1958-1978) and three negative periods (before 1930, 1944-1958 and 1980-2005). The variability of the filtered time series of MADI is higher (45%) during negative NAO stages and lower (25%) in the positive NAO stages (Fig. 7, De Vita et alii, 2012). As done for the climate indexes, even for MADI were analyzed linear and 11-year moving average trends and correlation with NAOI.
MADI and NAOI, coherently with other climate parameters, show a good co-movement and a strong correlation with raw data ($r = -0.506$) and with 11-year moving average data ($r = -0.780$) (Fig. 8, De Vita et alii, 2012). The same results are obtained considering indexes calculated on Maretto and Cassano Irpino karst springs for a shorter time period (Fig. 9, De Vita et alii, 2012).

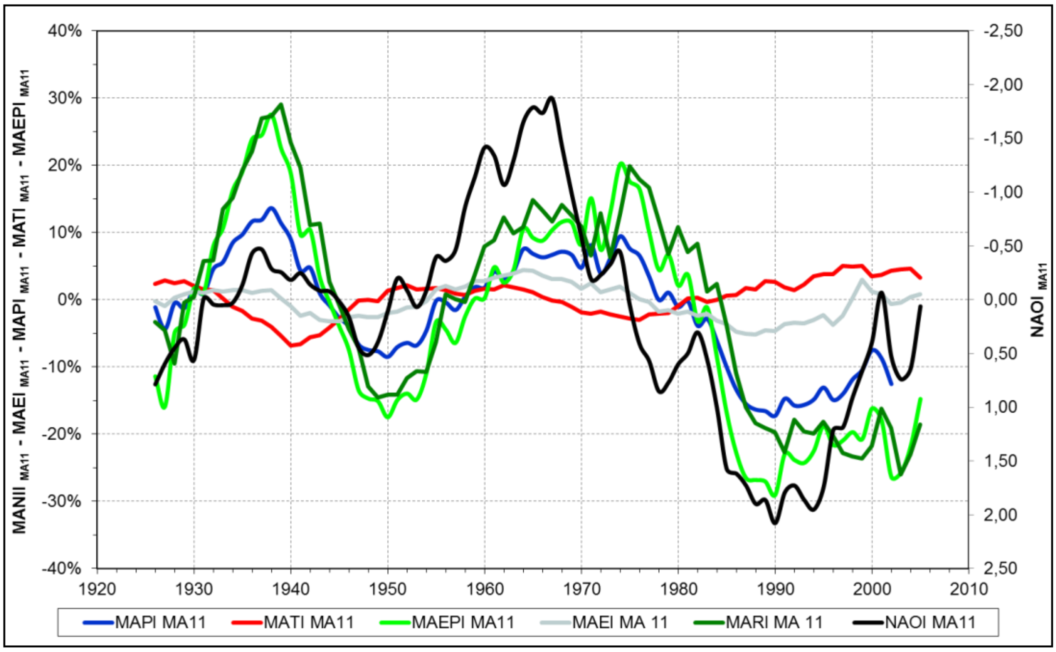

Fig. 5/2- Comparison of the 11-yr moving averages (MM11) of winter NAOI (Nord Atlantic Oscillation Index), MAPI (Mean Annual Precipitation Index), MATI (Mean Annual Temperature Index), MAEPI (Mean Annual Effective Precipitation Index), MAEI (Mean Annual Evapotraspiration Index) and MARI (Mean Annual groundwater Recharge Index) time series (Allocca et alii, 2012).

Cross-spectrum analysis of NAOI, MAPI and MADI

In order to understand the temporal structures and periodicities of NAOI, MAPI and MADI was carried out a Fourier analysis. It consists of the decomposition of a complex oscillation in simple functions finding their amplitudes and wavelengths and reconstructing their power spectra.

The observed spectrum for the winter NAOI displays principal periodogram peaks characterised by periodicities from 2 to 3 years, from 5 to 9 years, and at 30 and 45 years. At the same time periodogram's peaks of MAPI and MADI were found at 2, 5, 15, 22 and 45 years and matching with those of the NAOI 2, 3, 5 and 45 years (Fig. 5/3).
To find a periodicities of MAPI and MADI cross-spectral analysis was performed. Through it were recognised a periodicities from 2 to 3 years, from 3 to 4 years, for periods of around 5 years and 8 years and for periods from 30 to 45 years (Fig. 11, De Vita et alii, 2012).

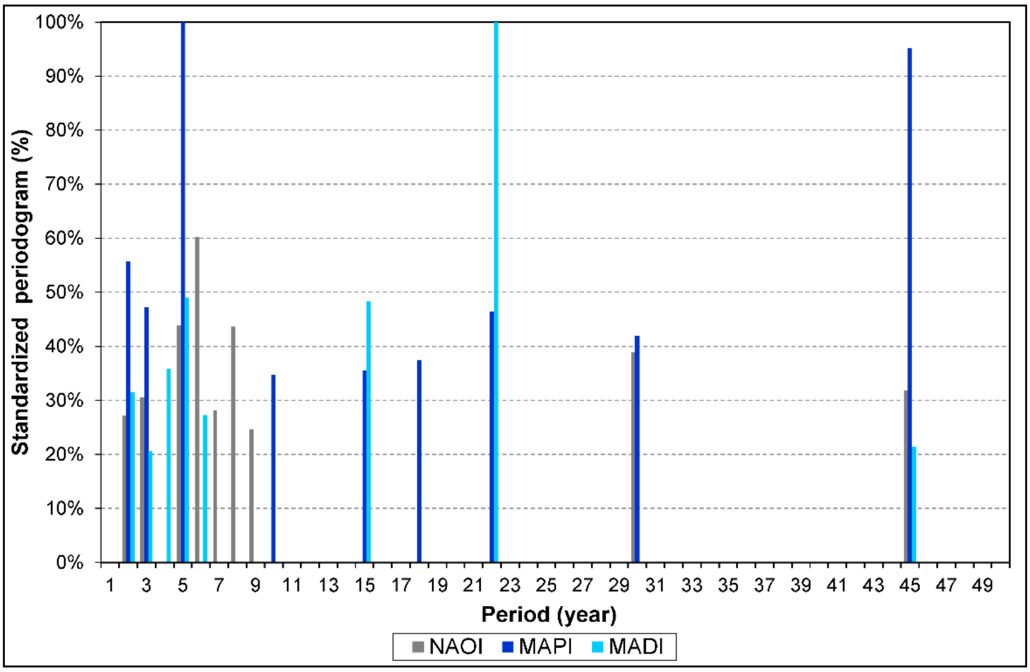

Fig. 5/3 – Largest periodogram peaks for the NAOI, MAPI and MADI time series (De Vita et alii, 2012).

Basin and mean-annual scale

Lithology, soil type, land use and geomorphological features

Analyzing the regional hydrogeological map of the southern Apennines, karst aquifer are made up of limestone, dolomitic and marly units. Specifically, the four sample karst aquifers were representative for extension and outcropping lithology: Matese (a) (120 km^2; 97% limestone and 3% dolomite); Accellica (a) (35 km^2; 68% dolomite and 32% limestone); Terminio (167 km^2; 100% limestone) and Cervialto (129 km^2; 98% limestone and 2% dolomite) (Fig. 3/1).
The prevailing category of soil covering the four sample karst aquifers is the loamy sand (LS), with an extension of about the 90% of the total area. Only for Terminio karst aquifer there is a percentage of the 14% of sandy loam coming from the accumulation of finest ash fall deposits (Fig. 5/4a). These results are consistent with the analysis of the other 36 karst aquifers for which the soils are homogeneous with sand in every category (Fig. 3a, Allocca et alii, 2014).
For the land use, the most significant category is the woodland with an extension of about 85%, followed by the meadowland (14%). Only small percentage of territory are occupied by areas without vegetation and urban areas (Fig. 5/4b). This distribution reflects the situation observed for the other aquifers. In fact, considering the 40 aquifers, the average woodland area

is 69%, meadowland 25%, areas without vegetation 5%, urban areas 1% (Fig. 3b, Allocca et alii, 2014).
The cumulative distribution of the slope angle were similar across the sample (Fig. 5/4c) and other (Fig. 3c, Allocca et alii, 2014) aquifers with a median value of 25°. Among the higher classes of slopes, the most frequent is the 30-35°.
Different extensions of the endorheic areas characterizes the sample aquifers: 0% Acellica (a); 20% Cervialto; 35% Matese (a); 43% Terminio (Fig. 5/4d). The same range was observed also for the other aquifers with maxima located in the northern and southern parts of the study area (Fig. 3d, Allocca et alii, 2014).

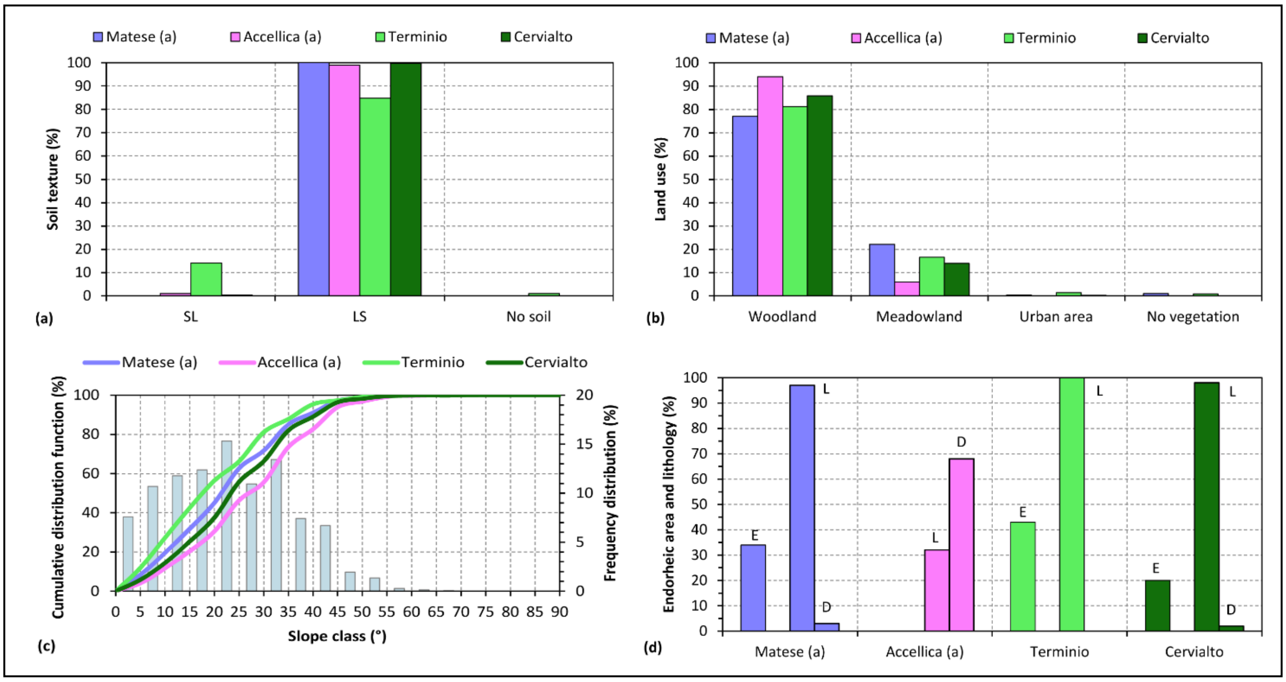

Figure 5/4 – Soil texture type, land use and geomorphological characteristics of the four sample karst aquifers. (a) Soil texture frequency (SL Sandy Loam, LS Loamy Sand. (b) Land use frequency. (c) Slope of karst aquifers frequency. (d) Summit endorheic and plateau areas frequency (E) and lithology (L = limestone; D = dolomite) (from Allocca et alii, 2014).

Annual Precipitation minus actual evapotranspiration (P-ETR)

Even though the spatial distribution of the rain gauge stations and of the air temperature stations seems to be homogeneous over the territory, the distribution respect to the altitude is strongly inhomogeneous. Comparing the distribution of karst area and the elevation of the monitoring stations, the 50% of the area lies at an altitude between 800 and 2200 m a.s.l. but in this fraction where only 10% of rain gauge and air temperature stations are. This lack of data at high altitude is a crucial issue to solve (Fig. 4, Allocca et alii, 2014).
To overcome the lack of stations at high altitude were identified three homogenous precipitation zones based on a correlation between P-ETR and elevation. An upwind zone, extending from the coastline to the principal Apennine morphological divide, and two downwind zones eastward of the same divide were identified, considering the orographic barrier effect and the rain shadowing effect. For each zone, was found a linear correlation between P-ETR and elevation, weighted on the years of functioning of the stations. These equations show an

increasing of P-ETR values with the altitude even considering three different laws (Fig. 5/5.). On the basis of these latter, a distributed model of P-ETR was created by integrating the three equations in GIS layers. The values range from 1606 mm (upwind zone) to 200 (downwind zone) (Fig. 6b, Allocca et alii, 2014).

Moreover was calculated for each rain gauge station the ratio (P-ETR)/P, finding values ranging from 0.11 to 0.82 with a mean value of 0.48. This result testified the great importance of the evapotranspiration effect controlled by spatial variability of both mean annual air temperature and precipitation (Fig. 6c, Allocca et alii, 2014).

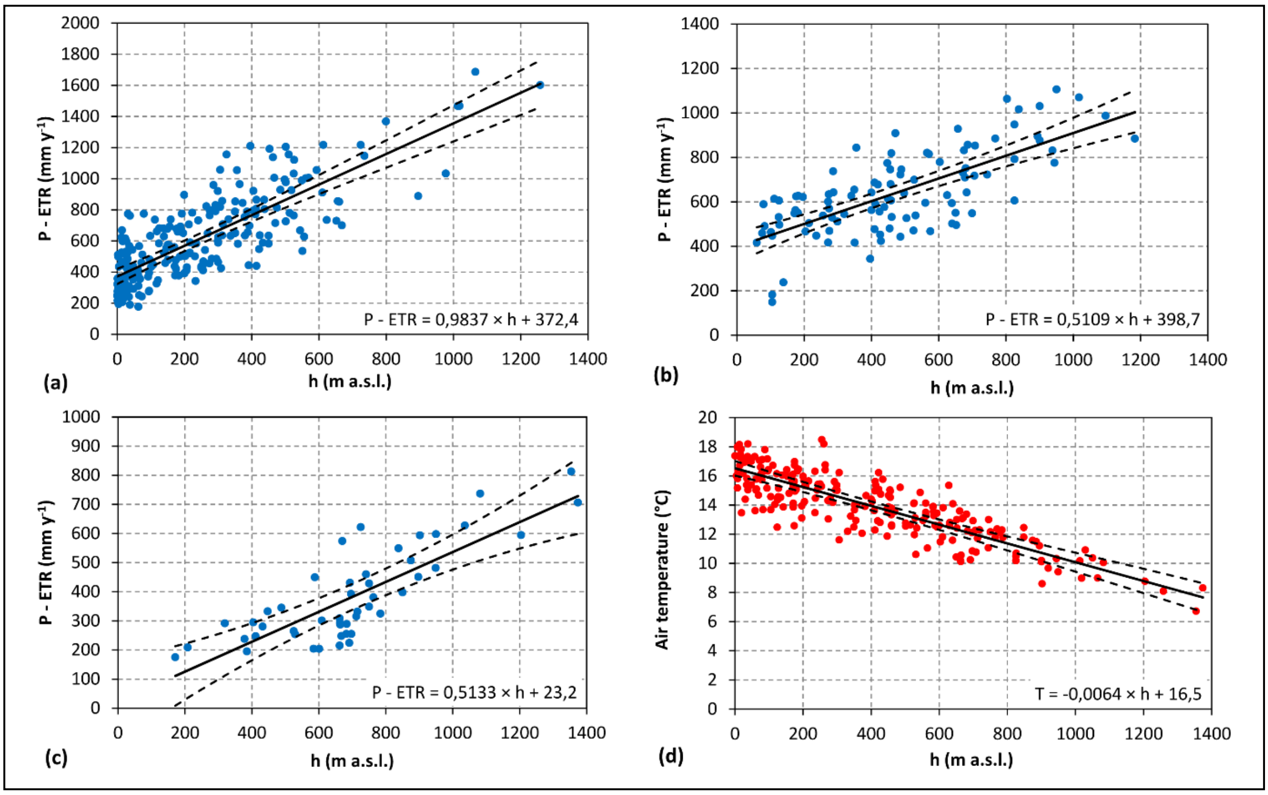

Fig. 5/5 – Linear correlations and confidence limits (95%) between mean annual P-ETR and altitude for upwind zone (a), first downwind zone (b) and second downwind zone (c). The correlation between mean annual air temperature and altitude is also shown (d) (Allocca et alii, 2014).

AGRC and AGRCS estimations and regional assessment of groundwater recharge

AGRC and AGRCs were estimated for the four sample aquifers also taking into account uncertainties due to the linear estimation of P-ETR (95% confidence limits) . Considering the obtained mean value, similar AGRC value were found for Termino (79%), Cervialto (71%) and Matese (a) (69%) whereas a value of 50% was found for Accellica (a). This difference appears to be correlated to the different lithology and the lack of endorheic area and summit plateau for Accellica (a). Corresponding AGRCs and ARC values were estimated as ranging from 50% to 64% and from 50% to 36%, respectively (Tab. 5/1) (Fig. 7, Allocca et alii, 2014).

ID	Karst aquifer	Area (km^2)	Summit plateau / endorheic area	$V_{outflow}$ (10^6 m^3 y^{-1})	V_{inflow} (10^6 m^3 y^{-1})	AGRC (%)	$AGRC_S$ (%)	ARC (%)
17a	Matese (a)	120	34	95.2	138.1	69	52	48
27	Terminio	167	43	169.7	213.3	79	64	36
31a	Accellica (a)	35	0	18.3	36.9	50	50	50
32	Cervialto	129	20	126.1	178.4	71	63	37

Tab. 5/1 - AGRC and mean $AGRC_S$ estimation for the investigated sample karst aquifers. Values are related to the mean value of the P-ETR linear regression models with altitude (Allocca et alii, 2014).

To regionalize the results of the estimation of the AGRC, a multivariate analysis was carried out between AGRC and the studied parameters (limestone area, summit plateau and endorheic area, woodland area, loamy sand soil type area and mean slope angle). A correlation was found for limestone (L) and summit plateau/endorheic areas (E) and, through a multiple linear regression, was calculated an equation to correlate these variables.

$$AGRC = 47.99 + 0.08L + 0.51E \qquad (5.1)$$

which was statistically significant (r^2 = 0.968; Prob. F-Fisher = 3.0%; Standard errors of 5.92, 0.06 and 0.07 for the intercept, first and second coefficient, respectively).
Using the equation AGRC and $AGRC_S$ were assessed for the 40 regional karst aquifers. The minimum value was 48% (Circeo) and the maximum 78% (Terminio) with a mean of 59%.

ID	Karst aquifer	Area (km^2)	Mean annual P-ETR (mm)	Limestone area (%)	Summit plateau and endorheic area (%)	AGRC (%)	$AGRC_S$ (%)	ARC (%)	Mean annual groundwater recharge (10^6 m^3 y^{-1})	Mean annual groundwater outflow (10^6 m^3 y^{-1})
1	Cerella	137	738	100	0	56	56	44	56.6	-
2	Simbruini	1075	896	94	12	62	57	43	597.2	-
3	Cornacchia	723	940	90	7	59	56	44	401.0	-
4	Marsicano	204	845	94	5	58	56	44	100.0	-
5	Genzana	277	814	10	34	66	49	51	148.8	-
6	Rotella	40	800	100	40	77	62	38	24.6	-
7	Porrara	63	753	100	25	69	59	41	32.7	-
8	Lepini	483	990	100	2	57	57	43	272.6	400.5
9	Colli Campanari	88	702	0	12	54	48	52	33.4	-
10	Capraro	70	586	0	5	51	48	52	20.9	-
11	Campo	16	692	0	13	55	48	52	6.1	-
12	Circeo	6	548	0	0	48	48	52	1.6	-
13	Ausoni	822	835	99	15	64	58	42	439.3	507.7
14	Venafro	362	796	74	11	60	55	45	172.9	269.3
15	Totila	183	535	0	8	52	48	52	50.9	-
16	Maio	93	706	98	12	63	58	42	41.4	-
17a	Matese (a)	120	1151	97	34	74	60	26	102.2	95.2
17b	Matese (b)	480	1151	65	15	61	55	39	303.8	375
18	Tre confini	28	887	0	4	50	48	52	11.6	-
19	Moschiaturo	85	700	0	7	51	48	52	38.5	-
20	Massico	29	719	89	0	55	55	45	11.2	-

21	Maggiore	157	935	99	0	56	56	44	63.2	56.7
22	Camposauro	50	646	99	4	58	56	44	27.1	-
23	Tifatini	80	1212	90	2	56	56	44	28.9	25.2
24	Taburno	43	775	81	4	57	55	45	29.7	-
25	Durazzano	52	983	100	0	56	56	44	22.6	-
26	Avella	334	1277	100	9	61	57	43	200.3	-
27	Terminio	167	565	100	43	78	62	38	166.3	169.7
28	Capri	9	868	93	0	56	56	44	2.8	-
29	Lattari	244	734	75	0	54	54	46	114.4	-
30	Salerno	46	1055	13	0	49	49	51	16.5	21.1
31a	Accellica (a)	35	1055	32	0	51	51	49	18,8	18.3
31b	Accellica (b)	171	1383	33	0	51	51	49	92.0	107.6
32	Cervialto	129	776	98	20	67	58	42	119.5	126.1
33	Polveracchio	117	1162	81	0	55	55	45	80.9	103.1
34	Marzano	292	1225	97	13	63	57	43	142.8	-
35	Alburni	254	1179	99	42	78	62	38	230.2	233.4
36	Cervati	318	859	81	13	62	56	44	241.5	220.8
37	Motola	52	965	100	4	59	57	43	36.2	37.8
38	Maddalena	307	785	59	21	64	54	46	168.8	97.8
39	Forcella	217	738	86	5	58	56	44	121.5	-
40	Bulgheria	100	896	68	1	54	54	46	42.4	42.5

Tab. 5/2- Data and estimations of AGRC, $AGRC_s$, ARC and mean annual groundwater recharge for karst aquifers of the study area (Allocca et alii, 2014).

Multiplying the AGRC value by the mean annual P-ETR, was possible to estimate the recharge for each karst aquifer (Tab. 5/2). In addition, an original map of the distribution of the mean annual recharge for karst aquifers of southern Apennines was created by the overlay of P-ETR, $AGRC_S$ and endorheic area maps (Fig. 8, Allocca et alii, 2014).
To validate this result, the predicted recharge was compared to the non-systematic measure of outflow for 18 of the 40 aquifers. The resulting residuals between the predicted recharge and measured outflow was considered to be negligible, ranging between 0% and 10% (Fig. 9, Allocca et alii, 2014).

Local and episodic scale

Aquifer response time

The water table of the perched karst aquifer during the considered year 2008 fluctuated of about 6 meters between the minimum and the maximum level (respectively +3.2 and +9.4 respect to an arbitrary datum lying at 1165 m a.s.l.)(Fig. 5/6a). The minimum level is recorded at 2nd of October, at the end of the main recession period, coincident with the summer season, when precipitation are very low (2.4 mm in July; 6.2 in August). The maximum level is at the beginning of December. During the recession periods, water-table levels were observed to decrease gradually (Fig. 2a) and to rise rapidly after rainfall events, with a velocity up to 0.92 m day^{-1}.
Comparing precipitation and water table data, there is a strong correlation with a fast response of the aquifer. In order to estimate the lag time, i.e. the time between the precipitation and the respective change in the water-table, was carried out a cross correlation analysis between the

precipitation and the water table fluctuation rate (difference between water table elevation in the considered day minus the water table elevation of the previous day) (Fig. 5/6b). The maximum value of correlation was found at a lag time of 2 days (r=0.53; t-Student<0.1 %).
Analyzing the soil water content distribution, it is possible distinguish three periods with homogeneous values of θ during the year: a first from March to June with a mean value of 20%, a second, corresponding with summer season (July to September), with a mean value of 12% and a third from October to December with the higher mean value (35%).
The analysis of θ and the precipitation shows a good overlap of the peaks and a faster response of the soil to the pluviometric input, confirmed by the cross-correlation carried out between θ and precipitation that reveals the strongest correlation at a time lag of 0 (r=0.45; t-Student<0.1 %).

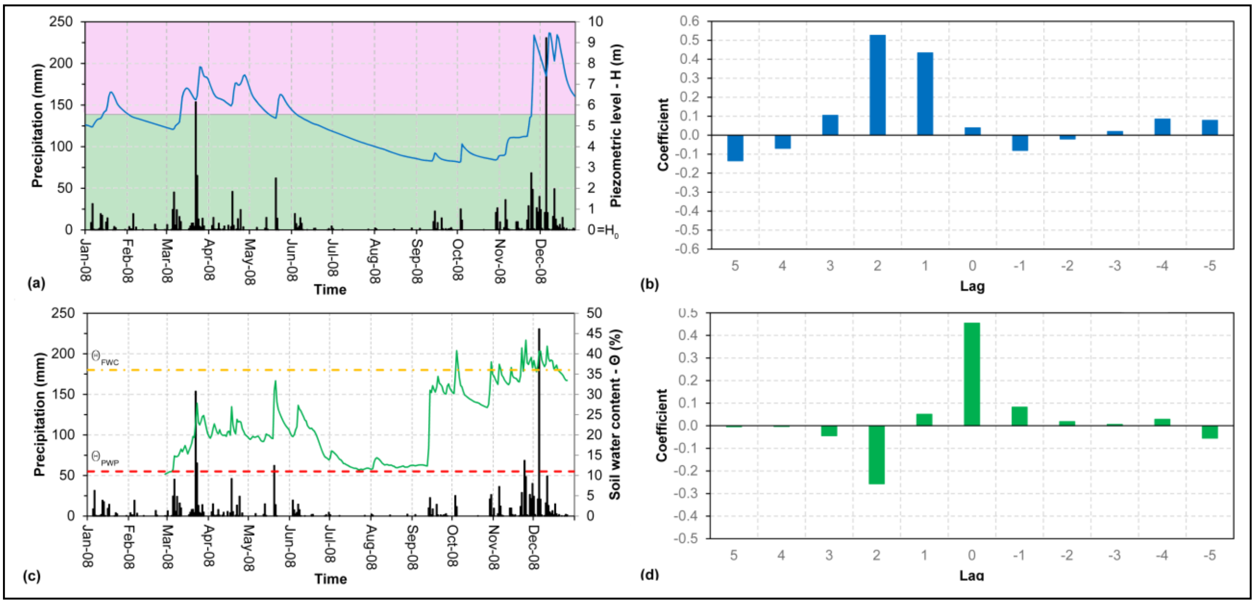

Fig. 5/6 – (a) Time series of piezometric level (blu line) and precipitation (black histogram). (b) Cross-correlation analysis between piezometric level and precipitation. (c) Time series of soil water content (green line) at 10 cm depth and precipitation (black histogram). (d) Cross-correlation analysis between soil water content at 10 cm depth and precipitation (Allocca et alii, 2015).

Episodic and annual groundwater recharge assessment

The MRC algorithm that identified automatically subsets corresponding to recessional limbs, namely all phases in which water-table levels decreased following a lack of precipitation. Considering the distribution of dH/dt vs H points, was fitted a third order polynomial curve (r = 0.906; prob t-Student < 0.1%) (Fig. 5/7). It is possible to split the entire dataset in two parts reflecting the different lithology. In detail, for values of H lower than 5.4 m, water-table levels were considered to lie into the karst aquifer only. For greater values of H, the saturation zone was recognized to comprehend also a portion of the pyroclastic aquifer. The points in the karst part are aligned with a slope less than indicated by those in pyroclastic soil. In the karst part of the aquifer the decline rate varies from 0 to 0.05 m per day while in the pyroclastic the range is wider, going from 0.05 to 0.45.

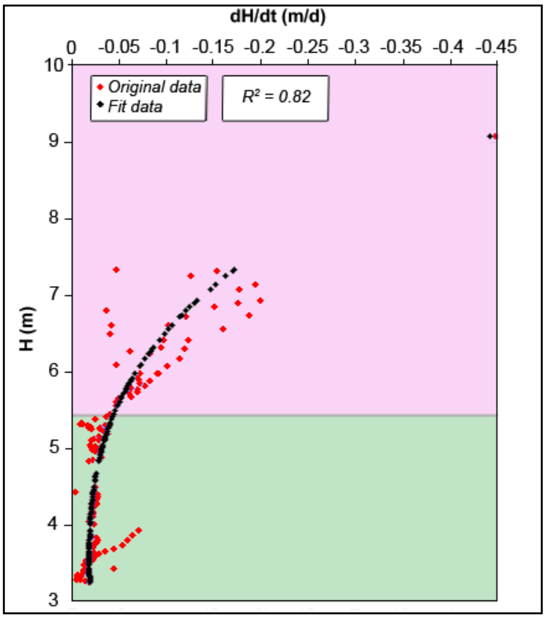

Fig. 5/7 – Master Recession Curve (Allocca et alii, 2015).

This vertical variation of the rate decline of groundwater levels, during drainage is attributable to a perched aquifer model characterized from two hydrostragraphic layers with different geometry (Fig. 1d, Allocca et alii, 2014) and thickness-volume saturated (Fig. 1c and Table 1, Allocca et alii, 2014). The layer of pyroclastic deposits, despite the higher value of effective porosity, has a thickness saturated more reduced and a higher hydraulic conductivity, if compared to the underlying layer of fractured carbonate substrate, and this leads to a higher rate of emptying during the recession phases.
Were identified 12 recharge episodes (Figs. 5 and 6, Allocca et alii, 2015) with a duration ranging from 5 to 37 days, with a mean value of 12 days(Tab. 5/3). The RPR values range from 35% to 97%, with a mean annual value of 73% (Tab. 5/3). This value is strongly consistent with the actual evapotranspiration annual value, equal to 30% of the annual precipitation, estimated through the Thornthwaite and Mater water balance ; moreover, it is not far from the Annual Groundwater Recharge Coefficient (AGRC) of about 70% calculated for that portion of the Terminio karst aquifer (Allocca et alii, 2014), at regional-annual scale.

Recharge episode	Start time (day)	End time (day)	Duration (day)	Recharge (m)	Precipitation (m)	RPR (Recharge to Precipitation Ratio)	Average storm intensity (m/d)	Max storm intensity (mm/d)	Soil water content (%)
1	04-gen	21-gen	18	0.1	0.104	0.97	0.006	31.4	-
2	05-feb	15-feb	10	0.011	0.019	0.59	0.002	19.2	-
3	03-mar	18-mar	15	0.11	0.129	0.86	0.009	45.2	-
4	21-mar	27-mar	6	0.093	0.247	0.37	0.038	153.6	23.49
5	28-mar	01-apr	5	0.014	0.017	0.87	0.003	4.6	24.16
6	05-apr	29-apr	24	0.107	0.12	0.89	0.005	46	20.45
7	18-mag	26-mag	8	0.064	0.076	0.84	0.01	62	27.78
8	10-set	16-set	5	0.019	0.033	0.57	0.006	22.4	12.42
9	01-ott	06-ott	5	0.039	0.042	0.92	0.008	25	30.51
10	27-ott	03-dic	37	0.261	0.404	0.65	0.011	68.4	34.01
11	05-dic	10-dic	6	0.107	0.272	0.39	0.046	230.6	39.45
12	12-dic	17-dic	6	0.072	0.089	0.81	0.014	49.2	39.42

Tab. 5/3 - Characteristics of recharge episodes (Allocca et alii, 2015).

Sensitivity of RPR to antecedent soil moisture and storm intensity

The aquifer's recharge dynamics reported in Tab. (5/3), suggest that in addition to the air temperature and evapotranspiration effects, the RPR values are influenced by storm intensity and antecedent soil moisture. In fact, the two lowest RPR values calculated for the episode 4 and the episode 11, respectively equal to 37% and 39%, corresponded to the highest rainfall intensities, respectively 0.038 m day^{-1} and 0.046 m day^{-1}. Moreover, the observation of groundwater recharge episodes allowed identifying a direct relationship between antecedent soil water content and RPR coefficients, thus expecting lower RPR coefficient values in correspondence of a lower soil water content.

Through a multiple regression was found a relation between RPR, average intensity of rainfall recharging events (i) and average soil water content (Θ_{av}) (Fig. 5/8).

The equation ($r = 0.894$; prob. t-Student < 0.1%) is:

$$\mathrm{RPR}(\%) = 0.67 + 0.8 \cdot \theta_{av} - 13.41 \cdot \mathrm{i} \quad (5.2)$$

Its form confirms the opposite role played by both independent variables (Θ_{av} and i) and the greater sensitivity of the RPR coefficient to average intensity of rainfall recharging events (i) than to average soil water content (Θ_{av}).

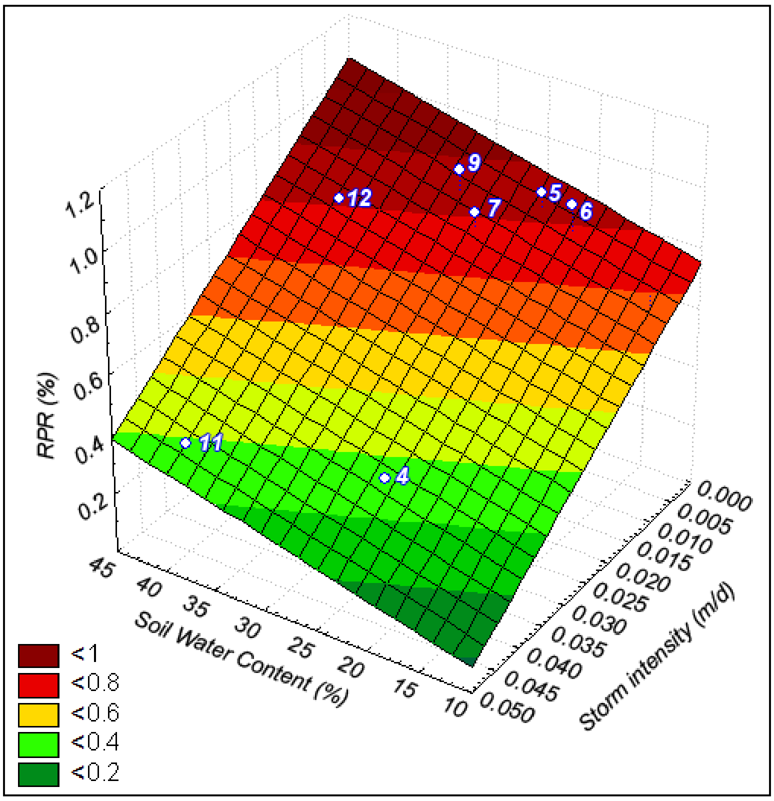

Fig. 5/8– Multiple linear regression between RPR, antecedent soil water content and storm intensity. The colors represent the RPR values (%) (Allocca et alii, 2015).

Soil water balance

At annual scale, the potential evapotranspiration is about 591.6 mm, equal to 33% of the precipitation, whereas the actual evapotranspiration amount to 542.8 mm, corresponding at

30% of the annual precipitation. The latter value is almost complementary to the mean RPR (73%) calculated with the EMR method, confirming the goodness of both methods adopted.
At monthly scale, from January to July and from September to December, the actual evapotranspiration is always maximum, and equal to potential evapotranspiration (Fig. 5/9). In these periods, the comparison between monthly precipitation and monthly evapotranspiration evidence the condition of soil water surplus and, hence, recharge for aquifer. Conversely, in August, the actual evapotranspiration is less than the potential evapotranspiration, and therefore there is a condition of soil water deficit.
To confirm the importance of antecedent soil moisture and of the evapotranspiration on the recharge process, it is possible to highlight that the 8th recharge episode (Tab. 5/3), showing one of lowest RPR, occurs in at beginning of September when there is the maximum effect of evapotranspiration and there is soil water deficit, while there are highest RPR during the winter season when evapotranspiration reaches its minimum.

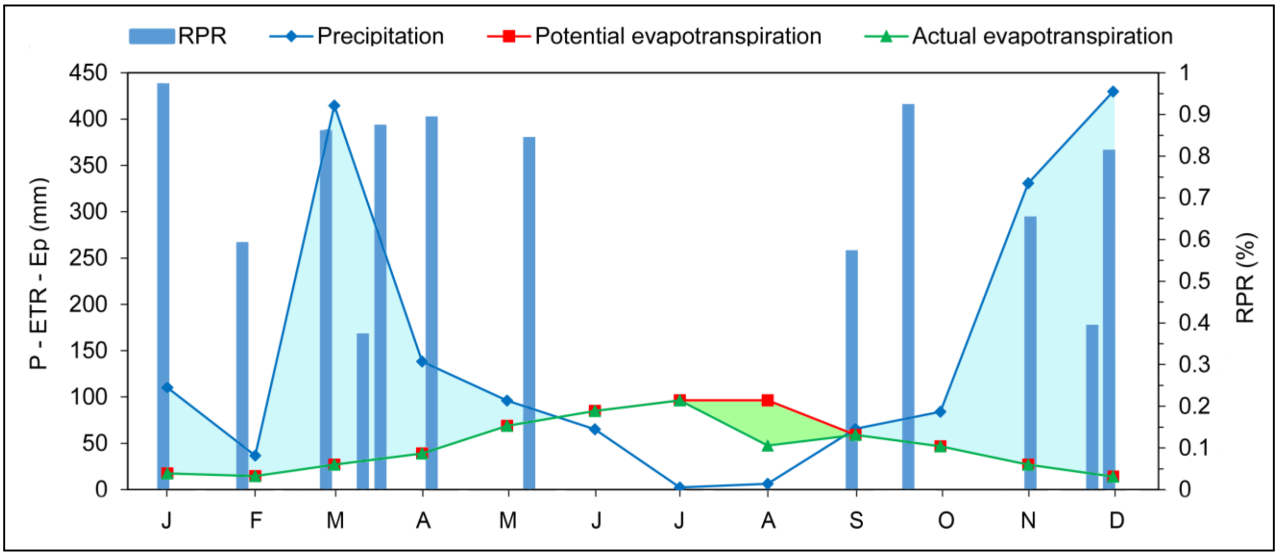

Fig. 5/9 – Comparison between precipitation (blue line), actual evapotranspiration (green line) and potential evapotranspiration (red line). The shaded area represent the soil water surplus (blu) and soil water deficit (green) (Allocca et alii, 2015).

6. Discussion and conclusions

Regional and mean-annual scale

In the southern Apennines, a complex cyclical periodicity of rainfall patterns that was mainly teleconnected with the North Atlantic Oscillation was discovered, confirming that previously observed for other regions of western Europe and North America (Hurrell and van Loon, 1997; Vincente-Serrano and Trigo, 2011). The significant correlations found between the NAOI and the examined hydrological time series demonstrated the strong influence of the NAO on the hydrological cycle of the karst aquifers. Therefore, the winter NAOI can be considered as an effective proxy to forecast the decadal variability of the groundwater resources in Mediterranean karst areas, allowing the modelling, forecasting and planning of their sustainable management.

The analysis of the temporal structure of the time series showed stronger correlations for periodicities varying from the interannual to decadal time scales, with the greatest correlation at the periodicity from 30 to 45 years.

Moreover, the correlations can be conceived as a basis in formulating groundwater recharge models of carbonate karst aquifers and in planning appropriate management scenarios of aqueduct feeding from the interannual to the decadal time scales.

Basin and mean-annual scale

The AGRC estimation appears an acceptable first step to estimate the groundwater recharge of karst aquifers in order to carry out water budget at the annual scale and to manage water resources, also considering effects of climate changes. Moreover, the methodology can be conceived as a first step to overcome the lack of spring discharges and piezometric levels time series and a deeper understanding of groundwater hydrology in karst aquifers.

The estimations of the AGRC for four sample karst aquifers varied from 50% to 79% with a mean value of 67%. These results are similar to those estimations carried out previously by others Italian (Celico, 1988; Allocca, 2007) and comparable with those of European authors (Burdon, 1965; Vilimonovic, 1965; Drogue, 1971; Bonacci, 2001).

The proposed approach highlights another complementary aspect related to the estimation of annual runoff along slope areas, which is particularly relevant for the management of surficial water resources. The calculated mean ARC values varying from 36% to 50% can be approximately compared with those determined for Dinaric karst aquifers (Horvat and Rubinic, 2006) and some river basins of the southern continental Italy (Del Giudice et alii, 2013).

Local and episodic scale

Main result of the application of the EMR method is the estimation of a mean RPR value, equal to 73%. This value is very close to the 70% estimated for that portion of the Terminio karst aquifer by Allocca et alii, 2014 on a regional scale using an integrated approach based on hydrogeological, hydrological, geomorphological, land use and soil cover analyses.

Moreover, the results coming from the estimation of the actual evapotranspiration confirm the goodness of the methods and permit us to discretize the different components of the soil water balance. In fact, the calculated actual evapotranspiration (30%) matches well with the 73% of the mean RPR. Considering geomorphological and hydrogeological characteristics of the study area, the evapotranspiration is the only loss of water. Therefore, soil water budget is verified.
The good results obtained from the application of the EMR codes to a complex hydrogeological situation represent a progress in the case studies. So far, the method was applied only in case with homogeneous porous aquifers: Masser site, Pennsylvania and the glacial aquifer of Silstrup in Denmark (Nimmo et alii, 2015). The code confirmed to be a valid tool for quantify the recharge process at detailed scale of observation and minimize errors coming from overestimation typical of WTF methods.
The sensitivity of RPR to storm intensity and antecedent soil water content is a reason to deep the understanding of the influence of hydrological and climates variables on the recharge process.

References

Alcalá F.J. and Custodio E., 2008. *Using the Cl/Br ratio as a tracer to identify the origin of salinity in aquifers in Spain and Portugal* . Journal of Hydrology 359, 189-207.

Alcalá F.J., Cantón Y., Contreras S., Were A., Serrano-Ortiz P., Puigdefábregas J., Solé-Benet A., Custodio E. and Domingo F., 2011. *Diffuse and concentrated recharge evaluation using physical and tracer techniques: results from a semiarid carbonate massif aquifer in southeastern Spain*. Environmental Earth Sciences 62 (3), 541e557. doi:10.1007/s12665-010-0546-y.

Aller L., Bennet T., Lehr J.H., Petty R.J. and Hackett G., 1987. *DRASTIC: a standardized system for evaluating groundwater potential using hydrogeological settings*. NWWA/EPA SER., EPA 600/2-87-035, P. 455.

Allocca V., Celico F., Celico P., De Vita P., Fabbrocino S., Mattia S., Monacelli G., Musilli I., Piscopo V., Scalise A. R, Summa G. and Tranfaglia G., 2007. *Illustrative Notes of the Hydrogeological Map of Southern Italy*. Ist. Poligrafico e Zecca dello Stato, Rome, 211 pp.

Allocca V., Celico F., Petrella E., Marzullo G. and Naclerio G., 2008. *The role of land use and environmental factors on microbial pollution of mountainous limestone aquifers*. Environmental Geology, 55, 277-283.

Allocca V., Manna F. and De Vita P., 2014. *Estimating annual groundwater recharge coefficient for karst aquifers of the southern Apennines (Italy)*. Hydrology Earth System Sciences, 18(2), 803–817.

Andreo B., Vías J., Durán J.J., Jiménez P., López-Geta J.A. and Carrasco F., 2008. *Methodology for groundwater recharge assessment in carbonate aquifers: application to pilot sites in southern Spain*. Hydrogeology Journal, 16, 911-925.

Andreu J.M., Alcalà F.J., Vallejo A. and Pulido-Bosch A., 2011. Recharge to mountainous carbonated aquifers in SE Spain: Different approaches and new challenges. J. Arid Environ., 75(12), 1262–1270.

Aquilina L., Ladouche B. and Dorfliger N., 2005. *Recharge processes in karstic systems investigated through the correlation of chemical and isotopic composition of rain and spring-waters*. Appl. Geochem., 20(12), 2189–2206, doi:10.1016/j.apgeochem.2005.07.011.

Arnold J.G. and Fohrer N., 2005. *SWAT2000: Current capabilities and research opportunities in applied watershed modelling*. Hydrological Processes 19(3), 563–572.

Arnold J.G., Srinivasan R., Muttiah R.S. and Williams J.R., 1998. *Large-area hydrologic modelling and assessment: Part I. Model development*. Journal of the American Water Resources Association 34(1), 73–89.

Atkinson T.C., 1977. *Diffuse flow and conduit flow in limestone terrain in the Mendip Hills, Somerset (Great Britain)*. Journal of Hydrology, 35, 93-110.

Amatya, D. M., Jha, M. K., Williams, T. M., Edwards, A. E., and Hitchcock, D. R., 2011a. *SWAT-based streamflow and embayment modeling of a karst affected Chapel Branch watershed, SC.* Trans. ASABE, 54(4), 1311–1323

Baffaut, C., and Benson, V. W., 2009. *Modeling the flow and pollutant transport in a karst watershed with SWAT*. Trans. ASABE, 52(2), 469–479.

Bakalowicz, M., Blavoux, B. and Mangin, A., 1974. *Apports du traçage isotopique naturel à la connaissance du fonctionnement d'un système karstique - teneurs en oxygène 18 de trois systèmes des Pyrénées, France*. Journal of Hydrology, 23, 141-158.

Bakalowicz M., 1995. *La zone d'infiltration des aquifères karstiques. Méthodes d'étude. Structure et fonctionnement*. Hydrogéologie, 4, 3-21.

Bakalowicz M., 2003. *Epikarst, the skin of karst*. Conference on Epikarst, Shepherdstown, West Virginia. The Karst Water Institute, Special publication, 9, 16-22.

Bakalowicz M., 2004. *Comments on "Carbon isotope exchange rate of DIC in karst groundwater by R. Gonfiantini and G.M. Zuppi"*. Chem Geol., 204(1–2),183–185.

Bandini A., 1931. *Tipi pluviometrici dominanti sulle regioni italiane*. Il Servizio Idrografico Italiano. Ministero dei Lavori Pubblici, Roma, (in Italian).

Bedinger M.S., 1966. *Electric analog study of cave formation*. Nat. Speleol. Soc. Bull., 28 (3), 127-132.

Bellot J., Sánchez J.R., Chirino E., Hernández N., Abdelli F. and Martinez J.M., 1999. *Effect of different vegetation type on the soil water balance in semiarid areas of South Eastern Spain.* Physics and Chemistry of the Earth (B) 24, 353–357.

Bellot J., Bonet A., Sánchez J.R. and Chirino E., 2001. *Likely effects of land use changes on the runoff and aquifer recharge in a semiarid landscape using a hydrological model*. Landscape and Urban Planning 55, 41–53.

Blasco O., San Roman J. and García Vera M.A., 2004. *Modelado numerico de flujo de la Unidad Hidrogeologica de Gallocanta (Cuenca del Ebro).* In *VIII Simposio de Hidrogeología*, ed. Asociacion Espanola de Hidrogeologos (AEH), 513–523.

Bonacci O., 2001. *Montly and annual effective infiltration coefficients in Dinaric karst: example of the Gradole karst spring catchment*. Hydrological Sciences - Journal des Sciences Hydrologiques, 46, 2.

Bonacci O., 1993. *Karst springs hydrographs as indicators of karst aquifers*. J. Hydrol. Sciences, 38(1-2), 51-62.

Burdon D.J., 1965. *Hydrogeology of some karstic areas of Greece. Actes de Colloque de Dubrovnik sur l'Hydrologie des roches calcaires fessures*. A.I.H.S.-UNESCO, 73, 308-317.

Cantón Y., Villagarcía L., Moro M.J., Serrano-Ortíz P., Were A., Alcalá F.J., Kowalski A.S., Solé-Benet A., Lázaro R. and Domingo F., 2010. *Temporal dynamics of soil water balance components* *in a karst range in southeastern Spain: estimation of potential recharge*. Hydrological Sciences Journal 55, 737-753.

Carter J. and Driscoll D., 2006. *Estimating recharge using relations between precipitation and yield in a mountainous area with large variability in precipitation*. J. Hydrol., 316, 71–83, doi:10.1016/j.jhydrol.2005.04.012.

Celico P. , 1978. *Schema idrogeologico dell'Appenninico carbonatico centro-meridionale.* Mem. e Ist. Geol. Appl. Napoli, 14, 1-97.

Celico P., 1981. *Relazioni tra idrodinamica sotterranea e terremoti in Irpinia (Campania).* Rendiconti Società Geologica Italiana, 4, 103-108.

Celico P., 1983a. *Idrogeologia dei massicci carbonatici, delle piane quaternarie e delle aree vulcaniche dell'Italia centro-meridionale (Marche e Lazio meridionale, Abruzzo, Molise e Campania).* Quaderni CASMEZ, 4/2, 1-225.

Celico P. , 1983b. *Le risorse idriche sotterranee dell'Appennino carbonatico centro-meridionale.* Idrotecnica, 1, 3-17.

Celico P., 1986. *Prospezioni idrogeologiche*. Vol. 1. Liguori Editore, Napoli.

Celico P., 1988. *Prospezioni idrogeologiche*. Vol. 2. Liguori Editore, Napoli.

Celico F., 1996. *Vulnerabilità all'inquinamento degli acquiferi e delle risorse idriche sotterranee in realtà idrogeologiche complesse: i metodi DAC e VIR*. Quad. di Geol. Appl., 1, 93-116.

Celico F., Celico P., De Vita P. and Piscopo V., 2000. *Groundwater flow and protection in the Southern Apennines (Italy)*. Hydrogéologie. 4, 39-46.

Celico F. and Petrella E., 2008. *Updated hydrogeological model of the north-western part of Matese carbonate aquifer - preliminary study*. Mem. Descr. Carta Geol. d'It. LXXVII (2008), 177 - 182 figg. 2.

Celico, F., Naclerio, G., Bucci, A., Nerone, V., Capuano, P., Carcione, M., Allocca, V. and Celico, P. (2010). *Influence of pyroclastic soil on epikarst formation: a test study in southern Italy.* Terra Nova, 22, 110–115. doi: 10.1111/j.1365-3121.2009.00923.x

Chirino E., 2003*. Influencia de las precipitaciones y de la cubierta vegetal en el balance hídrico superficial y en la recarga de acuíferos en clima semiárido.* Ph.D. Thesis, University of Alicante. Spain, 387.

Civita M., 1988. *Le Carte della Vulnerabilità degli acquiferi all'inquinamento*. In: Proposta di normativa per l'istituzione delle fasce di rispetto per le opere di captazione di acque sotterranee. Pubbl. n. 75 C.N.R.-G.N.D.C.I., Ed. V. Francani, Coed. M. Civita, Geograph, Milano.

Civita M., Manzone L. and Vigna B., 1999. *Rilevamenti strutturali ed idrodinamica dei sistemi acquiferi carbonatici*. In: 1. Convegno nazionale dei giovani ricercatori in geologia applicata, Gragnano, 22-23 ottobre 1991, 327-336.

Civita M.,1994. *Le carte della vulnerabilità degli acquiferi all'inquinamento: teoria e pratica*. Pitagora Ed., Bologna.

Civita M. and De Maio M., 1997. *Un sistema parametrico per la valutazione e la cartografia della vulnerabilità degli acquiferi all'inquinamento. Metodologia e automatizzazione*. Pitagora Ed., Bologna.

Civita .M, De Maio M., 2001. *Average groundwater recharge in carbonate aquifers: a GIS processed numerical model*. 7th Conference on Limestone Hydrology and Fissured Media, Besançon, France, September 2001, 93–100.

Cook P. G. and Solomon D. K., 1997. *Recent advances in dating young groundwater: chlorofluorocarbons, 3H/3He and 85Kr.* J. Hydrol., 191, 245–265, doi:10.1016/s0022-1694(96)03051-x.

Coutagne A., 1968. *Les variations de débit en periode non influencée par les précipitations*. La Houille Blanche. Sept.– Oct., 416–436.

Coutagne A., 1954. *Study of some regional hydrometereological correlations and their algebraic interpretation* (in French).

Dar F.A., Perrin J., Ahmed S. and Narayana A.C., 2014. *Review: carbonate aquifers and future perspectives of Karst hydrogeology in India.* Hydrogeology Journal, Volume 22, 7, 1493-1506.

Davies W.E., Simpson J.H., Ohlmacher G.C., Kirk, W.S. and Newton, E.G., 1984. *Engineering aspects of karst, national atlas.* 38077-AWNA-07M- 00, 1 sheet p.

De Vita P., and Fabbrocino S., 2007. *Influence of the North Atlantic Oscillation on the climatic variability and groundwater resources in carbonate aquifers of Southern Italy*. Italian Journal of Engineering Geology and Environment, 1, 33-48.

De Vita P., Allocca V., Manna F. and Fabbrocino S., 2012*. Coupled decadal variability of the North Atlantic Oscillation, regional rainfall and karst spring discharges in the Campania region (southern Italy)*. Hydrology and Earth System Sciences, 16, 1389-1399.

Delin, G., Healy, R., Lorenz, D., and Nimmo, J., 2007. *Comparison of local- to regional-scale estimates of ground-water recharge in Minnesota, USA.* Journal of Hydrology, 334, 1-2, 231-249.

Drogue C., 1971. *Coefficient d'infiltration ou infiltration efficace, sur les roches calcaires*. Actes colloque d'hydrologie en pays calcaire, Besançon, 121-131.

Drogue C., 1974. *Structure de certains aquifères karstiques d'après les résultats de travaux de forage. (Structure of certain karst aquifers from drilling data).* CR Acad. Sc. Paris, série III (278), 2621–2624.

Drogue C., 1992. *Hydrodynamic of karstic aquifers: Experimental sites in the Mediterranea karst, Southern France.* Inter. Contr. to Hydrogeol. I.A.H., 13, 133-149.

Dunkle S. A., Plummer L. N., Busenberg E., Phillips P. J., Denver J. M., Hamilton P. A., Michel R. L., and Coplen T. B., 1993. *Chlorofluorocarbons (CCl3F and CCl2F2) as dating tools and hydrologic tracers in shallow groundwater of the Delmarva Peninsula, Atlantic Coastal Plain, United States*. Water Resour. Res., 29, 3837–3860, doi:10.1029/93wr02073.

Ebrahimi B., Mehradad P. and Mohammad R. A., 2007. *Hydrodynamic behaviour of karstic aquifers in Boroujerd, western Iran*. Hydrological Sciences, 52(1), 192-205.

Eriksson, E., and Khunakasem V.. 1969. *Chloride concentrations in groundwater, recharge rate and rate of deposition of chloride in the Israel coastal plain*. Journal of Hydrology 7, 178–179.

Fayer M.J., Gee G.W., Rockhold M.L., Freshley M.D. and Walters T.B., 1996*. Estimating recharge rates for a groundwater model using GIS*. J Environ Qual, 25, 510–518.

Fiorillo F., 2011. *Tank-reservoir drainage as a simulation of the recession limb of karst spring hydrographs*. Hydrogeology Journal, 19, 1009–1019.

Fiorillo, F., Pagnozzi, M., Ventafridda, G., 2014. *A model to simulate recharge processes of karst massifs.* Hydrological Processes DOI: 10.1002/hyp.10353.

Fleury P., Plagnes V. and Bakalowicz M., 2007. *Modelling of the functioning of karst aquifers with a reservoir model: Application to Fontaine de Vaucluse (South of France).* J. Hydrol., 345, 38–49.

Ford D. and Williams P., 2007. *Karst hydrogeology and geomorphology*. Wiley J. & Sons, Ltd, 1-576, ISBN 978-0-470-84996-5.

Frot E. and van Wesemael B., 2009. *Predicting runoff from semi-arid hillslopes as source areas* for water harvesting in the Sierra de Gador, southeast Spain. Catena 79, 83e92

Galleani L., Vigna B., Banzato C. and Lo Russo S., 2011. *Validation of a Vulnerability Estimator for Spring Protection Areas: the VESPA index.* Journal of Hydrology, 396, 233-245.

Geyer T., Birk S., Liedl R. and Sauter M., 2008. *Quantification of temporal distribution of recharge in karst systems from spring hydrographs*. J. Hydrol., 348, 452–463.

Geiger R., 1954. Landolt-Börnstein - *Zahlenwerte und Funktionen aus Physik, Chemie, Astronomie, Geophysik und Technik*, alte Serie Vol. 3, Ch. Klassifikation der Klimate nach W. Köppen. – Springer, Berlin. 603–607.

Goldscheider N. and Drew D., 2007*. Methods in karst hydrogeology.* Taylor & Francis, London, 1-264.

Grindley J., 1967. *The estimation of soil moisture deficits*. Meterological Magazine, 96, 97–108.

Guardiola-Albert C., Martos-Rosillo S., Pardo-Igúzquiza E., Durán Valsero J. J., Pedrera A., Jiménez-Gavilán P. and Liñán Baena C., 2014. *Comparison of Recharge Estimation Methods During a Wet Period in a Karst Aquifer*. Groundwater. doi: 10.1111/gwat.12310.

Gunn J., 1983. *Point recharge of limestone aquifers - a model from New Zealand karst.* Journal of Hydrology, 61, 19-29.

Gunn J., 1981. *Hydrological processes in karst depressions*. Zeit. Geomorph. NF, 25, 313-331.

Hargreaves G.H. and Samani Z.A., 1982. *Estimating potential evapotranspiration*. Tech.Note, Journal of Irrigation and drainage Engineering, ASCE 108(3), 225–230.

Hartmann A., Lange J., Weiler M., Arbel Y. and Greenbaum N., 2012. *A new approach to model the spatial and temporal variability of recharge to karst aquifers.* Hydrology Earth System Sciences, 16, 2219-2231, 2012.

Hartmann A., Gleeson T., Rosolem R., Pianosi F., Wada Y., and Wagener T., 2014. *A simulation model to assess groundwater recharge over Europe's karst regions.* Geosci. Model Dev. Discuss., 7, 7887–7935.

Healy, R.W. and Cook, P.G., 2002. *Using groundwater levels to estimate recharge*. Hydrogeology Journal, 10, 91–109.

Heppner, C., and Nimmo, J., 2005. *A computer program for predicting recharge with a master recession curve*. U.S. Geological Survey Scientific Investigations Report 2005-5172, 1-8.

Heppner, C.S., Nimmo, J.R., Folmar, G.J., Gburek, W.J., and Risser D.W., 2007. *Multiple-Methods Investigation of Recharge at a Humid-Region Fractured Rock Site, Pennsylvania, USA*. Hydrogeology Journal, 15, 5: 915-927.

Horton, R.E. 1933. *The role of infiltration in the hydrologic cycle.* Transactions of the American Geophysical Union 14, 446–460.

Horvat B. and Rubinic J., 2006. *Annual runoff estimation - an example of karstic aquifers in the transboundary region of Croatia and Slovenia.* Hydrological Sciences Journal, 51, 2, 314-324.

Houze R.A., 2012. *Orographic effects on precipitating clouds*. Reviews of Geophysics, 50, 1-47.

Hughes A.G, Mansour M.M. and Robins N.S., 2008. *Evaluation of distributed recharge in an upland semi-arid karst system: the West Bank Mountain Aquifer*. Hydrogeology Journal, doi: 10.1007/s10040-008-0273-6.

Hurrell J. W., Kushirn Y., Ottersen G. and Visbeck N., 2003. A*n Overview of the North Atlantic Oscillation*. The North Atlantic Oscillation: Climatic Significance and Environmental Impact. Geophysical Monograph, American Geophysical Union, 134, 10.1029/134GM01.

Hurrell J. W., and van Loon H., 1997. *Decadal variations in climate associated with the North Atlantic Oscillation*. Climatic Change, 36, 301-326.

Jocson J. M. U., Jenson J. W., and Contractor D. N., 2002. *Recharge and aquifer response: Northern Guam Lens Aquifer, Guam, Mariana Islands*. J. Hydrol., 260, 231–254, doi:10.1016/s0022-1694(01)00617-5.

Johnston C. D., 1987. *Preferred water flow and localised recharge in a variable regolith*. J. Hydrol., 94, 129–142, doi:10.1016/0022- 1694(87)90036-9.

Jukić D. and Denić-Jukić V., 2008. *Estimating parameters of groundwater recharge model in frequency domain: Karst springs Jadro and Žrnovnica*. Hydrol. Process., 22: 4532–4542. doi: 10.1002/hyp.7057.

Jukić D. and Denić-Jukić V., 2009. *Groundwater balance estimation in karst by using a conceptual rainfall-runoff model*. J. Hydrol., 373(3– 4), 302–315.

Kessler, H., 1965. *Water balance investigation in the karstic region of Hungary.* Actes de Colloque de Dubrovnik sur l'Hydrologie des roches calcaires fessures. A.I.H.S.-UNESCO, 73, 91-105.

Kiraly L., 1975. *Rapport sur l'état actuel des connaissances dans le domaines des caractères physiques des roches karstiques*. Burger A. and Dubertret L. (Eds), Hydrogeology of karstic terrains, Int. Union of Geol. Sciences, B, 3, 53-67.

Kiraly L., 1997. *Modelling karst aquifers by the combined discrete channel and continuum approach*. 6th Conference on limestone hydrology and fissured aquifers, session on modelling karst aquifers. Université de Franche-Comté, Sciences et Technique de l'Environnement, La Chaux-de-Fonds, 1–26

Kiraly, L., 1998. *Modelling karst aquifers by the combined discrete channel and continuum approach*. Bulletin d'Hydrogéologie, 16, 77-98.

Kiraly L. 2002. Karstification and Groundwater flow. Gabrov.ek, F. (Ed.), *Evolution of karst: from prekarst to cessation*. Postojna- Ljubljana, Zalozba ZRC, 155-190.

Klimchouk, A., 1997. *The nature and principal characteristics of epikarst*. P.-Y. Jeannin (Editor), 12th International Congress of Speleology, La Chaux-de-Fonds, 306.

Klimchouk, A.B., 2000. *The formation of Epikarst and its role in Vadose Speleogenesis*. A.B. Klimchouk, D.C. Ford, A.N. Palmer and W. Dreybrodt (Editors), Speleogenesis. Evolution of Karst Aquifers. Huntsville. Natl. Speleol. Soc., 91-99.

Lastennet R., Puig J.M., Emblanch C. and Blavoux B., 1995. *Influence de la zone non saturée sur le fonctionnement des systèmes karstiques. Mises en évidence dans les sources du Nord-Vaucluse. (Influence of the non saturated zone on the functioning of karst systems. Demonstration from springs in northern Vaucluse, France..* Hydrogeologie, 4, 57–66.

Le Moine N., Andreassian V., and Mathevet T., 2008. *Confronting surface- and groundwater balances on the La RochefoucauldTouvre karstic system (Charente, France)*. Water Resour. Res., 44, W03403, doi:10.1029/2007WR005984.

LeGrand H.E. and Stringfield V.T., 1966. *Development of permeability and storage in the Tertiary limestones of the south eastern states, USA*. Bull. AIHS, 11 (4), 61-73.

Maillet E., 1905. *Essais d Hydraulique Souterraine et Fluvial* . Eyroles, Paris, France.

Mandel S., 1966. *A conceptual model of karstic erosion by groundwater*. Bull. AIHS, XI/1, 5-7.

Manna, F., Allocca, V., De Vita, P., Fusco, F. and Napolitano, E., 2013a. *Groundwater recharge assessment in karst aquifers of southern Apennines (Italy).* Rend. Online Soc. Geol. It., 24, 202-204.

Manna, F., Allocca, V., Fusco, F., Napolitano, E. and De Vita, P., 2013b. *Effect of the North Atlantic Oscillation on groundwater recharge in karst aquifers of the Cilento Geopark (Italy)*. Rend. Online Soc. Geol. It., 28, 106-109.

Mangin, A., 1975. *Contribution à l'étude hydrodynamique des aquifères karstiques.* Thèse Univ. Dijon. Annales de spéléologie, 29/3: 283-332, 29/4: 495-601, 30/1: 21-124.

Mangin A., 1994. *Karst hydrogeology.* Stanford J, Gibert J, Danielopol D. (eds) Groundwater ecology. Academic Press., 43–67.

Mansour M.M., and Hughes A.G., 2004. *User's manual for the distributed recharge model ZOODRM*. In British Geological Survey Internal Report IR/04/150.

Mazzarella A.,1999. *Rainfall multifractal dynamic processes in Italy.* Theor. Appl. Climatol., 63, 301-326.

Meinzer, O.E., 1923. *The occurrence of groundwater in the United States with a discussion of principles*. U.S. Geological Survey Water- Supply Paper, 489, 1-321.

Mudry J., 1990. *Les courbes flux chimique-débit et le fonctionnement des aquifères karstiques*. (Chemical mass flow vs. Discharge and the functioning of karst aquifers). J. Hydrol, 120 (1–4), 283–294.

Naclerio G., Petrella E., Nerone V., Allocca V., De Vita P. and Celico F., 2008. *Influence of topsoil of pyroclastic origin on microbial contamination of groundwater in fractured carbonate aquifers*. Hydrogeology Journal, 16, 1057–1064.

Nimmo J.R., Horowitz C. and Mitchell L., 2015. *Discrete-Storm Water-Table Fluctuation Method to Estimate Episodic Recharge.* Groundwater, 53(2), 282-292.

Nizinski J. and Saugier B., 1989. *A model of transpiration and soil-water balance for a Mature Oak Forest.* Agricultural and Forest Meteorology 47, 1–17.

Parajka J. and Szolgay J., 1998. *Grid based mapping of long-term mean annual potential and actual evapotranspiration in Slovakia*. In Kovar K (ed.) Hydrology, Water Resources and Ecology in Headwaters. Wallingford, International Association for Hydrological Sciences, 248, 123-129

Penman H.L., 1948. *Natural evaporation from open water, bares oil and grass.* Proceedings of the Royal Society of London Series A 193, 120–145.

Perrin J., 2003. *A conceptual model of flow and transport in a karst aquifer based on a spatial and temporal variations of natural tracers*. PhD Thesis, Faculty of Sciences of the University of Neuchatel.

Perrin J., Jeannin P.-Y. and Zwahlen F., 2003. *Epikarst storage in a karst aquifer: a conceptual model based on isotopic data, Milandre test site, Switzerland*. Journal of Hydrology ,279, 106-124.

Petrella E., Capuano P. and Celico F., 2007. *Unusual behaviour of epikarst in the Acqua dei Faggi carbonate aquifer (Southern Italy)*. Terra Nova, 19, 82-88.

Petrella, E., Falasca, A. and Celico, F., 2008. *Natural-gradient tracer experiments in epikarst: a test study in the Acqua dei Faggi experimental site, southern Italy*. Geofluids, 8, 159–166. doi: 10.1111/j.1468-8123.2008.00214.x.

Petrella, E., Capuano, P., Carcione, M. and Celico, F., 2009. *A high-altitude temporary spring in a compartmentalized carbonate aquifer: the role of low-permeability faults and karst conduits.* Hydrol. Process., 23: 3354–3364. doi: 10.1002/hyp.7454

Petrella, E., Aquino, D., Fiorillo, F. and Celico, F., 2014. *The effect of low-permeability fault zones on groundwater flow in a compartmentalized system. Experimental evidence from a carbonate aquifer (Southern Italy).* Hydrol. Process. doi: 10.1002/hyp.10294

Plummer L. N., Busenberg E.. McConnell J. B., Drenkard S., Schlosser P., and Michel R. L., 1998. *Flow of river water into a Karstic limestone aquifer.* 1. Tracing the young fraction in groundwater mixtures in the Upper Floridan Aquifer near Valdosta, Georgia. Appl. Geochem., 13(8), 995–1015, doi:10.1016/s0883-2927(98)00031-6.

Quinlan JF. and Ewers RO., 1989. *Subsurface drainage in the Mammoth Cave area*. In: White WB, White EL, editors. Karst hydrology: Concepts from the Mammoth Cave area. Van Nostrand Reinhold; New York. pp. 65–103.

Roe, G.H., 2005. *Orographic precipitation*. Annual Review Earth Planetary Science, 33, 645-671.

Rhodes R. and Sinacori M.N., 1941. *Pattern of ground-water flow and solution*. J. of Geology, 49 (8), 785-794.

Ries, F., Lange, J., Schmidt, S., Puhlmann, H., and Sauter, M., 2014. *Recharge estimation and soil moisture dynamics in a Mediterranean karst aquifer*. Hydrol. Earth Syst. Sci. Discuss., 11, 8803-8844, doi:10.5194/hessd-11-8803-2014.

Rimmer A., and Salingar Y., 2006. *Modelling precipitation-streamflow processes in karst basin: The case of the Jordan River sources, Israel*. J. Hydrol., 331, 524–542.

Samper J. 1997. *Evaluacion de la recarga a partir de modelos numericos de flujo en acuíferos.* In La evaluacion de larecarga a los acuíferos en la Planificacion Hidrologica, ed. E. Custodio, M.R. Llamas, and J. Samper, 153–180.Madrid, Spain: AIH-GE & ITGE.

Samper J. and García Vera M.A., 1997. *Estimación de la recarga producida por la lluvia y los excedentes de riego mediante balances diarios de agua en el suelo: Experiencias en diferentes zonas climáticas*. Seminario sobre la evaluación de la recarga a los acuíferos en la Planificación Hidrológica, Las Palmas de Gran Canaria. (eds). ITGE, 367–379.

Samper J., L. Huguet J. Ares, and. García Vera M.A, 1999. *Manual del usuario del programa Visual BALAN v. 1.0*. Publicacion tecnica de ENRESA 5, no. 99: 1–132.

Samper J., Alvares D., Pisani B. and García Vera M.A., 2007. *Evaluation of climate change impacts on water resources of Ebre River Basin with GIS-BALAN*. In: XXXV AIH Congress (Lisboa): Groundwater and Ecosystems, 11.

Scanlon B., Healy R., and Cook P., 2002. *Choosing appropriate techniques for quantifying groundwater recharge*. Hydrogeol. J., 10, 18–39.

SCS., 1993. *National engineering handbook.* Section 4, Hydrology, Chapter 4. Soil Conservation Service. Washington, DC: USDA.

Sheffer N. A., Cohen M., Morin E., Grodek T., Gimburg A., Magal E., Gvirtzman H., Nied M., Isele D., and Frumkin A., 2011. *Integrated cave drip monitoring for epikarst recharge estimation in a dry Mediterranean area, Sif Cave, Israel.* Hydrol. Process., online first:doi:10.1002/hyp.8046.

Somaratne, N., 2014. *Characteristics of Point Recharge in Karst Aquifers*. Water 2014, 6, 2782-2807.

Soulios, G., 1984. *Infiltration efficace dans le karst hellenique*. Journal of Hydrology, 75, 343-356.

Swinnerton A.C., 1949. *Hydrology of limestone terrains*. Meinzer O.E. (Ed.), Hydrology, Physics of the Earth. New York: Dover Publ.

Thornthwaite, C. W., and J. R. Mather, 1955. *The Water Balance*. Publ. Climatol., 8 (1): 1-104, Drexel Institute of Climatology, Centerton, New Jersey.

Thornthwaite C.V. and Mather, J. R., 1957. *Instructions and tables for computing potential evapotranspiration and the water balance*. Publ. Climatol., 10 (3):1-311.

Trcek B., Krothe N.C., 2002. *The role of the epikarst zone in karst aquifer recharge processes*. Geologija, 45(2), 579–584

Trcek B., 2006. *How can the epikarst zone influence the karst aquifer hydraulic behaviour?*. Environ Geol (2007), 51, 761-765.

Tritz S.,. Guinot V, and Jourde H., 2011. *Modelling the behaviour of a karst system catchment using non-linear hysteretic conceptual model.* J. Hydrol., 397(3–4), 250–262.

Turc L., 1954. *The soil balance: relations between rainfall, evaporation and flow* (in French). Geogr Rev., 38, 36–44

Sodeman P. C. and Tysinger J. E., 1965. *Effect of forest cover upon hydrologic characteristics of a small watershed in limestone region of East Tennesse*. Actes de Colloque de Dubrovnik sur l'Hydrologie des roches calcaires fessures. A.I.H.S.-UNESCO, 73, 135-151.

Sophocleous M., 1992. *Groundwater recharge estimation and regionalization: The Great Bend Prairie of central Kansas and its recharge statistics*. J Hydrol 137:113–140

Touhami, I., Andreu, J. M., Chirino, E., Sánchez, J. R., Moutahir, H., Pulido-Bosch, A., Martínez-Santos, P. and Bellot, J., 2013. *Recharge estimation of a small karstic aquifer in a semiarid Mediterranean region (southeastern Spain) using a hydrological model*. Hydrol. Process., 27, 165–174. doi: 10.1002/hyp.9200

Vigna B., 2002. *Monitoring and evaluation of the vulnerability of karst aquifers*. Conference proceedings"Le risorse idriche sotterranee delle Alpi Apuane:conoscenze attuali e prospettive di utilizzo". Forno di Massa, Italy - 22 giugno 2002, 23-35.

Vigna, B., 2007. *Classification and operation of aquifer systems in carbonate rocks*. Memorie dell'Istituto Italiano di Speleologia XIX, 21–26. ISBN: 978-88-89897-03-4 (in Italian).

Vilimonovic J., 1965. *A contribution of the study of groundwater intake recharge in karst*. Actes de Colloque de Dubrovnik sur l'Hydrologie des roches calcaires fessures. A.I.H.S.-UNESCO. 73, 482-499.

Vicente-Serrano S.M. and Trigo R.M. (Eds.), 2011. *Hydrological, Socioeconomic and Ecological Impacts of the North Atlantic Oscillation in the Mediterranean Region (Advances in Global Change Research)*. Springer, 1-236, 2011.

White, W. B. 1969. *Conceptual models for limestone aquifers*. Groundwater, 7 (3), 15-21.

White W.B., 2002. *Karst hydrology: recent developments and open questions*. Engineering Geology, 65, 85-105.

Williams P.W., 1983. *The role of the subcutaneous zone in karst hydrology*. Journal of Hydrology, 61, 1, 45-67.

Williams P.W., 1985. *Subcutaneous hydrology and the development of doline and cockpit karst*. Zeit. Geomorph. NF., 29, 463-482.

Williams P.W., 2008. *The role of the epikarst and cave hydrogeology : a review*. International Journal of Speleology, 37(1), 1- 10, Bologna (Italy).

Wood W. W. and Sanford W. E., 1995. *Chemical and Isotopic Methods for Quantifying Ground-Water Recharge in a Regional, Semiarid Environment*. Ground Water, 33, 458–468, doi:10.1111/j.1745- 6584.1995.tb00302.x.

Hydrol. Earth Syst. Sci., 16, 1389–1399, 2012
www.hydrol-earth-syst-sci.net/16/1389/2012/
doi:10.5194/hess-16-1389-2012

Hydrology and Earth System Sciences

Coupled decadal variability of the North Atlantic Oscillation, regional rainfall and karst spring discharges in the Campania region (southern Italy)

P. De Vita, V. Allocca, F. Manna, and S. Fabbrocino

Dipartimento di Scienze della Terra – University of Naples "Federico II", Italy

Correspondence to: P. De Vita (padevita@unina.it)

Received: 23 November 2011 – Published in Hydrol. Earth Syst. Sci. Discuss.: 16 December 2011
Revised: 16 April 2012 – Accepted: 24 April 2012 – Published: 11 May 2012

Abstract. Thus far, studies on climate change have focused mainly on the variability of the atmospheric and surface components of the hydrologic cycle, investigating the impact of this variability on the environment, especially with respect to the risks of desertification, droughts and floods. Conversely, the impacts of climate change on the recharge of aquifers and on the variability of groundwater flow have been less investigated, especially in Mediterranean karst areas whose water supply systems depend heavily upon groundwater exploitation.

In this paper, long-term climatic variability and its influence on groundwater recharge were analysed by examining decadal patterns of precipitation, air temperature and spring discharges in the Campania region (southern Italy), coupled with the North Atlantic Oscillation (NAO).

The time series of precipitation and air temperature were gathered over 90 yr, from 1921 to 2010, using 18 rain gauges and 9 air temperature stations with the most continuous functioning. The time series of the winter NAO index and of the discharges of 3 karst springs, selected from those feeding the major aqueducts systems, were collected for the same period.

Regional normalised indexes of the precipitation, air temperature and karst spring discharges were calculated, and different methods were applied to analyse the related time series, including long-term trend analysis using smoothing numerical techniques, cross-correlation and Fourier analysis.

The investigation of the normalised indexes highlighted the existence of long-term complex periodicities, from 2 to more than 30 yr, with differences in average values of up to approximately ±30 % for precipitation and karst spring discharges, which were both strongly correlated with the winter NAO index.

Although the effects of the North Atlantic Oscillation (NAO) had already been demonstrated in the long-term precipitation and streamflow patterns of different European countries and Mediterranean areas, the results of this study allow for the establishment of a link between a large-scale atmospheric cycle and the groundwater recharge of carbonate karst aquifers. Consequently, the winter NAO index could also be considered as a proxy to forecast the decadal variability of groundwater flow in Mediterranean karst areas.

1 Introduction

In the last few decades, the international scientific community has intensely debated climate change on a global scale (WMO, 1979) and the influence of anthropogenic activities. Since 1979, several international research programs (e.g. World Climate Programme – WCP, World Climate Data and Monitoring Programme – WCDMP; http://www.wmo.int/pages/prog/wcp/wcdmp/index_en.php) have been developed to analyse the state of knowledge on climate change, to start global monitoring of the climate systems and to fully understand the causes of its variability. Different groups of international experts (Intergovernmental Panel on Climate Change – IPCC) have been called to analyse the different causes and effects of these changes on the environment. Numerous reports have been published (IPCC, 1990, 2001, 2007) that summarise the current state of climate change and

Published by Copernicus Publications on behalf of the European Geosciences Union.

evaluate different scenarios for the impact of greenhouse gas pollution on global climate.

On a national scale, many hydrological and climatological studies (Lo Vecchio and Nanni, 1995; Brunetti et al., 2000, 2006), following different methodological approaches, have analysed the decadal climatic variations in Italy and the Mediterranean area with the long-term trends of annual precipitation and mean annual air temperature time series. Other studies in Italy have assessed the relationship between climate change and groundwater circulation (Dragoni and Sukhija, 2008; Cambi and Dragoni, 2000). To assess the impact of the climate variability on the water budget particularly for the Campania region, a reduction of precipitation of approximately 20 % in the last 20 yr was estimated (Ducci and Tranfaglia, 2008).

Numerous studies analysed the influence of the North Atlantic Oscillation (hereafter NAO) (Walker, 1924; Walker and Bliss, 1932) on the annual variability of precipitation in the Northern Hemisphere (Barnston and Livezey, 1987; Hurrell, 1995; Hurrell and van Loon, 1997), particularly in Northern Europe, the Iberian Peninsula and the European Alps (Rodriguez-Puebla et al., 1998; Uvo, 2003; López-Moreno and Vicente-Serrano, 2008; Bartolini et al., 2009; Rodriguez-Puebla and Nieto, 2010), and its impact on river flows in European hydrographic basins (Rimbu et al., 2002; Trigo et al., 2004; López-Moreno et al., 2007; Massei et al., 2009; Morán-Tejeda et al., 2011; Lorenzo-Lacruz et al., 2011).

In the Mediterranean area, a correlation between the NAO, precipitation, river discharges and lake levels was also found in the Middle East and in Turkey (Cullen and deMenocal, 2000; Cullen et al., 2002; Karabörk et al., 2005; Türkes and Erlat, 2005; Kücük et al., 2009). A strong interdependence among the NAO, precipitation, river discharges and air temperature in some southern Italy regions (Brandimarte et al., 2011; Caloiero et al., 2011) was discovered. Recent studies revealed that the impact of the NAO in Mediterranean areas can also be widely conceived as extendable to snow accumulation, crop production, landslides and soil erosivity (Vicente-Serrano and Trigo, 2011). Finally, the NAO was also found to extend its control on climate in northern Africa (Hasanean, 2004) and eastern North America (Sheridan, 2003; Tootle et al., 2005).

The temporal structure of the NAO and periodicities of its impacts on climate have been analysed (Greatbatch, 2000; Wanner et al., 2001; Hurrell et al., 2003), concluding that no preferred time scale of NAO variability exists and a general increase of power with period length in the spectrum of the NAOI. In detail, a quasi-biennial periodicity, a deficit in power from 3 to 5 yr and an increase in power from 8 to 10 yr, which was more enhanced in the second half of the 20th century (Hurrell and van Loon, 1997), were recognised. A recent study based on the reconstruction of the NAO since 1650, by means of instrumental and documentary proxy predictors, showed a dominant quasi 60-yr periodicity (Mazzarella and Scafetta, 2012).

None of the abovementioned studies analysed the impact of climatic variability due to the NAO on the aquifer recharge and groundwater regime from the interannual to decadal time scales.

The objective of this study was to examine, on a regional scale, the relationship between the NAO and groundwater recharge by analysing the patterns of an NAO Index (hereafter NAOI), precipitation, air temperature and spring discharge in the Campania region over a multi-decadal period. Datasets covering a period of 90 yr (1921–2010), composed of data gathered from 18 rain gauges and 9 temperature gauges, chosen for their regular functioning during the whole period and their homogeneous distribution over the territory, were elaborated. Additionally, the discharge time series of the Sanità karst spring, fed by the groundwater circulation of an extended fractured and karstified carbonate aquifer, were analysed together with two other shorter time series of karst spring discharges.

The present research represents the continuation and updating of previous studies conducted on the climatic variability of southern Italy due to the NAO (De Vita and Fabbrocino, 2005, 2007). These studies provided a preliminary analysis of regional precipitation and air temperature, having given a first insight into the correlation between the NAO and the decadal variability of groundwater recharge in a test carbonate aquifer.

The paper is organised as follows. After a description of the issue (Sect. 1), the hydrogeological and climate characteristics of the study area are explained (Sect. 2). Subsequently, hydrologic data and methods of analysis (Sect. 3), results (Sect. 4) and concluding remarks are reported (Sect. 5).

2 Climate and hydrogeological characteristics of the Campania region

The Campania region is located in the southern part of the Italian Peninsula and has an extension of approximately 13 590 km^2. It can be subdivided by the fundamental geomorphological features in the Apennine mountain ranges that reach altitudes of 1000 to 2000 m a.s.l., accounting for 30 % of the total area; coastal plains account for a further 18 %, and a remnant part of this region consists of low-altitude hills and alluvial valleys. The climate of the Campania region is of a Mediterranean type with hot dry summers and moderately cool and rainy winters. Mean annual air temperatures are in the range of approximately 10–12 °C in the mountainous interior, 13–15 °C in the coastal areas, and 12–13 °C in the plains surrounded by carbonate mountains. Rainfall regimes vary from the coastal or Mediterranean type to the Apennine sublittoral (Bandini, 1931), which is characterised by a principal maximum in autumn-winter and a minimum in the summer. The distribution of precipitation over the region is mainly controlled by the Apennine Mountains, which, acting as a barrier against humid air masses coming from the Tyrrhenian Sea, induce orographic precipitation (Henderson-Sellers and Robinson, 1986). The lowest mean annual rainfall, approximately 700–900 mm, occurs in the western and eastern parts of the Campania region; the highest mean annual rainfall, approximately 1700–2000 mm, occurs in the central part of the Apennine ridge.

The regional hydrogeological setting (Fig. 1) is essentially characterised by carbonate karst aquifers, with a high degree of permeability due to fracturing and karst. These aquifers, formed by limestone, dolomitic limestone and a dolomitic series of carbonate platform facies (Trias – Paleogene), are confined by aquitards or aquicludes composed of flysch and basinal series (Celico, 1978, 1983; Celico et al., 2000; Allocca et al., 2007, 2009). Morphologically, the first aquifers correspond to the higher mountains (carbonate massifs), while the second ones correspond to the low-altitude hills. Both types of hydrostratigraphic units originate from tectonic units thrust in the Apennines chain. They are typically characterised by a basal groundwater flow, outflowing in huge basal springs, with an average discharge frequently greater than $1.0\,m^3\,s^{-1}$. The patterns of groundwater flow are greatly conditioned both by the altimetry of the boundary with the juxtaposing lower-permeability flysch deposits, as well as by the position and permeability of cataclastic bands associated with main faults and thrusts. The latter, behaving as aquitards, determine the fractioning of the groundwater flow into several groundwater basins. Where the carbonate aquifers are juxtaposed with medium permeable Plio-Quaternary epiclastic and alluvial deposits, a groundwater exchange can exist. A subordinate perched groundwater flow also occurs in the surficial part of karst aquifers, where the different deepening of the epikarst (Celico et al., 2010), as well as stratigraphic and tectonic factors, can generate seasonal and ephemeral springs. The groundwater yield of the Campania's karst aquifers varies from 0.015 to $0.038\,m^3\,s^{-1}\,km^{-2}$ (Allocca et al., 2007, 2009). Given the high quality of their groundwater and their availability for exploitation, basal springs are, for the most part, tapped; thus, carbonate aquifers represent strategic resources for the socio-economic development of the Campania region and southern Italy.

The hydrography of the Campania region is mainly characterised by three principal rivers (Garigliano, Volturno and Sele) and by numerous minor streams, mostly draining towards the Tyrrhenian Sea. The morphology of the drainage network is irregular and controlled by geological and structural features. The principal rivers have a perennial regime in the terminal segments due to the feeding of groundwater that outflows from carbonate aquifers, directly from springs and indirectly through alluvial aquifers. Instead, the streamflow of minor watersheds is frequently ephemeral and more dependent on the precipitation regime.

3 Hydrologic data and methods of analysis

Different methods of analysis were applied to investigate decadal variability and correlations among hydrologic time series, including trend analysis using smoothing numerical techniques, cross-correlation and spectrum and cross-spectrum analyses through Fourier transform. The trend analysis was performed both with linear regression techniques and with low-pass numerical filtering of time series to provide evidence of their decadal components. In this approach, the moving average over 11 yr, centred on the sixth year, was applied, providing a good smoothing of the periodicities shorter than one decade. With the purpose of estimating the variability around the mean value and of recognising anomalous annual values outside the 90 % frequency range, moving 5th and 95th percentiles over 11 yr, centred in the sixth year, were calculated.

3.1 NAO index time series

Different NAOIs exist depending on the barometric stations and on the period of the year considered (Hurrell et al., 2003). For the case study, the analyses were performed with a subset (1921–2010) of the winter NAOI (December through March mean – DJFM) time series, calculated from the records of the Lisbon (Portugal) and Stikkishlomur (Iceland) barometric stations since 1864 (http://www.cgd.ucar.edu/cas/jhurrell/indices.html).

3.2 Precipitation and air temperature time series

To study the fundamental climatic variables that control groundwater recharge, the total annual precipitation and the mean annual air temperature were gathered from the official monitoring network for the period 1921–2010 (90 yr). Since 2000, the management of the monitoring network was changed from the national technical service and agency (SIMN – *Servizio Idrografico Mareografico Nazionale* and ISPRA – *Istituto Superiore per la Protezione e la Ricerca Ambientale*, http://www.isprambiente.gov.it) to the regional Civil Protection agency (http://www.protezionecivile.gov.it). On the basis of the temporal continuity of the record and of the homogeneous distribution over the territory, 18 rain gauge stations were selected. Similarly, 9 thermometric stations were identified (Fig. 1). In this case, the smaller number reflected the sparser density of the monitoring network due to the low spatial variability of air temperature, mostly depending on the altitude.

The assessment of a climate trend at the regional scale was performed by defining the indexes representative of the annual anomalies with respect to the mean value, which minimised variations due to local factors. To obtain such an index for precipitation, the Mean Annual Precipitation Index

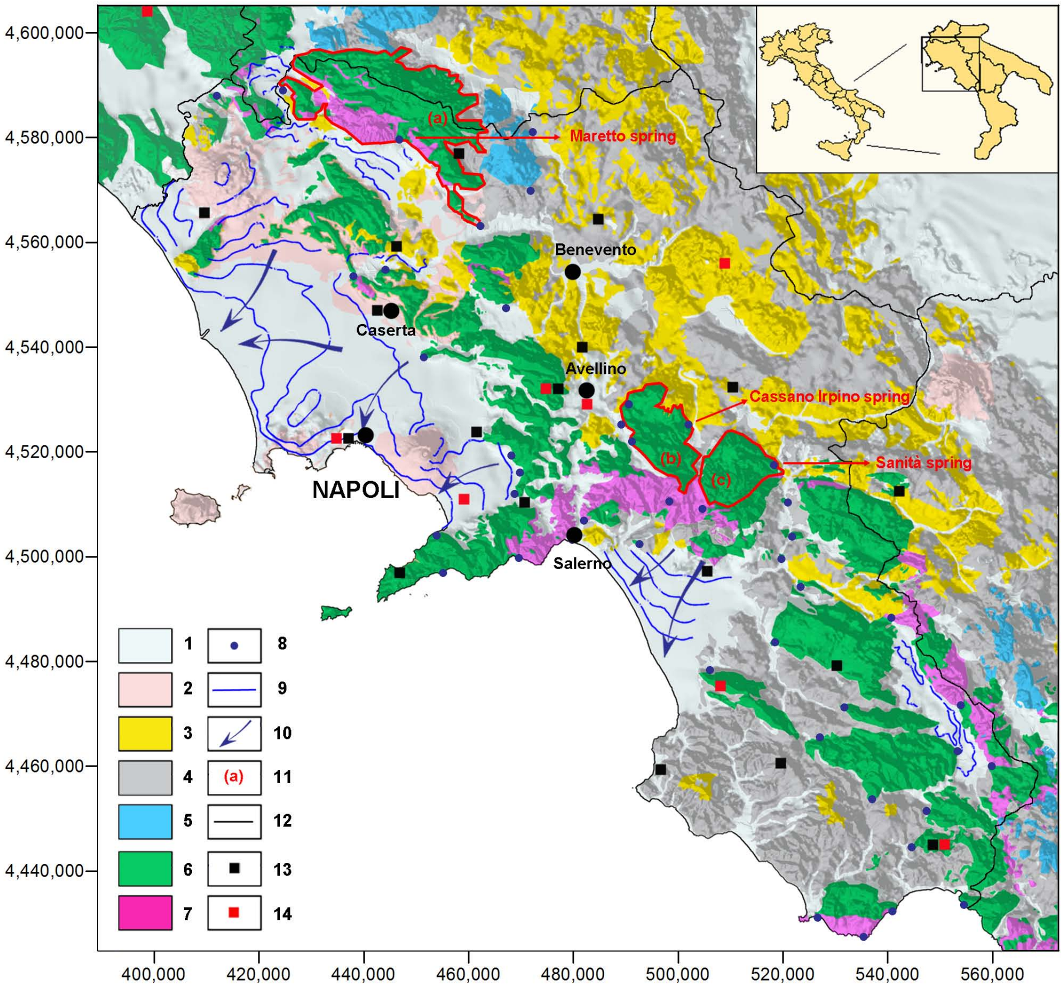

Fig. 1. Hydrogeological map of the Campania region. Hydrostratigraphic units and key to symbols: (1) alluvial and epiclastic units (Quaternary); (2) volcanic units (Pliocene-Quaternary); (3) late orogenic molasses and terrigenous units (Upper Miocene-Pliocene); (4) pre-orogenic and syn-orogenic terrigenous units of inner and thrust-top basins series (Cretaceous-Upper Miocene); (5) siliceous-marly units of outer basin series (Trias-Paleogene); (6) limestone and dolomitic limestone units of carbonate platform series (Jurassic-Paleogene); (7) dolomitic units of carbonate platform series (Trias-Jurassic); (8) main basal springs of carbonate karst aquifers; (9) groundwater head contour lines in alluvial and volcanic aquifers; (10) main preferential drainage axes of groundwater flow in alluvial aquifers; (11) identification of the carbonate karst aquifers analysed: **(a)** Matese Mount; **(b)** Terminio Mount; **(c)** Cervialto Mount; (12) regional boundary; (13) rain gauge stations; (14) air temperature monitoring stations.

(hereafter MAPI) was calculated as follows:

$$\mathrm{MAPI}_i = \frac{\sum_{j=1}^{18} \frac{\mathrm{AP}_{ji}\text{-}\mathrm{MAP}_j}{\mathrm{MAP}_j}}{\sum_{j=1}^{18} j} \tag{1}$$

where MAPI_i = Mean Annual Precipitation Index for the i year (%); AP_{ji} = Annual Precipitation for the j rain gauge station and the i year (mm); MAP_j = Mean Annual Precipitation of the whole time series for the j rain gauge station (mm).

Similarly and with reference to the identical observation period (1921–2010), the Mean Annual air Temperature Index (hereafter MATI) was calculated as follows:

$$\mathrm{MATI}_i = \frac{\sum_{k=1}^{9} \frac{\mathrm{AT}_{ki}\text{-}\mathrm{MAT}_k}{\mathrm{MAT}_k}}{\sum_{k=1}^{9} k} \tag{2}$$

where MATI_i = Mean Annual air Temperature Index for the i year (%); AT_{ki} = Annual air Temperature for the k air temperature gauge station and the i year (°C); MAT_k = Mean Annual air Temperature of the whole time series for the k air temperature gauge station (°C).

3.3 Effective precipitation time series

To assess the mean annual effective precipitation, which regulates groundwater recharge, the mean annual real evapotranspiration for each rain gauge station was estimated by applying the empirical formula of Turc (1954), as several studies have confirmed its reliability for Mediterranean areas and southern Italy (Santoro, 1970; Boni et al., 1982; Celico, 1983):

$$\mathrm{ET}_{ji} = \frac{\mathrm{AP}_{ji}}{\sqrt{0.9 + \left(\frac{\mathrm{AP}_{ji}}{300+25\cdot \mathrm{AT}_{ji}+0.05\cdot \mathrm{AT}_{ji}^{3}}\right)^{2}}} \tag{3}$$

where ET_{ji} = real EvapoTranspiration for the j rain gauge station and the i year (mm); AP_{ji} = Annual Precipitation for the j rain gauge station and the i year (mm); AT_{ji} = Annual air Temperature for the j rain gauge station and the i year (°C); for the rain gauge stations without air temperature gauges, mean annual air temperature values were extrapolated using linear correlations with altitude that were statistically robust in all cases.

Finally, for each year of the time series, the Mean Annual Effective Precipitation Index (hereafter MAEPI) was calculated as follows:

$$\mathrm{MAEPI}_i = \frac{\sum_{j=1}^{18} \frac{\mathrm{AEP}_{ji}\text{-}\mathrm{MAEP}_j}{\mathrm{MAEP}_j}}{\sum_{j=1}^{18} j} \tag{4}$$

where MAEPI_i = Mean Annual Effective Precipitation Index for the i year (%); AEP_{ji} = Annual Effective Precipitation for the j rain gauge station and the i year (mm); MAEP_j = Mean Annual Effective Precipitation of the whole time series for the j rain gauge station (mm).

3.4 Spring discharge time series

The discharge time series (1921–2010) of the Sanità karst spring was analysed. This is a unique case for the Campania region and southern Italy, both for its length and for the thorough continuity of the recording, as well as for the hydrogeological representativeness of the feeding aquifer. The Sanità karst spring (15°13′14.8559″ E, 40°49′5.3808″ N; 420 m a.s.l.) represents the sole groundwater outflow of the Cervialto Mount (15°7′50.4237″ E, 40°46′54.1411″ N; 1808 m a.s.l.) karst aquifer, which extends for over 128 km^2 and is confined by hydrostratigraphic units of the pre-orogenic and syn-orogenic terrigenous basinal series, with a lower degree of permeability (Celico, 1978, 1983). It is located in the upper part of the Sele River watershed (Fig. 1), close to the settlement of Caposele (Province of Avellino). The karst spring was tapped in 1906 by the Apulian Aqueduct (www.aqp.it), which by extension and capability is among the most important works of hydraulic engineering ever made in Italy. The spring discharges have been measured with a bi-weekly frequency until 1964 and daily in the following years, allowing the estimation of the mean annual discharge (3.95 m^3 s^{-1}). The carbonate aquifer suffered strong seismic shaking due to the proximity (<10 km) of the epicentre of the 23 November 1980 earthquake (Ms = 6.9 and a focal depth of 16 km) that caused anomalous high spring discharges during the period 1980–1981, followed by a gradual recovery of normal values until 1984 (Celico, 1981; Celico and Mattia, 2002). The same time series was already analysed by other authors in order to discover a method for analysing and forecasting drought periods (Fiorillo, 2009; Fiorillo and Guadagno, 2010).

For this time series, the Mean Annual Discharge Index (hereafter MADI) was calculated as follows:

$$\mathrm{MADI}_i = \frac{\mathrm{MAD}_i\text{-}\mathrm{MAD}}{\mathrm{MAD}} \tag{5}$$

where MADI_i = Mean Annual Discharge Index for the i year (%); MAD_i = Mean Annual Discharge for the i year (m^3 yr^{-1}); MAD = Mean Annual Discharge of the whole time series (m^3 yr^{-1}).

With the same approach, equivalent indexes for the time series of annual maximum and minimum discharges ($\mathrm{MADI_{max}}$ and $\mathrm{MADI_{min}}$) were calculated. Due to the dependency of the aqueduct feeding, the latter was considered particularly significant.

Two additional time series of karst spring discharge were chosen among those of greater duration, the Cassano Irpino and Maretto karst springs (Fig. 1), which belong to the Mount Terminio and the Mount Matese karst aquifers, respectively. The recording period under consideration was 1965–2010 for the first time series and 1965–2000 for the second, with an interval partially overlapping that of the Sanità karst spring of 45 and 35 yr, respectively.

4 Results and discussion

4.1 Correlation of the NAOI and regional climatic indexes

The time series of the winter NAOI, MAPI, MATI and MAEPI were first analysed with a least squares linear regression approach (Fig. 2). This analysis showed a general decreasing linear trend for the MAPI and the MAEPI with annual decreasing rates of −0.13 %, with respect to the mean value (1160.2 mm) (r = −0.203; Prob. t-Student = 5.4 %), for the MAPI and of −0.26 %, with respect to the mean value (625.2 mm) (r = −0.196; Prob. t-Student = 7.2 %) for the MAEPI. In contrast, for the MATI, a more significant linear trend was found with an annual increasing rate of 0.6 %, with respect to the mean value of (14.3 °C) (r = 0.262; Prob. t-Student = 1.5 %).

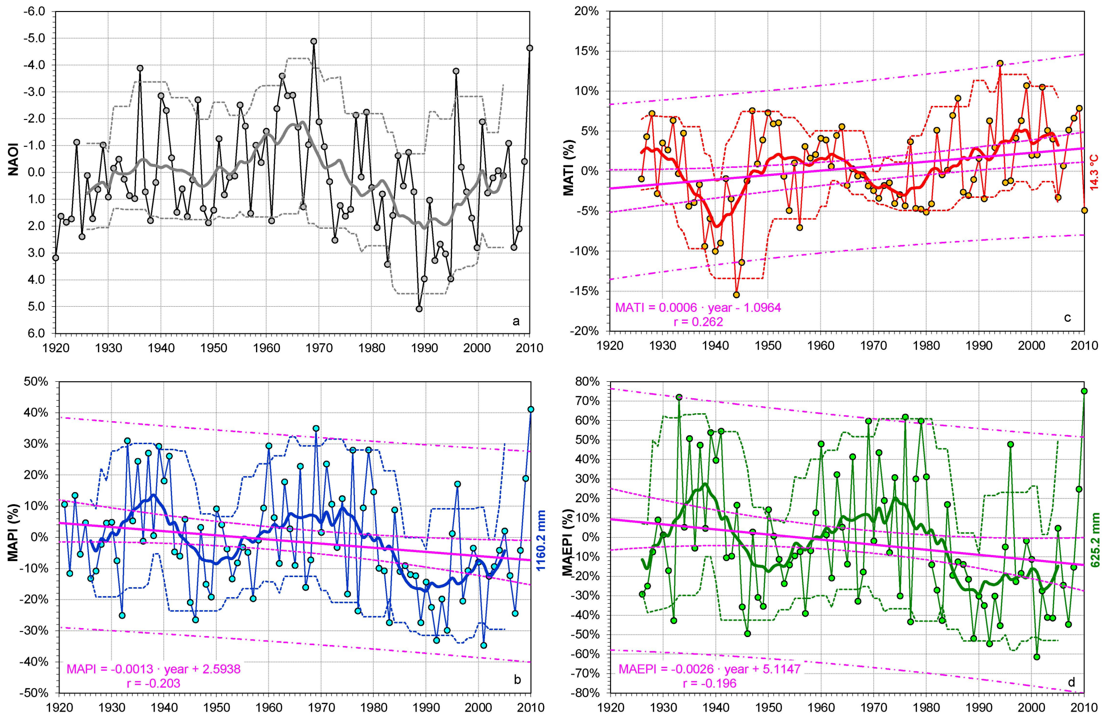

Fig. 2. Time series of **(a)** winter NAOI time series monitored between Lisbon (Portugal) and Stykkisholmur/Reykjavik (Iceland). **(b)** MAPI; **(c)** MATI; **(d)** MAEPI. Key to symbols: continuous magenta lines = linear trend of the whole time series (equation and coefficient of correlation in the lower left corner); dashed magenta lines = 95 % confidence interval of the expected mean value; dash-dotted magenta lines = 95 % prediction interval of the expected value; continuous thick line = 11-yr moving average centred on the sixth year; dashed lines = 11-yr moving percentiles of 5th and 95th centred on the sixth year; number on right side of the graphs = absolute mean value of the whole time series.

The long-term declining linear trend over the whole observed time period of the MAPI was in accordance with the findings of other authors for precipitation in southern Italy (Cotecchia et al., 2003; Polemio and Casarano, 2008; Ducci and Tranfaglia, 2008; Brandimarte et al., 2011). In addition, by observing the 11-yr moving average pattern with respect to the normal value (mean value of the whole time series), a complex cyclical dynamic was recognised (Fig. 2b). Two phases characterised by values above the normal value were identified in the periods 1930–1944 and 1958–1978, and three phases below the normal value were identified in the years preceding 1930 and in the periods 1944–1958 and 1980–2005. These long-term fluctuations were found as inversely coincident with those of the winter NAOI (Fig. 2a). Interestingly, for the last part of the time series, an increased frequency of MAPI values below the average value, which were not reached during previous periods, demonstrated a downward shifting trend. From 1985 to 2008, negative values (down to $<-30\,\%$ in 1992) were continuously observed, except in 1995, 1996 and 2005. Similar low levels also occurred in the 1930s and the 1940s (1932 and 1946) but with lower frequency (Fig. 2b). The maximum values of the time series were as follows: +31 % (1933), +35 % (1969) and +41 % (2010).

The long-term trend of the MATI (Fig. 2c) displayed an increasing pattern, although a complex cyclical dynamic was also observed in fluctuations of the 11-yr moving average. The minimum value of the MATI was −15 % (1944), and the maximum was +14 % (1994). The trends over the last two decades of both the MAPI and the MATI were found to be consistent with what was previously found by other researchers for the Campania region (Ducci and Tranfaglia, 2008).

The long-term trend of the MAEPI (Fig. 2d) showed a decreasing linear trend; however, very remarkable fluctuations around the mean value, with cyclical long-term dynamics, were observed. The extreme values of the time series, ranging from +72 % (1933) to −61 % (2001), were identified as matching those of the MAPI time series, therefore demonstrating the amplification effect due to the nonlinear behaviour of the actual evapotranspiration. Similar to the MAPI, a downward shift was observed for the MAEPI in the last decades of the time series.

The variability of the MAPI and the MAEPI, identified as the difference between the 5th and the 95th 11-yr moving percentiles, appeared inconstant during the time series with high ranges (Fig. 2b and d) of up to 50 % (from +30 % to −20 %) and 90 % (from +60 % and −30 %), respectively, in the periods characterised by the negative phase of the NAO.

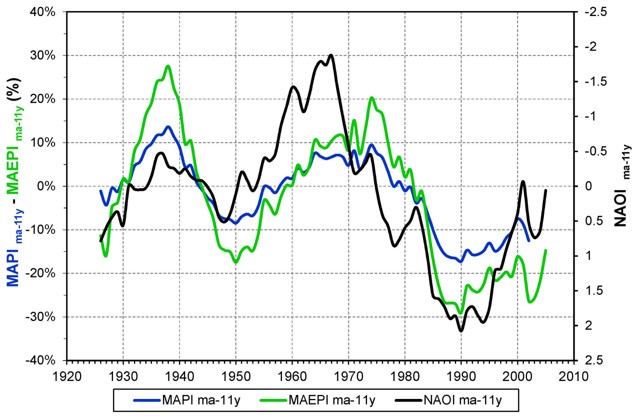

Fig. 3. Comparison of the 11-yr moving averages of the winter NAOI, MAPI, MATI and MAEPI time series for the Campania region.

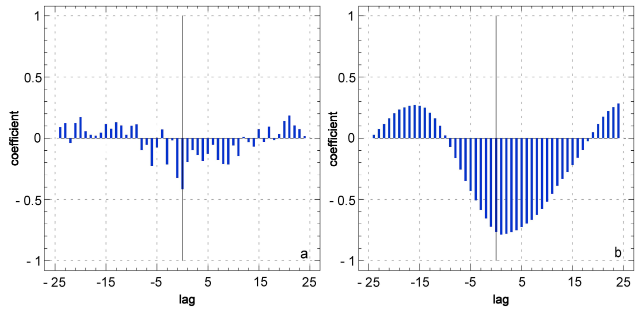

Fig. 4. Cross-correlation analysis between the winter NAOI and the MAPI carried out on **(a)** the original time series and **(b)** the 11-yr moving average time series.

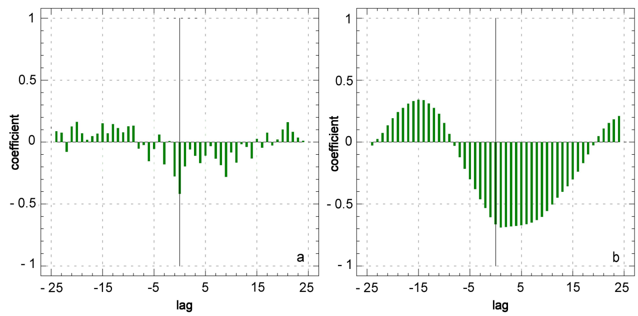

Fig. 5. Cross-correlation analysis between the long-term components of the winter NAOI and the MAEPI carried out on **(a)** the original time series data and **(b)** the 11-yr moving average.

In contrast, lower variability in the positive phase of the NAO was observed, with ranges of 35 % (from +5 % to −30 %) and 70 % (from +20 % to −50 %), respectively.

The integrated analysis among the different components of the long-term time series of the NAOI, the MAPI and the MAEPI showed, after filtering with the 11-yr moving averages, a strong co-movement and a good overlapping of the positive and negative peaks (Fig. 3). Particularly, the more simplified periodicity of the time series showed two decadal cycles and the beginning of a third cycle starting at approximately 1990.

A significant correlation between the winter NAOI and the MAPI was verified using a cross-correlation analysis performed with the raw data of these two time series. In this case, the absolute maximum value of the correlation ($r = -0.422$; Prob. t-Student < 0.1 %) was found at a lag time variable from 0 to +1 yr (Fig. 4). Considering the 11-yr moving average time series, the absolute maximum value of the resulting correlation increased ($r = -0.767$; Prob. t-Student < 0.1 %). The cross-correlation analysis between the winter NAOI and the MAEPI (Fig. 5) revealed a stronger correlation for the raw data of the time series ($r = -0.431$; Prob. t-Student < 0.1 %).

4.2 Correlation of the NAOI and spring discharges

A general linear decreasing trend with a rate of −0.14 % per year, with respect to the mean value ($3.95\,\mathrm{m^3\,s^{-1}}$) ($r = -0.300$; Prob. t-Student $= 0.5$ %), and high annual fluctuations around the mean, with extremes of +38 % (1941) and −25 % (2002), were found for the MADI time series (Fig. 6a). Specifically, a complex multi-year cyclicality was identified by the 11-yr moving average, which showed two phases of maxima corresponding to the years 1930–1944 and 1958–1978 and two phases of minima corresponding to the years before 1930, the period 1944–1958 and the years after 1980 (Fig. 8a and b). The variability of the MADI, identified as the difference between the 5th and the 95th 11-yr moving percentiles, was observed to be higher in the negative phase of the NAO, with a range of 45 % (from +30 % and −15 %), and lower in the positive phase of the NAO, with a range of 25 % (from +5 % and −20 %) (Fig. 6a). In contrast, for the $\mathrm{MADI_{min}}$ time series, a lower variability was recognised (Fig. 6b).

The integrated analysis of the long-term components of the winter NAOI and MADI time series, expressed by the 11-yr moving averages, showed a phase coherence (Fig. 7), except for the period 1980–1981, which was influenced by the earthquake shaking. This observation was confirmed by the analysis of cross-correlation (Fig. 8), carried out both on the raw data of the time series ($r = -0.506$; Prob. t-Student < 0.1 %) and for the 11-yr moving averages ($r = -0.780$; Prob. t-Student < 0.1 %). The maximum correlation was found for both at lag times of 0 and +1 yr.

The comparison of the discharge time series of the Sanità karst spring with two other time series of spring discharge belonging to the Cassano Irpino and Maretto karst springs, even if for a limited overlapping period (1965–2010 and 1965–2000) (Fig. 9), permitted the recognition of a coherent descending pattern until 1990 and a rising trend in the

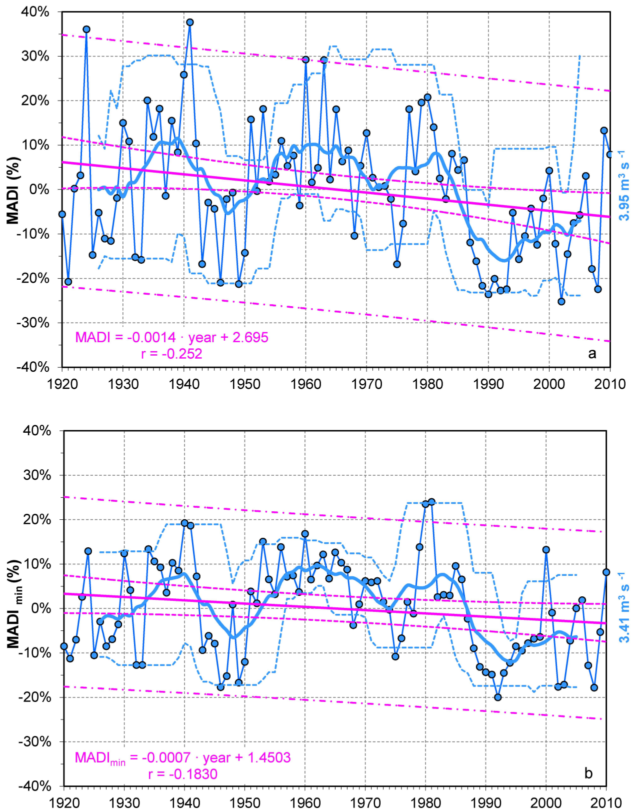

Fig. 6. (a) MADI time series; **(b)** $\mathrm{MADI_{min}}$ time series. Key to symbols: continuous magenta line = linear trend of the whole time series (equation and coefficient of correlation in the lower left corner); dashed magenta lines = 95 % confidence interval of the expected mean value; dash-dotted magenta lines = 95 % prediction interval of the expected value; continuous thick line = 11-yr moving average centred on the sixth year; dashed lines = 11-yr moving percentiles of 5th and 95th centred on the sixth year; number on right side of the graphs = absolute mean value of the whole time series.

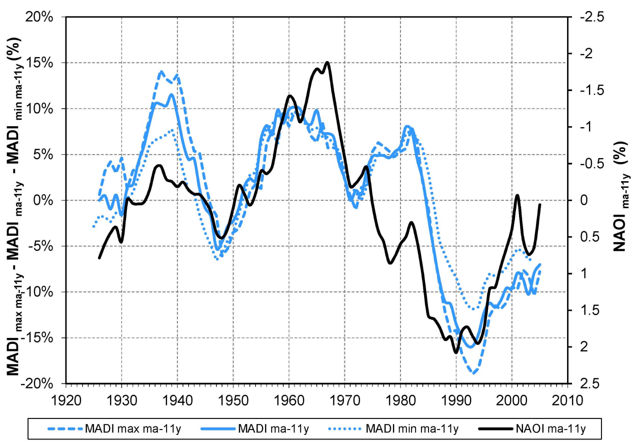

Fig. 7. Comparison between the 11-yr moving averages of the NAOI time series and the $\mathrm{MADI_{max}}$, MADI and $\mathrm{MADI_{min}}$ time series of the Sanità spring.

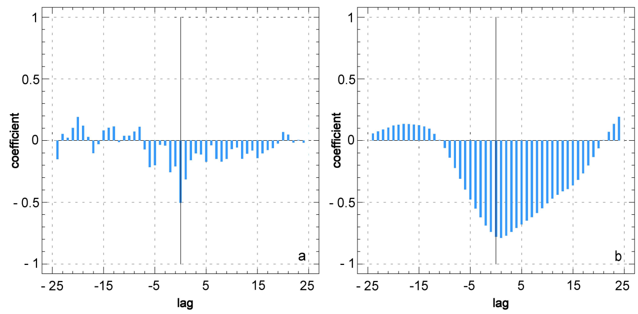

Fig. 8. Cross-correlation analysis between the NAOI and the MADI, carried out on **(a)** the original time series and **(b)** the 11-yr moving averages.

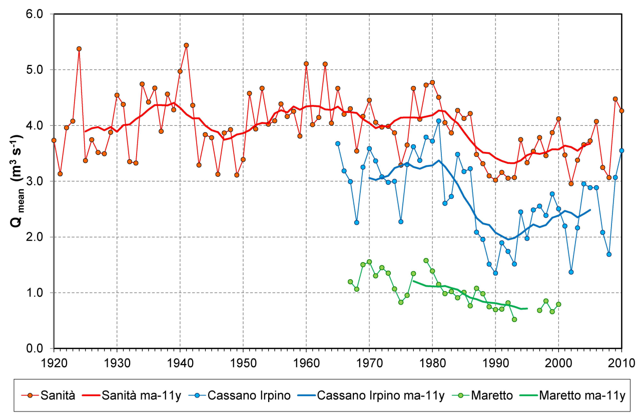

Fig. 9. Graphical comparison of annual mean discharges (Q_{mean}) of the Sanità, Cassano Irpino and Maretto karst springs (Fig. 1). Key to symbol: continuous thick line = 11-yr moving average centred on the sixth year.

following years, according to the pattern of the NAOI for the same period (Fig. 2a).

4.3 Cross-spectrum analysis of the NAOI, the MAPI and the MADI

A Fourier analysis was applied to the NAOI, MAPI and MADI time series in order to understand their temporal structures, periodicities and respective coherency. The purpose of this analysis is to decompose complex time series with cyclical components into fundamental underlying sinusoidal functions (sine and cosine), finding their amplitudes and wavelengths and reconstructing their power spectra.

The observed spectrum for the winter NAOI results were similar to that previously observed by other authors (Sect. 1), with principal periodogram peaks characterised by periodicities from 2 to 3 yr, from 5 to 9 yr, and at 30 and 45 yr (Fig. 10). Due to the length of the time series, longer periodicities were not found. The principal periodogram peaks for the MAPI and MADI time series were simultaneously observed at 2, 5, 15, 22 and 45 yr and appeared to match those

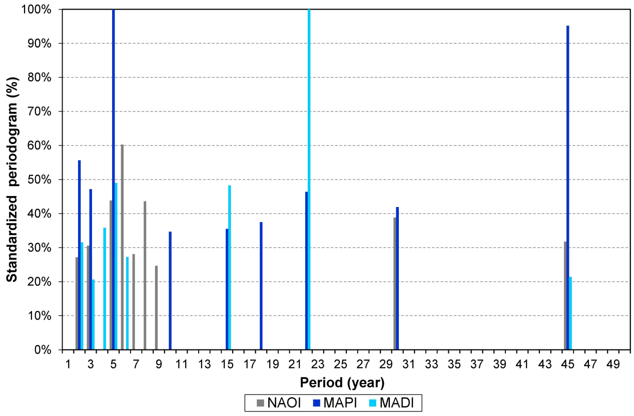

Fig. 10. Largest periodogram peaks for the NAOI, MAPI and MADI time series.

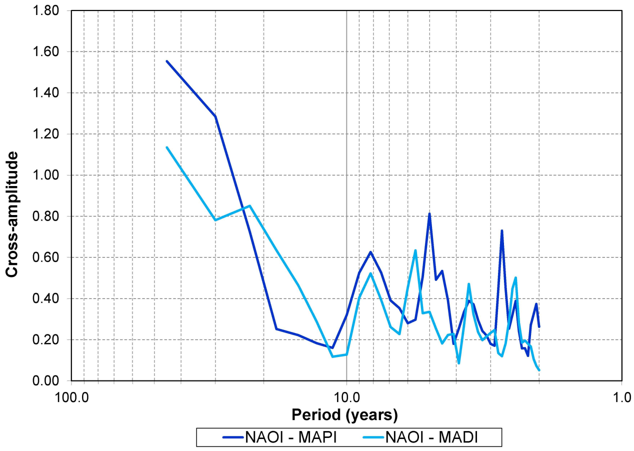

Fig. 11. Cross-amplitude of the MAPI and MADI time series compared to the NAOI time series.

belonging to the winter NAOI for periodicities from 2 to 3 yr, at 5 yr and at 45 yr (Fig. 10).

To find periodicities of the MAPI and the MADI that were synchronous with the winter NAOI, a cross-spectral analysis (Shumway and Stoffer, 2006) was performed to obtain cross-amplitude values of the cross periodogram, corresponding to a measure of the covariance between the respective frequency components in the two time series.

From this analysis (Fig. 11), correlations for periodicities from 2 to 3 yr, from 3 to 4 yr, for periods of around 5 yr and 8 yr and for periods from 30 to 45 yr were discovered. The longer periodicities, which were characterised by the greatest cross-amplitude, were also recognised by the observation of the fluctuation of the 11-yr moving averages, whose minima peaks occurred simultaneously for the three time series after approximately 45 yr (Figs. 4 and 9).

5 Conclusions

In the Campania region, a complex cyclical periodicity of rainfall patterns that was mainly teleconnected with the North Atlantic Oscillation was discovered, confirming that previously observed for other regions of western Europe and North America (Hurrell and van Loon, 1997; Vicente-Serrano and Trigo, 2011). The integrated analyses of regional indexes of precipitation, air temperature and effective precipitation in the period 1921–2010 (90 yr) revealed a significant impact of the NAO on processes of groundwater recharge. This was confirmed by the robust correlation between the winter NAO index and the annual spring discharges of a unique long-lasting karst spring discharge time series, as well as of other shorter time series.

The analysis of the temporal structure of the time series showed stronger correlations for periodicities varying from the interannual to decadal time scales, with the greatest correlation at the periodicity from 30 to 45 yr. This periodicity determined a decadal variability of the precipitation and spring discharge, configuring two complete long-term cycles with minima corresponding to 1925, 1948 and 1990 and displaying a new cycle starting in the early 1990s. The latter has been characterised by an increase in precipitation and the spring discharges as well as by the rising of piezometric levels and the return of karst springs, which disappeared during the 1980s and 1990s.

The results obtained can be considered a first attempt to extend understanding of the impact of the NAO on the hydrological variability over Europe and Mediterranean karst areas, including the underground component of the hydrological cycle on large and strategic regional aquifers. Moreover, the correlations can be conceived as a basis in formulating groundwater recharge models of carbonate karst aquifers and in planning appropriate management scenarios of aqueduct feeding from the interannual to the decadal time scales. Due to this teleconnection, the NAO would be conceived as a proxy to forecast climate change (Mazzarella and Scafetta, 2012) the decadal variability of groundwater recharge in Mediterranean karst areas. This consideration is enhanced by the wide interest of the scientific community in the North Atlantic Oscillation, which continuously operates, monitoring and interpretations of this large-scale atmospheric phenomenon.

Acknowledgements. The authors wish to thank Gerardo Ventafridda of the AQP Aquedotto Pugliese S.p.A. (http://www.aqp.it) who provided data for the Cassano Irpino and the Sanità karst springs. The authors are also grateful to the Department of Civil Protection of the Campania region (http://www.regione.campania.it), which has kindly provided the rainfall and temperature data. Finally, the authors are grateful to anonymous reviewers for constructive criticism.

Edited by: N. Romano

References

Allocca, V., Celico, F., Celico, P., De Vita, P., Fabbrocino, S., Mattia, S., Monacelli, G., Musilli, I., Piscopo, V., Scalise, A. R., Summa, G., and Tranfaglia, G.: Illustrative Notes of the Hydrogeological Map of Southern Italy, Istituto Poligrafico e Zecca dello Stato, ISBN 88-448-0215-5, 1–211, 2007.

Allocca, V., Celico, F., Celico, P., De Vita, P., Fabbrocino, S., Mattia, C., Monacelli, G., Musilli, I., Piscopo, V., Scalise, A. R., Summa, G., and Tranfaglia, G.: La carta idrogeologica dell'Italia meridionale. Metodi ed analisi territoriali per l'identificazione e la caratterizzazione dei corpi idrici sotterranei (Direttiva 2000/60/CE), L'ACQUA, 4, 21–32, 2009 (in Italian).

Bandini, A.: Tipi pluviometrici dominanti sulle regioni italiane, Il Servizio Idrografico Italiano. Ministero dei Lavori Pubblici, Roma, 1931 (in Italian).

Barnston, A. G. and Livezey, R. E.: Classification, Seasonality, and Persistence of Low-Frequency Atmospheric Circulation Patterns, Mon. Weather Rev., 115, 1083–1126, 1987.

Bartolini, E., Claps, P., and D'Odorico, P.: Interannual variability of winter precipitation in the European Alps: relations with the North Atlantic Oscillation, Hydrol. Earth Syst. Sci., 13, 17–25, doi:10.5194/hess-13-17-2009, 2009.

Boni, C., Bono, P., and Capelli, G.: Valutazione quantitativa dell'infiltrazione efficace in un bacino dell'Italia centrale: confronto con analoghi bacini rappresentativi di diversa litologia, Geologia Applicata e Idrogeologia, 17, 437–452, 1982.

Brandimarte, L., Di Baldassarre, G., Bruni, G., D'Odorico, P., and Montanari, A.: Relation Between the North-Atlantic Oscillation and Hydroclimatic Conditions in Mediterranean Areas, Water Resour. Manage., 25, 1269–1279, 2011.

Brunetti, M., Maugeri, M., and Nanni, T.: Variations of temperature and precipitation in Italy from 1866–1995, Theor. Appl. Climatol., 65, 165–174, 2000.

Brunetti, M., Maugeri, M., Monti, F., and Nanni, T.: Temperature and precipitation variability in Italy in the last two centuries from homogenized instrumental time series, Int. J. Climatol., 26, 345–381, 2006.

Caloiero, T., Coscarelli, R., Ferrari, E., and Mancini, M.: Precipitation change in Southern Italy linked to global scale oscillation indexes, Nat. Hazards Earth Syst. Sci., 11, 1683–1694, doi:10.5194/nhess-11-1683-2011, 2011.

Cambi, C. and Dragoni, W.: Groundwater, recharge variability and climatic changes: some consideration out of the modeling of an Apenninic spring, Hydrogeology, 4, 11–25, 2000.

Celico, F. and Mattia, C.: Analisi degli effetti indotti dal sisma del 23/11/1980 sugli equilibri idrogeologici della sorgente Sanità (Campania), mediante simulazione ragionata delle dinamiche di ricarica e esaurimento, Quaderni di Geologia Applicata, 1, 5–18, 2002 (in Italian).

Celico, F., Celico, P., De Vita, P., and Piscopo, V.: Groundwater flow and protection in the Southern Apennines (Italy), Hydrogéologie, 4, 39–47, 2000.

Celico, F., Naclerio, G., Bucci, A., Nerone, V., Capuano, P., Carcione, M., Allocca, V., and Celico, P.: Influence of pyroclastic soil on epikarst formation: a test study in southern Italy, Terra Nova, 22, 110–115, 2010.

Celico, P.: Schema idrogeologico dell'Appennino carbonatico centro-meridonale, Memorie e Note Istituto di Geologia Applicata, Napoli, 14, 1–97, 1978 (in Italian).

Celico, P.: Relazioni tra idrodinamica sotterranea e terremoti in Irpinia (Campania), Rendiconti Società Geologica Italiana, 4, 103–108, 1981 (in Italian).

Celico, P.: Idrogeologia dei massicci carbonatici, delle piane quaternarie e delle aree vulcaniche dell'Italia centro-meridionale (Marche e Lazio meridionale, Abruzzo, Molise e Campania), Quaderni della Cassa per il Mezzogiorno, 4/2, 1–203, 1983.

Cotecchia, V., Casarano, D., and Polemio, M.: Piovosità e siccità in Italia meridionale tra il 1821 ed il 2001, L'ACQUA, 2, 99–106, 2003 (in Italian).

Cullen, H. M. and deMenocal, P. B.: North Atlantic Influence on Tigris-Euphrates streamflow, Int. J. Climatol., 20, 853–863, 2000.

Cullen, H. M., Kaplan, A., Arkin, P. A., and deMenocal, P. B.: Impact of the North Atlantic Influence on the middle eastern climate and streamflow, Climatic Change, 55, 315–338, 2002.

De Vita, P. and Fabbrocino, S.: L'oscillazione del Nord Atlantico e la variabilità pluriennale delle risorse idriche sotterranee negli acquiferi carbonatici dell'Italia meridionale, Giornale di Geologia Applicata, 2, 357–362, 2005 (in Italian).

De Vita, P. and Fabbrocino, S.: Influence of the North Atlantic Oscillation on the climatic variability and groundwater resources in carbonate aquifers of Southern Italy, Italian Journal of Engineering Geology and Environment, 1, 33–48, 2007.

Dragoni, W. and Sukhija, B. S.: Climate change and groundwater: a short review, Geological Society, London, Special Publications, 288, 1–12, 2008.

Ducci, D. and Tranfaglia, G.: The Effect of Climate Change on the Hydrogeological Resources in Campania Region – Italy, in: Groundwater and climatic changes, edited by: Dragoni, W., Geological Society, London, Special Publications, 288, 25–38, 2008.

Fiorillo, F.: Spring hydrographs as indicators of droughts in a karst environment, J. Hydrol., 373, 290–301, 2009.

Fiorillo, F. and Guadagno, F. M.: Karst Spring Discharges Analysis in Relation to Drought Periods, Using the SPI, Water Resour. Manage., 24, 1867–1884, 2010.

Greatbatch, R. J.: The North Atlantic Oscillation, Stoch. Env. Res. Risk A., 14, 213–242, 2000.

Hasanean, H. M.: Wintertime surface temperature in Egypt in relation to the associated atmospheric circulation, Int. J. Climatol., 24, 985–999, 2004.

Henderson-Sellers, A. and Robinson, P. J.: Contemporary Climatology, John Wiley & Sons, New York, 1986.

Hurrell, J. W.: Decadal Trends in the North Atlantic Oscillation: Regional Temperatures and Precipitation, Science, 269, 676–679, 1995.

Hurrell, J. W. and van Loon, H.: Decadal variations in climate associated with the North Atlantic Oscillation, Climatic Change, 36, 301–326, 1997.

Hurrell, J. W., Kushirn, Y., Ottersen, G., and Visbeck, N.: An Overview of the North Atlantic Oscillation, in: The North Atlantic Oscillation: Climatic Significance and Environmental Impact, Geophysical Monograph, American Geophysical Union, 134, doi:10.1029/134GM01, 2003.

IPCC: Climate Change, The IPPC Scientific Assessment, edited by: Houghton, J. T., Jenkins, G. J., and Ephraums, J. J., ISBN 052140360X, 1-414, Cambridge University Press, UK, 1990.

IPCC: The scientific basis. Contribution of working group I to the third assessment report of the Intergovernmental Panel on

Climate Change (ICCP), edited by: Houghton, J. T., Ding, Y., Griggs, D. J., Noguer, M., Van der Linden, P. J., and Xiaosu, D., Cambridge University Press, UK, 2001.

IPCC: Climate Change, Synthesis Report. Contribution of Working Groups I, II and III to the Fourth Assessment Report of the Intergovernmental Panel on Climate Change, edited by: Pachauri, R. K. and Reisinger, A., Geneva, Switzerland, 1–104, 2007, available at: http://www.ipcc.ch/publications_and_data/publications_ipcc_fourth_assessment_report_synthesis_report.htm, 2007.

Karabörk, M. C., Kahya, E., and Karaca, M.: The influences of the Southern and North Atlantic Oscillation on climatic surface variables in Turkey, Hydrolog. Process., 19, 1185–1211, 2005.

Kücük, M., Kahya, E., Cengiz, T. M., and Karaca, M.: North Atlantic Oscillation influences on Turkish lake levels, Hydrolog. Process., 23, 893–906, 2009.

López-Moreno, J. I. and Vicente-Serrano, S. M.: Positive and negtive Phases of the Winter-time North Atlantic Oscillation and Drought occurrence over Europe: multitemporal-scale approach, J. Climate, 21, 1220–1241, 2008.

López-Moreno, J. I., Beguería, S., Vicente-Serrano, S. M., and García-Ruiz, J. M.: Influence of the North Atlantic Oscillation on water resources in central Iberia: Precipitation, stream-flow anomalies, and reservoir management strategies, Water Resour. Res., 43, W09411, doi:10.1029/2007WR005864, 2007.

Lorenzo-Lacruz, J., Vicente-Serrano, S. M., López-Moreno, J. I., González-Hidalgo, J. C., and Morán-Tejeda, E.: The response of Iberian rivers to the North Atlantic Oscillation, Hydrol. Earth Syst. Sci., 15, 2581—2597, doi:10.5194/hess-15-2581-2011, 2011.

Lo Vecchio, G. and Nanni, T.: The variation of the atmospheric temperature in Italy during the last hundred years and its relationship with solar output, Theor. Appl. Climatol., 51, 159–146, 1995.

Massei, N., Laignel, B., Deloffre, J., Mesquita, J., Motelay, A., Lafite, R., and Durand, A.: Long-term hydrological changes of the Seine River flow (France) and their relation to the North Atlantic Oscillation over the period 1950–2008, Int. J. Climatol., 30, 2146–2154, 2009.

Mazzarella, A. and Scafetta, N.: Evidences for a quasi 60-year North Atlantic Oscillation since 1700 and its meaning for global climate change, Theor. Appl. Climatol., 107, 599–609, 2012.

Morán-Tejeda, E., López-Moreno, I., Ceballos-Barbancho, A., and Vicente-Serrano, S. M.: Evaluating Duero's basin (Spain) response to the NAO phases: spatial and seasonal variability, Hydrolog. Process., 25, 1313–1326, 2011.

Polemio, M. and Casarano, D.: Climate change, drought and groundwater availability in Southern Italy, Geological Society, London, Special Publications, 288, 39–51, 2008.

Rimbu, N., Boroneant, C., Buta, C., and Dima, M.: Decadal variability of the Danube river flow in the lower basin and its relation with the North Atlantic Oscillation, Int. J. Climatol., 22, 1169–1179, 2002.

Rodriguez-Puebla, C. and Nieto, S.: Trends of precipitation over the Iberian Peninsula and the North Atlantic Oscillation under climate change conditions, Int. J. Climatol., 30, 1807–1815, 2010.

Rodriguez-Puebla, C., Encinas, A. H., Nieto, S., and Garmendia, J.: Spatial and temporal patterns of annual precipitation variability over the Iberian Peninsula, Int. J. Climatol., 18, 299–316, 1998.

Santoro, M.: Sulla applicabilità della formula di Turc per il calcolo della evapotraspirazione effettiva in Sicilia, Proceedings I International Conference on Groundwater, I.A.H., Palermo, 1970 (in Italian).

Sheridan, S. C.: North American weather-type frequency and teleconnection indices, Int. J. Climatol., 23, 27–45, 2003.

Shumway, R. H. and Stoffer, D. S.: Time Series Analysis and its Application (2 Edn.), Springer, 1–588, 2006.

Tootle, G., Piechota, T., and Singh, A.: Coupled oceanic-atmospheric variability and U. S. streamflow, Water Resour. Res., 41, 1–11, 2005.

Trigo, R. M., Pozo-Vázquez, D., Osborn, T. J., Castro-Díez, Y., Gámiz-Fortis, S., and Esteban-Parra, M. J.: North Atlantic Oscillation influence on precipitation, river flow and water resources in the Iberian Peninsula, Int. J. Climatol., 24, 925–944, 2004.

Turc, L.: Le bilan d'eau des sols: relations entre les précipitations, l'évaporation et l'éecolument, Annales agronomiques, Paris, 5, 491–595, 1954 (in French).

Türkes, M. and Erlat, E.: Climatological responses of winter precipitation in Turkey to variability of the North Atlantic Oscillation during the period 1930–2001, Theor. Appl. Climatol., 81, 45–69, 2005.

Uvo, C.: Analysis and regionalization of northern European winter precipitation based on its relationship with the North Atlantic Oscillation, Int. J. Climatol., 23, 1185–1194, 2003.

Vicente-Serrano, S. M. and Trigo, R. M. (Eds.): Hydrological, Socioeconomic and Ecological Impacts of the North Atlantic Oscillation in the Mediterranean Region (Advances in Global Change Research), Springer, 1–236, 2011.

Walker, G. T.: Correlation in seasonal variation of weather, IX Memories of the Indian Meteorological Department, 24, 275–332, 1924.

Walker, G. T. and Bliss, E. W.: World Weather V, Memories of the Royal Meteorological Society, 4, 53–84, 1932.

Wanner, H., Brönnimann, S., Casty, C., Gyalistras, D., Luterbacher, J., Schmutz, C., Stephenson, D. B., and Xoplaki, E.: North Atlantic Oscillation – concepts and studies, Survey Geophysics Journal, 22, 321–381, 2001.

WMO: World Climate Conference, WMO, No. 537, ISBN 92-63-10537-5. Proceedings of the World Climate Conference, Geneva, Switzerland, 12–23 February 1979.

Impact of the NAO on the hydrological cycle of karst aquifers in southern Apennines

Vincenzo Allocca[1], Pantaleone De Vita[1], and Ferdinando Manna[2]

1. Dipartimento di Scienze della Terra, Università degli Studi di Napoli Federico II, Napoli, Italy, vallocca@unina.it; padevita@unina.it.
2. Dipartimento di Scienze della Terra, Università degli Studi di Napoli Federico II, Napoli, Italy, PhD Student in "*Internal Dynamics of Volcanic Systems and Hydrogeological and Environmental Risks*", mannaferdinando@gmail.com.

Key-words: NAO, hydrological cycle, karst aquifer, Southern Apennines.

1. Introduction

The karst aquifers represent important groundwater resources in Italy, Europe and in the world. In southern Italy they are the main source of drinking and thermo-mineral waters, due their annual groundwater flow approximately amounting to 4.100×10^6 m^3/year (Celico, 1983; Allocca et al., 2007). Recent researches (De Vita et al., 2012; Allocca et al., 2012) provided evidence of a decadal relationship between the NAO (North Atlantic Oscillation), the regional rainfall and the discharges of some karst springs. In this paper we discuss about the impact of the NAO on the long-term components of the hydrological cycle for the karst aquifers of the southern Apennines (Fig. 2).

2. Material and Methods

In order to examine the decadal variability of karst aquifers recharge, we used rainfall data collected by 18 rain gauge stations and air temperature data recorded in 9 thermometric stations, for the period 1921÷2010 (Fig. 2). We reconstructed time series of regional normalized indexes (De Vita et al., 2012) for precipitations (MAPI), air temperature (MATI), effective precipitation (MAEPI), real evapotranspiration (MAEI) and effective infiltration (MANII) (Fig. 1). To the scope of analyzing the relationship between the NAO and the hydrological cycle of the investigated area, we have also considered the winter NAO Index (NAOI) existing between the station in Lisbon (Portugal) and the one in Stikkishlomur (Iceland), calculated for the period 1921÷2010.

3. Results

The pattern of the hydrological parameters was observed as characterized by a cyclical evolution, which resulted strongly correlated with the variation of the NAO Index (Fig. 1).

Moreover, a significant correlation between the NAOI and the MAPI, MAEPI, MAEI and MANII was found. The respective correlation coefficients (r), calculated by using the moving average (11 years) of each series were: –0,76, –0,66, –0,82 and –0,32. The correlation between the NAOI and the MATI was not significant (r = +0,29). Finally, during last decades (1980÷2010), the analysis showed a reduction of 10% in the volume of total annual rainfall, respect to the average of the whole time series. Similarly, a reduction was observed also for the real evapotranspiration (–2%) and in net infiltration (–15%) (Fig. 2). By contrast, an increase in air temperature (+0,05 °C) was recognized.

4. Conclusions

The significant correlations found between the NAOI and the examined hydrological time series demonstrated the strong influence of the NAO on the hydrological cycle of the karst aquifers. Therefore, the winter NAOI can be considered as an effective proxy to forecast the decadal variability of the groundwater resources in Mediterranean karst areas, allowing the modelling, forecasting and planning of their sustainable management.

References

Allocca V., Celico F., Celico P., De Vita P., Fabbrocino S., Mattia S., Monacelli G., Musilli I., Piscopo V., Scalise A.R., Summa G., Tranfaglia G. (2007). *Note illustrative della Carta idrogeologica dell'Italia meridionale*. Istituto Poligrafico e Zecca dello Stato, 1-211, ISBN 88-448-0215-5.

Allocca V., De Vita P., Manna F. (2012). *La variabilità climatica in Italia meridionale e gli effetti sulla ricarica degli acquiferi carbonatici.* EngHydriEnv Geology 14 B (2012), 9-10, doi: 10.1474/EHEGeology. 2012-14-B.51, ISSN 2038-0801.

Celico P. (1983). *Idrogeologia dei massicci carbonatici, delle piane quaternarie e delle aree vulcaniche dell'Italia centro-meridionale (Marche e Lazio meridionale, Abruzzo, Molise e Campania).* Quaderni della Cassa per il Mezzogiorno, 4/2, 1-203, 1983.

De Vita P., Allocca V., Manna F., Fabbrocino S. (2012). *Coupled decadal variability of the North Atlantic Oscillation, regional rainfall and karst spring discharges in the Campania region (southern Italy)*. Hydrol. Earth Syst. Sci., 16, 1389-1399, 2012, doi:10.5194/hessd-16-1389-2012.

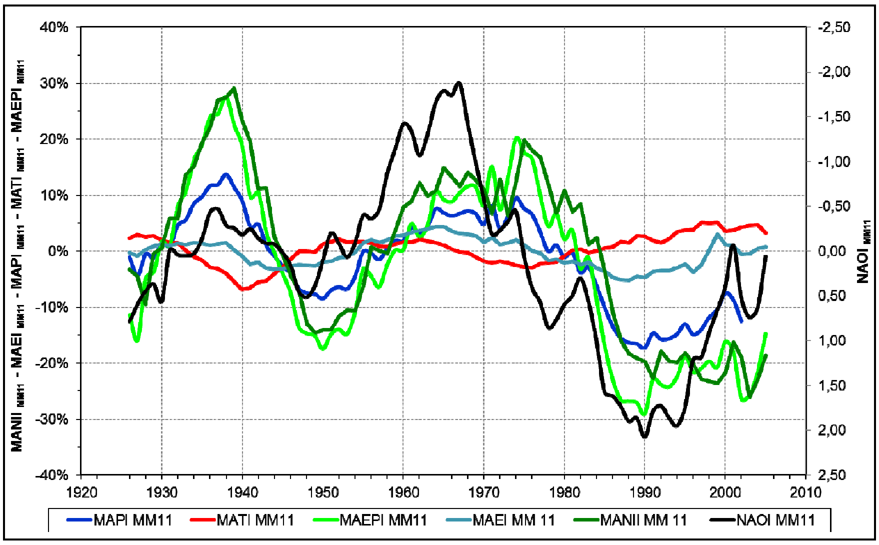

Fig. 1 – Comparison of the 11-yr moving averages (MM11) of winter NAOI (Nord Atlantic Oscillation Index), MAPI (Mean Annual Precipitation Index), MATI (Mean Annual Temperature Index), MAEPI (Mean Annual Effective Precipitation Index), MAEI (Mean Annual Evapotraspiration Index) and MANII (Mean Annual Net Infiltration Index) time series.

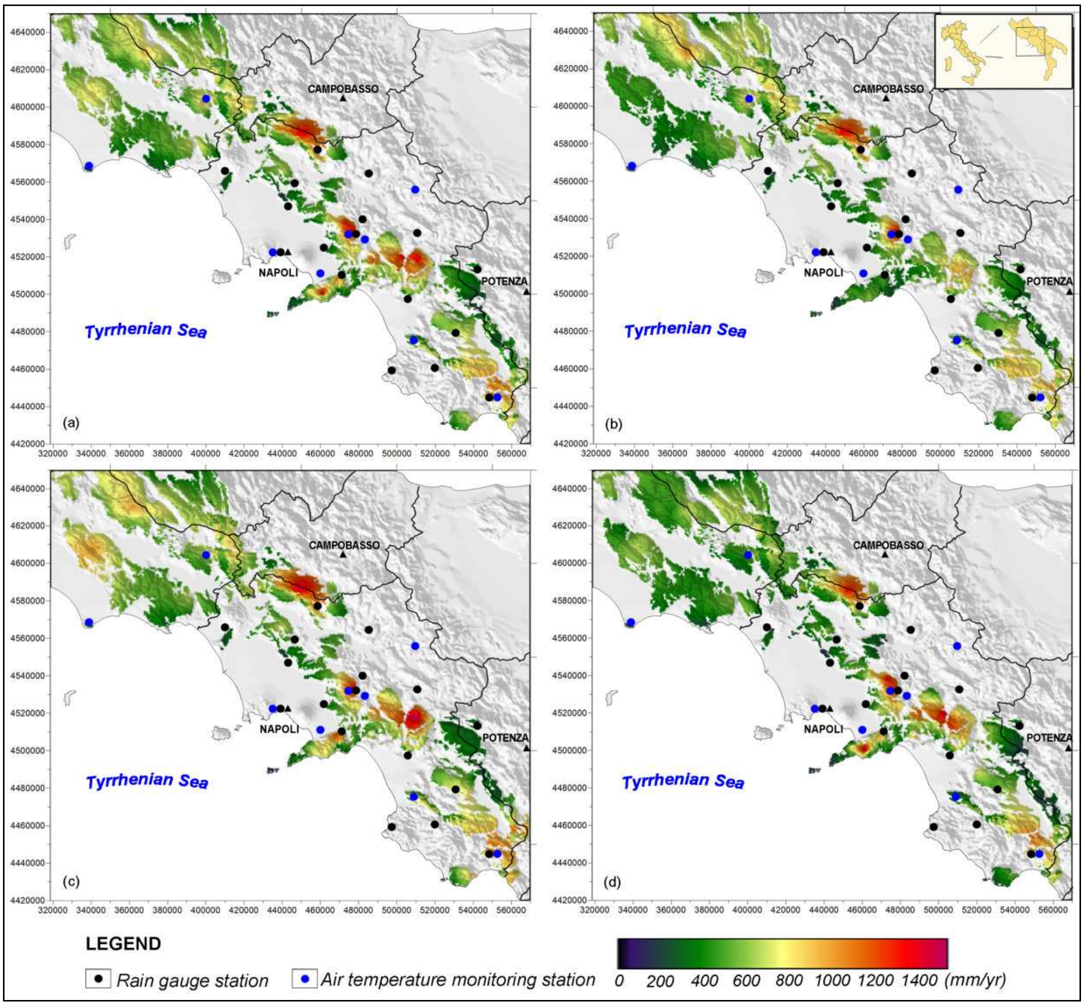

Fig. 2 – Spatial and temporal variation of mean net infiltration; (a): 1921÷2010; (b): 1926÷1950; (c): 1951÷1980; (d): 1981÷2010.

ISSN 2035-8008

RENDICONTI *Online* della *Società Geologica Italiana*

Volume 28 - Settembre 2013

12th European Geoparks Conference

An innovative approach to raise public awareness about geohazard, climate change, and the sustainable use of our natural resources

Selected short notes
Ascea, Italy, 4-7 September 2013

edited by: A. Aloia, D. Calcaterra, A. Cuomo, D. Guida

ROMA
SOCIETÀ GEOLOGICA ITALIANA
2013
www.socgeol.it

Rend. Online Soc. Geol. It., Vol. 28 (2013), pp. 106-109, 2 figs., 1 tab.

Effect of the North Atlantic Oscillation on groundwater recharge in karst aquifers of the Cilento Geopark (Italy)

Ferdinando Manna (*), Vincenzo Allocca (*), Francesco Fusco (**), Elisabetta Napolitano (*), Pantaleone De Vita (*)

(*) Dipartimento di Scienze della Terra, dell'Ambiente e delle Risorse - University of Naples "Federico II"
(**) External collaborator

Document type: Short note
Manuscript history: received 1 July 2013; accepted 22 July 2013; editorial responsibility and handling by Domenico Calcaterra.

ABSTRACT

The assessment of groundwater recharge for aquifers of a Geopark is an essential issue to plan water management based on balancing both human uses and river ecology. The relevance of this topic is enhanced by the climatic variability which constraints to analyze water budget with a non-stationary methodology. In this paper, an approach for evaluating the effects of climatic variability on the groundwater recharge of karst aquifers of the Cilento Geopark is proposed, focusing on the influence of the North Atlantic Oscillation (NAO). Such karst aquifers store invaluable groundwater resources feeding settlements of the Geopark and maintaining ecological equilibrium of the main rivers. With such purpose, time series of annual precipitation and air temperature, recorded by a meteorological network covering the Cilento Geopark, were gathered for the period 1921-2010 and analyzed. The most important result is the finding of a complexly cyclical variability of precipitation, with periodicities from yearly to decadal, which is strongly correlated to the NAO. During the examined period, the annual precipitation and effective precipitation ranged around the mean value, respectively for about ±40% and ±70%. Due to the continental influence of the NAO, the proposed approach can be conceived as being extendable to other Geoparks, climatically controlled by the NAO, in which the management of the groundwater resources is crucial for river ecological systems.

KEY WORDS: Cilento Geopark, climate variability, groundwater recharge, karst aquifers, North Atlantic oscillation.

INTRODUCTION

The karst aquifers store important groundwater resources in Italy, Europe and in the world. In southern Italy, they are the main source of drinking waters because of their annual groundwater yield, which amounts globally to 4100×10^6 m^3/year and outflows from huge springs and/or through other adjoining aquifers (Celico, 1983; Allocca et al., 2007). Due to climate variability, the assessment of groundwater recharge processes is an essential and challenging issue for a correct management of groundwater resources along with respecting the EU Water Framework Directive 2000/60/EC. Among the continental-scale phenomena influencing the atmospheric circulation, the most important one for the Northern hemisphere and the European continent, is the North Atlantic Oscillation (NAO), which is an oscillation with a complex periodicity, varying from yearly to decadal time scales, of the atmospheric masses comprised between the Azores Islands (barometric high) and Iceland (barometric low). The NAO is analyzed through the NAO Index (NAOI), which is the barometric anomaly between the Iceland's barometric low and Azores's barometric high (Hurrell et al., 2003), with respect to the standard difference.

Numerous studies analysed the impact of the NAO on the annual variability of precipitation in European countries (Rodriguez-Puebla & Nieto, 2010) and its impact on river flows of Mediterranean hydrographic basins (Lorenzo-Lacruz et al., 2011). Recent studies revealed that the NAO influences also snow accumulation, crop production, landslide occurrences and soil erosivity in Mediterranean areas (Vicente-Serrano & Trigo, 2011).

In the Campania region, the integrated analyses of regional indexes of precipitation, air temperature and effective precipitation in the period 1921-2010 has already revealed a significant impact of the NAO on spring discharges (De Vita et al., 2012), namely on groundwater recharge.

In this paper, the long-term climatic variability and its influence on groundwater recharge were analysed by examining decadal patterns of precipitation in the Cilento Geopark area (Italy), coupled with the North Atlantic Oscillation.

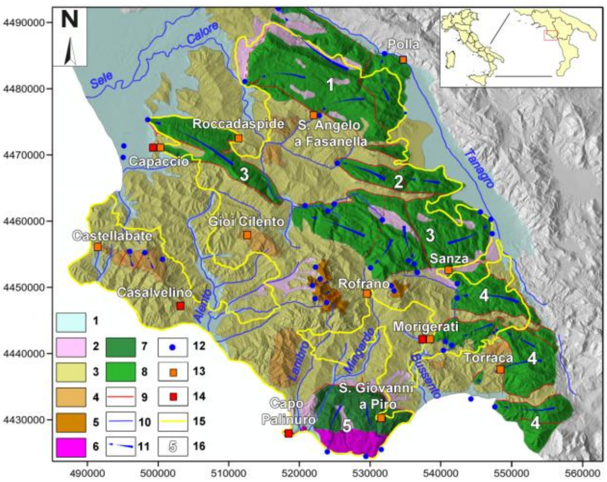

Fig. 1 – Hydrogeological map of the Cilento Geopark. Key to symbols: 1) Alluvial complex; 2) Detrital complex; 3) Pelitic-arenaceous-calcareous complex; 4) Arenaceous-conglomeratic complex; 5) Conglomeratic-arenaceous complex; 6) Dolomitic complex; 7) Calcareous-marly complex; 8) Calcareous complex; 9) Main faults of hydrogeological relevance; 10) River; 11) Direction of groundwater flow; 12) Springs; 13) Rain gauge station; 14) Air temperature stations; 15) Boundary of the Cilento Geopark; 16) ID of karst aquifers.

DATA AND METHODS

The Cilento Geopark is located in the southern Italy and has an extension of about 1810 km^2, with a mean altitude of about 550 m a.s.l. and a Mediterranean climate type (Csa) (Geiger, 1954). The hydrogeological setting (Fig. 1) is essentially characterised by carbonate aquifers (50% of total area), with a high degree of permeability due to fracturing and karst. These aquifers, formed by limestone, dolomitic limestone and dolomitic series of carbonate platform facies (Trias-Paleogene), are confined by aquitards or aquicludes, composed of flysch and basinal series (Paleogene), or by alluvial/detrital aquifers (Quaternary) (Celico, 1983; De Vita, 1994; Allocca et al., 2007; Allocca et al., 2009). They are typically characterised by a basal groundwater flow, outflowing in huge basal springs, which in several cases have an average discharge greater than 1.0 m^3/s. A subordinate perched groundwater flow also occurs in the surficial part of the karst aquifers (Allocca et al., 2008), where the different deepening of the epikarst (Celico et al., 2010), as well as stratigraphic and tectonic factors, allow generating seasonal and ephemeral springs. Unlike the other karst aquifers of Campania (Naclerio et al., 2008; Naclerio et al., 2009), the hydrogeological role of ash-fall pyroclastic overburdens (Fusco et al., 2013) is less important for those of the Cilento Geopark, because of the lowest thickness, which is due to the greater distance from the main eruptive centres of the Campania region (e.g. Phegrean Fields and Somma-Vesuvius).

To investigate decadal variability and correlations among hydrological time series, trend analysis was applied, by using smoothing numerical techniques. In particular, the moving average over 11 years, centred on the sixth year, provided a good smoothing of the periodicities shorter than one decade.

The analyses were performed by means of a subset (1921-2010) of the winter NAOI (December through March mean - DJFM) time series, calculated by the records of the Lisbon (Portugal) and Stikkishlomur (Iceland) barometric stations since 1864 (http://www.cgd.ucar.edu/cas/jhurrell/indices.html).

In order to examine the decadal variability of karst aquifers recharge, annual rainfall data recorded by 11 rain gauge stations for the period 1921-2010 (Fig. 1) were used: Capaccio, Castellabate, Gioi Cilento, Morigerati, Polla, Roccadaspide, Rofrano, S. Angelo a Fasanella, S. Giovanni a Piro, Sanza and Torraca. In addition, mean annual air temperature data recorded by the Capaccio, Capo Palinuro, Casalvelino and Morigerati monitoring stations (Fig. 1) were collected. This meteorological monitoring network was formerly controlled (1921-2000) by the National Hydrographic and Tidal Service (SIMN - *Servizio Idrografico Mareografico Nazionale* - http://www.isprambiente.gov.it); subsequently its management was in charge of the Regional Civil Protection Agency (http://www.protezionecivile.gov.it).

The time series of normalized index (De Vita et al., 2012) for mean annual precipitations (MAPI) (Fig. 2) was reconstructed by:

$$MAPI_i = \frac{\sum_{j=1}^{11} \frac{AP_{ji} - MAP_j}{MAP_j}}{\sum_{j=1}^{11} j}$$

where, $MAPI_i$ is the Mean Annual Precipitation Index for the i year (%), AP_{ji} is the Annual Precipitation for the j rain gauge station and the i year (mm), MAP_j is the Mean Annual Precipitation of the whole time series for the j rain gauge station (mm).

To assess the mean annual effective precipitation, which regulates groundwater recharge, the mean annual real evapotranspiration was estimated for each rain gauge station by applying the empirical formula of Turc (1954), as several studies have confirmed its reliability for Mediterranean areas and southern Italy (Celico, 1983):

$$ET_{ji} = \frac{AP_{ji}}{\sqrt{0.9 + \left(\frac{AP_{ji}}{300 + 25 \cdot AT_{ji} + 0.05 \cdot AT_{ji}^3}\right)^2}}$$

where ET_{ji} is the real evapotranspiration for the j rain gauge station and the i year (mm), AP_{ji} is the Annual Precipitation for the j rain gauge station and the i year (mm), AT_{ji} is the Annual air Temperature for the j rain gauge station and the i year (°C).

For the rain gauge stations without air temperature gauges, the mean annual air temperature values were extrapolated using linear correlations with altitude that were statistically robust in all cases.

Finally, for each year of the time series, the Mean Annual Effective Precipitation Index (hereafter MAEPI) was calculated by:

$$MAEPI_i = \frac{\sum_{j=1}^{18} \frac{AEP_{ji} - MAEP_j}{MAEP_j}}{\sum_{j=1}^{11} j}$$

where, $MAEPI_i$ is the Mean Annual Effective Precipitation Index for the i year (%), AEP_{ji} is the Annual Effective Precipitation for the j rain gauge station and the i year (mm), $MAEP_j$ is the Mean Annual Effective Precipitation of the whole time series for the j rain gauge station (mm).

To estimate the mean annual effective infiltration, the calculation of the water budget was carried out for all the karst aquifers (Fig. 1), by adapting the hydrological budget equation:

$$AP + U_i = ETR + R + IE + U_u + Q_s + Q_t$$

where, AP is the mean annual precipitation, U_i is the mean annual indirect inflow recharge, ETR is the mean annual actual evapotranspiration, R is the mean annual runoff, IE is the mean annual direct net infiltration, U_u is the mean annual indirect outflow discharge, Q_s is the mean annual spring discharges, Q_t is the mean annual tapped discharge.

The value of effective infiltration (IE), which represents the direct groundwater recharge due to precipitation, was calculated by means of coefficients of potential infiltration (CIP) (Celico, 1983; Allocca et al., 2007). These coefficients express the percentage of effective precipitation (AEP = AP – ETR) that potentially recharge groundwater circulation (CIP =

IE / AEP). Due to the hydrogeological settings, other indirect inflow recharge of karst aquifers were considered negligible.

RESULTS AND CONCLUSIONS

By observing the pattern of the MAPI 11-year moving average (Fig. 2b), a complex cyclical dynamic was recognised with respect to the normal value (mean value of the whole time series). Two decadal phases characterized by values above the normal value were identified for the periods 1930-1944 and 1958-1978, instead three phases below the normal value were recognized for years preceding 1930 and for the periods 1944-1958 and 1980-2005. These long-term fluctuations were found as inversely corresponding with those of the winter NAOI (Fig. 2a). For the last part of the time series, an increased frequency of MAPI values below the average value, indicated a downward shifting trend. From 1985 to 2008, negative values (down to -39% in 1992) were continuously observed, except in 1996 and 2002. Similar low levels also occurred in 1932 and 1946 but with lower frequency (Fig. 2b). The maximum values of the time series were estimated as follows: +44% (1963), +46% (1976) and +47% (2010).

The long-term trend of the MAEPI (Fig. 2c) showed a very remarkable fluctuations around the mean value, with cyclical decadal dynamics. The extreme values of the time series, ranging from +70% (1976) to -63% (1992), were identified as matching those of the MAPI time series. This observation was correlated to the amplification effect due to the nonlinear behaviour of the evapotranspiration process. Similarly to the MAPI, a downward shift trend was observed for the MAEPI in the last decades of the time series.

The integrated analysis among the different components of long-term time series of the NAOI, MAPI and MAEPI showed a strong coherence of the 11-year moving averages by a good overlapping of the positive and negative peaks (Fig. 2d). Particularly, the long-term periodicity of the time series indicated two decadal cycles and the beginning of a third cycle, starting approximately from 1990.

Taking into account the fluctuation of MAEPI around the mean value, the decadal groundwater recharge variability was modelled. In particular, minimum and maximum values of recharge were estimated by considering the minimum (-36%) and the maximum (+20%) of the MAEPI 11-year moving average (Table 1). This approach was considered useful to recognize the long-term variability of groundwater resources, even if stronger fluctuations occur on shorter time scales.

According to Celico (1983) and Allocca et al. (2007), a mean CIP value of 90% for Alburni, Cervati, Motola and Forcella karst aquifers was assigned, considering their typical summit flat and endorheic morphologies and of 70% for Bulgheria karst aquifer, owing to the different lithology (Fig. 1).

The values of effective precipitation were obtained from a regional distributed model of mean annual effective precipitation (Manna et al., 2013), which accounts for spatial variability of precipitation due to both the orographic and altitude controls. The aquifer extension, spatial distribution of effective precipitation and different values of CIP control the net infiltration process, causing a very high volume of recharge for Alburni and Cervati aquifers and a lower volume for the

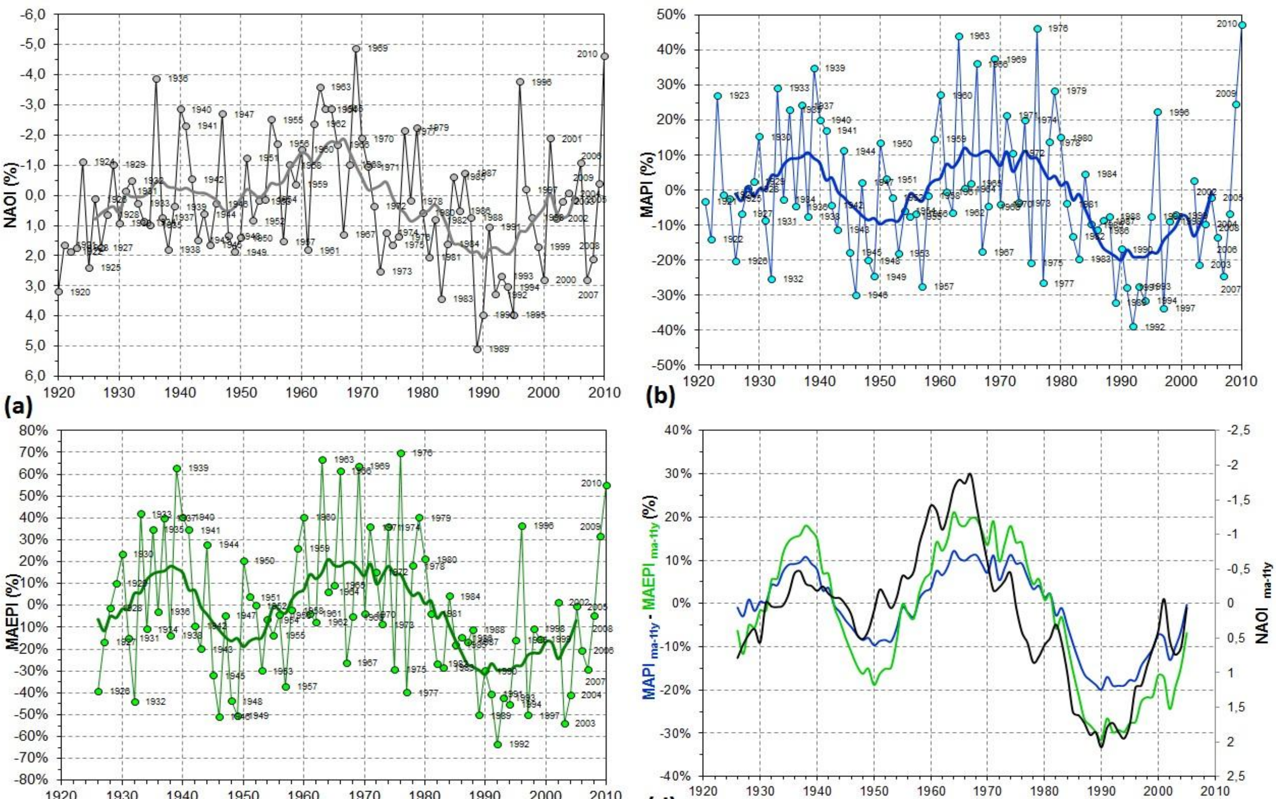

Fig. 2 – Time series of a) winter NAOI; b) MAPI; c) MAEPI. Key to symbols: continuous thick line = 11-year moving average centred on the sixth year; d) Comparison of the 11-year moving averages of the winter NAOI, MAPI and MAEPI time series for the Cilento Geopark.

Table 1 – Mean, min and max annual groundwater recharge estimated for the investigated karst aquifers of the Cilento Geopark. Minimum and maximum values were calculated respect to the variability of 11-year moving average.

ID	Karst aquifer	Area (Km^2)	Annual effective precipitation (10^6 m^3)			Mean CIP (%)	Groundwater recharge (10^6 m^3)		
			Min	Mean	Max		Min	Mean	Max
1	Alburni	254	189	295	354	90	170	265	318
2	Cervati	318	250	390	468	90	225	351	421
3	Motola	52	39	61	73	90	35	55	66
4	Forcella	217	134	210	252	90	121	189	227
5	Bulgheria	100	50	79	94	70	35	55	66

Bulgheria one, which is the closest to the coast line (Table 1).

By simulating the recharge process, it was taken into account the variability due to the NAO influence. For the Cervati karst aquifer a difference between minimum and maximum annual groundwater recharge of about 200×10^6 m^3/year was found; while for the Motola and Bulgheria aquifers, which have a lower extension, a difference of about 30×10^6 m^3/year was calculated (Table 1).

The significant correlations found between the NAOI and the examined hydrological time series demonstrated the strong influence of the NAO on the hydrological cycle of the karst aquifers in the Cilento Geopark. Therefore, this study demonstrates that the winter NAOI can be considered as an effective proxy to forecast the decadal variability of the groundwater resources. This understanding will allow to model and plan a sustainable management of water resources in protected areas as the Geoparks belonging to those zones of the Northern hemisphere, and particularly of the Mediterranean, which are under the influence of the NAO.

REFERENCES

Allocca V., Celico F., Celico P., De vita P., Fabbrocino S., Mattia S., Monacelli G., Musilli I., Piscopo V., Scalise A. R., Summa G. & Tranfaglia G. (2007) – Illustrative Notes of the Hydrogeological Map of Southern Italy. Istituto Poligrafico e Zecca dello Stato, ISBN 88-448-0215-5, 1-211.

Allocca V., Celico F., Petrella E., Marzullo G. & Naclerio G. (2008) - The role of land use and environmental factors on microbial pollution of mountainous limestone aquifers, Environ Geol, 55, 277-283.

Allocca V., Celico F., Celico P., De Vita P., Fabbrocino S., Mattia S., Monacelli G., Musilli I., Piscopo V., Scalise A.R., Summa G. & Tranfaglia G. (2009) – La carta idrogeologica dell'Italia meridionale. Metodi ed analisi territoriali per l'identificazione e la caratterizzazione dei corpi idrici sotterranei (Direttiva 2000/60/CE). L'ACQUA, 4, 21-32.

Celico F., Naclerio G., Bucci A., Nerone V., Capuano P., Carcione M., Allocca V. & Celico P. (2010) – Influence of pyroclastic soil on epikarst formation: a test study in southern Italy. Terra Nova, 22, 110-115.Celico P. (1983) – Idrogeologia dei massicci carbonatici, delle piane quaternarie e delle aree vulcaniche dell'Italia centro-meridionale (Marche e Lazio meridionale, Abruzzo, Molise e Campania). Quaderni della Cassa per il Mezzogiorno, 4/2, 1-203.

De Vita P. (1994) – La pianificazione delle risorse idriche nel Parco del Cilento e Vallo di Diano. Notiziario della SIGEA (Società Italiana di Geologia Ambientale), anno 2, 1, 6-8.

De Vita P., Allocca V., Manna F. & Fabbrocino S. (2012) – Coupled decadal variability of the North Atlantic Oscillation, regional rainfall and karst spring discharges in the Campania region (southern Italy). Hydrol. Earth Syst. Sci., 16, 1389-1399.

Fusco F., De Vita P., Napolitano E., Allocca V. & Manna F. (2013) – Monitoring the soil suction regime of landslide-prone ash-fall pyroclastics deposits covering slopes in the Sarno area (Campania – southern Italy). Rend. Online Soc. Geol. It, 24, 202 - 204.

Geiger R. (1954) – Landolt-Börnstein - Zahlenwerte und Funktionen aus Physik, Chemie, Astronomie, Geophysik und Technik, alte Serie Vol. 3, Ch. Klassifikation der Klimate nach W. Köppen. Springer. 603-607.

Hurrell J.W., Kushirn Y., Ottersen G. & Visbeck N. (2003) - An Overview of the North Atlantic Oscillation, in: The North Atlantic Oscillation: Climatic Significance and Environmental Impact. Geophysical Monograph, American Geophysical Union, 134, 10.1029/134GM01.

Lorenzo-Lacruz J., Vicente-Serrano S.M., López-Moreno J.I., González-Hidalgo J.C. & Morán-Tejeda E. (2011) – The response of Iberian rivers to the North Atlantic Oscillation. Hydrology and Earth System Sciences, 15, 2581 - 2597.

Manna F., Allocca V., De Vita P., Fusco F. & Napolitano E. (2013) – Groundwater recharge assessment in karst aquifers of southern Apennines (Italy). Rend. Online Soc. Geol. It, 24, 202 - 204.

Naclerio G., Petrella E., Nerone V., Allocca V., De Vita P. & Celico F. (2008) - Influence of topsoil of pyroclastic origin on microbial contamination of groundwater in fractured carbonate aquifers, Hydrogeology Journal, 16, 1057-1064.

Naclerio G., Nerone V., Bucci A., Allocca V. & Celico F. (2009) - Role of organic matter and clay fraction on migration of Escherichia Coli cells through pyroclastic soils, southern Italy, Colloids and Surfaces B: Biointerfaces, 72, 57-61.

Rodriguez-Puebla C. & Nieto S. (2010) – Trends of precipitation over the Iberian Peninsula and the North Atlantic Oscillation under climate change conditions. International Journal Climatology, 30, 1807 - 1815.

Turc L. (1954) – Le bilan d'eau des sols: relations entre les précipitations, l'évaporation et l'éecolument. Annales Agronomiques, 5, 491-595.

Vicente-Serrano S. M. & Trigo R. M. (2011) – Hydrological, Socioeconomic and Ecological Impacts of the North Atlantic Oscillation in the Mediterranean Region. Advances in Global Change Research, 46, 244 pp.

RENDICONTI *Online* della Società Geologica Italiana
Volume 28 - Settembre 2013

Cover: Molpa di Palinuro coast, Italy. (Photo: Aniello Aloia)

RENDICONTI ONLINE DELLA SOCIETÀ GEOLOGICA ITALIANA
Direttore responsabile: DOMENICO CALCATERRA
Iscrizione ROC 18414.
Pubblicato online il 1 settembre 2013.

ISSN 2035-8008

RENDICONTI *Online* della Società Geologica Italiana

Volume 24 - Febbraio 2013

Atti del IX Convegno Nazionale dei Giovani Ricercatori di Geologia Applicata

Napoli, 14-15 Febbraio 2013

A cura di: Domenico Calcaterra & Silvia Fabbrocino

ROMA
SOCIETÀ GEOLOGICA ITALIANA
2013
www.socgeol.it

Rend. Online Soc. Geol. It., Vol. 24 (2013), pp. 202-204, 2 figs., 2 tabs.

Groundwater recharge assessment in karst aquifers of southern Apennines (Italy)

FERDINANDO MANNA (*), VINCENZO ALLOCCA (*), PANTALEONE DE VITA (*), FRANCESCO FUSCO (°), ELISABETTA NAPOLITANO (*)

RIASSUNTO

Valutazione della ricarica degli acquiferi carsici dell'Appennino meridionale (Italia).

L'obiettivo di questo lavoro è la stima del coefficiente d'infiltrazione efficace medio annuo per quattro acquiferi carsici, rappresentativi dei numerosi altri dell'Appennino meridionale, i cui deflussi idrici sotterranei costituiscono insostituibili risorse idropotabili e controllano l'equilibrio ecologico di numerosi corsi d'acqua alla scala regionale.

Gli acquiferi campione sono stati caratterizzati mediante un approccio multidisciplinare basato sull'analisi delle proprietà idrogeologiche e morfologiche, dell'uso e del tipo di suolo e della copertura vegetale. Sulla base della raccolta di dati termo-pluviometrici a scala regionale nel periodo 1921-2012 e dei deflussi idrici sotterranei disponibili per lo stesso intervallo temporale, sono stati effettuati il calcolo del bilancio idrologico e la stima dei valori del coefficiente di infiltrazione efficace.

I coefficienti stimati rappresentano un avanzamento delle conoscenze idrogeologiche riguardanti i rapporti tra afflussi meteorici e ricarica degli acquiferi. Essi potranno essere utilizzati per la valutazione, dalla scala del singolo acquifero a quella regionale, dei valori di ricarica/infiltrazione, consentendo la gestione sostenibile delle risorse idriche sotterranee, anche simulando gli effetti dei cambiamenti climatici.

KEY WORDS: *Effective Infiltration Coefficient, karst aquifers, groundwater recharge, southern Apennines.*

INTRODUCTION

In most areas in the word, karst aquifers are important groundwater resources. For southern Italy, these aquifers represent the main source for drinking water and a strategic resource to socio-economic and environmental development (CELICO, 1983; ALLOCCA *et alii*, 2007). Therefore the correct estimation of groundwater recharge processes, at different space-time scales, taking into account the atmospheric factors affecting the climate variability (DE VITA *et alii*, 2012), is a fundamental and challenging issue.

Sedimentary series belonging to carbonate platform palaeographic units, Triassic to Paleogene in age, were piled up in the thrust-belt Apennine structure together with basinal and flysch series, during the Miocene orogenesis. They crop out forming both the highest mountain ranges and large karst aquifers, which are constituted of limestone, dolomitic-limestone and dolomite, with a high permeability degree, due to fracturing and karst processes (Fig. 1). An appropriate conceptual model to describe the hydrogeological features was depicted by several studies (CELICO, 1983; ALLOCCA *et alii*, 2007) that recognized 33 karst aquifers with autonomous groundwater circulation existing in the southern Apennines, from Abruzzo to Basilicata regions.

In scientific literature there is a wide range of direct and indirect approaches aiming to estimate the groundwater recharge (SCANLON *et alii*, 2002 and references therein): lysimeters measurements, soil moisture budgets, effective infiltration coefficients, water table rise method, tracer method, remote sensing method. However, each of them displays a degree of approximation depending upon the space-time scale

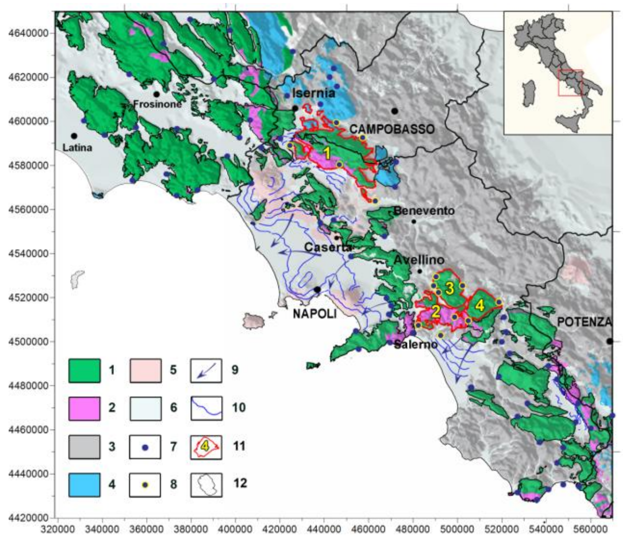

Fig. 1 – Hydrogeological map of southern Apennines. Hydrostratigraphic units and key to symbols: 1) Limestone and dolomitic limestone units of carbonate platform series (Jurassic-Paleogene); 2) Dolomitic units of carbonate platform series (Trias-Jurassic); 3) Pre-orogenic and syn-orogenic terrigenous units of inner and thrust-top basins series (Cretaceous-Upper Miocene); 4) Siliceous-marly units of outer basin series (Trias-Paleogene); 5) Volcanic units (Pliocene-Quaternary); 6) Alluvial and epiclastic units (Quaternary); 7) Main basal springs of carbonate karst aquifers; 8) Basal springs considered in water budget; 9) Main preferential drainage axes of groundwater flow in alluvial aquifers; 10) Groundwater head contour lines in alluvial and volcanic aquifers; 11) Identification of sample karst aquifers: 1. Matese; 2. Accellica; 3. Terminio; 4. Cervialto; 12) Hydrogeological boundary of the karst aquifers.

(*) Dipartimento di Scienze della Terra, dell'Ambiente e delle Risorse - University of Naples "Federico II"

(°) External collaborator

This study was supported in part by MIUR (Research Program PRIN 2010-2011).

investigated. At regional scale, the degree of approximation can be lowered by employing time series analysis and GIS instruments within a multi-disciplinary approach to estimate endogenous and exogenous variables affecting the recharge processes.

The aim of this paper is to quantify the groundwater recharge through the estimation of the Annual Effective Infiltration Coefficient (AEIC) in four representative karst aquifers of southern Apennines (Italy).

The AEIC is defined as the ratio between the outflow discharges and the volume of effective rainfall in a specified time unit (DROGUE, 1971; BONACCI, 2001). This hydrological parameter summarizes the effect of infiltration, soil-moisture deficiency, and runoff potential.

Several researches were carried out for characterizing the AEIC in carbonate aquifers. The measurement for AEIC carried out by KESSLER (1965) in Hungary karst area has shown a value of 51.6%. For Greek karst, in Parnassos-Ghiona aquifer, BURDON (1965) found a value of 45.2% consistent with the 49.8% recorded by SOULIOS (1984). DROGUE (1971) estimated a coefficient of about 50% in Saugras basin in France. For different calcareous basin of Croatia, values of AEIC from 35% to 70% (VILIMONOVIC, 1965), from 35% to 76%, with a mean value of 57% (BONACCI, 2001), from 23% to 77%, with mean value of 54% (HORVAT & RUBINIC, 2006), were found. For the dolomitic basin Tennesee a low value of 27% was assessed (SODEMAN & TYSINGER, 1965).

In Italy, BONI & BONO (1982) found a value of AEIC of 70% for some karst aquifers of the central Apennines, while CELICO (1983) and ALLOCCA *et alii* (2007) provided a preliminary estimate for southern Apennines karst aquifers ranging from 70% to 90%.

DATA AND METHODS

Karst aquifers of the southern Apennines constitute massifs with special morphological features, being characterized by large flat surface and endorheic zones on the top, and by having an average slope angle of about 30°-35° derived by the morphological evolution of original fault line scarps. These aquifers, in Campania and surrounding regions, are singularly covered by discontinuous pyroclastic soils, erupted from Campanian volcanic centers during the Quaternary.

Due to these complex features, a multidisciplinary approach was conducted for characterizing the four sample karst aquifers. The following aspects were analyzed: i) hydrogeological and geomorphological characteristics; ii) soil type, land use, and vegetation cover type; iii) time series of outflow discharge and effective precipitations.

The hydrogeological analysis of such aquifers was based on previous studies (CELICO, 1983; ALLOCCA *et alii*, 2007), while the morphological analysis was carried out analysing topographic digital elevation models derived from the I.G.M. (Italian Army Geographical Institute) topographic maps (1:25.000 scale). Data from Corine Land Cover (2006) were collected and analysed (http://www.sinanet.isprambiente.it), reclassifying them in four principal complexes: woodland, meadowland, urban area and areas without vegetation cover. Moreover, the *Soil Map of Campania region* (http://www.risorsa.info) and the *Ecopedological Map of Italy* (http://www.pcn.minambiente.it) were analysed, allowing to identify three soil types along with their texture (fine, medium and coarse) as well areas without soil cover.

Data of total annual precipitation and annual mean air temperature from 1926 to 2012 were collected from the National Technical Service Agency annals (http://www.isprambiente.gov.it) and Regional Civil Protection Agency databases (http://www.protezionecivile.gov.it). These data sets were used to reconstruct a regional-scale model of effective rainfall in a GIS platform, by means of geostatistical techniques. Annual groundwater outflows from sample karst aquifers were also estimated both considering spring discharge time series and other groundwater losses.

The AEIC (%) in karst aquifers was defined as follows:

$$\mathrm{AEIC} = \left[\frac{Q_{\mathrm{outflow}}}{Q_{\mathrm{inflow}}}\right] \times 100$$

where $Q_{outflow}$ is the annual mean of the outflow discharges (m^3/s) while Q_{inflow} is the annual mean of effective precipitation volume (mm/year) referred to the area recharge of the karst aquifer (km^2). Furthermore, having identified the endorheic basins and flat areas in which the infiltration value is maximum ($AEIC_E = 1$), we calculated the AEIC for the slope part of the karst aquifers ($AEIC_S$), by means of the following formula:

$$\mathrm{AEIC_S} = \left[\frac{(\mathrm{AEIC} \times A_T) - (1 \times A_E)}{A_S}\right] \times 100$$

where A_T is the total area of karst aquifer (km^2); A_E is the surface of endorheic basin (km^2); A_S is the slope surface (km^2).

To obtain the annual mean effective precipitation, the annual mean real evapotranspiration for each rain gauge station was estimated by applying the empirical formula of Turc (TURC, 1954).

$$\mathrm{ET_{ji}} = \frac{\mathrm{AP_{ji}}}{\sqrt{0.9 + \left(\frac{\mathrm{AP_{ji}}}{300 + 25 \cdot \mathrm{AT_{ji}} + 0.05 \cdot \mathrm{AT_{ji}}^3}\right)^2}}$$

where, ETji is the real evapotranspiration for the j rain gauge station and the i year (mm); APji is the annual precipitation for the j rain gauge station and the i year (mm); ATji is the Annual air Temperature for the j rain gauge station and the i year (°C). For the rain gauge stations without air temperature gauges, annual mean air temperature values were extrapolated using linear correlations with altitude that were found statistically robust in all cases (Fig. 2d).

RESULTS AND CONCLUSIONS

At a regional and mean annual scales, three homogeneous pluviometric zones, characterized by different correlations between the annual mean effective precipitation and altitude (Figs. 2b, c and d) were recognized: in particular, an upwind zone, extending from the coastal line to the principal Apennine morphological divide, and two downwind zones behind the same divide. Based on such finding, the spatial distribution of effective precipitations was reconstructed at the regional scale (Fig. 2). This model shows that the values of effective mean annual rainfall progressively increase with the altitude, whereas they decrease behind the Apennine watershed.

The AEIC and AEICs values were found reaching the highest value for Terminio and Cervialto karst aquifers (77% and 75% respectively). However, the $AEIC_S$ for Terminio karst aquifer was found lower due to a wider endorheic and flat karst surface (Table 1). For the Matese karst aquifer an AEIC value was estimated around 65%, because of the presence of 10% siliceous-marly units in its area (Table 2). The lowest value, around 49% was identified for the Accellica karst aquifer and it was justified by the prevailing dolomitic lithology (Table 2).

Since the examined aquifers are properly representative of typical features of such aquifers in southern Apennine, the practical applicability of AEICS values is possible at a regional scale. This practical approach appears an acceptable first step to estimate the groundwater recharge of karst aquifers in order to carry out water budget at the annual scale and to manage water resources, also considering effects of climate changes.

TABLE 1
Hydrological parameters and AEIC and $AEIC_S$ estimated for the investigated karst aquifers.

Number	Karst Aquifer	Area (Km^2)	Endorheic Zone (%)	Annual Mean Air Temperature (°C)	Annual Mean Effective Precipitation (mm)	Annual Mean Outflow Discharge (m^3/s)	Annual Mean Inflow Volume (cm^3)	Annual Mean Outflow Volume (cm^3)	AEIC (%)	$AEIC_S$ (%)
1	Matese	600	18	7,9	1175	3,0	146,9	95,4	65	57
2	Accellica	206	0	9,6	1077	0,6	37,5	18,4	49	49
3	Terminio	167	42	8,1	1312	5,4	219,5	169,8	77	61
4	Cervialto	129	20	6,8	1422	4,4	183,2	137,2	75	68

TABLE 2
Hydrogeological parameters of the investigated karst aquifers.

Number	Karst Aquifer	Lithology (%)			Soil Type (%)				Land Use (%)			
		Limestone	Dolomitic	Siliceous-marly	Fine	Medium	Coarse	No soil	Woodland	Meadowland	Urban area	No vegetation
1	Matese	68	21	10	7	83	6	5	73	22	0	5
2	Accellica	34	65	0	4	80	16	0	90	8	2	0
3	Terminio	100	0	0	14	85	0	1	81	17	1	1
4	Cervialto	98	2	0	0	100	0	0	86	14	0	0

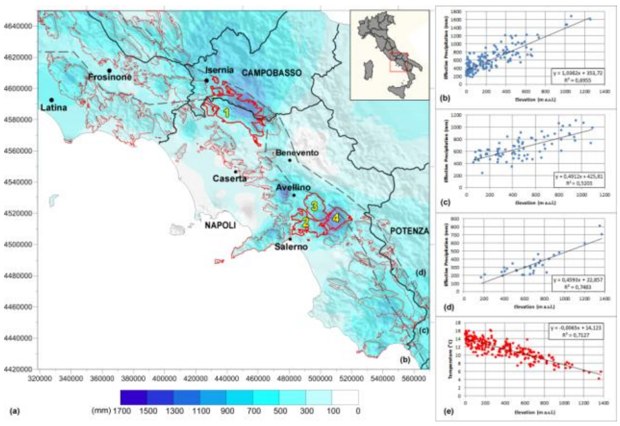

Fig. 2 – Spatial distribution of annual mean effective precipitation (a), effective precipitation *vs* altitude correlations (b, c and d) and annual mean air temperature *vs* altitude correlation (e). Upwind zone (a); first downwind zone (b); second downwind zone (c). Grey dashed lines are the limit of homogeneous rainfall zones.

REFERENCES

ALLOCCA V., CELICO F., CELICO P., DE VITA P., FABBROCINO S., MATTIA S., MONACELLI G., MUSILLI I., PISCOPO V., SCALISE A.R., SUMMA G. & TRANFAGLIA G. (2007) – *Note illustrative della Carta idrogeologica dell'Italia meridionale*. Istituto Poligrafico e Zecca dello Stato, 1-211.

BONACCI O. (2001) – *Monthly and annual effective infiltration coefficients in Dinaric karst: example of the Gradole karst spring catchment.* Hydrological Sciences - Journal des Sciences Hydrologiques, **46**(2), 287-299.

BONI C.F. & BONO P. (1982) – *Prima valutazione dell'infiltrazione efficace sui sistemi carsici della piattaforma carbonatica laziale-abruzzese e nei sistemi di facies pelagica umbro-marchigiana-sabina (Italia centrale).* Geologia Applicata e Idrogeologia, **17**, 427-436.

BURDON (1965) – *Hydrogeology of some karstic areas of Greece.* Actes de Colloque de Dubrovnik sur l'Hydrologie des roches calcaires fessures, A.I.H.S.-UNESCO, **73**, 308-317.

CELICO P. (1983) – *Idrogeologia dei massicci carbonatici, delle piane quaternarie e delle aree vulcaniche dell'Italia centro-meridionale (Marche e Lazio meridionale, Abruzzo, Molise e Campania)*. Quaderni della Cassa per il Mezzogiorno, **4/2**, 203 pp.

DE VITA P., ALLOCCA V., MANNA F., FABBROCINO S. (2012) – *Coupled decadal variability of the North Atlantic Oscillation, regional rainfall and karst spring discharges in the Campania region (southern Italy).* Hydrol. Earth Syst. Sci., **16**, 1389-1399.

DROGUE C. (1971) – *Coefficient d'infiltration ou infiltration eficace, sur le roches calcaires.* Actes du Colloque d'Hydrologie en Pays Calcaire, Besancon, **15** (3° série), 121-130.

HORVAT B. & RUBINIC J. (2006) – *Annual runoff estimation-an Example of karstic aquifers in the transboundary region of Croatia and Slovenia.* Hydrological Sciences Journal, **51**(2), 314-324.

KESSLER H. (1965) – *Water balance investigation in the karstic region of Hungary*. Actes de Colloque de Dubrovnik sur l'Hydrologie des roches calcaires fessures, A.I.H.S.-UNESCO, **73**, 91-105.

SCANLON B.R., HEALY R. W. & COOK P.G. (2002) – *Choosing appropriate techniques for quantifying groundwater recharge*. Hydrogeology Journal, **10**,18–39.

SODEMAN P.C. & TYSINGER J.E. (1965) – *Effect of forest cover upon hydrologic characteristics of a small watershed in limestone region of East Tennesse.* Actes de Colloque de Dubrovnik sur l'Hydrologie des roches calcaires fessures, A.I.H.S.-UNESCO, **73**, 135-151.

SOULIOS G. (1984) – *Infiltration efficace dans le karst hellenique*. Journal of Hydrology, **75**, 343-356.

TURC L. (1954) – *Le bilan d'eau des sols: relations entre les précipitations, l'évaporation et l'éecolument.* Annales Agronomiques, **5**, 491-595.

VILIMONOVIC J. (1965) – *A contribution of the study of groundwater intake recharge in karst.* Actes de Colloque de Dubrovnik sur l'Hydrologie des roches calcaires fessures, A.I.H.S.-UNESCO, **73**, 482-499.

Hydrol. Earth Syst. Sci., 18, 803–817, 2014
www.hydrol-earth-syst-sci.net/18/803/2014/
doi:10.5194/hess-18-803-2014

Hydrology and Earth System Sciences
Open Access

Estimating annual groundwater recharge coefficient for karst aquifers of the southern Apennines (Italy)

V. Allocca, F. Manna, and P. De Vita

Dipartimento di Scienze della Terra, dell'Ambiente e delle Risorse – University of Naples "Federico II", Naples, Italy

Correspondence to: P. De Vita (padevita@unina.it)

Received: 24 July 2013 – Published in Hydrol. Earth Syst. Sci. Discuss.: 7 August 2013
Revised: 30 November 2013 – Accepted: 5 January 2014 – Published: 27 February 2014

Abstract. To assess the mean annual groundwater recharge of the karst aquifers in the southern Apennines (Italy), the estimation of the mean annual groundwater recharge coefficient (AGRC) was conducted by means of an integrated approach based on hydrogeological, hydrological, geomorphological, land use and soil cover analyses. Starting from the hydrological budget equation, the coefficient was conceived as the ratio between the net groundwater outflow and the precipitation minus actual evapotranspiration ($P-\mathrm{ETR}$) for a karst aquifer. A large part of the southern Apennines, which is covered by a meteorological network containing 40 principal karst aquifers, was studied. Using precipitation and air temperature time series gathered through monitoring stations operating in the period 1926–2012, the mean annual $P-\mathrm{ETR}$ was estimated, and its distribution was modelled at a regional scale by considering the orographic barrier and rain shadow effects of the Apennine chain, as well as the altitudinal control. Four sample karst aquifers with available long spring discharge time series were identified for estimating the AGRC. The resulting values were correlated with other parameters that control groundwater recharge, such as the extension of outcropping karst rocks, morphological settings, land use and covering soil type. A multiple linear regression between the AGRC, lithology and the summit plateau and endorheic areas was found. This empirical model was used to assess the AGRC and mean annual groundwater recharge in other regional karst aquifers. The coefficient was calculated as ranging between 50 and 79 %, thus being comparable with other similar estimations carried out for karst aquifers of European and Mediterranean countries. The mean annual groundwater recharge for karst aquifers of the southern Apennines was assessed by these characterizations and validated by a comparison with available groundwater outflow measurements.

These results represent a deeper understanding of an aspect of groundwater hydrology in karst aquifers which is fundamental for the formulation of appropriate management models of groundwater resources at a regional scale, also taking into account mitigation strategies for climate change impacts. Finally, the proposed hydrological characterizations are also supposed to be useful for the assessment of mean annual runoff over carbonate mountains, which is another important topic concerning water management in the southern Apennines.

1 Introduction

Karst aquifers host important groundwater resources for human and agricultural use in many areas of the world and include natural landscapes and ecosystems with great geo- and biodiversities (Goldscheider, 2012). For regions in southern Italy, these aquifers are the primary source of drinking water and a strategic resource for socio-economic and environmental development (Allocca et al., 2007b); moreover their groundwater resources play a primary role in regulating the hydro-ecological regime of rivers. In this area, the public water supplies of major cities, such as Naples, which has approximately 1 million inhabitants, and many small towns and countless settlements are fed by large and small karst springs. Karst groundwater resources have also been utilized since the Roman epoch for drinking water (for example Augustan Aqueduct, dated 33–12 BC) and thermal and mineral water. These aquifers are currently important sources for several bottling plants as well. Hence, the correct estimation at

Published by Copernicus Publications on behalf of the European Geosciences Union.

various spatio-temporal scales of groundwater recharge processes in karst systems, corresponding to mean annual replenishment of aquifers by infiltration processes through the vadose zone (Lerner et al., 1990; Stephens, 1995; Scanlon et al., 2006; Delin et al., 2007; Healy, 2010), is a fundamental and challenging issue to be investigated for a proper management of groundwater and surface water resources. In addition, this quantitative assessment is a required approach for respecting the EU Water Framework Directive (European Commission, 2000) and taking into account effects of climatic decadal variability (De Vita et al., 2012).

A wide range of direct and indirect methods to estimate groundwater recharge processes, with a degree of approximation depending on different spatio-temporal scales, have been proposed (Scanlon et al., 2002 and references therein). Examples include lysimeter measurements, soil moisture budgets and effective infiltration coefficients, as well as water table rise, tracer and remote sensing methods. At a regional scale, to estimate the endogenous and exogenous variables controlling groundwater recharge processes, multidisciplinary analyses of hydrological time series, hydrogeological and geomorphological data have been implemented in a GIS environment (Andreo et al., 2008; Dripps and Bradbury, 2010). Moreover, conceptual and physically based models accounting for the spatial variability of parameters which controll recharge have been proposed (Hartmann et al., 2012).

For many karst aquifers around the world, the assessment of the groundwater recharge has been carried out by estimating the effective infiltration coefficient (EIC), which was defined as the ratio between the groundwater replenishment, corresponding to the net groundwater outflow, and the rainfall in a specified timescale (usually monthly or yearly) and at the aquifer scale (Drogue, 1971; Bonacci, 2001). Therefore this ratio incorporates complex processes existing in the vadose zone such as water storage, evapotranspiration, runoff and percolation to the saturated zone; it was conceived as a practical tool to assess monthly or annual groundwater recharge of an aquifer by the rainfall measurements. In karst aquifers, the EIC is controlled by several factors, among which the composition of carbonate rocks, fracturing degree, development of epikarst and deeper karst processes, slope steepness, land use and covering soil type can be basically recognized. Several estimations and applications of EIC for calcareous karst aquifers were carried out in Hungary (Kessler, 1965), Greece (Burdon, 1965; Soulios, 1984), France (Drogue, 1971) and Croatia (Vilimonovic, 1965; Bonacci, 2001), at the annual timescale, finding values ranging from 35 to 76 %, with a mean value around 51 %. Finally, for other non-European countries, a value of 27 % was assessed for the dolomitic basin of Tennesee (Sodeman and Tysinger, 1965). In Italy, Boni et al. (1982) reported an annual EIC value of 70 % for some karst aquifers in the central Apennines.

The aim of this study was to assess the average annual groundwater recharge of the main karst aquifers of the southern Apennines (Italy) by estimating the annual groundwater recharge coefficient (AGRC), which was set similarly to the EIC (Drogue, 1971; Bonacci, 2001) and adapted to be more suitable for a regional-scale application. This assessment was conceived as a key aspect of groundwater hydrology in karst aquifers of the southern Apennines which would provide an effective tool to estimate annual groundwater recharge. To achieve this objective, an integrated approach based on the hydrological budget applied to precipitation, evapotranspiration and spring discharge time series, as well as geomorphological settings, land use and type of soil cover analyses was carried out. The applied methods were based on all the available data and were set up to solve the temporal and spatial discontinuities of hydrological time series, specifically the lack of significant measurements for both springs discharge and precipitation in the high altitude ranges.

The paper is organized as follows: after a description of the issue and a review of the literature in Sect. 1, the hydrogeological characteristics of the karst aquifers of the southern Apennines are described in Sect. 2, which are followed by the data and methods, results, discussion and concluding remarks in Sects. 3, 4 and 5, respectively.

2 Hydrogeology of karst aquifers and climatic characteristics of the southern Apennines

The southern Apennines consist of a series of mountain ranges in which karst aquifers form the major massifs (Fig. 1). In this area, karst aquifers cover approximately 8560 km^2 (Fig. 1) and consist mainly of Triassic-Liassic dolomites, Jurassic limestones and Paleogene marly limestones of the Mesozoic carbonate platform series, which were tectonically deformed and piled up in the fold-and-thrust belt Apennine structure during the Miocene orogenic phases (Patacca and Scandone, 2007). The karst aquifers of the southern Apennines in several cases are characterized by large plateau and endorheic zones on the top and exhibit an average inclination of structurally controlled slopes of approximately 30–35°, related to the morphological evolution of original fault line scarps (Brancaccio et al., 1978; Bull, 2007). Moreover, given their proximity to volcanic centers (Fig. 1), these aquifers were singularly covered by variable thicknesses of ash-fall pyroclastic deposits (De Vita et al., 2006, 2013) that erupted during the Quaternary, whose presence influences the epikarst development (Celico et al., 2010).

Regional hydrogeological studies carried out in the southern Apennines analysed groundwater circulation in main karst aquifers by understanding geological and structural constraints that control groundwater paths and assessing large groundwater bodies outflowing chiefly in basal springs, with mean annual discharges varying from 0.1 to 5.5 $m^3\,s^{-1}$.

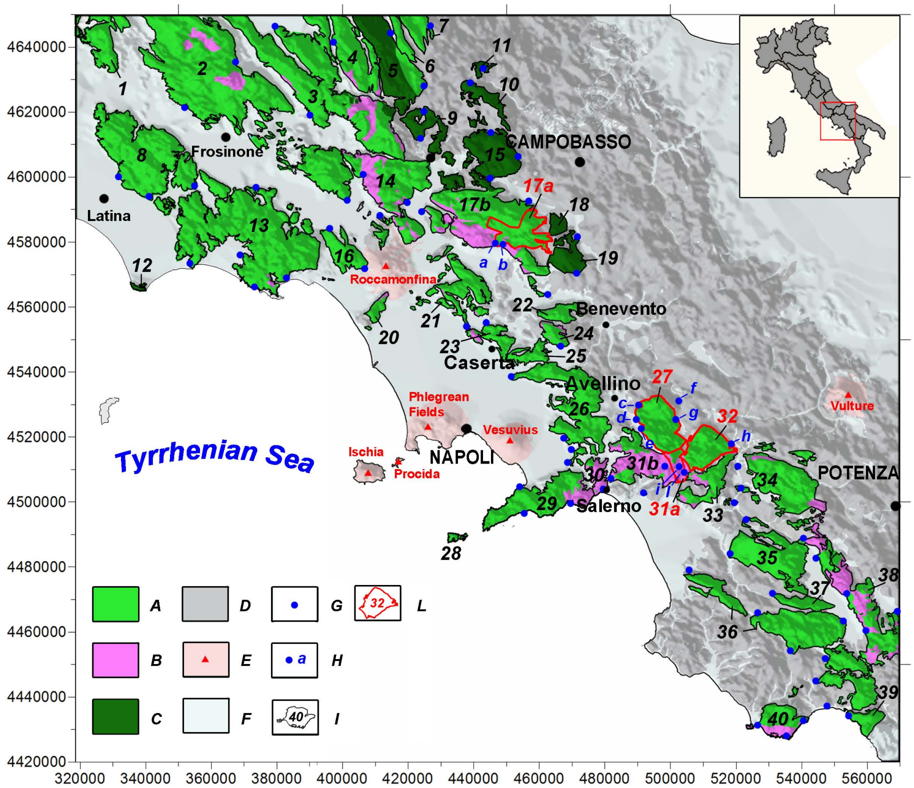

Fig. 1. Map of the karst aquifers of the southern Apennines. Key to symbols: (A) limestone and dolomitic limestone units of the carbonate platform series (Jurassic-Paleogene); (B) dolomitic units of the carbonate platform series (Trias-Liassic); (C) calcareous-marly units of the outer basin series (Trias-Paleogene); (D) pre-, syn- and late- orogenic molasses and terrigenous units (Cretaceous-Pliocene); (E) volcanic centers (Pliocene-Quaternary); (F) alluvial and epiclastic units (Quaternary); (G) main basal springs of karst aquifers; (H) basal karst springs considered in the hydrological budget (a and b: Maretto and Torano; c: Salza Irpina; d and e: Serino; f: Baiardo; g: Cassano Irpino; h: Sanità; i: Avella; l: Ausino-Ausinetto); (I) hydrogeological boundary and identification number of the karst aquifers; (L) hydrogeological boundary and identification number of the karst aquifers considered for the hydrological budget.

The hydrogeological behaviour of these aquifers (Celico, 1988; Allocca et al., 2007a) is in accordance with principal conceptual models proposed for karst aquifers (White, 1969, 2002; Mangin, 1975; Kiraly, 1975, 2002; Drogue, 1992; Bonacci, 1993; Klimchouk, 2000; Civita et al., 1992; Jeannin, 1998; Goldscheider and Drew, 2007; Fiorillo, 2011a). Due to the fold-and-thrust belt structure of the Apennine, karst aquifers are tectonically juxtaposed to hydrostratigraphic units of lower permeability belonging to pre- and syn-orogenic basinal and flysch series. Therefore, the groundwater circulation of karst aquifers is basically controlled by the geometry of stratigraphic or tectonic contacts with these units of lower permeability, being generally oriented toward the lowest point of the hydrogeological boundary (Celico, 1983; Allocca et al., 2007a), where basal springs are located (Fig. 1). In these zones, the groundwater circulation can also feed alluvial and detrital aquifers in lateral contact with karst aquifers. Inversely, in other specific conditions, groundwater circulation of alluvial and detrital aquifers can feed that of karst aquifers. Other minor stratigraphic or tectonic factors subdivide the basal groundwater circulation inside karst aquifers. These include faults with low-permeability damage and core zones or intervals in the carbonate series with marly or argillaceous composition that compartmentalize the aquifers in basin-in-series systems (Celico, 1988; Celico et al., 2006). Though karst systems (ISSKA, 2012) belonging to the same aquifer can be fed by variable contributing areas (Ravbar et al., 2011), in the cases of the southern Apennines the whole recharge area of a karst aquifer can be considered constant and corresponding to the outcrop of karst rocks, owing to distinct structural and stratigraphic constraints with juxtaposing hydrogeological units of lower permeability. An exception is given for those very limited cases of allogenic recharge coming from adjoining alluvial aquifers or concentrated-secondary infiltration of runoff formed on the surrounding or overlying non-karst terrains.

A subordinate perched groundwater flow, related to epikarst and/or superimposed aquifers, also occurs in the surficial part, where stratigraphic and structural factors or the presence of small karst conduits can generate high-altitude seasonal and ephemeral springs characterized by mean annual discharges generally lower than $0.01\,\mathrm{m^3\,s^{-1}}$. The groundwater recharge of karst aquifers occurs chiefly by autogenic recharge due to diffuse-direct net infiltration through the epikarst. For several karst aquifers of the southern Apennines, the mean annual groundwater flow was assessed mostly on the basis of short-duration and discontinuous time series (frequently less than three years) or few non-systematic instantaneous measurements of spring discharges.

The climatic characteristics of the southern Apennines and their temporal variability strongly control the recharge processes in karst aquifers, and both are influenced by the North Atlantic Oscillation (De Vita et al., 2012). The climate of this sector of Italy varies from Mediterranean type (Csa) in the coastal sector to Mediterranean mild climate (CSb) in the inland areas (Geiger, 1954). The spatial distribution of mean annual precipitation is mainly influenced by the orographic effect (Henderson-Sellers and Robinson, 1986) of the Apennine mountain ranges on humid air masses moving eastward from the Tyrrhenian Sea. According to the location of the Apennine chain, higher orographic precipitation occurs in the western sector, with maximum values up to 1700–2000 mm along the Apennine ridge itself. Eastward of the Apennine ridge, lower precipitations down to 700–900 mm are recorded because of the rain shadow effect.

3 Data and methods

This study was carried out in a large sector of the southern Apennines covering approximately 19 339 km^2, corresponding to the regional hydrological network of the National Hydrographic and Tidal Service, Department of Naples. The basic hydrogeological characteristics that control groundwater recharge in karst aquifers over this territory (Fig. 1) were assessed: extension of the recharge areas, outcropping lithology, morphological settings (slope angle distribution and summit plateau/endorheic areas), land use and type of soil cover. Precipitation and air temperature time series recorded by all monitoring stations functioning over the same territory in the period 1926–2012 were also collected and analysed. Moreover, four sample karst aquifers were identified to estimate the AGRC on the basis of the availability of significant spring discharge time series and representativeness of the lithological and morphological settings (Fig. 1): the Matese (a), Accellica (a), Terminio and Cervialto karst aquifers. Although not numerous, the examined sample aquifers are the only ones for which long time series of spring discharges are available in the southern Apennines.

3.1 Estimation of annual groundwater recharge coefficient

The EIC (Drogue, 1971; Bonacci, 2001) being essentially the ratio between the net groundwater outflow (Q_{OUT}) and rainfall (P) for an analysed karst aquifer and a fixed timescale (monthly or annual),

$$\mathrm{EIC} = \frac{Q_{\mathrm{OUT}}}{P} \tag{1}$$

was conceived incorporating the evapotranspiration loss. For this reason the EIC was not considered applicable to a regional scale such as the southern Apennines, where differences in the spatial distributions of rainfall and air temperature lead to different evapotranspiration rates over karst aquifers (Fiorillo, 2011b), and not exportable even in the cases of lithological and morphological similarities. Therefore the EIC structure was modified for taking into account the role of the evapotranspiration, in a form of a new coefficient calculated at the annual timescale, named annual groundwater recharge coefficient (AGRC).

The AGRC was estimated for each of the four sample karst aquifers, by applying the hydrological budget equation to the whole recharge area, equivalent to the outcropping extension of the aquifer, and considering average values for the period 1926–2012:

$$P - \mathrm{ETR} = R + (Q_{\mathrm{s}} + Q_{\mathrm{t}}) + (U_{\mathrm{o}} - U_{\mathrm{i}}) \pm \Delta W_{\mathrm{r}}, \tag{2}$$

where P is the mean annual precipitation, ETR is the mean annual actual evapotranspiration, R is the mean annual runoff, Q_{s} is the mean annual spring discharge, Q_{t} is the mean annual tapped discharge, U_{o} is the mean annual groundwater outflow through adjoining aquifers, U_{i} is the mean annual groundwater inflow from adjoining aquifers and other allogenic recharge, and $\pm\Delta W_{\mathrm{r}}$ is the interannual variation of groundwater reserves.

Because interannual variation of groundwater reserves ($\pm\Delta W_{\mathrm{r}}$) is approximately negligible in the long-term timescale, as it results by the complexly cyclical decadal variability around the mean value found (De Vita et al., 2012) for the Cervialto, Terminio and Matese karst aquifers (No. 32, 27 and 17 in Fig. 1), Eq. (2) can be simplified as follows:

$$P - \mathrm{ETR} - R = (Q_{\mathrm{s}} + Q_{\mathrm{t}}) + (U_{\mathrm{o}} - U_{\mathrm{i}}). \tag{3}$$

The mean AGRC was estimated for each karst aquifer as the ratio between the mean annual net groundwater outflow [$Q_{\mathrm{OUT}} = (Q_{\mathrm{s}} + Q_{\mathrm{t}}) + (U_{\mathrm{o}} - U_{\mathrm{i}})$] and the mean annual precipitation minus actual evapotranspiration ($P - \mathrm{ETR}$), where both were related to the whole recharge area:

$$\mathrm{AGRC} = \frac{(Q_{\mathrm{s}} + Q_{\mathrm{t}}) + (U_{\mathrm{o}} - U_{\mathrm{i}})}{P - \mathrm{ETR}}. \tag{4}$$

Due to the general hydrogeological settings along the boundaries, mean annual groundwater outflows (U_{o}) through juxtaposed alluvial and detrital aquifers were considered significant for the Matese (a), Terminio and Accellica (a) cases only; instead, groundwater inflows (U_{i}) were assessed as negligible or non-existent. Groundwater outflows (U_{o}) were estimated by the application of Darcy's law (Darcy, 1856) to measurements of hydraulic transmissivity, length of the draining section and hydraulic gradient, known from preceding hydrogeological studies (Celico, 1983; Allocca et al., 2007a). In detail, groundwater outflows (U_o) were assessed as a very limited fraction of the mean annual net groundwater outflow (Q_{OUT}), corresponding to 3, 2 and 7 %, respectively for the three sample aquifers.

The annual EIC (AEIC) and AGRC are linked by a simple relationship, which can be obtained by combining Eqs. (1) and (4):

$$\text{AEIC} = \text{AGRC} \times \frac{P - \text{ETR}}{P}. \tag{5}$$

Furthermore, due the peculiar morphological setting of karst aquifers, summit plateau areas (slope angle $\leq 5°$) and endorheic watersheds, in which the infiltration value reaches the maximum value (AGRC = 100 %), were identified and measured. The annual effective infiltration coefficient for the slope part (AGRC_S), in non-endorheic conditions and with a slope angle greater than 5°, was therefore calculated by the following formula:

$$\text{AGRC}_\text{S} = \left[\frac{(\text{AGRC} \times A_\text{T}) - (1 \times A_\text{E})}{A_\text{T} - A_\text{E}}\right] \times 100, \tag{6}$$

where A_T is the total area of the karst aquifer (km^2), and A_E is the cumulative extension of summit plateau areas and/or endorheic watersheds (km^2).

This estimation was considered useful for a comprehensive understanding of the hydrological role of karst aquifers, and thus also for taking into account a general assessment of runoff formation along karst slopes (Horvat and Rubinic, 2006) by estimating the annual runoff coefficient (ARC), which is the complementary part of the AGRC:

$$\text{ARC} = 100 - \text{AGRC}_\text{S}. \tag{7}$$

The ARC can be compared to runoff coefficients, which are usually calculated as the ratio between surface runoff and rainfall, by considering the ratio $(P - \text{ETR})/P$ homologously as for Eq. (5).

3.2 Hydrological data

The mean annual precipitation data (387 rain gauge stations) and air temperatures (228 monitoring stations) were gathered from the annals of the National Hydrographic and Tidal Service in the period 1926–1999 (www.isprambiente.gov.it) and the Regional Civil Protection Agency databases (www.protezionecivile.gov.it) for the remaining interval from 2000 to 2012. During the entire period, the number of rain gauge stations varied from a total of 175 in 1926 to a minimum of 52 during 1943–1944, up to a maximum of 225 from 1972 to 1984 to a current value of 171. The number of the air temperature stations began with 19 in 1926, increased to 90 in 1975, and then oscillated around this number up to now. Nevertheless, more than 50 % of the monitoring stations worked for longer than 30 yr and approximately 10 % of the stations ran for more than 70 yr. Another issue of this monitoring network was the prevailing distribution of stations in the lower-middle altitude ranges (0–600 m a.s.l.), which is a limiting factor in assessing hydrological data at the highest altitude ranges.

Time series were analysed to reconstruct regional distribution models of mean annual precipitation (P), air temperature (T) and precipitation minus actual evapotranspiration ($P - \text{ETR}$), thereby accounting for variations due to orographic control of mountain ranges (Roe, 2005; Houze, 2012) and altitude (Vuglinski, 1972; Brunsdon et al., 2001) in a GIS environment. For the $P - \text{ETR}$ data set, a linear correlation analysis between mean annual values and altitude was carried out identifying homogeneous precipitation zones by distinctive relationships between $P - \text{ETR}$ and altitude as well as according to geographical location of rain gauge stations respect to the principal morphological divide of the Apennine chain. For each precipitation zone, an empirical model was calculated by means of a linear regression weighted by the number of years of functioning of each station (Carroll and Ruppert, 1988).

To estimate the mean annual $P - \text{ETR}$ over the period 1926–2012, the actual evapotranspiration was calculated for each rain gauge station by Turc's formula (Turc, 1954), which was based on annual runoff, air temperature and precipitation of 254 drainage basins distributed in different climates and continents. The reliability of this empirical model, was also confirmed by studies in the Mediterranean (Santoro, 1970) and European areas (Parajka and Szolgay, 1998; Horvat and Rubinic, 2006) as well as through mean annual hydrological budgets carried out for principal aquifers of southern Italy (Boni et al., 1982; Celico, 1983; Allocca et al., 2007a):

$$\text{ETR}_j = \frac{P_j}{\sqrt{0.9 + \left(\frac{P_j}{300 + 25 \cdot T_j + 0.05 \cdot T_j^3}\right)^2}}, \tag{8}$$

where ETR_j is the mean annual actual evapotranspiration (mm) for the j rain gauge station; P_j is the mean annual precipitation (mm) for the j rain gauge station; and T_j is the mean annual air temperature (°C) for the j air temperature-rain gauge station.

The actual evapotranspiration was also calculated for those rain gauge stations not provided with an air temperature sensor. In these cases, the mean annual air temperature was estimated by the empirical linear regression model with the altitude. Moreover, in order to assess the regional variability of the mean annual actual evapotranspiration, the ratio $(P - \text{ETR})/P$ was calculated for each rain gauge station.

By the daily discharge time series of basal springs of the sample karst aquifers, the mean annual spring discharges

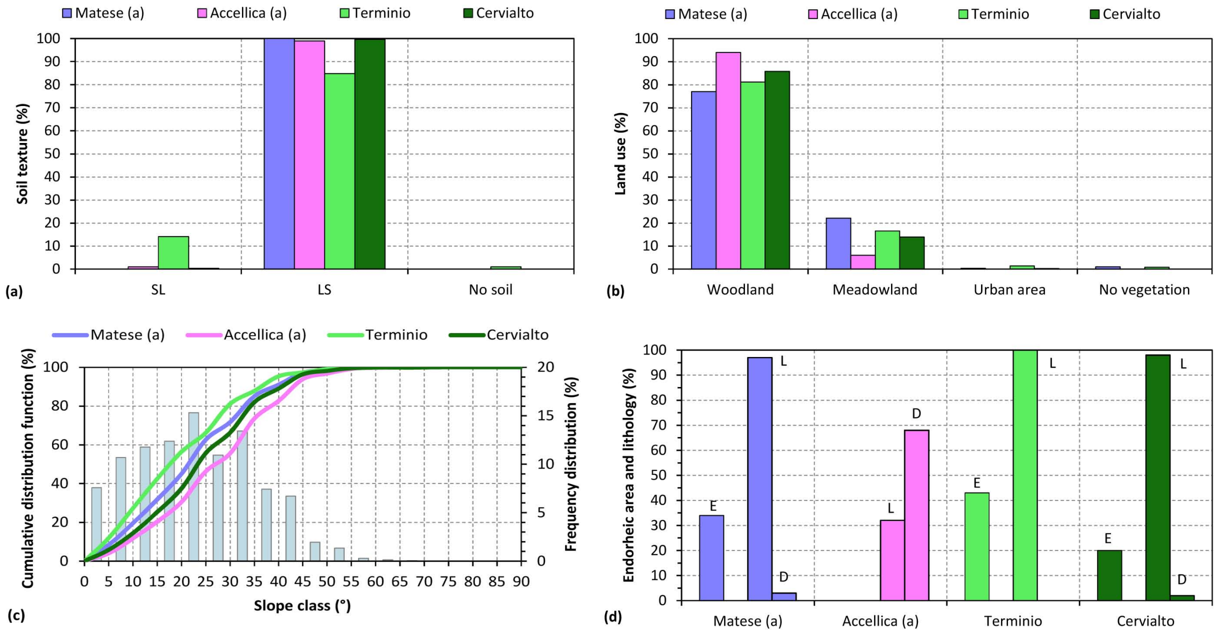

Fig. 2. Soil texture type, land use and geomorphological characteristics of the four sample karst aquifers. **(a)** Soil texture frequency (SL Sandy Loam, LS Loamy Sand. **(b)** Land use frequency. **(c)** Slope of karst aquifers frequency. **(d)** Summit endorheic and plateau areas frequency (E) and lithology (L = limestone; D = dolomite).

were calculated (Fig. 1). Specifically for the Matese (a) karst aquifer, the Maretto and Torano springs were considered (recording period from 1967–2000 and 1957–2000, respectively). For the Terminio aquifer, the Cassano Irpino (recording period 1965–2010), Serino (recording period 1887–2010) and Baiardo and Salza Irpina springs (recording period 1970–2000) were analysed. For the Cervialto aquifer, the Sanità spring, which represents the sole outflow of the entire karst aquifer and a unique case for the duration of its time series (recording period 1921–2012), was considered (De Vita et al., 2012). For the Accellica (a) karst aquifer, the Avella and Ausino–Ausinetto springs (recording period 1967–1989) were considered.

3.3 Aquifer lithology, covering soil type, land use and geomorphological data

On the basis of preceding hydrogeological studies carried out for singular aquifers and synthesized in reviews of regional relevance (Celico, 1983; Allocca et al., 2009), 40 principal karst aquifers were identified (Fig. 1). The outcropping lithology of the karst aquifers were assessed by analysing hydrogeological maps of southern Italy, 1 : 250 000 scale (Allocca et al., 2007a).

To analyse the types of soil covering such aquifers, the Land System Map of the Campania Region, 1 : 250 000 scale (www.risorsa.info), and the Ecopedological Map of Italy, 1 : 250 000 scale (www.pcn.minambiente.it), were consulted. In addition, data from Corine Land Cover 2006 (www.eea.europa.eu) were collected to analyse land use. A national 20 m grid spacing digital elevation model (http://www.sinanet.isprambiente.it) was analysed to examine the morphological features of the karst aquifers, giving special attention to slope angle and extension of the endorheic catchments. The above-mentioned spatial data were implemented in a geographical information system, which allowed for the analysis of the spatial frequency of such parameters for each examined karst aquifer.

4 Results

4.1 Extension and lithology of the recharge areas

Extension and lithology of the recharge areas of the 40 karst aquifers were assessed by analysing regional hydrogeological maps (Allocca et al., 2007a). Specifically, the four sample karst aquifers were shown to be representative, both by their significant extensions and their outcropping lithology (Fig. 2): Matese (a) (120 km^2; 97 % limestone and 3 % dolomite); Accellica (a) (35 km^2; 68 % dolomite and 32 % limestone); Terminio (167 km^2; 100 % limestone) and Cervialto (129 km^2; 98 % limestone and 2 % dolomite).

4.2 Soil type, land use and geomorphological features

The analysis of soil types covering karst aquifers identified the loamy sand type (coded as LS in Figs. 2a and 3a) as the prevailing one with a percentage greater than 90 % for three of the four karst aquifers considered, which is consistent with

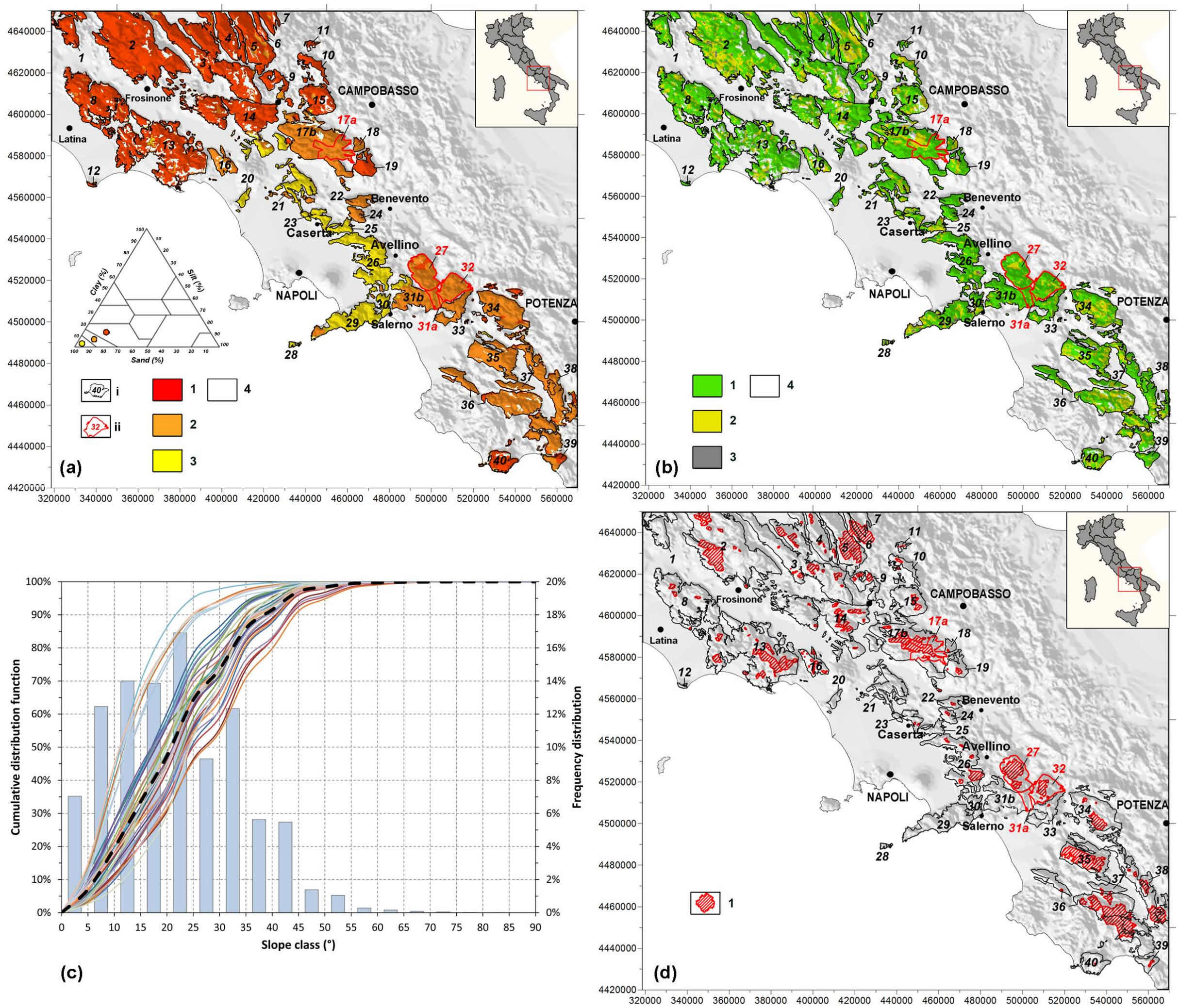

Fig. 3. **(a)** Soil texture map. Common symbols: (i) hydrogeological boundary and identification number of the karst aquifers; (ii) hydrogeological boundary and identification number of the sample karst aquifers. Key to symbols: (1) sandy loam soil; (2) loamy sand soil; (3) sandy soil; (4) area with no soil. **(b)** Land use map. Key to symbols: (1) woodland; (2) meadowland; (3) urban area; (4) no vegetation area. **(c)** Frequency analysis of the slope angle distribution for the karst aquifers. Key to symbol: (coloured line) Cumulative distribution of single karst aquifer; (dashed black line) Mean cumulative distribution; (histogram) Mean frequency distribution. **(d)** Summit plateau areas and endorheic watersheds map. Key to symbol: (1) limits of endorheic watershed.

Naclerio et al. (2008, 2009). A fraction of a coarser soil type, 14 % of sandy loam soils (coded as SL in Fig. 3a), was identified for the Terminio karst aquifer according to other studies carried out at a detailed scale (Allocca et al., 2008; Fiorillo, 2011b) and the proximity to the Somma-Vesuvius volcano, which led to the deposition both of greater thicknesses of ash-fall pyroclastic deposits (De Vita et al., 2006) and coarser grain sizes.

Land use varied among four principal typologies: woodland, meadowland, areas without vegetation cover and urban areas. Specifically, the woodland and meadowland classes were the dominant ones in the four sample karst aquifers, extending for approximately 85 and 14 % of the total area, respectively (Figs. 2b and 3b).

The sample karst aquifers were found to have extensions of summit plateau areas and endorheic zones (Figs. 2d and 3d) varying from 43 % in the case of Terminio to 0 % for Accellica (a), with intermediate values of approximately 35 and 20 % for Matese (a) and Cervialto, respectively. Moreover, the cumulative distributions of slope angle were found to be similar across the sample and other aquifers (Figs. 2c and 3c), showing a similar median value of 25°.

Considering the 40 karst aquifers identified at a regional scale (Fig. 1), the soil type was notably homogeneous (Fig. 3a) with a prevalence of sand in each category. Average land use values of 69 % for woodland, 25 % for meadowland, 5 % for areas without vegetation and 1% for urban areas were estimated (Fig. 3b). The morphological settings

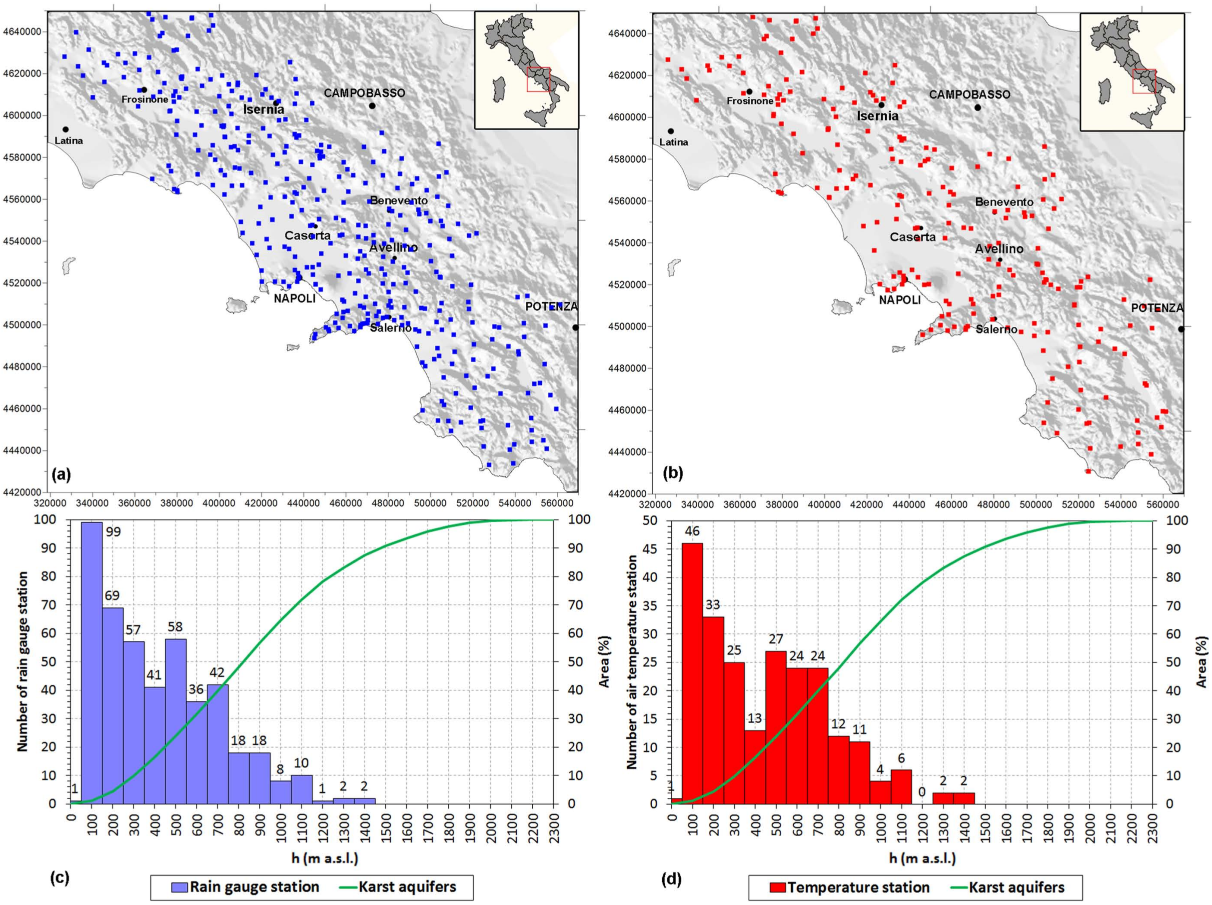

Fig. 4. Spatial distributions of rain gauge stations **(a)** and air temperature stations **(b)**. Comparisons between the hypsometric curve of the 40 karst aquifers in the study area and the altitudinal distribution of rain gauge stations **(c)** and air temperature stations **(d)**.

of all karst aquifers showed very similar cumulative distributions of slope angles, with a median of 25° and a modal value ranging within 20–25°. In contrast, the most frequent higher value slope angle class was 30–35°, according to the typical morphological setting, due to the erosional evolution of fault-line scarps in carbonate mountains of the southern Apennines (Brancaccio et al., 1978; Bull, 2007). Significant differences were observed in the distribution and extent of the summit plateau and endorheic areas (Fig. 3d and Table 2) according to the different structural settings of the karst aquifers. More extended summit plateau and endorheic watersheds were detected in the northern and in the southern parts of the study area. In particular, more than 40 % of the total area of the Terminio and Alburni karst aquifers (Fig. 3d and Table 2) were characterized by summit plateau area and endorheic watersheds, and hence by a complete infiltration of the $P-\mathrm{ETR}$ amount.

4.3 Annual precipitation minus actual evapotranspiration ($P-\mathrm{ETR}$)

Despite the apparent homogeneous distribution of rain gauges and air temperature stations over the territory (Fig. 4a and b), the assessment of the spatial distribution of these stations revealed an inhomogeneous scattering with altitude, with a dominant presence in the lower-middle ranges (Fig. 4c and d). This scarcity of a monitoring network at higher altitude ranges was recognized as a principal issue to overcome in order to assess the groundwater recharge of karst aquifers, which have a mountainous morphology extending up to the highest altitudes. In fact, the statistical comparison between the altitude of the monitoring stations and the karst aquifers showed that 50 % of these areas lie at altitudes between 800 and 2280 m a.s.l., where only 10 % of rain gauge and air temperature stations are located (Fig. 4c and d).

At the regional scale, despite of the mean annual precipitation, the spatial variability of the mean annual air temperature was found to be correlated with the altitude by a unique and statistically robust linear regression model (Fig. 5d): $T\,(°\mathrm{C}) = -0.0064 \times h\,(\mathrm{m\ a.s.l.}) + 16.5$ ($r^2 = 0.733$;

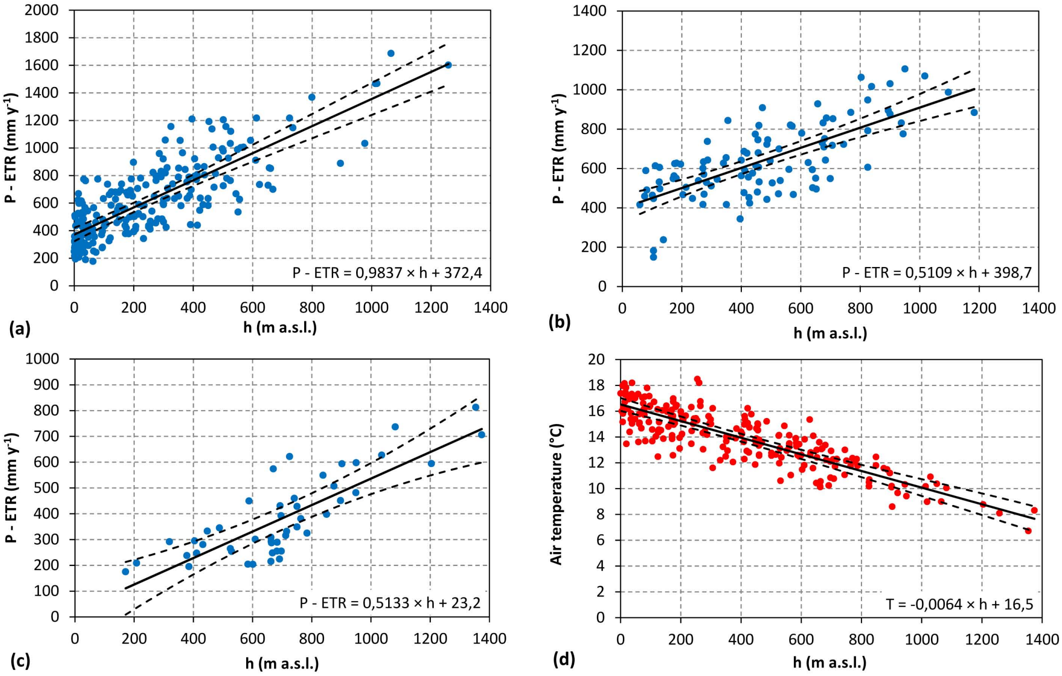

Fig. 5. Linear correlations and confidence limits (95 %) between mean annual $P-\mathrm{ETR}$ and altitude for upwind zone **(a)**, first downwind zone **(b)** and second downwind zone **(c)**. The correlation between mean annual air temperature and altitude is also shown **(d)**.

Prob. F-Fisher < 0.1 %). This empirical model was applied to estimate the mean annual air temperature for rain gauge stations not provided with air temperature sensors, thus permitting to calculate mean annual ETR for all the 387 rain gauge stations.

To estimate groundwater recharge at a regional scale, a distributed model of the mean annual $P-\mathrm{ETR}$ was reconstructed by considering the spatial variability due to both orographic and altitudinal controls. By analysing the correlation of $P-\mathrm{ETR}$ data with the altitudes of the rain gauge stations, three homogeneous precipitation zones were found, according to the orographic barrier effect (Vuglinski, 1972; Brunsdon et al., 2001) of the Apennine chain. An upwind zone, extending from the coastline to the principal Apennine morphological divide, and two downwind zones eastward of the same divide were identified (Figs. 5 and 6), which resulted from a rain shadowing effect (Roe, 2005). For each zone, a specific linear regression model, weighted by the years of functioning of each rain gauge station, was identified between $P-\mathrm{ETR}$ and altitude (Fig. 5a–c). These models showed that the $P-\mathrm{ETR}$ values progressively increase with altitude, even considering three different empirical laws across the Apennine chain, which were always statistically significant if considering the 95 % confidence interval ($r^2_{\mathrm{min}} = 0.510$ and Prob. F-Fisher < 0.1 %).

On the basis of such findings, a general distributed model of $P-\mathrm{ETR}$ was reconstructed by integrating the three precipitation zones in a GIS layer (Fig. 6a and b). For the upwind pluviometric zone, the recorded values of mean $P-\mathrm{ETR}$ ranged between 373 and 1606 mm, but varied from 200 to 1010 mm for the two downwind zones.

The ratio $(P-\mathrm{ETR})/P$ was analysed for all the available rain gauge stations, finding a significant variability from 0.11 to 0.82, a mean value of 0.48 ± 0.21 (95 % confidence interval) and a linear correlation with the altitude $(P-\mathrm{ETR})/P\,(\mathrm{ad.}) = 0.0002 \times h\,(\mathrm{m\ a.s.l.}) + 0.398$ ($r^2 = 0.396$; Prob. F-Fisher < 0.1 %). This result, also represented as a map (Fig. 6c), testified to the strong differences of the mean annual ETR at the regional scale, which are controlled by spatial variability of both mean annual air temperature and precipitation (Eq. 8).

4.4 AGRC and AGRC$_\mathrm{S}$ estimations

From the calculation of the variables forming Eqs. (4) and (6), the AGRC and AGRC$_\mathrm{S}$ were estimated for the four sample karst aquifers (Table 1), which also took into account the uncertainties due to the linear regression models (95 % confidence limits) of $P-\mathrm{ETR}$ and altitude (Fig. 7). Due to the structure of Eq. (4) and the different uncertainty of its variables (Q_{OUT} and $P-\mathrm{ETR}$), the AGRC uncertainty is chiefly controlled by that of the $P-\mathrm{ETR}$ and altitude regression models. Considering the results related to the mean value of the regression models, similar values of the AGRC were found for the Terminio, Cervialto and Matese (a) karst aquifers, corresponding to 79, 71 and 69 %, respectively, whereas a value of 50 % was calculated for the Accellica (a) karst aquifer. This difference appeared to be mainly

Table 1. AGRC and mean $AGRC_S$ estimation for the investigated sample karst aquifers. Values are related to the mean value of the $P-ETR$ linear regression models with altitude.

ID	Karst aquifer	Area (km^2)	Summit plateau/ endorheic area (%)	$V_{outflow}$ ($10^6\,m^3\,yr^{-1}$)	V_{inflow} ($10^6\,m^3\,yr^{-1}$)	AGRC (%)	$AGRC_S$ (%)	ARC (%)
17a	Matese (a)	120	34	95.2	138.1	69	52	48
27	Terminio	167	43	169.7	213.3	79	64	36
31a	Accellica (a)	35	0	18.3	36.9	50	50	50
32	Cervialto	129	20	126.1	178.4	71	63	37

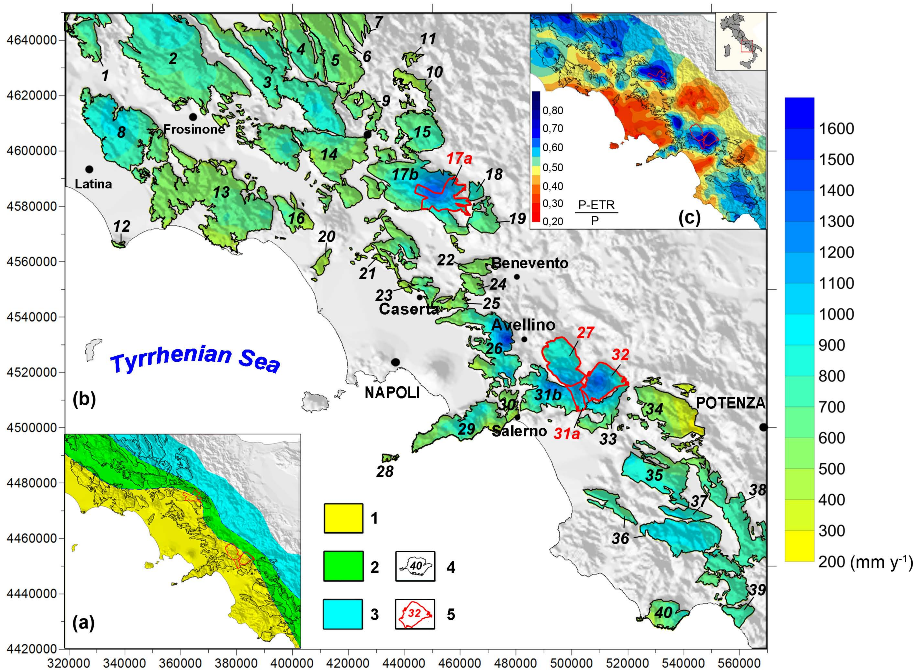

Fig. 6. Homogeneous precipitation zones **(a)**, distributed model of mean annual $P-ETR$ **(b)** and of mean annual $(P-ETR)/P$ ratio **(c)**. Key to symbol: (1) upwind zone; (2) first downwind zone; (3) second downwind zone; (4) hydrogeological boundaries and identification number of the karst aquifers; (5) hydrogeological boundaries and identification number of the karst aquifers considered for the hydrological budget.

correlated to the different lithology, which is prevailingly dolomitic, and the lack of summit plateau and endorheic areas for the latter case. Corresponding $AGRC_S$ and ARC values (Table 1 and Fig. 7) were estimated as ranging from 50 to 64 % and from 50 to 36 %, respectively.

4.5 Regional assessment of the groundwater recharge

To generalize the results obtained for the four sample karst aquifers at a regional scale, a bivariate correlation analysis was carried out between the AGRC and limestone area, summit plateau and endorheic area, woodland area, loamy sand soil type area and mean slope angle. A significant correlation was found for limestone ($r^2=0.901$; Prob. F-Fisher = 1.3 %) and summit plateau endorheic areas ($r^2=0.931$; Prob. F-Fisher = 0.14 %) only. Instead, the correlation analyses revealed a scarce statistical significance (Prob. F-Fisher ≥ 15 %) of the last three parameters on the AGRC variability. Consequently, a multiple linear regression to empirically correlate the mean AGRC to the basic controlling variables, namely limestone area (L %) and summit plateau and endorheic area (E %), was found:

$$\mathrm{AGRC} = 47.99 + 0.08\,\mathrm{L} + 0.51\,\mathrm{E}, \tag{9}$$

which was statistically significant ($r^2=0.968$; Prob. F-Fisher = 3.0 %; standard errors of 5.92, 0.06 and 0.07 for the intercept, first and second coefficient, respectively).

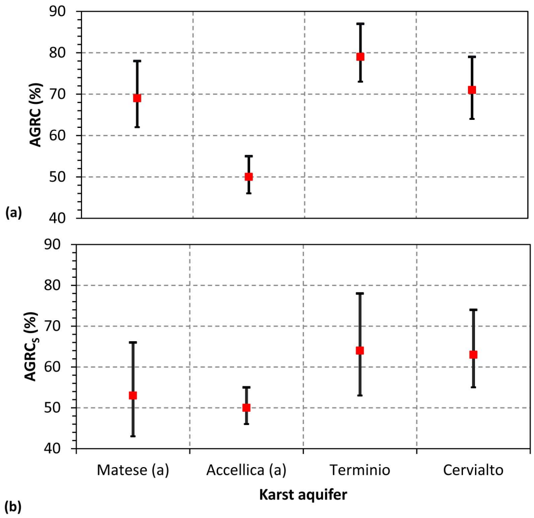

Fig. 7. AGRC **(a)** and AGRC$_S$ **(b)** estimations for the four sample karst aquifers obtained considering uncertainties of the annual $P-\mathrm{ETR}$ and air temperature regression models (95 % confidence limits).

The preceding equation confirms the insight that the plateau and endorheic area is a factor affecting the mean AGRC more strongly than lithology (outcrop of karst rocks).

The AGRC and AGRCs values for the 40 regional karst aquifers by applying the empirical Eqs. (9) and (6) (Table 2) were assessed. The minimum estimated AGRC value was calculated for the Circeo karst aquifer (48 %); the maximum value was found for the Terminio karst aquifer (78 %), with a residual of 1 % respect directly calculated to that (Table 1) and a mean global value of 59 %.

The estimation of the AGRC and $P-\mathrm{ETR}$ values (Fig. 6) for each karst aquifer allowed for the assessment of the respective mean annual groundwater recharge (Table 2), which was assessed at the regional scale (Fig. 8). To validate this empirical estimation, the recharge values calculated by Eq. (9) for the four sample karst aquifers were compared with the outflow discharges. The resulting residuals between the predicted recharge and measured outflow was considered to be negligible, ranging between 0 and 10 % (Table 2 and Fig. 9), and thus supporting the reliability of the empirical estimations. Moreover, the correlation between the estimated mean annual groundwater recharge and the measured groundwater outflow, appraised for 18 of the 40 karst aquifers by non-systematic spring discharges measurements carried out during the 1970s and 1980s (Celico, 1983; Allocca et al., 2007a), showed consistent results (Fig. 9) both in terms of angular coefficient and statistical significance (Prob. F-Fisher < 0.1 %).

5 Discussion and conclusions

The estimation of the AGRC is proposed as a practical tool to assess annual groundwater recharge in karst aquifers of the southern Apennines and forecast the effects of annual to decadal climatic variability. The applied methods were oriented to account for the lack of temporal and spatial hydrological time series, namely the availability of significant spring discharge measurements and precipitation records in the high altitude ranges. Consequently, results are based on all existing and available hydrological data.

A contribution to reconstruct a regional distributed model of $P-\mathrm{ETR}$ that also accounts for orographic barrier and altitude controls of the Apennine chain is provided by identifying three homogeneous zones in which distinctive empirical laws exist relatively to altitude. This approach is proposed as a simpler and more direct method for distributively assessing the amount of $P-\mathrm{ETR}$, potentially involved in groundwater recharge, which is not based on geostatistical analyses (Goovaerts, 2000; Marquínez et al., 2003) but on the recognition of the orographic barrier and altitude controls (Vuglinski, 1972; Brunsdon et al., 2001).

The estimations of the AGRC for four sample karst aquifers varied from 50 to 79 % with a mean value of 67 %. These results are similar to those estimations carried out previously by Celico (1988) and Allocca et al. (2007a), who heuristically assessed AGRC values up to 90 % for karst aquifers of the southern Apennines, taking their typical summit plateau and endorheic morphologies into account.

No other comparisons are possible due to the new structure of the proposed coefficient. Nonetheless, by means of Eq. (5) and considering a mean annual value of the $(P-\mathrm{ETR})/P$ ratio approximately equal to 0.7 for the four sample karst aquifers, the AGRC values are quite comparable to those of annual EIC (AEIC), which were determined in the European and peri-Mediterranean areas (Burdon, 1965; Vilimonovic, 1965; Drogue, 1971; Bonacci, 2001) and previously as described in the Introduction section.

The four sample karst aquifers are the only cases for which spring discharges were measured for a long duration and the AGRC is more accurately estimable. Because of the accurate assessment of mean annual groundwater outflow and inflow volumes for the four sample karst aquifers, the calculated values of the AGRC represent a reliable approach to model groundwater recharge for these aquifers.

Owing to the similarity of the other karst aquifers, an empirical estimate of the mean AGRC was also proposed for those aquifers, hence attempting a regionalization of the groundwater recharge modelling. Using a correlation analysis of other factors recognisable as affecting groundwater recharge in sample karst aquifers, such as lithology, morphological settings, land use and covering soil type, an empirical relationship between AGRC, summit plateau and/or endorheic areas and lithology was found. In spite of the limited number of data, this empirical relationship is statistically

Table 2. Data and estimations of AGRC, $AGRC_S$, ARC and mean annual groundwater recharge for karst aquifers of the study area. In the last column, the mean annual groundwater outflow, estimated for some of the karst aquifers by other hydrogeological studies (Celico, 1983; Allocca et al., 2007) are reported; values estimated in this study for the four sample karst aquifers (ID 17a, 27, 31a and 32) are reported.

ID	Karst aquifer	Area (km^2)	Mean annual $P-$ETR (mm)	Limestone area (%)	Summit plateau and endorheic area (%)	AGRC (%)	$AGRC_S$ (%)	ARC (%)	Mean annual groundwater recharge ($10^6\,m^3\,yr^{-1}$)	Mean annual groundwater outflow ($10^6\,m^3\,yr^{-1}$)
1	Cerella	137	738	100	0	56	56	44	57.0	–
2	Simbruini	1075	896	94	12	62	57	43	596.7	–
3	Cornacchia	723	940	90	7	59	56	44	402.6	–
4	Marsicano	204	845	94	5	58	56	44	100.8	–
5	Genzana	277	814	10	34	66	49	51	149.6	–
6	Rotella	40	800	100	40	77	62	38	24.6	–
7	Porrara	63	753	100	25	69	59	41	32.9	–
8	Lepini	483	990	100	2	57	57	43	274.3	400.5
9	Colli Campanari	88	702	0	12	54	48	52	33.4	–
10	Capraro	70	586	0	5	51	48	52	20.7	–
11	Campo	16	692	0	13	55	48	52	6.1	–
12	Circeo	6	548	0	0	48	48	52	1.7	–
13	Ausoni	822	835	99	15	64	58	42	438.2	507.7
14	Venafro	362	796	74	11	60	55	45	172.4	269.3
15	Totila	183	535	0	8	52	48	52	51.2	–
16	Maio	93	706	98	12	63	58	42	41.0	–
17a	Matese (a)	120	1151	97	34	74	60	40	101.8	95.2
17b	Matese (b)	480	1151	65	15	61	55	45	338.1	375.0
18	Tre Confini	28	830	0	4	50	48	52	11.6	–
19	Moschiaturo	85	887	0	7	51	48	52	38.6	–
20	Massico	29	700	89	0	55	55	45	11.4	–
21	Maggiore	157	719	99	0	56	56	44	63.5	56.7
22	Camposauro	50	935	99	4	58	56	44	27.4	–
23	Tifatini	80	646	90	2	56	56	44	29.2	25.2
24	Taburno	43	1212	81	4	57	55	45	29.8	–
25	Durazzano	52	775	100	0	56	56	44	22.7	–
26	Avella	334	983	100	9	61	57	43	201.2	–
27	Terminio	167	1277	100	43	78	62	38	167.4	169.7
28	Capri	9	565	93	0	56	56	44	2.7	–
29	Lattari	244	868	75	0	54	54	46	115.2	–
30	Salerno	46	734	13	0	49	49	51	16.6	21.1
31a	Accellica (a)	35	1055	32	0	51	51	49	18.7	18.3
31b	Accellica (b)	171	1055	33	0	51	51	49	91.6	107.6
32	Cervialto	129	1383	98	20	67	58	42	119.0	126.1
33	Polveracchio	117	1257	81	0	55	55	45	80.9	103.1
34	Marzano	292	776	97	13	63	57	43	142.0	–
35	Alburni	254	1162	99	42	78	62	38	230.5	233.4
36	Cervati	318	1225	81	13	62	56	44	241.0	220.8
37	Motola	52	1179	100	4	59	57	43	35.7	37.8
38	Maddalena	307	859	59	21	64	54	46	168.8	97.8
39	Forcella	217	965	86	5	58	56	44	121.4	–
40	Bulgheria	100	785	68	1	54	54	46	42.5	42.5

significant, allowing for the regionalization of the groundwater recharge for karst aquifers of the southern Apennines. A few other studies have tried to regionalize karst aquifer characteristics with topographic and climatic descriptors (Andreo et al., 2008) and by defining signatures derived from hydrodynamic and hydrochemical observations (Hartmann et al., 2013).

The proposed approach highlights another complementary aspect related to the estimation of annual runoff along slope areas, which is particularly relevant for the management of surficial water resources. The calculated mean ARC values

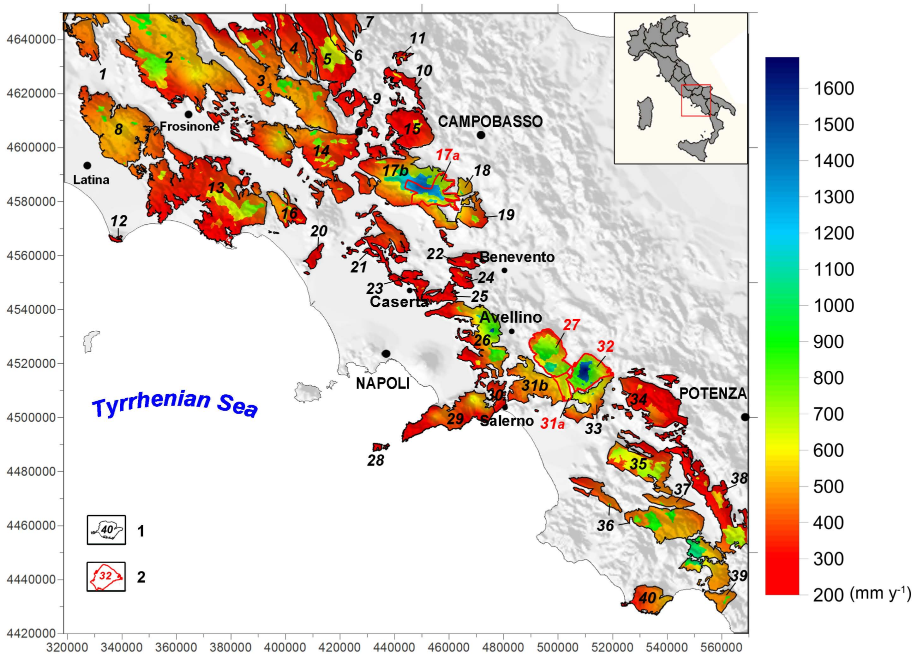

Fig. 8. Distributed model of the mean annual groundwater recharge for karst aquifers of the southern Apennines. Key to symbol: (1) hydrogeological boundaries and identification number of the karst aquifers; (2) hydrogeological boundaries and identification number of the karst aquifers considered for the hydrological budget.

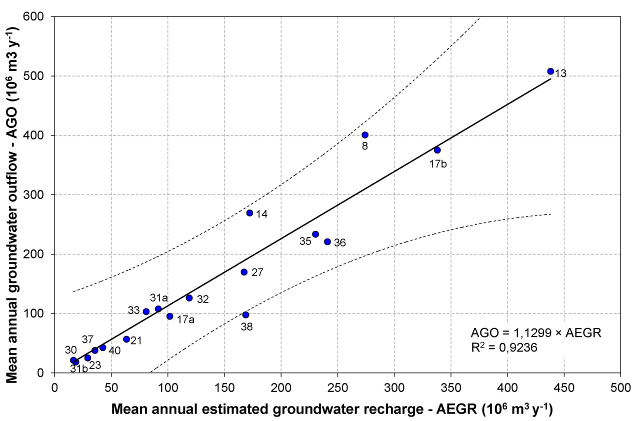

Fig. 9. Correlation between mean annual groundwater outflow (AGO) assessed by non-systematic spring discharges measurements and mean annual estimated groundwater recharge (AEGR). The numbers correspond to the aquifers' ID. The 95 % confidence bands are also shown.

varying from 36 to 50 % can be approximately compared with those determined for Dinaric karst aquifers (Horvat and Rubinic, 2006) and some river basins of southern continental Italy (Del Giudice et al., 2013).

The methodology is presented as a reliable and practical approach for modelling the groundwater recharge of karst aquifers at regional and mean annual scales in the case of a large territory with discontinuous and absent hydrological monitoring. It can be conceived as a deeper understanding of groundwater hydrology in karst aquifers and a first step to overcoming the lack of spring discharges and piezometric levels' time series. The application of this method would thus permit the design of appropriate management models for groundwater and surface resources of karst aquifers as well as the setting up of accurate strategies to mitigate the effects of climate change. This achievement would allow the balancing of environmental needs and societal impacts of water uses, as required by the EU Water Framework Directive (European Commission, 2000).

Acknowledgements. We thank Gerardo Ventafridda of the Apulian Aqueduct (www.aqp.it), who provided discharge data for the Cassano Irpino and the Sanità karst springs, and the Department of Civil Protection of the Campania region (www.regione.campania.it), which kindly provided the rainfall and temperature data. We are also grateful to Pierre-Yves Jeannin, Andrew J. Long and two other anonymous referees who provided constructive reviews of the manuscript.

Edited by: N. Romano

References

Allocca, V., Celico, F., Celico, P., De Vita, P., Fabbrocino, S., Mattia, S., Monacelli, G., Musilli, I., Piscopo, V., Scalise, A. R., Summa, G., and Tranfaglia, G.: Illustrative Notes of the Hydrogeological Map of Southern Italy, Istituto Poligrafico e Zecca dello Stato, Rome, 1–211, 2007a.

Allocca, V., De Vita, P., Fabbrocino, S., and Celico, P.: The karst aquifers of the southern Apennines (Italy): a strategic groundwater resource, Mem. Ist. It. Speleo, II, XIX, 65–72, 2007b.

Allocca, V., Celico, F., Petrella, E., Marzullo, G., and Naclerio, G.: The role of land use and environmental factors on microbial pollution of mountainous limestone aquifers, Environ. Geol., 55, 277–283, 2008.

Allocca, V., Celico, F., Celico, P., De Vita, P., Fabbrocino, S., Mattia, C., Monacelli, G., Musilli, I., Piscopo, V., Scalise, A. R., Summa, G., and Tranfaglia, G.: La carta idrogeologica dell'Italia meridionale. Metodi ed analisi territoriali per l'identificazione e la caratterizzazione dei corpi idrici sotterranei (Direttiva 2000/60/CE), L'Acqua, 4, 21–32, 2009.

Andreo, B., Vías, J., Durán, J. J., Jiménez, P., López-Geta, J. A., and Carrasco, F.: Methodology for groundwater recharge assessment in carbonate aquifers: application to pilot sites in southern Spain, Hydrogeol. J., 16, 911–925, 2008.

Bonacci, O.: Karst spring hydrographs as indicators of karst aquifers, Hydrolog. Sci. J., 38, 51–62, 1993.

Bonacci, O.: Montly and annual effective infiltration coefficients in Dinaric karst: example of the Gradole karst spring catchment, Hydrological Sciences – Journal des Sciences Hydrologiques, 46, 287–299, 2001.

Boni, C., Bono, P., and Capelli, G.: Valutazione quantitativa dell'infiltrazione efficace in un bacino dell'Italia centrale: confronto con analoghi bacini rappresentativi di diversa litologia, Geologia Applicata e Idrogeologia, 17, 437–452, 1982.

Brancaccio, L., Cinque, A., and Sgrosso, I.: L'analisi dei versanti di faglia come strumento per la ricostruzione di eventi neotettonici, Memorie Società Geologica Italiana, 19, 621–626, 1978.

Brusdon, C., Mc Clatchey, J., and Unwin, D. J.: Spatial variations in the average rainfall-altitude relationship in Great Britain: an approach using geographically weighted regression, Int. J. Climatol., 21, 455–466, 2001.

Bull, W. B.: Tectonic geomorphology of mountains, a new approach to paleoseismology, Blackwell Publishing, Malden, USA, 316 pp., 2007.

Burdon, D. J.: Hydrogeology of some karstic areas of Greece. Actes de Colloque de Dubrovnik sur l'Hydrologie des roches calcaires fessures, A.I.H.S.-UNESCO, 73, 308–317, 1965.

Carroll, R. J. and Ruppert, D.: Transformation and Weighting in Regression, Chapman and Hall, New York, 1988.

Celico, P.: Idrogeologia dei massicci carbonatici, delle piane quaternarie e delle aree vulcaniche dell'Italia centromeridionale (Marche e Lazio meridionale, Abruzzo, Molise e Campania), Quaderni della Cassa per il Mezzogiorno, 4/2, 1–203, 1983.

Celico, P.: Prospezioni idrogeologiche, vol. 2, edited and published by: Liguori, E., Naples, Italy, p. 536, 1988.

Celico, F., Petrella, P. and Celico, P.: Hydrogeological behaviour of some fault zones in a carbonate aquifer of Southern Italy: an experimentally based model, Terra Nova, 18, 308–313, 2006.

Celico, F., Naclerio, G., Bucci, A., Nerone, V., Capuano, P., Carcione, M., Allocca, V., and Celico, P.: Influence of pyroclastic soil on epikarst formation: a test study in southern Italy, Terra Nova, 22, 110–115, 2010.

Civita, M., Olivero, G., Manzone, L., and Vigna, B.: Approcci sinergici nelle ricerche sui sistemi idrogeologici carbonatici del Piemonte meridionale. Atti Conv, Ricerca e Protezione delle Risorse Idriche Sotterranee delle Aree Montuose", 1, 53–86, 1992.

Darcy, H.: Les Fountaines Publiques de la Ville de Dijon, Victor Dalmont, Paris, 1–647, 1856.

Del Giudice, G., Padulano, R., and Rasulo, G.: Spatial prediction of the runoff coefficient in Southern Peninsular Italy for the index flood estimation, Hydrology Research, doi:10.2166/nh.2013.243, in press, 2013.

Delin, G. F., Healy, R. W., Lorenz, D. L., and Nimmo, J. R.: Comparison of local- to regional-scale estimates of ground-water recharge in Minnesota, USA, J. Hydrol., 334, 231–249, 2007.

De Vita, P., Agrello, D., and Ambrosino, F.: Landslide susceptibility assessment in ash-fall pyroclastic deposits surrounding Somma-Vesuvius: application of geophysical surveys for soil thickness mapping, J. Appl. Geophys., 59/2, 126–139, 2006.

De Vita, P., Allocca, V., Manna, F., and Fabbrocino, S.: Coupled decadal variability of the North Atlantic Oscillation, regional rainfall and karst spring discharges in the Campania region (southern Italy), Hydrol. Earth Syst. Sci., 16, 1389–1399, doi:10.5194/hess-16-1389-2012, 2012.

De Vita, P., Napolitano, E., Godt, J. W., and Baum, R. L.: Deterministic estimation of hydrological thresholds for shallow landslide initiation and slope stability models: case study from the Somma-Vesuvius area of southern Italy, Landslides, 10, 713–728, doi:10.1007/s10346-012-0348-2, 2013.

Dripps, W. R. and Bradbury, K. R.: The spatial and temporal variability of groundwater recharge in a forested basin in northern Wisconsin, Hydrol. Process., 24, 383–392, 2010.

Drogue, C.: Coefficient d'infiltration ou infiltration eficace, sur le roches calcaires, Actes du Colloque d'Hydrologie en Pays Calcaire, Besancon, 15, 121–130, 1971.

Drogue, C.: Hydrodynamic of karstic aquifers: Experimental sites in the Mediterranea karst, Southern France, Inter. Contr. Hydrogeol. I.A.H., 13, 133–149, 1992.

European Commission: Directive 2000/60/EC of the European Parliament and of the Council of 23 October 2000 establishing a framework for community action in the field of water policy, Official Journal L327 of 22 December 2000, Bruxelles, 2000.

Fiorillo, F.: Tank-reservoir drainage as a simulation of the recession limb of karst spring hydrographs, Hydrogeol. J., 19, 1009–1019, 2011a.

Fiorillo, F.: The Role of the Evapotranspiration in the Aquifer Recharge Processes of Mediterranean Areas, in: "Evapotranspiration, From Measurements to Agricultural and Environmental Applications", edited by: Gerosa, G., InTech Publisher, Rijeka, Croatia, 373–388, 2011b.

Geiger, R.: Landolt-Börnstein – Zahlenwerte und Funktionen aus Physik, Chemie, Astronomie, Geophysik und Technik, alte Serie Vol. 3, in: Klassifikation der Klimate nach W. Köppen, Springer, Berlin, 603–607, 1954.

Goldscheider, N.: A holistic approach to groundwater protection and ecosystem services in karst terrains, Aqua Mundi – Am, 06046, 117–124, 2012.

Goldscheider, N. and Drew, D.: Methods in karst hydrogeology, Taylor & Francis, London, 1–264, 2007.

Goovaerts, P.: Geostatistical approaches for incorporating elevation into the spatial interpolation of rainfall, J. Hydrol., 228, 113–129, 2000.

Hartmann, A., Lange, J., Weiler, M., Arbel, Y., and Greenbaum, N.: A new approach to model the spatial and temporal variability of recharge to karst aquifers, Hydrol. Earth Syst. Sci., 16, 2219–2231, doi:10.5194/hess-16-2219-2012, 2012.

Hartmann, A., Weiler, M., Wagener, T., Lange, J., Kralik, M., Humer, F., Mizyed, N., Rimmer, A., Barberá, J. A., Andreo, B., Butscher, C., and Huggenberger, P.: Process-based karst modelling to relate hydrodynamic and hydrochemical characteristics to system properties, Hydrol. Earth Syst. Sci., 17, 3305–3321, doi:10.5194/hess-17-3305-2013, 2013.

Healy, R. W.: Estimating Groundwater Recharge, Cambridge University Press, 256 pp., 2010.

Henderson-Sellers, A. and Robinson, P. J.: Contemporary Climatology, John Wiley & Sons, New York, 1986.

Horvat, B. and Rubinic, J.: Annual runoff estimation - an example of karstic aquifers in the transboundary region of Croatia and Slovenia, Hydrolog. Sci. J., 51, 314–324, 2006.

Houze, R. A.: Orographic effects on precipitating clouds, Rev. Geophys., 50, 1–47, 2012.

ISSKA: Swisskarst Project – toward a sustainable management of karst waters in Switzerland. Swiss Institute for Speleology and Karst studies, Swiss National Science Foundation, La Chaux-de-Fonds, Switzerland, p. 47, 2012.

Jeannin, P.-Y.: Structure et comportement hydraulique des aquifères karstiques, PhD thesis, University of Neuchâtel, Neuchâtel, p. 244, 1998.

Kessler, H.: Water balance investigation in the karstic region of Hungary, Actes de Colloque de Dubrovnik sur l'Hydrologie des roches calcaires fessures, A.I.H.S.-UNESCO, 73, 91–105, 1965.

Kiraly, L.: Rapport sur l'état actuel des connaissances dans le domaines des caractères physiques des roches karstiques, edited by: Burger, A. and Dubertret, L., Hydrogeology of karstic terrains, Int. Union of Geol. Sci. B, 3, 53–67, 1975.

Kiraly, L.: Karstification and Groundwater Flow, in: Evolution of karst: from prekarst to cessation, Postojna-Ljubljana, edited by: Gabrovsek, F., Zalozba ZRC, Ljubljana, Slovenia, 155–190, 2002.

Klimchouk, A. B.: The formation of Epikarst and its role in Vadose Speleogenesis, in: Speleogenesis, Evolution of Karst Aquifers, edited by: Klimchouk, A. B., Ford, D. C., Palmer, A. N., and Dreybrodt, W., Nat. Speleol. Soc., Huntsville, 91–99, 2000.

Lerner, D. N., Issar, A. S., and Simmers, I.: Groundwater recharge, a guide to understanding and estimating natural recharge, Rep. 8, International Association of Hydrogeologists, Kenilworth, p. 354, 1990.

Mangin, A.: Contribution à l'étude hydrodynamique des aquifères karstiques, Ann. Spéléol., 29, 283–332; 29, 495–601, 30, 21–124, 1975.

Marquínez, J., Lastra, J., and García, P.: Estimation models for precipitation in mountainous regions: the use of GIS and multivariate analysis, J. Hydrol., 270, 1–11, 2003.

Naclerio, G., Petrella, E., Nerone, V., Allocca, V., De Vita, P., and Celico, F.: Influence of topsoil of pyroclastic origin on microbial contamination of groundwater in fractured carbonate aquifers, Hydrogeol. J., 16, 1057–1064, 2008.

Naclerio, G., Nerone, V., Bucci, A., Allocca, V., and Celico, F.: Role of organic matter and clay fraction on migration of Escherichia Coli cells through pyroclastic soils, southern Italy, Colloids Surf. B, 72, 57–61, 2009.

Parajka, J. and Szolgay, J.: Grid-based mapping of long-term mean annual potential and actual evapotranspiration in Slovakia, IAHS Publ., Proceedings of the HeadWater'98 Conference, April 1998, Merano, Italy, 123–129, 1998.

Patacca, E. and Scandone, P.: Geology of the Southern Apennines, Ital. J. Geosci., 7, 75–119, 2007.

Ravbar, N., Engelhardt, I., and Goldscheider, N.: Anomalous behaviour of specific electrical conductivity at a karst spring induced by variable catchment boundaries: the case of the Podstenjsek spring, Slovenia, Hydrol. Process., 25, 2130–2140, 2011.

Roe, G. H.: Orographic precipitation, Annu. Rev. Earth Planet. Sci., 33, 645–671, 2005.

Santoro, M.: Sulla applicabilità della formula di Turc per il calcolo della evapotraspirazione effettiva in Sicilia, Proceedings I International Conference on Groundwater, I.A.H., Palermo, 1970.

Scanlon, B. R., Healy, R. W., and Cook, P. G.: Choosing appropriate techniques for quantifying groundwater recharge, Hydrogeol. J., 10, 18–39, 2002.

Scanlon, B. R., Keese, K. E., Flint, A. L., Flint, L. E., Gaye, C. B., Edmunds, W. M., and Simmers, I.: Global synthesis of groundwater recharge in semiarid and arid regions, Hydrol. Process., 20, 3335–3370, 2006.

Sodeman, P. C. and Tysinger, J. E.: Effect of forest cover upon hydrologic characteristics of a small watershed in limestone region of East Tennesse, Actes de Colloque de Dubrovnik sur l'Hydrologie des roches calcaires fessures, A.I.H.S.-UNESCO, 73, 135–151, 1965.

Soulios, G.: Infiltration efficace dans le karst hellenique, J. Hydrol., 75, 343–356, 1984.

Stephens, D. B.: Vadose Zone Hydrology, CRC Press, Boca Raton, Florida, USA, 339 pp., 1995.

Turc, L.: Le bilan d'eau des sols: relations entre les précipitations, l'évaporation et l'éecolument, Annales Agronomiques, 5, 491–595, 1954.

Vilimonovic, J.: A contribution of the study of groundwater intake recharge in karst, Actes de Colloque de Dubrovnik sur l'Hydrologie des roches calcaires fessures, A.I.H.S.-UNESCO, 73, 482–499, 1965.

Vuglinski, V. S.: Methods for the study of laws for the distribution of precipitation in mediu-high mountains (illustrated by the Vitim River Basin), Distribution of precipitation in Mountainous Areas, WMO Publ., 326, 212–221, 1972.

White, W. B.: Conceptual models for carbonate aquifer, Ground Water, 7, 15–21, 1969.

White, W. B.: Karst hydrology: recent developments and open questions, Eng. Geol., 65, 85–105, 2002.

AGU FALL MEETING

San Francisco I 15–19 December 2014

Assessment of groundwater recharge in an ash-fall mantled karst aquifer of southern Italy

Manna F., Nimmo J.R., De Vita P., Allocca V.

In southern Italy, the Mesozoic carbonate platform series, covered by ash-fall pyroclastic soils, are large karst aquifers and major groundwater resources. For these aquifers, even though Allocca et al., 2014 estimated a mean annual groundwater recharge coefficient at regional scale, a more complete understanding of the recharge processes, at small spatio-temporal scale, is a primary scientific target to be achieved.

In this paper, we study groundwater recharge processes in the Acqua della Madonna test site (Allocca et al., 2008), through the integrated analysis of piezometric levels, rainfall, soil moisture and air temperature data. These were gathered, with hourly frequency, by a monitoring station in 2008.

To model groundwater recharge through the identification of episodes of recharge and the estimation of the Recharge to Precipitation Ratio (RPR) at both the individual-episode and annual time scale, the Episodic Master Recharge method (Nimmo et al., 2014) was applied.

For different episodes of recharge observed, RPR ranges from 97% to 37%, with an annual mean around 73%. This result, confirmed by a soil water balance and the application of the Thornthwaite-Mather method to estimate actual evapotranspiration, is very close to the mean annual groundwater recharge coefficient estimated, at regional scale, for the karst aquifers of southern Italy. In addition, the RPR is affected, at the daily scale, by both antecedent soil moisture and rainfall intensity, as demonstrated by a statistically significant multiple linear regression among such hydrological variables. In particular, the recharge magnitude is great for low storm intensity and high antecedent soil moisture value.

The results advance the comprehension of groundwater recharge processes in karst aquifers, and the sensitivity of RPR to antecedent soil moisture and rainfall intensity facilitates the prediction of the influence of climate and precipitation regime change on the groundwater recharge process.

Groundwater recharge assessment at local and episodic scale in a soil mantled perched karst aquifer of southern Italy

V. Allocca[1], P. De Vita[1], F. Manna[1], and J.R. Nimmo[2]

[1] Department of Earth, Environment and Resources Sciences, University of Naples "Federico II", Naples, Italy.

[2] U.S. Geological Survey, Menlo Park, California, United States

Correspondence to: V. Allocca (vincenzo.allocca@unina.it)

Abstract

Groundwater recharge assessment of karst aquifers in southern Italy, at various spatial and temporal scales, is a current and major scientific topic, since these aquifers play an essential role for both socio-economic development and fluvial ecosystems.

In this study, groundwater recharge was estimated at local and episodic scales in a representative perched karst aquifer of the southern Italy, covered by ash-fall pyroclastic soils and under Mediterranean-type climate. The research was carried out through precipitation, air temperature, soil water content and water-table level monitoring during 2008 in an experimental site, the Acqua della Madonna test area, belonging to the Terminio Mount karst aquifer (Campania region, southern Italy). An improvement of the Water Table Fluctuation (WTF) method, known as Episodic Master Recession (EMR) technique, was applied to assess the episodic aquifer recharge, generated by single rainfall events, by the estimation of the Recharge to the Precipitation Ratio (RPR).

Depending on seasonal variability of air temperature, precipitation pattern and evapotranspiration, the calculated values of RPR varied between 35% and 97%. A multiple linear correlation of the RPR with both the average intensity of recharging rainfall events and the antecedent soil water content was found. Given the accessibility of these two hydro-meteorological parameters, such an empirical model would have strong hydrogeological and practical implications since it would allow making forecasts of groundwater recharge in other karst aquifers of the Mediterranean region and, more generally, in other aquifers with similar hydrogeological characteristics.

Keywords: Groundwater recharge, local and episodic scales, perched karst aquifer, soil cover, Water Table Fluctuation method.

1. Introduction

Karst aquifers represent about 12% of the Earth's continental area and about one quarter of the global population is fed by drinking water from these hydrogeological systems (Ford and Williams, 2007). Many European and Mediterranean countries are completely or partially dependent on groundwater resources of karst aquifers. In southern Italy, these aquifers are the main source for drinking water supplies (Celico, 1983; Celico et al., 2000; Allocca et al., 2007a; Allocca et al., 2014) and they play also a vital role for groundwater-dependent fluvial ecosystems.

The mean annual yield of karst groundwater in southern Italy was estimated to be about $4{,}100\times10^{6}\ m^{3}year^{-1}$, with an average specific yield varying from 0.015 to 0.045 $m^{3}s^{-1}km^{-2}$ (Allocca et al., 2007a). The high productivity of karst aquifers in southern Italy is linked to high permeability of karst rocks, relevant precipitation during autumn and winter seasons and existence of large summit endorheic and/or flat areas that favour infiltration and groundwater recharge processes (Manna et al., 2013a; Allocca et al., 2014). Another peculiarity of such karst aquifers is the widespread existence of allochthonous soil mantles, formed by the deposition of ash-fall pyroclastic deposits (De Vita et al., 2013) erupted by the main volcanic centres of the Campania region (Ischia, Roccamonfina, Phlegraean Fields and Somma-Vesuvius). These surficial volcanic overburdens influence groundwater recharge, especially where they are thicker, by acting as a temporary water storage tank that modulates the infiltration processes into carbonate bedrock and enhances evapotranspiration. At the same time, this surficial hydrogeological subsystem, coupled with the abundant vegetation cover, obstructs the migration of microbial cells from the ground toward groundwater bodies (Naclerio et al., 2008; Naclerio et al., 2009; Bucci et al., 2015a; Bucci et al., 2015b) and fosters the development of epikarst (Petrella et al., 2007; Celico et al., 2010).

Karst aquifers of southern Italy are characterized by a prevalent groundwater basal flow, outflowing in major basal springs (Celico, 1978; Boni et al., 1986; Allocca et al., 2007b), but often by perched groundwater circulation feeding numerous high-altitude minor springs, whose groundwater resources are very relevant for local uses.

Advancing knowledge regarding suitable approaches to assess groundwater recharge processes, namely to quantify and model the replenishment of groundwater resources by infiltration processes through the unsaturated zone (Lerner et al., 1990; Stephen, 1995; Scanlon et al., 2006; Healy, 2010), is a fundamental and challenging issue to be investigated in different hydrogeological conditions. In such a view, given impacts of climate changes (VV.AA., 2007) on groundwater hydrology (De Vita et al., 2012; Manna et al., 2013b; Hartmann et al., 2014a) and the increasing demand of drinking water in various areas of the Mediterranean and of the world (Wada et al., 2010), to understand and model groundwater recharge processes in karst systems appears a fundamental requisite for sustainable management of groundwater resources as well as for protection of dependent fluvial ecosystems.

In addition, progressing hydrological studies on perched karst aquifers is a new research frontier owing to the high altitude of the related spring outflows, which represent valuable resources for mountainous areas as well as for development of mini-hydropower production.

Several direct and indirect methods, both empirical and numerical, are known in scientific literature for estimating groundwater recharge in karst aquifers at different spatial scales, from regional to local, and temporal scales, from annual to daily and episodic (Andreo et al., 2008; Hartmann et al., 2014b; Allocca et al., 2014; Fiorillo et al., 2014; Guardiola-Albert et al., 2014; Nimmo et al., 2015).

As regards direct approaches for estimating groundwater recharge (Scanlon et al., 2006), the Water Table Fluctuation (WTF) method is widely used (Healy and Cook, 2002) though is not usually applied to karst aquifers due to the frequently great depth of the water table, which usually prevents measurement and monitoring of groundwater levels. In recent years, several ways of implementing the WTF method have been developed, using different approaches, each one with its own limits and approximation (Todd, 2005; Coes et al., 2007). Among them, the RISE (Rutledge, 1998) and Master Recession Curve (MRC) (Heppner and Nimmo, 2005; Heppner et al., 2007; Delin et al., 2007) as well as other graphical approaches (Risser et al., 2005; Delin et al., 2007) can be mentioned. Recently, Nimmo et al. (2015) have developed an advancement of the WTF method, known as Episodic Master Recession (EMR) method, to estimate the groundwater recharge at local and episodic scale and to associate each recharge episode with a causal rainfall recharging event. Although the EMR method has already been tested (Nimmo et al., 2015) in a fractured sandstone aquifer (Masser Site, Pennsylvania, USA) and a glacial moraine aquifer (Silstrup Site, Denmark), it has never been applied in karst aquifers.

Through the application of the EMR method to a perched karst aquifer of the southern Italy, mantled by ash-fall pyroclastic soils, this research points to the following principal objectives: i) to assess the groundwater recharge, at local and episodic scales, by estimating the Recharge to Precipitation Ratio (RPR); ii) to find the relationship between RPR, average intensity of rainfall recharging events, and antecedent soil water content; iii) to check and validate the reliability of the RPR values by estimating actual evapotranspiration through a soil water budget.

The paper is organised as follows: after a description of the test area (Sect. 2), the hydrometeorological and hydrogeological data and methodology for estimating groundwater recharge are illustrated (Sect. 3). Following these, results (Sect. 4), discussion (Sect. 5) and conclusion (Sect. 6) are reported.

2. 2. Description of the research site

The Acqua della Madonna test area belongs to the central-southern sector of the Terminio Mount karst aquifer (Campania region, southern Italy), whose total extent is about 167 km^2 (Figs. 1a and 1b). This test area, extended for about 0.9 km^2 and lying around 1.200 m a. s. l. (Figs. 1b and 1d), is characterized by a perched karst aquifer that is formed mainly by a fractured and partially karstified Cretaceous limestone series. The area is covered by alkali-potassic ash-fall pyroclastic deposits derived mainly from the Somma-Vesuvius volcano (Allocca et al., 2008). Over such pyroclastic deposits, Molli-Eutrisilic Andosols and Molli-Vitric Andosols are present, with thicknesses up to 0.50-0.60 m, while in small karst plains (Fig. 1b), where the bedrock is deeper and pyroclastic mantle reaches a thickness up to 10÷20 m, Pachi-Eutrisilic Andosols are developed (Allocca et al., 2008). Moreover, along hillslopes, deciduous forest (*Fagus sylvatica L.*) is the predominant land use type, whereas in the flat karst endorheic areas grassland is the prevailing type (Allocca et al., 2008).

The limestone aquifer is characterized by a very low primary porosity (about 0.1÷0.6%) and a more relevant secondary one (about 2%), which is determined by a high degree of jointing and subordinately by the development of karst process along principal discontinuities. Several boreholes were drilled down to a depth of about 80 m in the test area and in its surroundings (Figs. 1b and 1d), detecting the existence of an unconfined karst aquifer under an ash-fall pyroclastic deposits about 8 m thick. Due to the high altitude of this groundwater body, with water-table levels ranging from 1.151 to 1.182 m a.s.l. (Figs. 1b and 1d), the Acqua della Madonna aquifer is clearly perched, with respect to the larger basal groundwater circulation, which feeds main karst springs outflowing at the base of the Mount Terminio aquifer with mean annual discharges and altitudes respectively varying from 0.1 to 1.4 m^{3}s^{-1} and from 330 to 473 m a.s.l. (Fig. 1a). Boreholes in the test area have not revealed any stratigraphic or structural factor leading to a local reduction of permeability which could be recognized to perch the studied aquifer.

According to the stratigraphic setting of the carbonate Mesozoic series, which is characterized by low-permeability marls and clayey interbeds in correspondence of the lower Cretaceous interval (D’Argenio et al., 1973), as well as the possible existence of low-permeability Miocene inverse faults or thrusts dislocating the carbonate series (Cello and Mazzoli, 1998), it is supposed that such stratigraphic or structural factors (Celico, 1988) could be found below the depths reached by the drilling.

The main hydrogeological lateral boundaries of the Acqua della Madonna aquifer (Fig. 1b) are Pleistocene direct fault systems that mostly act as barriers to groundwater flow, thus determining lateral compartmentalization of the perched aquifer and the existence of a basin-in-series aquifer system (Petrella et al., 2009; Petrella et al., 2014). In such a hydrogeological framework, high altitude springs are generally located in association with faults with a lower permeability of core zones (Figs. 1b and 1d), although limited groundwater flow can occur through fault zones themselves and hydraulic exchanges among groundwater basins is possible (Fig. 1d). Altitudes of springs and water-table levels support the hypothesis that the groundwater flow occurs from north-west toward south-east (Figs. 1b and 1d), through a well-connected fracture network, feeding a seasonal spring (S1), with discharge up to 0.025 $m^3 s^{-1}$ and two perennial springs (S2 and S3) with discharge from 0.005 $m^3 s^{-1}$ to 0.15 $m^3 s^{-1}$. Moreover, water-table levels display several meters of fluctuation and a rapid response to recharge rainfall events and related infiltration process. The annual fluctuation of groundwater levels crosses the boundary between pyroclastic cover and fractured carbonate bedrock (Fig. 1c). The recharge of the perched karst aquifer, which generally occurs from September to May and, after major precipitation events, between December to April, is mostly driven by autogenic recharge, namely by diffuse net infiltration and percolation processes through the vadose zone.

The main physical and hydraulic properties of the perched karst aquifer (Table 1) were determined by field and laboratory tests (Allocca et al., 2008; Naclerio et al., 2009) while water-table levels were measured and monitored in the P1 borehole (60 m deep), whose hydrostratigraphic setting is characterized by 8.5 m of pyroclastic deposits and 51.5 m of calcareous rock-mass (Fig. 1c).

The study area belongs to a Mediterranean-mild climate (CSb) type (Geiger, 1954). On the basis of records of a regional meteorological network covering a period of 90 years (1920 - 2012) and their extrapolation to higher altitudes, the estimated mean annual rainfall for the Mount Terminio karst aquifer is 1.730 mm and the mean annual air temperature is 8.4 °C, whereas the estimated average annual groundwater recharge is 1.280 mm, equal to about 74% of the mean annual precipitation (Allocca et al., 2014).

Perched karstic aquifer	Aquifer layer	Soil texture type (%)			Saturated thickness (m)		Specific yield (%)	Hydraulic conductivity (m/s)
		Gravel	Sand	Silt	Min	Max		
	Pyroclastic deposits	5	86	9	0	4	5	$5,6\times10^{-5}$
	Fractured carbonate substrate				> 49	> 51,5	2	$4,7\times10^{-7}$

Table 1 – Some physical and hydraulic properties of the perched karst aquifer

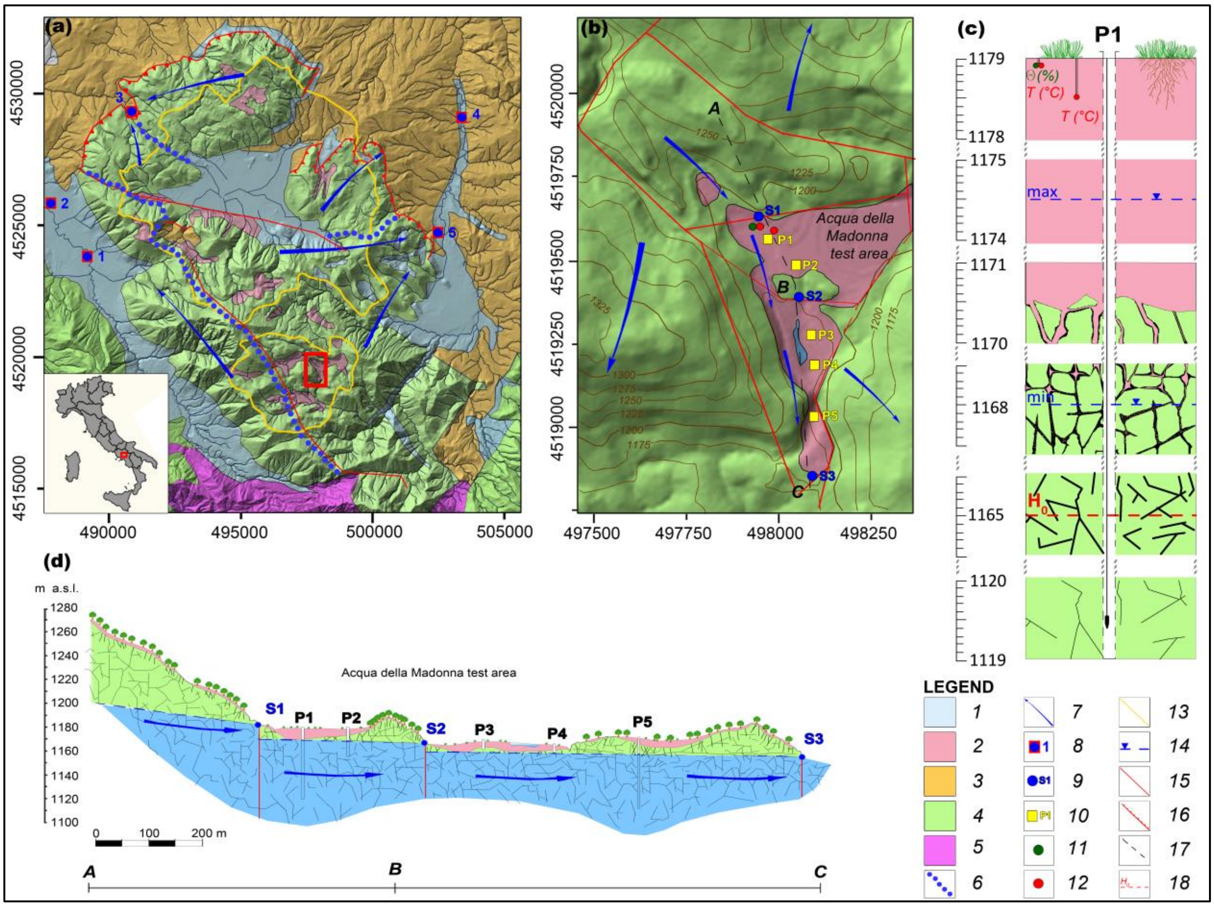

Figure 1. (**a**) Hydrogeological map of Terminio Mount karst aquifer. (**b**) Hydrogeological map of Acqua della Madonna perched aquifer. (**c**) Hydrostratigraphic scheme of P1 piezometer. (**d**) Hydrogeological section of Acqua della Madonna perched aquifer. Key to symbols: 1) Alluvial units (Quaternary); 2 Ash-fall units (Quaternary); 3) Terrigenous units (Cretaceous-Pliocene); 4) Limestone unit (Cretaceous); 5) Dolomitic unit (Trias); 6) Hydrogeological divide; 7) Main groundwater flow direction; 8) Basal springs [1) Acquaro-Pelosi spring, 376 m a.s.l.;2) Urciuoli spring, 330 m a.s.l.; 3) Sauceto spring, 465 m a.s.l.; 4) Baiardo spring, 470 m a.s.l.; 5) Cassano Irpino spring, 473 m a.s.l.]; 9) Perched springs [S1) Verteglia spring 1182 m a.s.l.; S2) Acqua della Madonna spring, 1168 m a.s.l.; S3) Giumenta spring, 1151 m a.s.l.] ; 10) Piezometers; 11) Soil water content sensor; 12) Soil temperature sensor; 13) Endorheic basin; 14) Water table level (min and max); 15) Thrust faults; 16) Faults; 17) Section profile.

3. Data and methodologies

3.1 Hydrological monitoring

In order to evaluate groundwater recharge episodes at local scale, daily thermo-pluviometric time series recorded by meteorological stations of the Regional Civil Protection Agency were collected from January to December 2008 (Fig. 2a). For the same period, hourly groundwater levels were measured in the P1 piezometer by a pressure head transducer (STS Inc., USA) provided with datalogger (Figs. 1b, 1c and 2a). In addition, hourly data of volumetric soil water content ($\theta=V_w/V_t$) were measured by a transducer provided with datalogger (SIAP-MICROS Inc., Italy) at a depth of 0.10 m (Figs. 1b, 1c and 2c). The chosen depth was considered representative of the upper portion of the unsaturated zone, which is mostly exposed to evapotranspiration processes due to the limited depth of roots of grassy vegetation.

3.2 Estimation of groundwater recharge at episodic and local scale

To assess groundwater recharge processes of the Acqua della Madonna aquifer at the episodic and local scales, we adopted the Episodic Master Recession (EMR) method (Nimmo et al., 2015), which is an advance of the Water Table Fluctuation (WTF) approach. The WTF technique is based on measurements of water-table heights (H), respect to a datum corresponding to the position of the water table in the absence of episodic recharge, and in the estimation of the related amount of groundwater replenished in the aquifer (Meinzer, 1923; Healy and Cook, 2002). It estimates the aquifer recharge by the following equation:

$$R_j = S_y \times \Delta H_j \qquad (1),$$

where: R_j (mm) is groundwater recharge of the j^{th} episode; S_y (%) is specific yield; ΔH_j (mm) is the maximum rise of water-table level for the j^{th} episode, given by the difference between the peak rise and the low point of extrapolated antecedent recession curve at the time of the peak.

The EMR method includes also the Master Recession Curve (MRC) technique (Heppner and Nimmo, 2005; Heppner et al., 2007; Delin et al., 2007), which is based on the following assumptions: a) there exists a characteristic functional correlation between decline rate of water-table (dH/dt) and respective heights in absence of recharge episodes; b) water-table fluctuations are caused only by natural groundwater recharge and discharge processes. In detail, the MRC method is based on an automated procedure that evaluates the rate of water-table level decline (dH/dt) as a function of (H) and, therefore, extrapolates the slope of water-table in absence of recharge. It has the advantage of taking into account the effect of unrealized recession by reconstructing the recessional limb after the onset of water-table rise, thus to assess the amount of water involved in the groundwater recharge for a single episode. The MRC algorithm first selects a subset of data from the original water-table level time series that represents a pure recessional limb, and uses it to develop an optimized master recession curve. The input data and respective formats required are: i) time (days); ii) precipitation (mm); iii) heights of water-table levels respect to an arbitrary datum (m); iv) storm recovery time value (days), which is the time between last precipitation event and the start of recession limb; v) mathematical form of the MRC, namely the equation that best fits the (dH/dt) versus (H) and simulates empirically the average behavior for water-table level recession at that site.

Specifically, the EMR method identifies discrete episodes of recharge based on water-table dynamics and precipitation records over a given period. The input data required by this method are: i) time unit (days); ii) heights of water-table levels with respect to a datum (m); iii) cumulative precipitation (m); iv) master recession curve type; v) specific yield (%) of saturated aquifer; vi) time lag, namely the time between a precipitation event and the associated recharge response; vii) fluctuation tolerance, corresponding to the measurement of the noise and indicating if a given fluctuation of (H) can be considered significant for the assessment of groundwater recharge at the episodic scale. The first step of the EMR technique is to identify the recharge episodes, defined as periods during which the observed water-table rate of change (dH/dt) exceeds water-table rate of change (dH/dT_{MRC}), predicted by the master recession curve, by an amount greater than the fluctuation tolerance (Fig. 3a). The initiation of a single recharge episode starts one lag time before dH/dt crosses the tolerance interval of the dH/dt_{MRC} curve. Similarly, the end a single recharge episode finishes one lag time before dH/dt re-entries within the tolerance interval of the dH/dt_{MRC} curve (Fig. 3a).

The rainfall event associated with a recharge episode begins one time lag before the start of the episode, and ends one time lag after the end of the episode (Fig. 3a). The recharge in a single episode is the product of the specific yield and the difference of two water-table heights (ΔH), respectively extrapolated by the recession limbs of the antecedent and the subsequent episodes at the time of the water-table peak (Fig. 3b). For each recharge episode, the EMR algorithm calculates start (t_o) and end (t_f) times (Figs. 3a and 3b), duration (D) and groundwater recharge (G_R). The RPR for each recharge episode is calculated by

$$RPR_j = \frac{G_{Rj}}{P_j} \qquad (2),$$

where: RPR_j (%) is the Recharge to Precipitation for the j^{th} recharge episode; G_{Rj} (mm) is the groundwater recharge for the j^{th} recharge episode; P (mm) is the precipitation for the j^{th} recharge episode.

To apply the MRC technique, water table levels measured from January to December 2008 were referred to a datum (H_0) lying at 1165 m a.s.l. (Figs. 1c). The aquifer response time was calculated by a cross-correlation analysis between precipitation and heights of water-table levels (Figs. 2a and 2b); the same approach was used to find the correlation between precipitation and θ (Figs. 2c and 2d). Finally, to assess the influence on groundwater recharge at the episodic time scale of other basic hydrological factors, which conceptually control processes of infiltration and percolation to water-table, a multiple regression analysis between the RPR coefficients, average intensity of the recharging rainfall events and antecedent soil water content status was performed. The antecedent soil water content was defined as the average soil water content (θ_{av}), measured at a depth of 0.10 m three days before the onset of the rainfall event.

3.3 Soil water balance

To understand more consistently hydrological processes occurring in the vadose zone and considering the available hydrological time series, we estimated potential evapotranspiration at the monthly time-scale by the Thornthwaite method (Thornthwaite, 1948):

$$Ep_i = K \times \left[1.6 \times \left(\frac{t_i}{I} \right)^{\alpha} \right] \tag{3}$$

where: Ep_i (mm) is the mean potential evapotranspiration for the i^{th} month; K is a dimensionless coefficient that depends on mean monthly hours of solar radiation, namely by the month of the year and latitude; t_i is the mean air temperature for the i month (°C); I is the annual heat index (adimensional); α is an exponent, given by:

$$\alpha = 675 \times 10^{-9} \times I^3 - 771 \times 10^{-7} \times I^2 + 1792 \times 10^{-5} \times I + 0.49239 \tag{4}$$

The monthly actual evapotranspiration (ETR_i) was calculated by the soil water balance method (Thornthwaite-Mather, 1955; 1957). Besides Ep_i, this method considers the monthly precipitation (P_i) and the total available water content ($\Delta\theta_{TAW}$) stored in the evapotranspiration zone, which corresponds to the difference between field capacity value (θ_{FWC}) and Permanent Wilting Point (θ_{PWP}). Typically, during humid season, soil water content in the evapotranspiration zone reaches the θ_{FWC} value, the stored amount of soil moisture available for the evapotranspiration is maximum ($\Delta\theta_{TAW}$) and ETR_i is equal to Ep_i. Under these conditions, when the soil water content exceeds the θ_{FWC} due to rainfall, monthly runoff (R_i) and net infiltration (I_{ei}) rise, and groundwater recharge occurs. Conversely, during months with rainfall amounts lower than Ep_i, ETR_i can equal Ep_i due to the loss of water content stored in the evapotranspiration zone in the antecedent month ($\theta_{i-1} - \theta_{PWP}$). Therefore, in the humid season, defined by:

$$P_i + (\theta_{i-1} - \theta_{PWP}) - Ep_i \geq 0 \qquad (5);$$

monthly groundwater recharge, or monthly effective infiltration (I_{ei}), is given by:

$$I_{ei} = [P_i + (\theta_{i-1} - \theta_{PWP}) - Ep_i] - R_i \qquad (6).$$

Finally, when soil moisture available for the evapotranspiration zone is completely lost ($\theta = \theta_{PWP}$), ETR_i is lower than Ep_i ($ETR_i < Ep_i$) and it corresponds to monthly rainfall (P_i). Consequently in the dry season, defined by:

$$P_i + (\theta_{i-1} - \theta_{PWP}) - Ep_i \leq 0 \qquad (7),$$

no monthly groundwater recharge episodes or runoff exist.

Owing to the flat and endorheic geomorphological features of the Acqua della Madonna test area, which permits negligible runoff toward the altimetrically lowest sector, monthly and annual amounts of water surplus estimated by soil water balance method, were considered, as an approximation, to contribute to groundwater recharge only.
θ_{FWC} and θ_{PWP} were respectively set equal to 36.9% and 11.0%, based on retention curves measured on undisturbed pyroclastic soil samples (De Vita et al., 2013). Therefore the $\Delta\theta_{TAW}$ value was equal to 26.0%. Knowing the maximum rooting depth (Fig. 1c) of local vegetation, equal to 0.60 m (Bucci et al., 2015a; Keller and Bliesner, 1990), it was possible to estimate the equivalent water height of $\Delta\theta_{TAW}$ as 156 mm.

4. Results

4.1 Aquifer response time

During 2008, water-table levels observed in the piezometer P1 and measured with respect to the considered datum (H_0=1165 m a.s.l.), varied between +3.2 m and +9.4 m, with an average value of +5.2 m (Fig. 2a). The maximum fluctuation range of the recorded water-table levels was about 6.20 m. The minimum water-table level was recorded on the 2nd of October 2008, at the end of a major recession period, which coincided with the summer season with very low rainfall events (2.4 mm in July 2008 and 6.2 mm in August 2008). The maximum value was detected at the beginning of December 2008.

During the recession periods, water-table levels were observed to decrease gradually (Fig. 2a) and to rise rapidly after rainfall events, with a velocity up to 0.92 m day^{-1}. A strong correlation between rainfall and water-table level time series was observed, therefore a clear and fast response of the aquifer was recognized. The maximum value of the correlation coefficient was found at a time lag of 2 days (Fig. 2b) (r = 0.53; t-Student < 0.1 %), which was considered as corresponding to the storm recovery time. In addition, the θ time series reflects the temporal pattern of daily precipitation (Fig. 2c), with highest value during the winter season (43.0%) and lower during the summer (10.0%). The temporal analysis (Fig. 2c) shows the existence of three phases with θ □omogeneous value of range: a first phase, from March to June, with a mean value of 20.0%; a second phase, corresponding to the summer season (July to September), with a mean value of 12.0%; a third phase, from October to December, with the highest mean value of 35.0%. A good cross-correlation between θ and rainfall time series was found (Fig. 2d) with a time lag of 0 (r = 0.535; prob. t-Student < 0.1 %).

Recharge occurs also under soil water content conditions lower than the θ_{FWC} value (Figs. 2a and 2c). This observation, which apparently contradicts what it is known for the soil water balance and groundwater recharge at the monthly time scale, could be explained by considering the existence of a heterogeneous pore size distribution at micro-scale that generates preferential micro-flow phenomena in the unsaturated zone (Mirus and Nimmo, 2013), even with soil water content drier than θ_{FWC}. This localized effective infiltration process can justify also the lack of instrumental records of increase in soil water content.

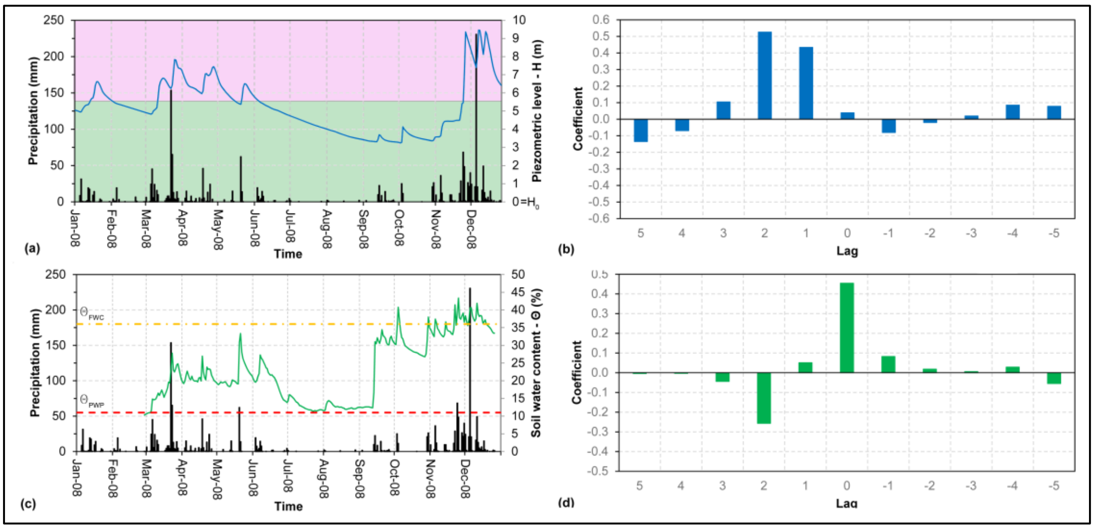

Figure 2. (**a**) Time series of piezometric level (blue line) and precipitation (black histogram). (**b**) Cross-correlation analysis between piezometric level and precipitation. (**c**) Time series of soil water content at 10 cm depth (green line) and precipitation (black histogram). (**d**) Cross-correlation analysis between soil water content at 10 cm depth and precipitation.

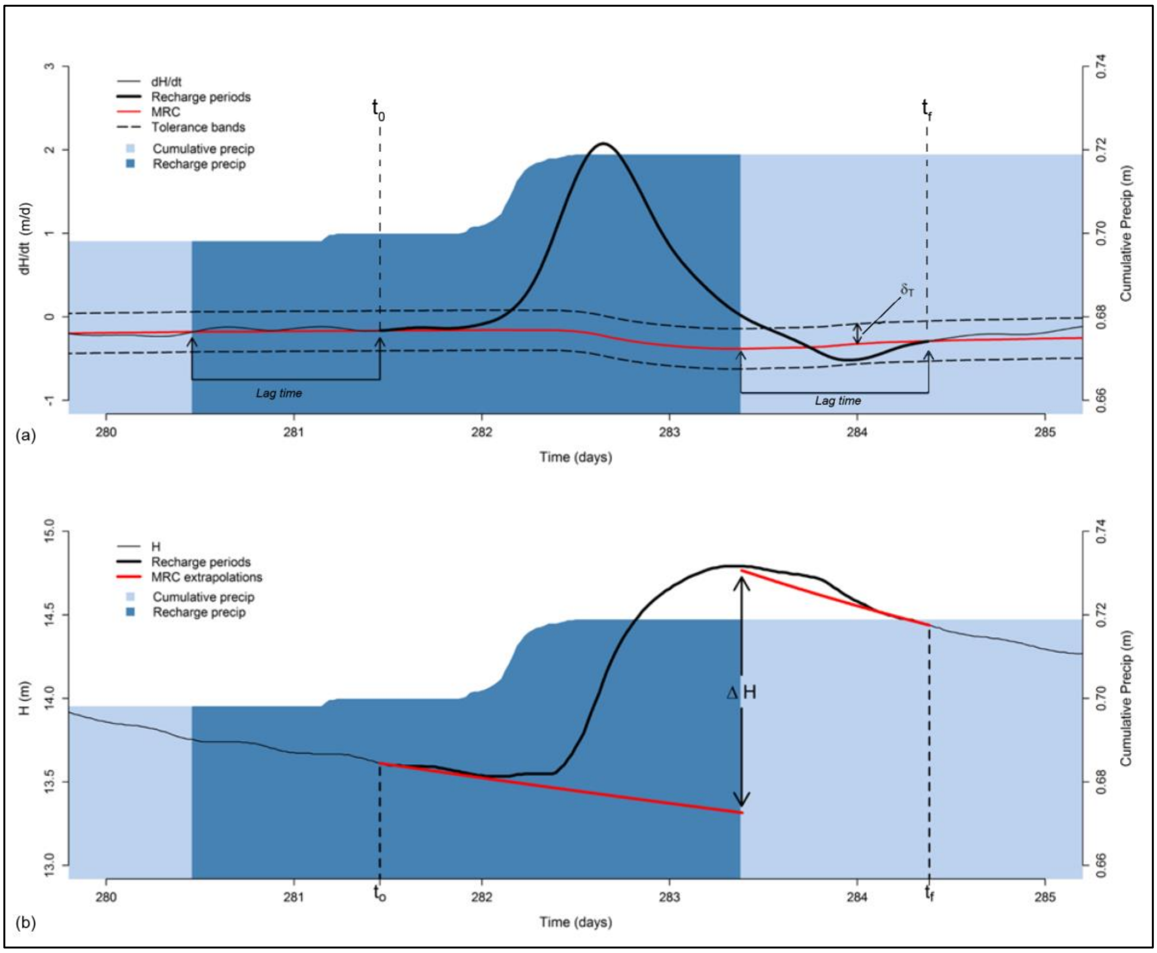

Figure 3. EMR method. (**a**) Detection of the recharge episodes based on dH/dt analysis. (**b**) Determination of the ΔH between the two MRC extrapolations.

4.2 Episodic groundwater recharge

The water-table level time-series recorded by the P1 piezometer in 2008 was analyzed by the MRC algorithm that identified automatically subsets corresponding to recessional limbs (Fig. 4a), namely all phases in which water-table levels decreased following a lack of precipitation (Fig. 4b) and due to groundwater drainage. The construction of the MRC as an empirical correlation between dH/dt and H (Fig. 5) was carried out by fitting recorded data by a third order polynomial equation ($r = 0.906$; prob t-Student < 0.1%). Considering changes in slope of the polynomial trend, it is possible to split the entire dataset into two parts with respect to whether the water-table height is above or below the interface between the pyroclastic soil cover and karst aquifer. For values of H lower than 5.4 m, water-table levels were considered to lie in the karst. For greater values of H, the saturation zone was recognized to include also a portion of the pyroclastic material. Given such a separation, decline rates of water-table levels (dH/dt) were found to vary from 0.00 to 0.05 m day^{-1} in the karst, and from 0.05 to 0.45 m day^{-1} in the pyroclastic interval (Fig. 5). This difference was related to a composite aquifer model characterized by two hydrostratigraphic layers with different geometry, thickness of saturation zone, specific yield and hydraulic conductivity (Figs. 1c and 1d, and Table 1). In detail, the pyroclastic aquifer, besides the higher value of specific yield, has a reduced thickness of the saturation zone and a higher hydraulic conductivity, compared to the underlying karst aquifer. These features may determine the greater recession rate of water-table levels in the pyroclastic interval.

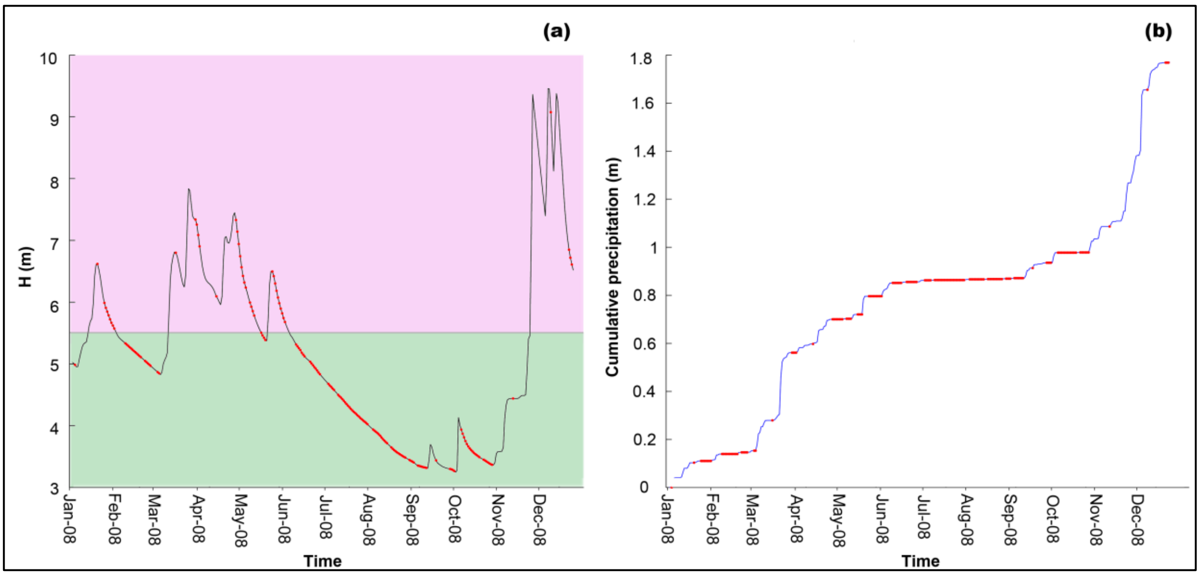

Figure 4. (**a**) Time series of piezometric level (H level referred to H_0=1165 m a.s.l.) with pure recessional data (red points). (**b**) Cumulative precipitation and pure recessional data (red points). The background color represent the fractured carbonate substrate (green) and pyroclastic deposits (pink).

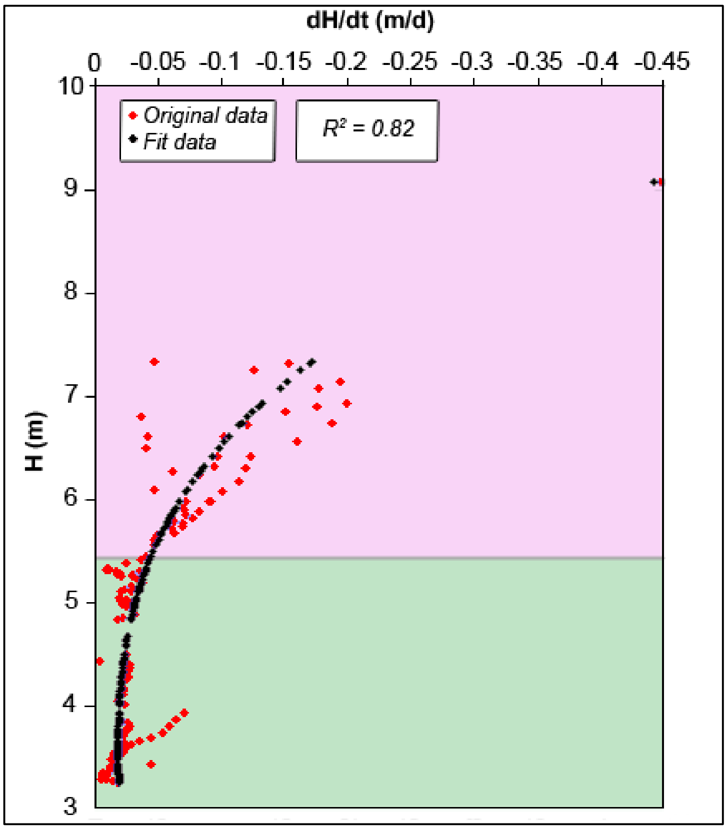

Figure 5. Master Recession Curve (MRC) for P1 piezometer. Red points represent the pure recession data (Fig. 4); black points are the points forming the Master Recession Curve. The background color represent the fractured carbonate substrate (green) and pyroclastic deposits (pink).

The analysis of water-table levels time series recognized 12 recharge episodes (Figs. 6 and 7). Duration of the recharge periods ranged from 5 to 37 days, with a mean value of 12 days, whereas the length of non-recharge periods varied from 0 to 107 days, corresponding chiefly to the summer season. The first nine recharge episodes showed a low range of water-table fluctuation rate (dH/dt), from 0.25 to 0.60 m day^{-1}, while episodes 10, 11 and 12 showed a greater variability in the fluctuation rate, and, among them, the episode 10 had the highest value (about 2 m day^{-1}).

Values of RPR, calculated by the EMR method and the application of Eq. 2, range from 35% to 97%, with a mean annual value of 73% (Table 2 and Fig. 8).

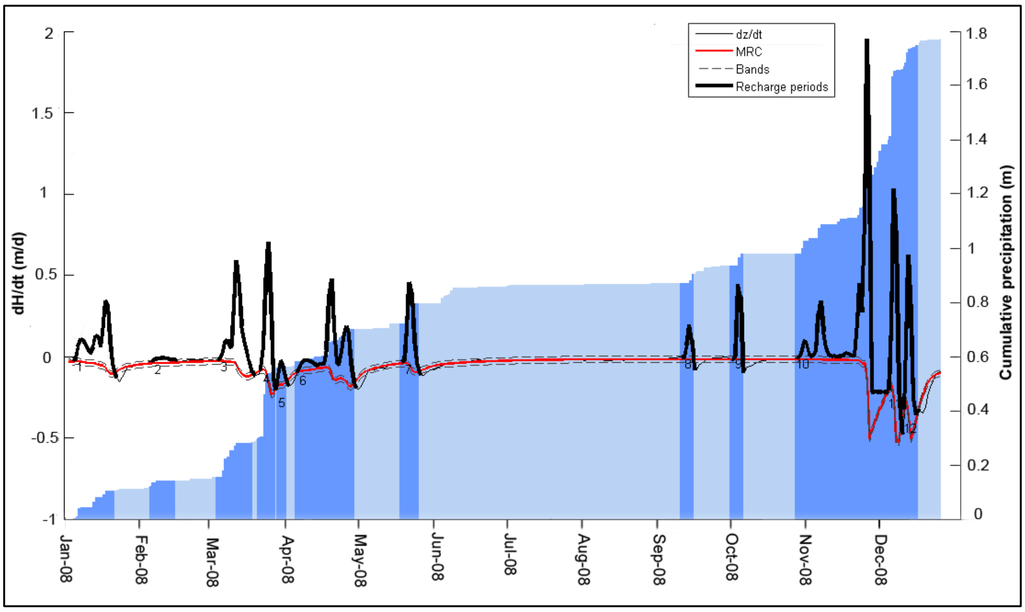

Figure 6. Episodic Master Recession analysis of dH/dt versus time. The numbers represent the recharge episodes.

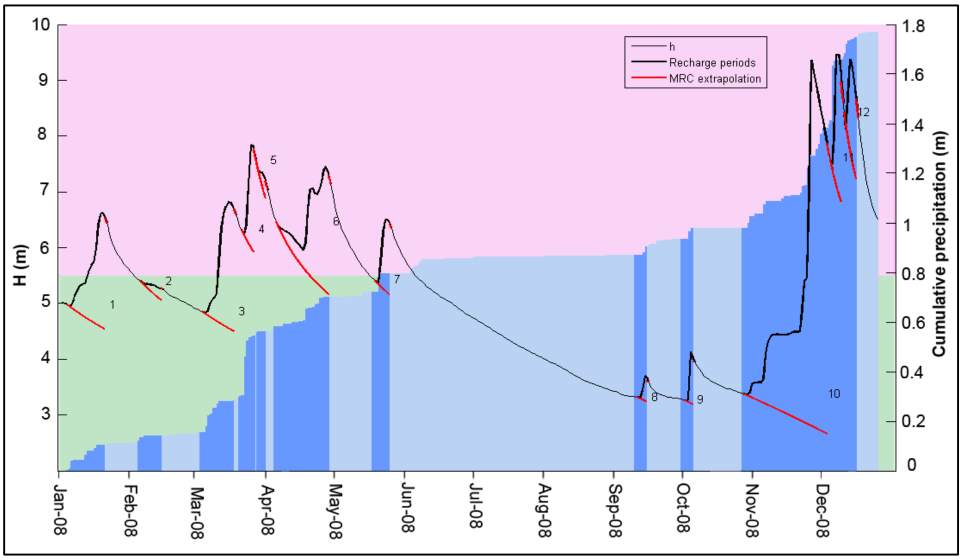

Figure 7. Episodic Master Recession analysis of H versus time. The background color represent the fractured carbonate substrate (green) and pyroclastic deposits (pink), and the numbers the recharge episodes.

Recharge episodes	Start time t_i (day)	End time t_f (day)	Duration D (day)	Groundwater Recharge G_R (m)	Precipitation P (m)	Recharge to Precipitation ratio RPR (%)	Av. storm intensity i (m/day)	Max storm intensity i_{max} (mm/day)	Average soil water content (Θav) (%)
1	4	22	18	0.1	0.104	97	0.006	31.4	-
2	36	46	10	0.011	0.019	59	0.002	19.2	-
3	63	78	15	0.11	0.129	86	0.009	45.2	-
4	81	87	6	0.093	0.247	37	0.038	153.6	23.49
5	87	92	5	0.014	0.017	87	0.003	4.6	24.16
6	96	120	24	0.107	0.12	89	0.005	46	20.45
7	139	147	8	0.064	0.076	84	0.01	62	27.78
8	254	260	5	0.019	0.033	57	0.006	22.4	12.42
9	275	280	5	0.039	0.042	92	0.008	25	30.51
10	301	339	37	0.261	0.404	65	0.011	68.4	34.01
11	339	345	6	0.107	0.272	39	0.046	230.6	39.45
12	345	352	6	0.072	0.089	81	0.014	49.2	39.42

Table 2 – Characteristics of the recharge episodes

This result was compared to that of an independent method, by carrying out a monthly soil water balance for 2008 by the Thornthwaite-Mather (1955; 1957) method. At monthly time-scale, from January to July and from September to December, actual evapotranspiration (ETR_i) was always a maximum, equal to the potential evapotranspiration (Ep_i). Therefore, in these months there existed a soil water surplus which allowed groundwater recharge (Fig. 8). Conversely, ETR_i of August was less than Ep_i, and therefore there occurred a condition of soil water deficit (Fig. 8), apparently with no possibility of groundwater recharge episodes.

At the annual scale, potential evapotranspiration (Ep) totaled about 591.6 mm, thus corresponding to 33% of P, whereas actual evapotranspiration (ETR) amounted totally to 542.8 mm, corresponding to 30% of P.

Parameters	Jan	Feb	Mar	Apr	May	Jun	Jul	Aug	Sep	Oct	Nov	Dec	Tot
Air T (°C)	5.9	5.0	7.4	9.8	15.4	18.9	21.2	22.7	15.9	13.6	9.2	4.9	
Heat index (I)	1.3	1.0	1.8	2.8	5.5	7.5	8.9	9.9	5.8	4.5	2.5	1.0	52.4
Ep_i' (mm)	20.9	17.7	26.3	35.1	55.1	67.5	75.8	81.0	56.9	48.6	32.9	17.6	535.4
Adjustment factor	0.8	0.8	1.0	1.1	1.3	1.3	1.3	1.2	1.0	1.0	0.8	0.8	
Ep_i (mm)	17.4	14.7	27.1	39	68.8	85.0	96.3	96.4	59.2	46.6	27.0	14.1	591.6
P_i (mm)	110.2	36.6	414.6	138.2	96.2	65.0	2.4	6.2	65.6	84.2	330.8	429.8	1779.8
Δ_i (mm)	92.8	21.9	387.5	99.2	27.4	-20.0	-93.9	-90.2	6.4	37.6	303.8	415.7	1188.2
A_i (mm)	155.4	155.4	155.4	155.4	155.4	135.4	41.4	0.0	6.4	44.0	155.4	155.4	1315.0
ΔAi (mm)	0.0	0.0	0.0	0.0	0.0	-20.0	-93.9	-41.4	6.4	37.6	111.4	0.0	0.0
ETR_i (mm)	17.4	14.7	27.1	39.0	68.8	85.0	96.3	47.6	59.2	46.6	27.0	14.1	542.8
S_i (mm)	92.8	21.9	387.5	99.2	27.4	0.0	0.0	0.0	0.0	0.0	192.4	415.7	1237.0
D_i (mm)	0.0	0.0	0.0	0.0	0.0	0.0	0.0	48.8	0.0	0.0	0.0	0.0	48.8

Table 3 – Results of the Thornthwaite and Mather water balance. Key to symbols: Epi' = unadjusted potential evapotranspiration for the ith month; Epi' = adjusted potential evapotranspiration for the ith month; Pi = precipitation for the ith month; Δi = precipitation minus potential evapotranspiration for the ith month; Ai = soil storage for the ith month; ΔAi= change in soil storage for the ith month; ETRi= actual evapotranspiration for the ith month; Si= water surplus for the ith month; Di= water deficit for the ith month.

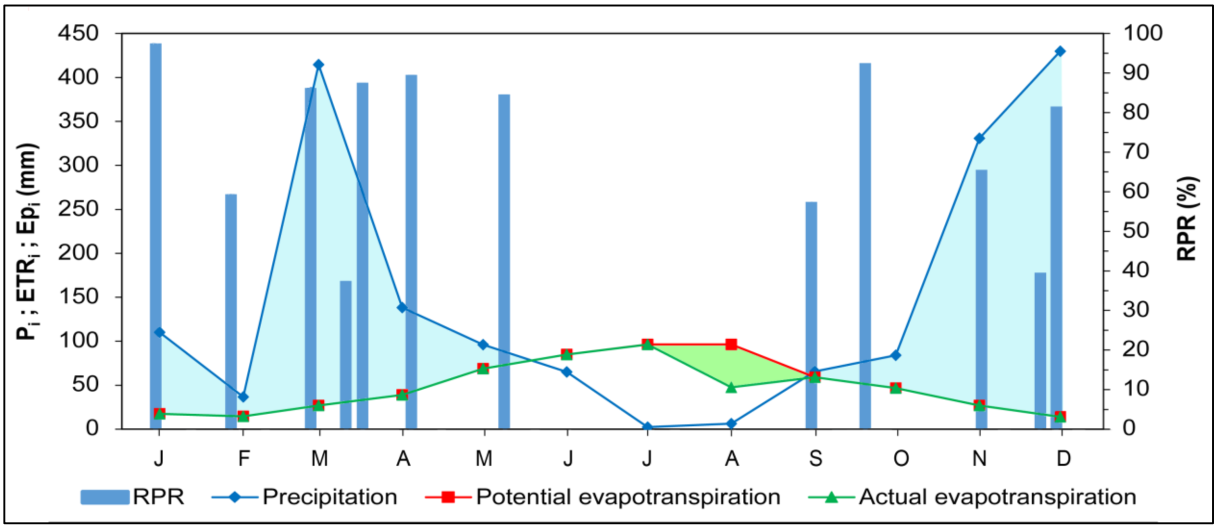

Figure 8. Monthly soil water balance carried out for 2008 by the Thorthwaite and Mather method (1955; 1957). Blue histogram represents groundwater recharge episodes and related values of RPR coefficients.

4.3 Dependence of RPR on soil water content and rainfall intensity

The comparison of groundwater recharge dynamics (Table 2) with rainfall patterns and seasonality allowed hypothesizing a dependence of RPR values based on rainstorm intensity and antecedent soil water content. For instance, the two lowest RPR values calculated for the episode 4 and the episode 11, respectively equal to 37% and 39%, corresponded to the highest rainfall intensities, respectively 0.038 m day^{-1} and 0.046 m day^{-1}. Moreover, the observation of groundwater recharge episodes (Figs. 7 and 8) allowed identifying a direct relationship between antecedent soil water content and RPR coefficients, which might associate lower RPR values with lower soil water content. For example, recharge episode 8, in September 2008, was characterized by a modest RPR value, 57%, notwithstanding the low rainfall intensity of about 0.006 m day^{-1}. This observation suggested a possible influence during this period of the soil water deficit on episodic groundwater recharge, due to the loss of soil water content by evapotranspiration that occurred during the summer dry season. Subsequently, by analyzing RPR values, average intensity of rainfall recharging events (i) and average soil water content (θ_{av}) estimated for the 12 recharge episodes (Table 2), we found a multiple linear regression (Fig. 9) between the RPR, our dependent variable, and the other two independent variables (r = 0.894; prob. t-Student < 0.1%):

$$\mathrm{RPR}(\%) = 0.67 + 0.8 \cdot \theta_{av} - 13.41 \cdot i \qquad (7).$$

This empirical equation is to be expected to be valid in the ranges of the observed variables (Table 2): 37% $\leq$ RPR $\leq$ 97%; 10.0% $\leq \theta_{av} \leq$ 43.0%; 0.001 m day$^{-1} \leq i \leq$ 0.046 m day^{-1}. Its form confirms the opposite role played by both independent variables (θ_{av} and i) and the greater sensitivity of the RPR coefficient to average intensity of rainfall recharging events (i) than to average soil water content (θ_{av}). The latter is demonstrated by the variability of the RPR coefficient (about 26%), given the recorded extreme values of θ_{av} and the same value of i, and its variability (about 60%), considering the recorded extreme values of i and the same value of θ_{av}.

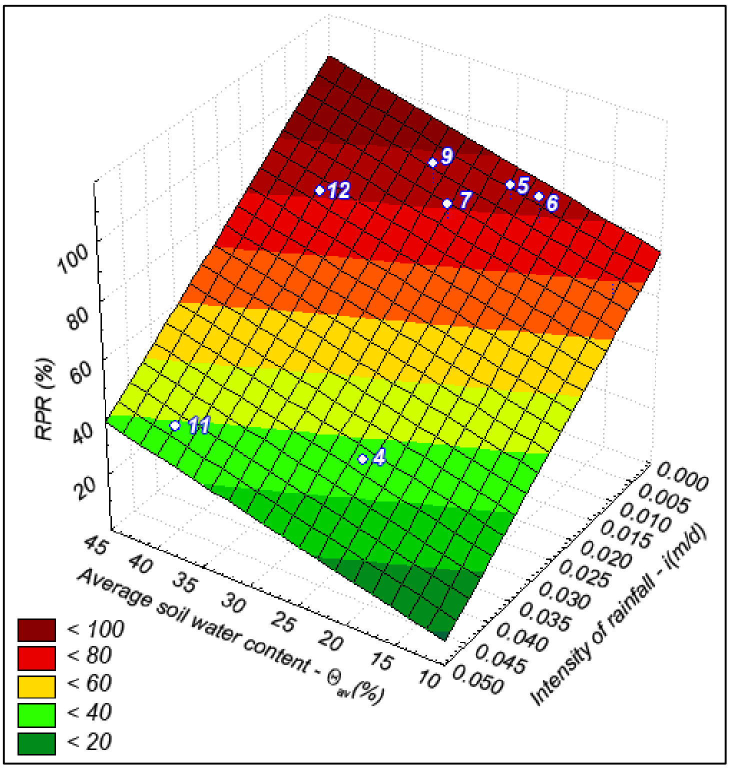

Figure 9. Multiple linear regression between RPR coefficient, antecedent average soil water content (θ_{av}) and average intensity of recharging rainfall events. The colors represent the RPR values and the numbers the recharge episodes.

5. Discussion

The application of the Episodic Master Recession (EMR) method (Nimmo et al., 2015), for estimating the RPR is tested in this research as a reliable tool to assess, at local and episodic scales, groundwater recharge in a perched karst aquifer of the southern Italy covered by ash-fall pyroclastic soil deposits. The existence of a soil cover is a fundamental factor that control groundwater recharge processes by permitting water losses due to evapotranspiration, therefore the studied case is referred to a specific condition of a soil mantled karst aquifer which is very common for karst aquifers of southern Italy as well as in other areas of the world.

In the period that we analyzed, which crossed all seasons and hydrological conditions of 2008, values of RPR varied from 37% to 97%, with a mean value of 73% (Table 2 and Fig. 8). The portion of precipitation that does not become recharge can be attributed to water losses due to both evapotranspiration and a slight runoff process toward the altimetrically lowest sector of the Acqua della Madonna test area. Nonetheless, due to endorheic morphological feature of this area, runoff is constrained to infiltrate and thus can be considered negligible in the monthly and annual water balance equation. This assumption allows considering, at the annual scale, water losses due to evapotranspiration as correspondent to the complement of the mean value of the RPR coefficient (27%). This value is closely comparable to that estimated independently by the Thorthwaite-Mather (1955; 1957) method, equal to about 30% at the annual scale (Table 3). This similarity of values provides good confirmation of both approaches.

At the episodic time scale, lower RPR coefficient values correspond generally to heavy rainstorm intensity episodes (i.e. episodes 4 and 11 in Table 2), and show a seasonal effect during summer, when the potential evapotranspiration is highest and soil water content stored into the evapotranspiration zone is lower that the θ_{FWC} (i.e. episodes 8 and 10 in Table 2). Conversely, highest RPR values occur during winter, when evapotranspiration is relatively low and soil water content stored into the evapotranspiration zone corresponds closely to θ_{FWC}. The effect of antecedent soil water content in the evapotranspiration zone on RPR values is also evident in some non-recharge period (Figs. 2a, 4a and 7), during which rainfall events with no recharge episodes were observed.

Given this phenomenological framework, we found new insights regarding groundwater recharge at locale and episodic scales by a multiple linear correlation between values of RPR and the average intensity of rainfall recharging events (i) and average antecedent soil water content (θ_{av}). In detail, at the episodic time scale, the influence of θ_{av} on value of RPR coefficient is conceptually related to effects of different amounts of water to be added to the evapotranspiration zone, given different values of initial θ_{av}. Nevertheless, it appears interesting the coincidence of the variability induced on RPR coefficient (26%) by the recorded extreme values of θ_{av} ($10.0\% \leq \theta_{av} \leq 43.0\%$) with the total available water content ($\Delta\theta_{TAW} = 26\%$). This correspondence was attributed to the fact that the extreme values of soil water content recorded at a depth of 0.1 m represent a proxy of soil moisture conditions of the whole evapotranspiration zone, which correspond to θ_{FWC} and θ_{PWP}, respectively.

In addition, the influence of average intensity of rainfall recharging events (i) was attributed to the formation of ponding and runoff flowing toward the altimetrically lowest sector of the Acqua della Madonna test area.

Finally, the results give further insights regarding the limits and approximations associated with the assessment of groundwater recharge by the monthly soil water balance or by the EMR technique. In this regard, assumming negligible runoff, monthly and annual amounts of groundwater recharge show a good match for both approaches.

6. Conclusions

The obtained results represent progress in the application and validation of the Episodic Master Recession (EMR) method to a new hydrogeological framework represented by a heterogeneous perched karst aquifer of southern Italy, in addition to the few cases of aquifers with homogeneous hydraulic properties, which were considered until now (Nimmo et al., 2015). Therefore, the EMR method can be conceived as a valid tool for quantifying the recharge process at the local and episodic scales, applicable in other Mediterranean karst areas wherever water-table level time series are available. Further insights were discovered at the episodic time scale concerning the dependence of RPR on basic hydrological parameters that control groundwater recharge. Therefore, the prediction of the groundwater recharge, knowing basic hydrological data, like precipitation and soil water content, may be used as a powerful tool for an equitable-sustainable management of karst systems and protection of groundwater-dependent ecosystems, in the current context of the climate change and increasing demand of drinking water in various areas of the world. These findings, which would be further developed by empirical or numerical approaches, could advance the assessment of groundwater recharge at episodic time scale also considering the possibility of artificial groundwater recharge.

Acknowledgements

This work was supported by the personnel short mobility and the doctorate programs of the University of Naples Federico II that funded scientific collaboration with the Unsaturated Zone Interest Group (UZIG) of the US Geological Survey.

References

Allocca V., Celico F., Petrella E., Marzullo G., and Naclerio G.: The role of land use and environmental factors on microbial pollution of mountainous limestone aquifers, Environ Geol, 55, 277-283, 2008.

Allocca, V., Celico, F., Celico, P., De Vita, P., Fabbrocino, S., Mattia, S., Monacelli, G., Musilli, I., Piscopo, V., Scalise, A. R., Summa, G., and Tranfaglia, G.: Illustrative Notes of the Hydrogeological Map of Southern Italy, Istituto Poligrafico e Zecca dello Stato, Rome, 1–211, ISBN 88-448-0223-6, 2007a.

Allocca, V., De Vita, P., Fabbrocino, S., and Celico, P.: The karst aquifers of the southern Apennines (Italy): a strategic groundwater resource, Memorie Istituto Italiano di Speleologia, 2, 19, 65–72, 2007b.

Allocca, V., Manna F., and De Vita, P.: Estimating annual groundwater recharge coefficient for karst aquifers of the southern Apennines (Italy), Hydrol. Earth Syst. Sci., 18, 803–817, 2014.

Andreo, B., Vías, J., Durán, J.J., Jiménez, P., López-Geta, J.A., and Carrasco, F.: Methodology for groundwater recharge assessment in carbonate aquifers: application to pilot sites in southern Spain, Hydrogeology Journal, 16, 911–925, 2008.

Boni, C.F., Bono, P., and Capelli, G.: Schema Idrogeologico dell’Italia Centrale (scala 1:500.000), Mem. Soc. Geol. It. , 35, 2, 991-1012, 1986.

Bucci, A., Allocca, V., Naclerio, G., Capobianco, G., Divino F., Fiorillo, F. and Celico, F.: Winter survival of microbial contaminants in soil: An in situ verification, Journal of Environmental Sciences, 27, 131-138, 2015a.

Bucci, A., Petrella, E., Naclerio, G., Allocca, V., and Celico, F.: Microorganisms as contaminants and natural tracers: a 10-year research in some carbonate aquifers (southern Italy), Environ Earth Sci, DOI 10.1007/s12665-015-4043-1, 2015b.

Celico, F., Celico, P., De Vita, P., and Piscopo, V.: Groundwater flow and protection in the Southern Apennines (Italy). Hydrogeology, 4, 39-47, 2000.

Celico, F., Naclerio, G., Bucci, A., Nerone, V., Capuano, P., Carcione, M., Allocca, V. and Celico, P.: Influence of pyroclastic soil on epikarst formation: a test study in southern Italy, Terra Nova, 22, 110–115, 2010.

Celico, P.: Falda in rete sospese nel massiccio carbonatico del monte Terminio (Campania) ed implicazioni idrogeologiche. L’Appennino Meridionale, 1, 99-112, 1988.

Celico, P.: Idrogeologia dei massicci carbonatici, delle piane quaternarie e delle aree vulcaniche dell'Italia centromeridionale (Marche e Lazio meridionale, Abruzzo, Molise e Campania), Quaderni della Cassa per il Mezzogiorno, 4/2, 1–203, 1983.

Celico, P.: Schema idrogeologico dell'Appennino carbonatico centro-meridionale. Mem. Note Ist. Geol. Appl., Napoli, 14, 1-97, 1978.

Cello, G. and Mazzoli, S.: Apennine tectonics in southern Italy: a review. Journal of Geodynamics, 27, 191-211, 1998.

Coes, A., Spruill, T., and Thomasson, M.: Multiple-method estimation of recharge rates at diverse locations in the North Carolina Coastal Plain, USA, Hydrogeology Journal, 5, Issue 4, 773-788, 2007.

D'Argenio, B., Pescatore, T. and Scandone, P.: Schema geologico dell'appennino meridionale (Campania, Lucania). Atti del Convegno: Moderne vedute sulla geologia dell'appennino. Accademia Nazionale dei Lincei, 183, 49-72, 1973.

De Vita, P., Allocca, V., Manna, F., and Fabbrocino, S.: Coupled decadal variability of the North Atlantic Oscillation, regional rainfall and karst spring discharges in the Campania region (southern Italy), Hydrology and Earth System Sciences, 16, 1389–1399, 2012.

De Vita, P., Napolitano, E., Godt, J.W. and Baum, R.L.: Deterministic estimation of hydrological thresholds for shallow landslide initiation and slope stability models: case study from the Somma-Vesuvius area of southern Italy. Landslides, 10, 713–728, 2013.

Delin, G., Healy, R., Lorenz, D., and Nimmo, J.: Comparison of local- to regional-scale estimates of ground-water recharge in Minnesota, USA: Journal of Hydrology, 334, 1-2, 231-249, 2007.

Fiorillo, F., Pagnozzi, M., Ventafridda, G.: A model to simulate recharge processes of karst massifs. Hydrological Processes DOI: 10.1002/hyp.10353, 2014.

Ford, D., Williams, P.: Karst hydrogeology and geomorphology. Wiley J. & Sons, Ltd, 1-576, ISBN 978-0-470-84996-5, 2007.

Geiger, R.: Landolt-Börnstein-Zahlenwerte und Funktionen aus Physik, Chemie, Astronomie, Geophysik und Technik, alte Serie Vol. 3, in: Klassifikation der Klimate nach W. Köppen, Springer, Berlin, 603–607, 1954.

Guardiola-Albert, C., Martos-Rosillo, S., Pardo-Igúzquiza, E., Durán Valsero, J. J., Pedrera, A., Jiménez-Gavilán, P. and Liñán Baena, C.: Comparison of Recharge Estimation Methods During a Wet Period in a Karst Aquifer. Groundwater. doi: 10.1111/gwat.12310, 2014.

Hartmann, A., Gleeson, T., Rosolem, R., Pianosi, F., Wada, Y., and Wagener, T.: A simulation model to assess groundwater recharge over Europe's karst regions. Geoscientific Model Development Discuss., 7, 7887–7935, 2014b.

Hartmann, A., Goldscheider, N., Wagener, T., Lange, J., and Weiler M.: Karst water resources in a changing world: Review of hydrological modeling approaches. Reviews of Geophysics, 52, 3, 218-242, 2014a.

Healy, R.W. and Cook, P.G.: Using groundwater levels to estimate recharge. Hydrogeology Journal, 10, 91–109, 2002.

Healy, R.W.: Estimating Groundwater Recharge. Cambridge University Press, 256 pp., ISBN 978-0-521-86396-4, 2010.

Heppner, C., and Nimmo, J.: A computer program for predicting recharge with a master recession curve: U.S. Geological Survey Scientific Investigations Report 2005-5172, 1-8, 2005.

Heppner, C.S., Nimmo, J.R., Folmar, G.J., Gburek, W.J., and Risser D.W.: Multiple-Methods Investigation of Recharge at a Humid-Region Fractured Rock Site, Pennsylvania, USA. Hydrogeology Journal, 15, 5: 915-927, 2007.

Keller, J. and Bliesner, R.D.: Sprinkle and Trickle Irrigation van Nostrand Reinhold., New York, NY. 1-652, 1990.

Lerner, D.N., Issar, A.S. and Simmers, I.: Groundwater recharge, a guide to understanding and estimating natural recharge. International Association of Hydrogeologists, Kenilworth, Rep. 8, 354 pp., ISSN 0936-3912, 1990.

Manna, F., Allocca, V., De Vita, P., Fusco, F. and Napolitano, E.: Groundwater recharge assessment in karst aquifers of southern Apennines (Italy). Rendiconti Online Società Geologica Italiana, 24, 202-204, 2013a.

Manna, F., Allocca, V., Fusco, F., Napolitano, E. and De Vita, P.: Effect of the North Atlantic Oscillation on groundwater recharge in karst aquifers of the Cilento Geopark (Italy). Rendiconti Online Società Geologica Italiana, 28, 106-109, 2013b.

Meinzer, O.E.: The occurrence of groundwater in the United States with a discussion of principles. U.S. Geological Survey Water- Supply Paper, 489, 1-321, 1923.

Mirus, B.B. and Nimmo, J.R.: Balancing practicality and hydrologic realism: A parsimonious approach for simulating rapid groundwater recharge via unsaturated-zone preferential flow. Water Resources Research, 49, 1458–1465, 2013.

Naclerio, G., Nerone, V., Bucci, A., Allocca, V., and Celico F.: Role of organic matter and clay fraction on migration of Escherichia coli cells through pyroclastic soils, southern Italy. Colloids and Surfaces B: Biointerfaces, 72, 57-61, 2009.

Naclerio, G., Petrella, E., Nerone, V., Allocca, V., De Vita, P. and Celico, F.: Influence of topsoil of pyroclastic origin on microbial contamination of groundwater in fractured carbonate aquifers. Hydrogeology Journal, 16: 1057–1064, 2008.

Nimmo, J.R., Horowitz, C., and Mitchell, L.: Discrete-Storm Water-Table Fluctuation Method to Estimate Episodic Recharge. Groundwater, 53, 282-292, 2015.

Petrella, E., Aquino, D., Fiorillo, F., and Celico, F.: The effect of low-permeability fault zones on groundwater flow in a compartmentalized system. Experimental evidence from a carbonate aquifer (Southern Italy). Hydrological Processes, 2014, Published online, DOI: 10.1002/hyp.10294

Petrella, E., Capuano, P., and Celico, F.: Unusual behaviour of epikarst in the Acqua dei Faggi carbonate aquifer (Southern Italy). Terra Nova, 19, 82–88, 2007.

Petrella, E., Capuano, P., Carcione, M., and Celico, F.: A high-altitude temporary spring in a compartmentalized carbonate aquifer: the role of low-permeability faults and karst conduits. Hydrological Processes 23, 3354–3364, 2009.

Risser, D., Gburek, W. and Folmar, G.: Comparison of methods for estimating ground-water recharge and base flow at a small watershed underlain by fractured bedrock in the eastern United States: U.S. Geological Survey Scientific Investigations Report, 2005-5038, 31, 2005.

Rutledge, A.T.: Computer Programs for Describing the Recession of Ground-Water Discharge and for Estimating Mean Ground-Water Recharge and Discharge from Streamflow Data–Update, Water-Resources Investigations Report 98–4148, US Geological Survey, 1998.

Scanlon, B.R., Keese, K.E., Flint, A.L., Flint, L.E., Gaye, C.B., Edmunds, W.M. and Simmers, I.: Global synthesis of groundwater recharge in semiarid and arid regions. Hydrological Processes, 20, 3335–3370, 2006.

- Stephens, D.B.: Vadose Zone Hydrology. CRC Press, 339 pp., ISBN-10: 0873714326, 1995.

Thornthwaite, C.W., 1948.: An Approach toward a Rational Classification of Climate. Geographical Review, 38, 55-94.

Thornthwaite, C.W., and Mather J.R.: The Water Balance. Publ. Climatol., 8 (1): 1-104, Drexel Institute of Climatology, Centerton, New Jersey, 1955.

Thornthwaite, C.W. and Mather, J.R.: Instructions and tables for computing potential evapotranspiration and the water balance. Publ. Climatol., 10 (3):1-311, 1957.

Todd D.K.: Groundwater Hydrology, 3rd edn. Wiley J., New York, 1-665535, ISBN 0-471-87616-X, 20051980.

VV.AA.: Regional Climate Projections, in Climate Change. Cap. 11 in “Climate Change 2007: The Physical Science Basis”. Contribution of Working Group I to the Fourth Assessment Report of the Intergovernmental Panel on Climate Change Solomon, S., D. Qin, M. Manning, Z. Chen, M. Marquis, K.B. Averyt, M. Tignor and H.L. Miller (eds.). Cambridge University Press, Cambridge, United Kingdom and New York, NY, USA, 996 pp.

Wada, Y., van Beek, L.P.H., van Kempen, C.M., Reckman, J.W.T.M., Vasak, S. and Bierkens M.F.P.: Global depletion of groundwater resources, Geophysical Research Letters, 37, 1-5, L20402, 2010.

V Congresso Nazionale AIGA

Cagliari, 29-30 Aprile 2015

Rend. Online Soc. Geol. It., Vol. XX (2013), pp. XX-XX, 1 fig., x pl., x tab.

Recharge in karst aquifers: from regional to local and annual to episodic scale

Ferdinando Manna ([a]), John R. Nimmo ([b]), Vincenzo Allocca ([a]) & Pantaleone De Vita ([a])

([a]) Department of Earth Science, Environment and Resources - University of Naples Federico II. E-mail: ferdinando.manna@unina.it

([b]) United States Geological Survey – Menlo Park (CA)

Document type: Short note.
Manuscript history: received 21 March 2013; accepted 25 April 2013; editorial responsibility and handling by Domenico Calcaterra.

ABSTRACT

The assessment of groundwater recharge for karst aquifers of southern Italy is a major scientific task due to the relevant socio-economic and environmental role of the related groundwater resources. In this paper, the results of two methods, applied at different spatial and time scales, are reported.

At regional and mean annual scales, through a multidisciplinary approach, the mean Annual Groudwater Recharge Coefficient (AGRC) was estimated for four sample karst aquifers, with available long-lasting spring discharge time series. Such estimations were extended to other karst aquifers of southern Italy by means of an empirical law that was found linking the AGRC to percentages of outcropping lithologies and endorheic/summit plateau areas.

At local and episodic scales, the groundwater recharge of a test perched karst aquifer, belonging to the Mount Terminio hydrogeological structure (Campania region, southern Italy) was estimated. For such a purpose, an improvement of the Water Table Fluctuation (WTF) method, known as Episodic Master Recession (EMR), was applied to estimate the Recharge to Precipitation Ratio (RPR) coefficient, which represents the amount of precipitation recharging groundwater.

Results obtained through the first approach furnished AGRC values varying between 50% and 79% and well matching with estimations of infiltration coefficients known in literature for other karst aquifers of Europe. Moreover, the mean value of RPR determined for the local karst aquifer (73%) resulted well matching with the AGRC estimated for the whole Mount Terminio karst aquifer (79%).

By the comparison of these outcomes, at the regional and mean annual scales, the groundwater recharge of karst aquifers was found as mainly controlled by both the extension of outcropping lithologies and endorheic/summit plateau zones. While at the local and episodic scales, the groundwater recharge was recognized as chiefly influenced by the rainfall intensity and soil hydrological condition.

KEY WORDS: Groundwater recharge, karst aquifer, Water Table Fluctuation.

INTRODUCTION

The assessment of the aquifer recharge has a key role in several hydrologic and hydrogeological fields: from the management of the water resources to the study of vulnerability and contamination. Groundwater recharge is defined as the water that moves from the land surface or unsaturated zone into the saturated zone (NIMMO *et alii*, 2005). This definition excludes flow coming from adjoining aquifers and include three main mechanisms of recharge (ANDREO *et alii*, 2008): a) direct recharge by percolation through the unsaturated zone; b) indirect recharge through the beds of continental water bodies (rivers and lakes); c) localized or concentrated recharge at specific points (e.g. dolines and karst conduits).

A correct estimation of this amount is difficult because it is controlled by several factors, which are very variable at different spatial and temporal scales of observation: soil type, land use, lithology, slope angle, altitude, geomorphological setting, precipitation, rainfall intensity, evapotranspiration, runoff, soil water content.

In scientific literature, a number of approaches to quantify the volume of recharge at different spatial and temporal scales can be found: hydrological budget methods, surface-water methods, analysis of groundwater data, Darcian methods, chemical tracers methods, heat-based methods and geophysical methods. The estimation of recharge from local to regional scales reveals numerous issues. Local-scale estimates are not generally representative of an entire watershed, and regional estimates may be too extensive to capture recharge variability within a watershed (DELIN *et alii*, 2007).

In this paper, we present and compare the results of two different approaches to quantify the recharge processes in karst aquifers of southern Apennines (Italy). The first was set on regional and mean annual scales, through the estimation of the Annual Groundwater Recharge Coefficient (AGRC) carried out for four sample regional karst aquifers. The second was accomplished on local and episodic scales, by the application of the Episodic Master Recession (EMR) on to the *Acqua della Madonna* perched karst aquifer, belonging to the Mount Terminio hydrogeological unit (Campania region, southern Italy).

HYDROGEOLOGICAL SETTING

In southern Apennines, on a regional scale, it is possible to identify 40 principal karst aquifers. These aquifers represent the main source of drinking water, a strategic resource for socio-economic development and a fundamental factor controlling ecological equilibrium of rivers. A mean groundwater yield of 4100×10^{6} m^{3} year^{-1} and a mean specific

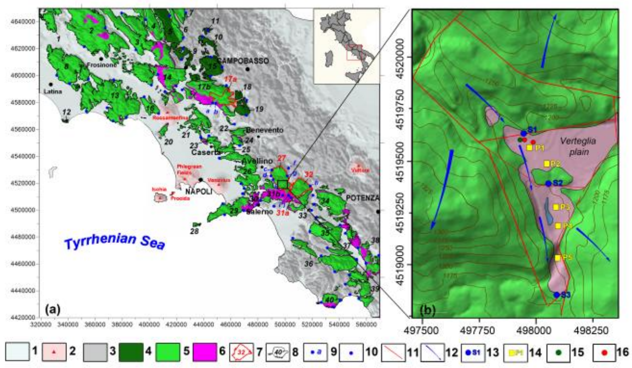

Fig. 1 – (a) Map of the karst aquifers of the southern Apennines. (b) Hydrogeological map of *Acqua della Madonna* perched karst aquifer. Key to symbols: 1) alluvial and epiclastic units (Quaternary); 2) volcanic centres (Pliocene-Quaternary); 3) pre-, syn- and late- orogenic molasses and terrigenous units (Cretaceous-Pliocene); 4) calcareous-marly units of the outer basin series (Trias-Paleogene); 5) limestone and dolomitic limestone units of the carbonate platform series (Jurassic-Paleogene); 6) dolomitic units of the carbonate platform series (Trias-Liassic); 7) hydrogeological boundary and identification number of the karst aquifers considered for the hydrological budget; 8) hydrogeological boundary and identification number of the karst aquifers; 9) basal karst springs considered in the hydrological budget (a and b: Maretto and Torano; c: Salza Irpina; d and e: Serino; f: Baiardo; g: Cassano Irpino; h: Sanità; i: Avella; l: Ausino-Ausinetto); 10) main basal springs of karst aquifers; 11) main faults; 12) groundwater flow direction; 13) perched springs; 14) piezometers; 15) soil water content sensor; 16) soil temperature sensor.

groundwater yield varying between 0.015 and 0.045 $m^3 s^{-1} km^{-2}$ were assessed by mean annual hydrological budget carried out (CELICO *et alii*, 2000; ALLOCCA *et alii*, 2007). These aquifers are formed by Mesozoic to Cenozoic carbonate series, which comprise rock types such as limestone, dolomitic-limestone, dolostones and marls. They are well hydraulically confined by low permeability terrigenous units, which adjoin by stratigraphic or tectonic boundaries. These aquifers are characterized by a basal groundwater circulation, outflowing in huge basal springs (Q_{mean} up to 5 m^3s^{-1}) located in the lowest point of the hydrogeological boundary at the contact with the low permeability units.

Unlike other karst aquifers in Europe, those of southern Italy have large endorheic and plateau areas on the top, which in several cases are covered by ash-fall pyroclastic deposits erupted from neighboring volcanic centers (DE VITA *et alii*, 2006; DE VITA *et alii*, 2013). In these aquifers, the groundwater recharge occurs by diffuse infiltration and/or secondary or concentrated infiltration in the endorheic areas.

DATA AND METHODS

Considering the principal factors affecting recharge of karst aquifers on a regional scale, the following factors were analysed for the estimation of the AGRC: a) lithology, through the use of a hydrogeological map of southern Italy, 1:250,000 scale, (ALLOCCA *et alii*, 2007); b) geomorphological features, by a national Digital Elevation Model (DEM) with cells of 20×20 m (http://www.sinanet.isprambiente.it); c) soil type, by the Land System Map of the Campania Region, 1:250,000 scale, (www.risorsa.info); d) land use, by the Corine Land Cover Project (2006). Moreover, mean annual precipitation data and mean annual air temperature data were gathered from the National Hydrographic and Tidal Service in the period 1926–1999 (www.isprambiente.gov.it) and the Regional Civil Protection Agency databases (www.protezionecivile.gov.it) for the period between 2000 and 2012. Considering the availability of long-duration time series of basal spring discharge, the Matese, Accellica, Terminio and Cervialto karst aquifers were analyzed among the 40 ones.

The Annual Groundwater Recharge Coefficient (AGRC) was estimated, by comparing terms of the hydrological budget, as the ratio between the mean annual net groundwater outflow (spring and other groundwater discharges) and the mean annual precipitation minus evapotranspiration:

$$AGRC = \frac{(Q_s + Q_t) + (U_o - U_i)}{P - ETR} \qquad (1).$$

Where: Q_s is the mean annual spring discharge; Q_t is the mean annual tapped discharge; U_o is the mean annual groundwater outflow through adjoining aquifers; U_i is the mean annual groundwater inflow from adjoining aquifers and other allogenic recharge; P is the mean annual precipitation; ETR is the mean annual actual evapotranspiration; R is the mean annual runoff.

For the calculation of the evapotranspiration, Turc's formula (1956) was applied:

$$ETR_j = \frac{P_j}{\sqrt{0.9 + \left(\frac{P_j}{300 + 25 \cdot T_j + 0.05 \cdot T_j^3}\right)^2}} \qquad (2).$$

Where: ETR_j is the mean annual actual evapotranspiration (mm) for the j rain gauge station; P_j is the mean annual precipitation (mm) for the j rain gauge station; and T_j is the mean annual air temperature (°C) for the j air temperature-rain gauge station.

Considering the peculiar geomorphological feature of the karst aquifers, characterized by huge summit plateau and endorheic areas, namely by a total infiltration and no runoff, an additional coefficient was assessed in order to estimate the recharge for the slope areas only:

$$AGRC_S = \left[\frac{(AGRC \times A_T) - (1 \times A_E)}{A_T - A_E}\right] \times 100 \qquad (3).$$

Where: $AGRC_S$ is the Annual Groundwater Recharge Coefficient for slope areas; A_T is the total area of the karst aquifer (km^2); A_E is the cumulative extension of summit plateau areas and/or endorheic watersheds (km^2). A complementary value of the $AGRC_S$ was calculated and named Annual Runoff Coefficient (ARC):

$$ARC = 100 - AGRC_S \qquad (4).$$

On a local scale, was analysed *Acqua della Madonna* test area (Terminio Mount karst aquifer, Campania region). Located in an endorheic area, it hosts a perched karstic aquifer formed by a carbonate bedrock, confined by a system of normal faults, and mantled by pyroclastic deposits (ALLOCCA *et alii*, 2008). For this sample area, daily rainfall and air temperature data were gathered from January to December 2008 by a thermo-pluviometric station belonging to the *Alto Calore S.p.A.* meteorological network

(http://www.altocalore.eu/). Moreover, were collected daily water table data by the P1 piezometer (Fig. 1), 60 m deep, whose stratigraphic setting is characterized, from the top, by 8.5 m of ash fall pyroclastic deposits and 51.5 m of karstified limestone and dolomitic-limestone.
Using precipitation and water table data (H), we analysed the recharge process by the WTF method and in particular using the EMR method (NIMMO *et alii*, 2015). The latter consists of two phases. The first is the reconstruction of the Master Recession Curve (MRC), which best fits the dH/dt *vs* H data and represents the average behavior for a declining water-table. The second is the application of the Episodic Master Recession (EMR) code to detect the episodes of recharge and calculate the Recharge to Precipitation Ratio (RPR), that is the amount of precipitations recharging the aquifer at the episodic time scale.
To validate the results of the methods to the discretization of the different components of the recharge process, was calculated a soil hydrological budget through the estimation of the actual evapotranspiration by the Thornthwaite-Mather method (1957).

RESULTS AND CONCLUSION

On a regional scale, on the basis of the empirical law found between P-ETR and the elevation of each rain gauge station, were found three homogeneous pluviometric zones and reconstructed a P-ETR map. Considering this regional distribution, were estimated the mean annual P-ETR values for the identified four sample karst aquifers. Then, considering the net groundwater outflow and applying the (1), were estimated the AGRC values (Tab. 1). For the Matese (a), Terminio and Cervialto, values of AGRC very similar (69%, 79% and 71%, respectively), while for the the Accellica aquifer was found a lower value (50%). The difference is due to the larger extension of dolomitic rocks and the lack of endorehic and summit plateau areas for the Accellica Mount karst aquifer.

ID	Karst aquifer	Area (km^2)	Summit plateau / endorheic area (%)	$V_{outflow}$ (10^6 m^3 y^{-1})	V_{inflow} (10^6 m^3 y^{-1})	AGRC (%)	$AGRC_S$ (%)	ARC (%)
17a	Matese (a)	120	34	95.2	138.1	69	52	48
27	Terminio	167	43	169.7	213.3	79	64	36
31a	Accellica (a)	35	0	18.3	36.9	50	50	50
32	Cervialto	129	20	126.1	178.4	71	63	37

Table 1 – AGRC and mean $AGRC_S$ estimation for the investigated sample karst aquifers. Values are related to the mean value of the P-ETR linear regression models with altitude (from ALLOCCA *et alii*, 2014).

Very similar values for the $AGRC_S$ and ARC, ranging respectively from 50% to 64% and from 50% to 36% were found. Moreover, to understand the influence of the considered factors, controlling the groundwater recharge on a regional scale (lithology, endorheic/summit plateau areas, soil type and land use), and to extend the results of this analysis to the other karst aquifers, was effected a bivariate correlation analysis. A significant empirical relationship between the AGRC and only the percentages of outcropping limestone (L) and endorheic/summit plateau (E) areas was discovered,

$$AGRC = 47.99 + 0.08L + 0.51E \qquad (5),$$

which resulted statistically significant (r^2 = 0.968; Prob. F-Fisher = 3.0%).
The application of the equation allowed to calculate the AGRC and the $AGRC_S$ also for those aquifers for which long time series of spring discharge measurements were not available. The values of the calculated AGRC vary from 48% to 79% with a mean value of 67% that is consistent with values found for other karst aquifers of Europe (BONACCI, 2001).
In a GIS environment, was reconstructed a distributed model of the mean annual groundwater recharge for the karst aquifers of the southern Apennines by the overlapping of the P-ETR and the $AGRC_S$ maps as well as considering a total infiltration condition for the endorheic/summit plateau areas.
At local scale, was reconstructed the MRC using the pure

Recharge episode	Start time	End time	Duration (day)	Recharge (m)	Precipitation (m)	RPR (Recharge to Precipitation Ratio)	Average storm intensity (m/d)	Max storm intensity (mm/d)	Soil water content (%)
1	04-gen	21-gen	18	0.1	0.104	0.97	0.006	31.4	-
2	05-feb	15-feb	10	0.011	0.019	0.59	0.002	19.2	-
3	03-mar	18-mar	15	0.11	0.129	0.86	0.009	45.2	-
4	21-mar	27-mar	6	0.093	0.247	0.37	0.038	153.6	23.49
5	28-mar	01-apr	5	0.014	0.017	0.87	0.003	4.6	24.16
6	05-apr	29-apr	24	0.107	0.12	0.89	0.005	46	20.45
7	18-mag	26-mag	8	0.064	0.076	0.84	0.01	62	27.78
8	10-set	16-set	5	0.019	0.033	0.57	0.006	22.4	12.42
9	01-ott	06-ott	5	0.039	0.042	0.92	0.008	25	30.51
10	27-ott	03-dic	37	0.261	0.404	0.65	0.011	68.4	34.01
11	05-dic	10-dic	6	0.107	0.272	0.39	0.046	230.6	39.45
12	12-dic	17-dic	6	0.072	0.089	0.81	0.014	49.2	39.42

Table 2 – Results of the EMR Matlab code. Average storm intensity and max storm intensity are user-supplied parameters.

recessional data, i.e. a subset formed by excluding data affected by input from recent rainfall. Looking at the distribution of dH/dt *vs* H points, a third order polynomial curve was fitted (r^2= 0.82). The entire dataset can be split in two parts according to the position of the water table respect the two lithologies. In the karst sector of the aquifer, varies from 0.00 to 0.05 meters/day, while in the pyroclastic the range is wider, going from 0.05 to 0.45 m/day. The main cause of this difference was considered to be the greater hydraulic conductivity and specific yield of the pyroclastic media respect to the karst bedrock one.

The application of the EMR code for the *Acqua della Madonna* perched aquifer, allowed us to identify for the considered year 12 episodes of recharge and 12 non-recharge periods (Tab. 2). Duration of the recharge periods ranged from 5 to 37 days, with a mean value of 12 days, whereas the length of non-recharge periods varied from 0 to 107 days, corresponding chiefly to the summer season. The RPR for each recharge episodes varies from 37% to 97% with a mean value of 73%.

The calculated value of the ETR (28% of P) provided a complementary value of P-ETR (72%), well matching with the 73% of the mean RPR if considering the endorheic morphology and the total infiltration condition of the sample area. The mean value of RPR (73%) is very close to the AGRC (79%), estimated for the whole Terminio Mount karst aquifer on a regional scale, and it is similar to values of infiltration coefficient estimated for other European karst aquifers (BONACCI, 2001).

Observing the results, at regional and mean annual time scales, groundwater recharge is influenced by the presence and extension of endorheic/summit plateaus areas and limestone lithology while, at local and episodic scale, the parameters affecting recharge are seasonality and intensity of precipitation. The soil type, covering the carbonate outcrops, and land use resulted to have a negligible control on the groundwater recharge process.

In conclusion, the obtained results permit consideration of the AGRC as a valid tool for the calculation of the annual hydrological budget in order to set up a sustainable and responsible management of water resources, also taking into account the decadal climate variability affecting the area (DE VITA *et alii*, 2012a; MANNA *et alii*, 2013). The adaption of EMR method to the WTF one is a valid approach to quantify the recharge at a detailed scale of observation and minimize errors coming from typical overestimation of others WTF methods (DELIN *et alii*, 2007; NIMMO *et alii*, 2015).

REFERENCES

Allocca V., Celico F., Celico P., De Vita P., Fabbrocino S., Mattia S., Monacelli G., Musilli I., Piscopo V., Scalise A. R, Summa G. & Tranfaglia G. (2007) - Illustrative Notes of the Hydrogeological Map of Southern Italy. Ist. Poligrafico e Zecca dello Stato, Rome, 211 pp.

Allocca V., Celico F., Petrella E., Marzullo G. & Naclerio G. (2008) - The role of land use and environmental factors on microbial pollution of mountainous limestone aquifers. Environmental Geology, 55, 277-283.

Allocca V., Manna F. & De Vita P. (2014) - Estimating annual groundwater recharge coefficient for karst aquifers of the southern Apennines (Italy). Hydrology Earth System Sciences, 18(2), 803–817.

Andreo B., Vías J., Durán J.J., Jiménez P., López-Geta J.A. & Carrasco F. (2008) - Methodology for groundwater recharge assessment in carbonate aquifers: application to pilot sites in southern Spain. Hydrogeology Journal, 16, 911-925.

Bonacci O. (2001) - Monthly and annual effective infiltration coefficients in Dinaric karst: example of the Gradole karst spring catchment. Hydrological Sciences, 46, 287-299.

Celico F., Celico P., De Vita P. & Piscopo V. (2000) - Groundwater flow and protection in the Southern Apennines (Italy). Hydrogéologie. 4, 39-46.

De Vita P., Agrello D. & Ambrosino F. (2006) - Landslide susceptibility assessment in ash-fall pyroclastic deposits surrounding Mount Somma-Vesuvius: application of geophysical surveys for soil thickness mapping. Journal of Applied Geophysics, 59, 126-139.

De Vita P., Allocca V., Manna F. & Fabbrocino S. (2012) - Coupled decadal variability of the North Atlantic Oscillation, regional rainfall and karst spring discharges in the Campania region (southern Italy). Hydrology and Earth System Sciences, 16, 1389-1399.

De Vita P., Napolitano E., Godt J.W. & Baum R.L. (2013) - Deterministic estimation of hydrological thresholds for shallow landslide initiation and slope stability models: case study from the Somma-Vesuvius area of southern Italy. Landslides, 10, 713–728.

Delin G., Healy R., Lorenz D., & Nimmo J. (2007) - Comparison of local- to regional-scale estimates of ground-water recharge in Minnesota, USA. Journal of Hydrology, 334, 1-2, 231-249.

Manna F., Allocca V., Fusco F., Napolitano E. & De Vita P. (2013) - Effect of the North Atlantic Oscillation on groundwater recharge in karst aquifers of the Cilento Geopark (Italy). Rendiconti Online Soc. Geol. Italiana, 28, 106-109.

Nimmo J.R., Healy R.W., & Stonestrom D.A. (2005) - Aquifer Recharge. In: Anderson M.G., & Bear J., eds., Encyclopedia of Hydrological Science, Chichester, UK, Wiley, 4, 2229-2246.

Nimmo J.R., Horowitz C. & Mitchell L. (2015) - Discrete-Storm Water-Table Fluctuation Method to Estimate Episodic Recharge. Groundwater, 53(2), 282-292.

Thornthwaite C.W. & Mather J.R. (1957) - Instructions and tables for computing potential evapo-traspiration and water balance. Climatology, 10, 3, Thornthwaite C.W. & Associates, Centerton, New Jersey.

Turc L. (1954) - Le bilan d’eau des sols: relations entre les précipitations, l’évaporation et l’éecolument. Annales Agronomiques, 5, 491-595.